DETERMINING MECHANICAL PROPERTIES OF LIME-STABILIZED CLAY

METİN BULUT

January, 1986

Boğaziçi University

DETERMINING MECHANICAL PROPERTIES OF LIME-STABILIZED CLAY

by

METİN BULUT

B.S. in C.E., Ege University, 1982

Submitted to the Institute for Graduate Studies in Science and Engineering in partial fulfillment of the requirements for the degree

Master of Science

in

Civil Engineering

Boğaziçi University

1986

DETERMINING MECHANICAL PROPERTIES
OF
LIME-STABILIZED CLAY

APPROVED BY :

Doç. Dr. Erol GÜLER
(Thesis Supervisor)

Prof. Dr. Ergün TOĞROL

Doç. Dr. Turan H. DURGUNOĞLU

Doç. Dr. Vural ALTIN

DATE OF APPROVAL : January 22, 1986

To my parents,

Sabahattin and Fati BULUT.

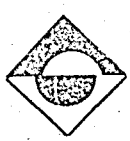

ACKNOWLEDGEMENT

I would like to express my sincere gratitude to Doç. Dr. Erol Güler, for his invaluable suggestions, guidence, encouragements throughout the course of my study and especially in evaluation of test results.

METİN BULUT

Istanbul, January 1986

ABSTRACT

The scientific investigations in geotechnical engineering field, up to present, has focused on understanding and predicting the behaviour of soil material using different types of tests. In this thesis, the behaviour of artificially lime added clayey soil is investigated within the framework of critical state theory. Therefore, a series of isotropically consolidated-undrained compression tests have been carried out on lime-stabilized clay by using triaxial testing equipment. Confining pressures were chosen as 2.0, 2.5, 3.0, 3.5, 4.0 and 5.0 kg/cm^2. Lime percentages were chosen to be 5%, 10% and 20%. The relationships of $q:\varepsilon_\alpha$, $U:\varepsilon_\alpha$, $q:p'$, $q/p':\varepsilon_\alpha$, $U:p'$, $A_p:\varepsilon_\alpha$, $Ap:p'$, $q/p'_{ei}:\varepsilon_\alpha$ *and* $\nu:lnp'$ *are tabulated and drawn.*

ÖZET

KİREÇ İLE STABİLİZE EDİLMİŞ KİLİN MEKANİK ÖZELLİKLERİNİN SAPTANMASI

Bugüne kadar zemin mekaniği alanındaki bilimsel çalışmalar zemin üzerinde çeşitli deneyler yaparak davranışını inceleme konusunda yoğunlaşmıştır. Bu tez çalışmasında kireç ile stabilize edilmiş kilin davranışı kritik durum teorisi çerçevesinde incelenmiştir. Bu nedenle, hazırlanan kireç katılmış ve katılmamış kil numuneleri üzerinde üç eksenli deney aletini kullanarak, konsolidasyonlu-drenajsız deneyler gerçekleştirilmiştir. Konsolidasyon sırasında 2.0, 2.5, 3.0, 3.5, 4.0, ve 5.0 kg/cm^2 hücre basınç uygulanmıştır. Ayrıca kireç yüdeleri de %5, %10 ve %20 olarak seçilmiştir. Tüm deney sonuçları tablolar halinde sunulmuş olup, değişik kireç yüzdelerine göre değişim gösteren q-ε, u-ε, q-p', q/p'-ε, A_p-ε, A_p-p', U-p', q/p_{ei}-ε ve U/P_{ei}-ε eğrileri çizilmiştir.

TABLE OF CONTENTS

LIST OF FIGURES

LIST OF TABLES

LIST OF SYMBOLS

A' : Cross-sectional area of specimen

A_o : Initial cross-sectional area of specimen

A_p : Pore-pressure parameter

CSL : Critical state line

e : Void ratio

ε_α : Axial strain

ε_f : Axial strain at failure

ε_v : Volumetric strain

g : Soil constant defining the Hvorslev surface

G_s : Specific gravity of soil grains

Γ : Specific volume of soil sample at critical state corresponding to p':1.0 kg/cm^2 in v:$\ell n p'$ space

h : Slope of the Hvorslev surface

λ : Slope of normal consolidation line and critical state line in v:$\ell n p'$ space

M : Slope of critical state line in q:p' space

N : Specific volume of isotropically normally consolidated sample at p'=10 kg/cm^2 in ν:ℓnp' space

ν : Specific volume

NCL : Normal consolidation line

OCR : Overconsolidation ratio

P : Total mean normal stress

p' : Effective mean normal stress

P_{ei} : Initial equivalent mean normall stress

q:q' : Deviator stress

q_f : Deviator stress at failure

σ_1 : Axial stress

σ_2:σ_3:σ_c: Cell pressure

U : Pore water pressure

U_f : Pore water pressure at failure

W : Water content

W_{LL} : Liquid limit

W_{opt} : Optimum water content

W_{pL} : Plastic limit

I. INTRODUCTION

Many researchers have, through extensive experimental results and analyses, provided the civil engineers, for all practical purposes, several means of predicting the different aspects of soil behaviour. Rcscoe, Schofield and Wroth brought a new understanding to the relations of water content, shear stress and effective mean normal stress by explaining the existing theories with the critical state theory.

In some cases, the soil material does not exhibit the desirable properties required in the construction of several projects such as dam, road, airfield, building and in other installements. Therefore, it becomes necessary to improve the soil characteristics for the purpose of obtaining a better soil for the intended engineering usage. The improvement of soil properties is carried out by altering properties of soil through several means of stabilization techniques, i.e. mechanical, electrical, thermal, chemical, bituminous and portland-cement stabilization procedures.

In this thesis resarch, the behaviour of artifically lime added clayey soil is investigated within the framework of critical state theory. For this purpose, a series of consolidated-undrained compression tests have been carried out on lime-stabilized clay through the use of common triaxial testing apparatus.

In chapter II, structure of cohesive soils, changes in structure during compaction and effects of structure and compaction on strength are explained. Soil-lime-water relations and mechanism of lime-stabilization are also mentioned.

A brief explanation of Critical State concept and Critical State Line is presented in chapter III. The complete state boundary surface, consisting of the Roscoe and Hvorslev surfaces, is also mentioned.

In chapter IV, the details of the triaxial compression testing equipment used in the experimental study, the material and preparation of samples are explained.

Effect of lime amount in soil-lime mixtures on deviator stress and pore-pressure is discussed in chapter V. Stress paths are presented, and effect of lime content on mechanical properties of lime-stabilized clay is also mentioned in this chapter.

A brief summary of thesis study and conclusions deduced from the previous studies and tests carried out in this research are presented in Chapter VI.

II. STRUCTURE OF COHESIVE SOILS

2.1 INTRODUCTION

When soil at a site is loose of highly compressible, or when it has unsuitable properties for use in a construction project, they have to be stabilized. Therefore, a knowledge of the behaviour of compacted clays stabilized with lime is necessary for satisfactory and economical design.

In this chapter, a short summary of existing knowledge on the structure of cohesive soils is presented. Changes in structure during compaction are discussed. Effects of structure and compaction on strength are mentioned. Soil-lime-water relations are discussed. The mechanism of lime-stabilization is also presented.

2.1.1 Structure of Clays

According to Lambe (1958), the term "Structure" is the arrangement of soil particles, which is controlled by the electrical forces acting between adjacent particles. Previously, "Structure" was limited to the arrangement of soil particles only. The concepts of electrical forces and environmental factors entered into the discussions

of structure with the principals of colloid chemistry.

A cohesive soil is defined as an aggregation of mineral particles which has plasticity index defined by the Atterberg limits and which forms into a choerent mass on drying such that force is necessary to seperate the individual microscopic grains (Bowles,1979).

A complete description of the structure of a fine-grained cohesive soil requires a knowledge of both the interparticle forces and geometrical arrangement of particles. The interpartide forces appear to be developed from two types of electrical charges.

The elements which are capable of chemical combination lack a complete of electrons in their outermost shells. One atom joins with another atom by adding electrons to its outer shell or shells, or by losing them, to arrive at a stable state. Atoms which have lost or gained electrons in this manner are called ions, and the forces binding them together are called ionic (primary) bonds (Scott, 1963).

As a result of movements of electrons in their orbits around atoms, any molecule posseses an associated electric field which is capable of interacting with the field of nearby molecules to give rise to an attractive force between the molecules; this attractive force is called Van der Waals-London force (Jumikis, 1962). The Van der Waals attractive forces between the surfaces of two parallel clay mineral particles seperated by water depend on the crystal structure of the minerals and on the distance of separation as seen in Fig. 2.1.

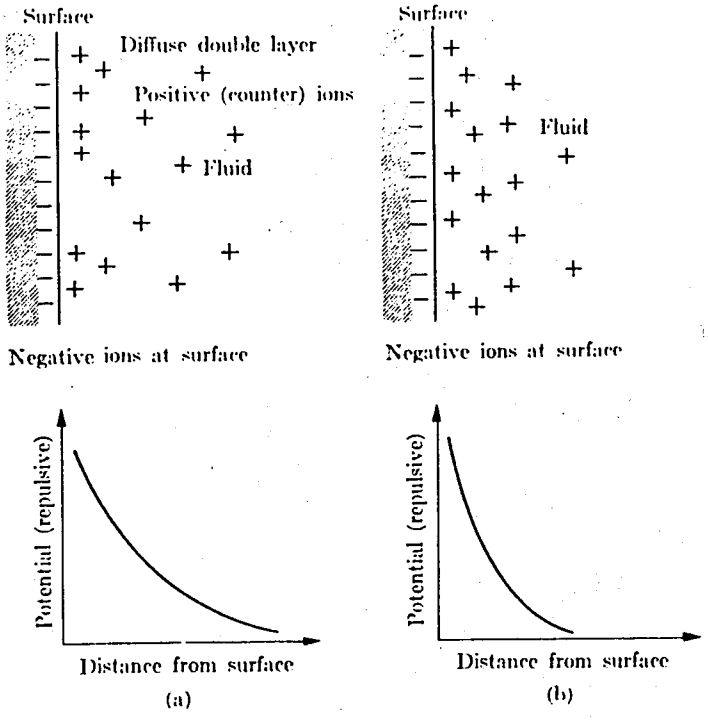

FIG.2.1 Repulsion Potential in the Diffuse Double Layer as a Function of Distance from the Surface (After Scott, 1963)

Clay particles are almost hydrated, i.e., surrounded by layers of water molecules called adsorbed water. In the presence of water, clay particles exhibit greatly different behaviour then do other minerals because of the interaction of the electrostatic fields, the diffuse double layers. The strongly held and charged cations at the surface of the particle and the relatively mobile counter-ions in the medium adjacent to the surface are generally considered to be two layers, and the whole system is referred to as the diffuse double layer.

The edges of all the clay minerals have net negative charges. This results in attempts to balance the charges by cation attraction. Owing to these charges, the H^+ ions in water, the Van der Waals forces, and small size of the particles, they tend to become attracted together in a solution. Several particles, thus attracted form a randomly oriented floc or structure of larger size which will settle out of suspension to form a very loose sediment. After the clay has been standing some time, it gains strength with aging, a thixotropic effect (Mitchell, 1960). Structure of sedimented clays and shematic diagram of thixotropic structure change in a fine grained soils is presented in Fig. 2.2.

2.1.2 Structure of Compacted Clays

In compacting any particular soil, the basic properties that affect the behaviour are the method or type of compaction, the compactive effort, the soil type, and the water content. Usually, the water content of compacted soil is referenced to the optimum mois-

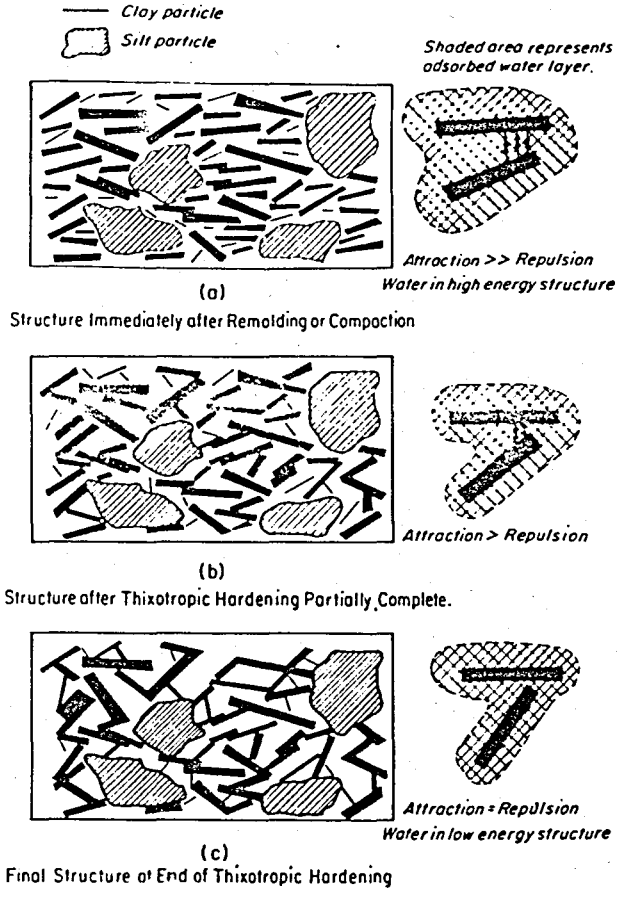

FIG.2.2 Schematic Diagram of Thioxotropic Structure Change in a Fine Grained Soil (After Mitchell, 1960)

ture content for the given type of compaction. Depending on the relative position, this may be "dry of optimum," "near or at optimum," or "wet of optimum".

Although Lambe (1958) stated that little is known on how the type of compaction influences the structures of compacted clays, Seed and Chan (1959) and later Seed et al.(1960) indicated that different types of compaction methods induce varying amounts of shear strains into the soil and increasing shear strains result in more dispersed structures with parallel arrangement of particles. Thus, changes in structure arise from the combined effect of both and increase in water content and induced shear strains.

Further, Seed and Chan (1959) observed that four basic types of compaction methods, i.e., static, vibratory, impact and kneading, result in different structures and different soil properties for samples compacted at wet of optimum. The induced shear strains tend to increase in the following order of compaction methods; static, vibratory, impact and kneading. Seed et al.(1960) also stated that all types of compaction methods produce similar structures. This is due to the fact that none of the compaction procedures can induce high shear strains below optimum water content. During compaction at wet of optimum, the increase in the degree of dispersion is directly related to the increasing shear strains induced by different types of compaction methods. Besides, the "lubrication" of clay particles of water is needed for shear strains to change the particle order into a more parallel arrangement.

By keeping the compaction energy and type constant, only one

dry density is obtained for a unique water content. Increasing compactive energy at any given water content increases the orientation of particles and thus gives a higher density. This was first investigated by Lambe (1958), and it is shown in Fig. 2.3. In that figure, at point A, there is not enough water for the diffuse double layers of the soil particles to develop fully, or clay is water deficient. Hence, the electric repulsive forces between particles are smaller than the attractive forces, resulting in a net attraction between particles, and the particles tend to flocculated in a disorderly array.

Clay particles under a given set of conditions have certain amount of water to fully develop their double layers. The difference between the existing water and needed water is called deficient water which the particles will try to adsorb. When the existing water content of a clay sample is less than the equilibrium water content, the net forces between particles are attractive and the structure is flocculated. If the necessary amount of water is given to the clay, the double layers are fully obtained, the net forces between particles become repulsive and the structure becomes dispersed.

When the water increased towards B,Fig. 2.3.,electrolyte concentration decreases, the repulsion between clay particles increases, and double layer becomes larger; therefore, flocculation decreases. Decreasing degree of flocculation permits a more orderly arrangement of particles. Increasing the order of particles increases the density until water content of point B is reached.

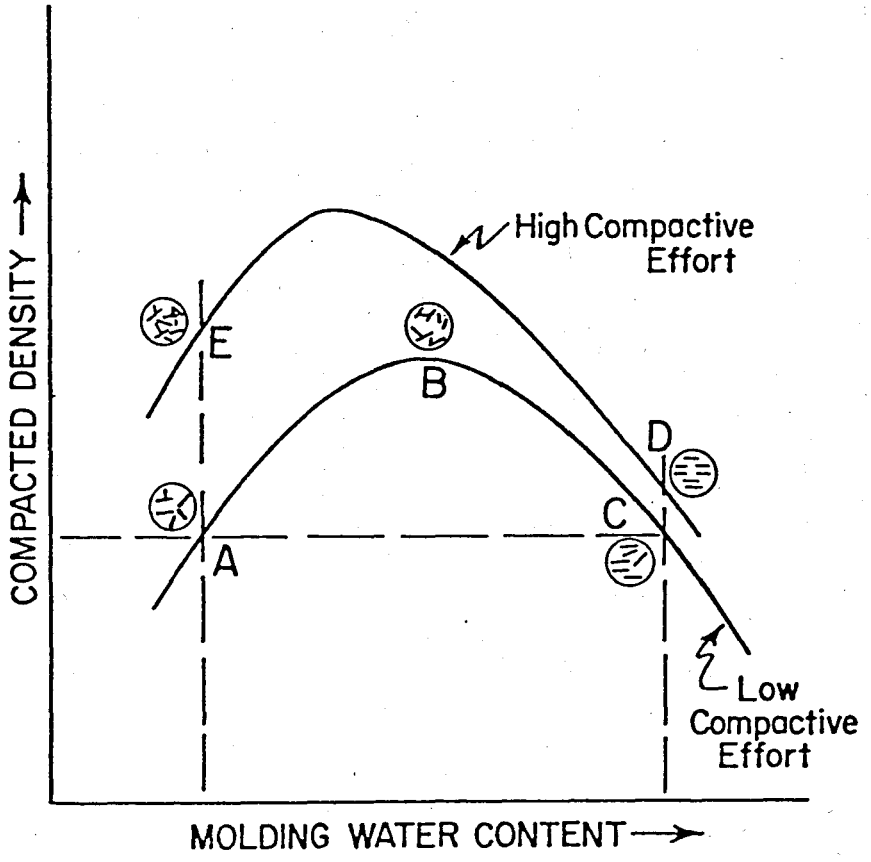

FIG.2.3 Effects of Compaction on Structure (After Lambe,1958)

Beyond point B, particle parallelism increases. A further expansion of the double layer causes the repulsion between particles to increase and the attractive force to decrease. Althouhg a more orderly arrangement exist, beyond point B the compacted density begins to decrease because water starts to occupy space which could be filled with soil particles.

The changes in structure which are described above can not be seen in all compacted clays, especially in the clays with particles having great tendencies to flocculate.

In this way, the particle orientation of a clay may be of any arrangement between two different cases; i.e., a completely random orientation which is a flocculated structure and a completely parallel orientation which is a dispersed structure.

2.1.3 Effect of Structure on Shear Strength

According to Lambe (1958), the entire force system between clay particles should be considered for studying the shear strength of the compacted clays. He explained that four main forces act between adjacent particles; these are : the externally applied intergranular stress, the electrical repulsion forces, the geometric interaction, i.e., contact pressure.

A particular phenomenon of clay that a clay mass which has dried from some initial water content forms a mass which has considerable strength. If these lumps are broken down to element particles, the material behaves as a cohesionless one. When water is

again added, the material becomes plastic with some strenth intermediate to the dry lump strength. If the wet clay is again dried, it forms hard, strong lumps. It follows that higher density resulting from packing and the close spacing resulting in the maximum effect of interparticle force attraction give this high strength. A recently conducted experimental research indicates that an increase in the shear strength takes place as the intrinsic effective stress increase due to bonds generated by wetting and drying (Allam and Sridharan, 1981).

Main factors affecting the strength are spacing, orientation of particles of clay and type of compaction used. When a clay specimen is compacted on the dry-side of optimum, a flocculated structure is formed and the edge-to-face contact between soil particles provides high resistance to load. On the other hand, when compacted on wet of optimum, the specimen has a dispersed structure with relatively strong interparticle contacts, resulting in a low shear strength. Besides, increased compactive energy at dry of optimum causes in an increase of strength. If clay with a flocculated structure is subjected to shear, some of the interparticle bonds break down in the course of shear deformations, while new ones are formed continuously. If the break down of the bonds become predominant, the clay suffers an essential change in its structural strength, so that constant shear strain can be maintened even by greatly reducing stresses. Interparticle forces of adhesion cease to exist because of the destruction of bonds;therefore the part of shearing stress due to cohesion decreases whereas the frictional resistance increases.

2.2 LIME STABILIZATION

2.2.1 History of Lime Stabilization

It is known that Romans have used quicklime for base construction 2200 years ago. The famous "Appian Way" included a 30 cm. layer of gravel and coarse sand mixed with "hot" lime and this road served well until the Seventh Century. There are also roads of antiquity in China, India and Burma when lime was used alone or burnt with clay.

The use of lime in the road construction began in the U.S.A. nearly 70 years ago. However, the scientific researchs started in the University of Missouri in 1924.

Although successfully used in the U.S.A, soil stabilization with lime was applied in the United Kingdom in country road, for the first time in Europe, in 1945. Later, France used this type of stabilization technique at the Orly Airport in Paris. And at present, soil satibilization with lime is widely applied especially in the developing countries.

2.2.2. Mechanism of Lime Stabilization

The nature of reactions accompanying the stabilization with lime and mechanism concerned with the alteration of soil-lime reactions have been studied by Z.C.Moh(1964). Using 10% cementing compounds on mono-mineral soils with or without sodium additives, he has examined the results by a number of analytical techniques after

compaction and various curing periods. Both mono-mineral soils, quartz and kaolinite, reacted with hydrated lime. Addition of sodium additives greatly intensified the reaction between the soil and the stabilizer, and increased the abundance of reaction products.

The response of soil to treatment with lime is complex;and number of explanations to take into account these unusual responses were proposed by Diamond and Kinter (1965), including,

i. Cation exchange, i.e., replacement of the exchangeable sodium, magnesium or other cations previously held by the clayey soil and by calcium cations from lime.

ii. Flocculation of clay, and consequent increase in effective grain size.

iii. Carbonation, i.e., reaction of lime with carbon-dioxide from the atmosphere to from calcium-carbonate which is said to exert cementing action.

iv. The co-called pozzolanic reactions with soil constituents to generate new minerals of a cementious nature.

The factor of cation exchange has been mentioned by many scientists (Eades, Nichols and Grim, 1962; Thompson, 1967, Bowles,1979), yet familarity with the cation exchange properties of soils should have eliminated this as a serious explanation for the stabilizing effects of lime on soil. Even though it may be suggested that complete, rather than predominant calcium saturation is required for

stabilization, it has been demonstrated that even lime is added in very large excess do dilute clay suspensions, under conditions where cation movement is faciliated, complete exchange for sodium does not take place (Ladd, Moh and Lambe, 1960; Moh, 1962).

The concept that flocculation plays a major part in soil-lime stabilization is often mentioned, but study of previously known facts reveals that this is also an inadequate explanation. The fact that flocculation of clay occurs as a consequence of the addition of lime is a well-known phenomenon, but the achievement of flocculation is clearly not the mechanism by which lime stabilizes soil.

The hypothesis that soil-lime stabilization depends on carbonation of lime to form calcium-carbonate can be dismissed by reference to any of the great number of studies, in which reaction with atmospheric carbon-dioxide was precluded by sealing the samples and in which characteristics modification of properties and development of strength associated with lime were observed. Carbonation does not take place in the field, however strength gain is said to occur by means of cementation of soil grains by $CaCo_3$ (Eades, Nichols and Grim, 1962). It appears that the additional benefit by long-term reaction of uncarbonated lime with the soil itself would far out outweigh any such contribution, and carbonation is probably a deleterious rather than a helpful phenomenon in soil-stabilization

Up to present, researchs reveal that there are at least two distinct stages of reaction involved.

i. The immediate process responsible for the amelioriation of the water-sensitive properties of untreated clay soil,

ii. The slower, long term reactions resulting in the formation of the final cementitious products that are indicated by the gradual development of strength in compacted soil-lime mixtures.

Among the effects observed in the first stage are large increases in the w_{PL}, generally leading to a reduction in the I_p. (Wang Mateos and Davidson 1963). The amount of increase in w_{PL} varies directly with the amount of lime added up to some limiting lime content; further increments of lime usually bring little or no additional increases (Mohammad and Walker, 1963). The point of inflection of the plot of lime added vs w_{PL} is called the "lime fixation point" (Hilt and Davidson, 1960).

The effect on the w_{LL} is less easy to summarize since the published data conflict.

The lime treatment substantially increased the shear strength of lime reactive soils. This improvement is due to a large increase in cohesion with small increase in the angle of internal friction. Similarly, the moduli of elasticity of the lime-soil mixture were much larger than the those of untreated soil (Thompson, 1966, 1967)

2.2.3 Reaction of Soil-Lime Mixtures

When a solution of lime comes into contact with clay particles, the covalent positively charged calcium ions tend to occupy the exchange positions of the clay; consequently, the following reactions are observed :

$$AOK_2 + Ca(OH)_2 \rightarrow AOCa_2 + 2KOH$$

$$AOH_2 + Ca(OH)_2 \rightarrow AOCa + 2H_2O$$

2.3 SUMMARY

In this chapter, particle orientations, the structure of compacted clay and effects of structure change due to compaction on strength is presented; te mechanism of lime stabilization is also mentioned; and the following conclusions are obtained.

The particle orientation of a clay may be of any arrangement between two different cases; i.e., a completely random orientation which is flocculated structure and a completely parallel orientation which is a dispersed structure.

The electrical forces acting between particles are most responsible for soil strength in compacted clay.

Different compaction types result in different structures in samples compacted at wet of optimum and have considerable effect on strength, however type of compaction method has little influence at dry of optimum.

Cation exchange, substitution of metallic ions of higher order, plays a major part in soil-lime mixtures.

Large increases in the w_{PL}, generally leading to a reduction in the I_p, are observed when lime is added to clayey soil; however, the amount of increase in w_{PL} varies directly with the amount of lime added up to some limiting content, further increments of lime give rise to little or no additional increases.

The lime treatment substantially increases the shear strength

of lime stabilized clay due to a large increase in cohesion with small increase in the angle of internal friction.

The modulus of elasticity of soil-lime mixture is larger than untreated soil.

III. CRITICAL STATE THEORY

3.1 INTRODUCTION

In this chapter, a brief explanation of critical state concept and critical state line is presented. The complete state boundary surface, consisting of the Roscoe and Hvorslev surfaces is also discussed.

3.1.1 Critical State Concept

The classic work of Hvorslev on the shear strength of remoulded saturated cohesive soils contains a clear statement of the fundamentals upon which the present knowledge of subject is based. He indicated that the peak shear stress at failure of such a soil is a function of the effective normal stress p_f' on, and of the void ratio of e_f in, the plane of failure at the moment of failure and this function is independent of the stress history of the sample.

The continuous yielding of a sample can be represented by a loading path which rises to the yield surface and then remains constant. The problem arises as to whether the path ends at any specific point. It is shown that the final portions of all paths lie in a

unique surface, and the paths end at a unique critical voids ratio line, and at the critical void ratio state unlimited deformations can take place while p', e(v) and q, deviator stress, remain constant (Roscoe, Schofield and Wroth, 1958).

In a drained triaxial test the critical void ratio can be defined as that ultimate state of a sample at which any arbitrary further increment of shear distortion will not result in any change of voids ratio. In an undrained test the sample remains at a constant voids ratio, but the effective stress p' will alter to bring the sample into an ultimate state such that particular voids ratio, at which it is compelled to remain during shear, becomes a critical voids ratio (Roscoe, Schofield and Wroth, 1958).

According to Schofield and Wroth (1968), who developed the critical state theory within the framework of experimental results of Roscoe (1958), Parry (1960) et al., soil and other granular materials, if continuously distorted until they flow as a frictional fluid, will come into a well-defined critical state, determined by the following two equations :

$$q = M.p' \qquad \ldots (3.1)$$

$$v = \Gamma - \lambda \ln p' \qquad \ldots (3.2)$$

The constants M, Γ and λ represent basic soil-material properties; and the parameters $q, v = 1+e$(void ratio), and p' are deviator stress, specific volume and effective mean normal stress, respectively.

The first equation of the critical states determines the magnitude of the deviator stress,q, needed to keep the soil flowing continuously as the product of a frictional constant with the effective mean pressure. The second equation states that the specific volume occupied by unit volume of flowing particles will decrease as the logarithm of the effective pressure increases, i.e. more water in the voids and a clay paste of a softer consistency that flows under less deviator stress.

3.3.2 Critical State Line

The failure states of drained and undrained triaxial compression tests, as seen in Fig. 3.1 and in Fig. 3.2, on isotropically compressed samples, when plotted together, the data points define a single straight line through the origin in q':p' space and a single curved line in v:p' space. This single and unique line of failure points of both drained and undrained tests is defined as the Critical State Line.

The crucial property of the Critical State Line (CSL) is that failure of initially isotropically compressed samples will occur once the stress states of the samples reach the line, irrespective of the test path followed by the samples of their way to the Critical State Line. Failure can be described as a state when large shear distortions occur with no change in stress, or in specific volume.

The projection of the Critical State Line onto the v vs $\ln p'$ plane as illustrated in Fig. 3.3, is described by the equation (3.1),

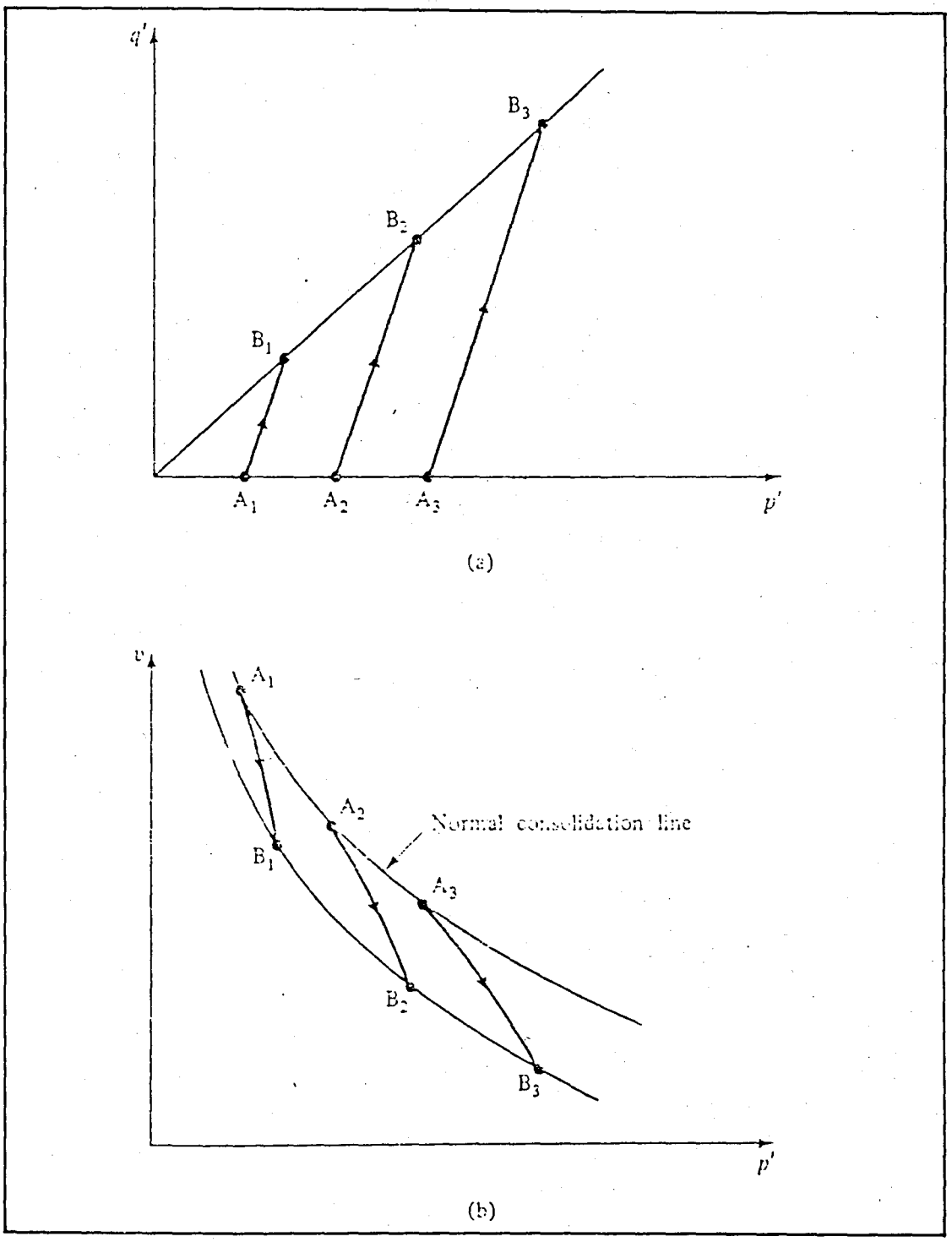

FIG.3.1 Stress Paths in a)q':p' and b)ν:p' Space for Drained Triaxial Tests on Normally Consolidated Samples (After Atkinson and Bransby, 1978)

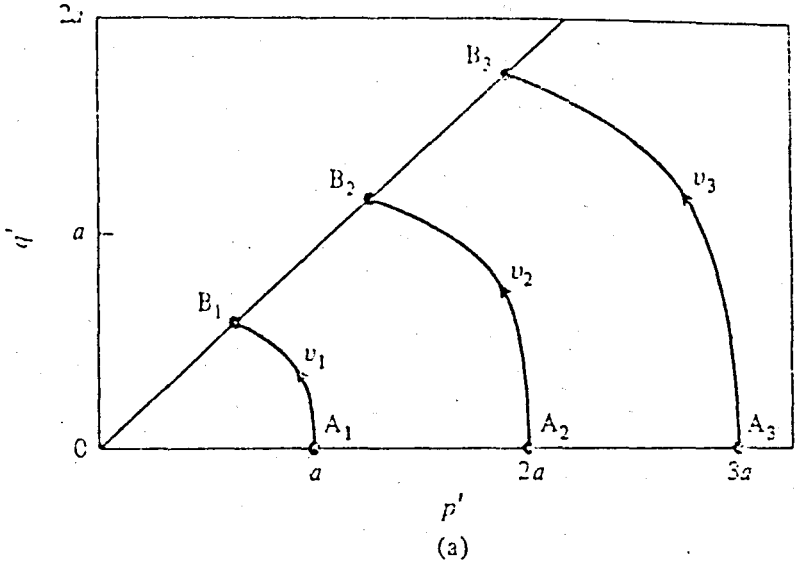

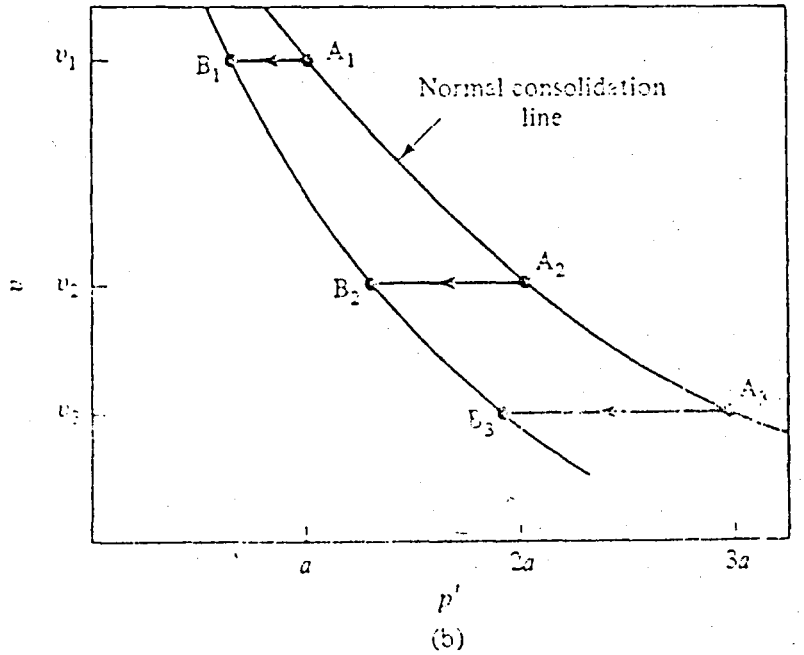

FIG.3.2 Stress Paths in a)q':p' and b)ν:p' Space for Undrained Tests on Normally Consolidated Samples (After Atkinson and Bransby,1978)

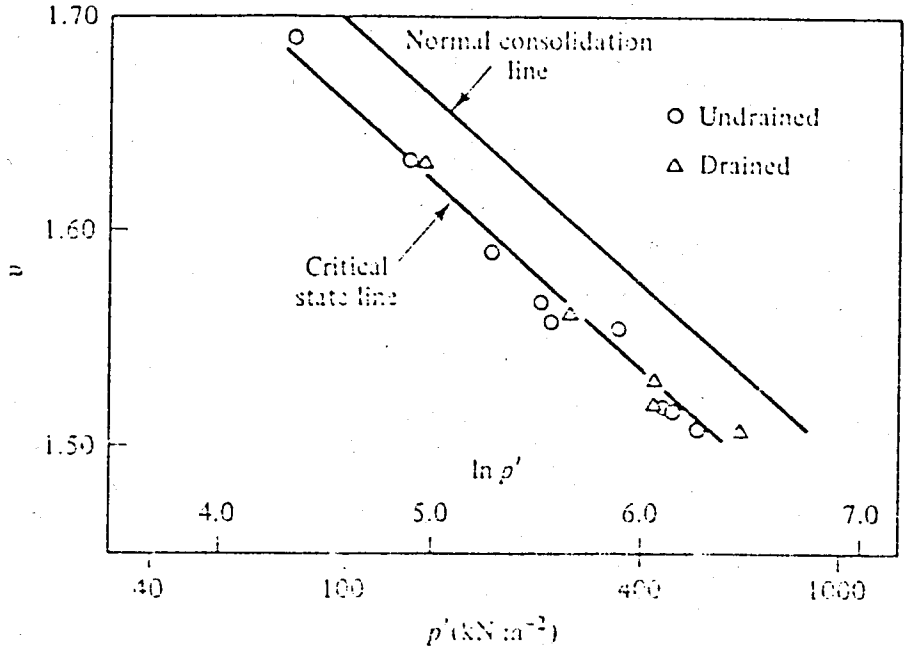

FIG.3.3 The Critical State Line in ν:lnp' space (Data from Parry,1960)

and for Normal Consolidation Line in the same plane

$$v = N - \lambda \ln p' \qquad \ldots(3.3)$$

where N and λ are the value of specific volume corrosponding to $p' = 1 kg/cm^2$ on the Normal Consolidation Line in the $v : \ln p'$ plane and the slope of the Critical State Line in the $v : \ln p'$ plane.

The position of the critical state of a sample is a function of q', p' and v; therefore it will be helpful to draw the Critical State Line in a three dimensional $q':p':v$ space, as sketched in Fig.3.4. The normal isotropic consolidation line is shown in the $q'=0$ plane, i.e., on the floor of the $q':p:v$ space The Critical State Line rises, i.e., q increases, as p' increases and v decreases. The projections of points ABC on the Critical State Line are shown as points A_1, B_1 and C_1 in the plane containing the q' and p' axes as points A_2, B_2 and C_2 on the $q' = 0$ plane.

The test paths followed in standard triaxial tests may also be represented in $q':p':v$ space. In view of undrained tests, a typical sample may be isotropically compressed to point A, as seen in Fig. 3.5, and then subjected to a standard undrained triaxial compression test until it fails at a point B on the Critical State Line. The test path can be projected into $q':p'$ space and is shown as path A_1B_1. The test is undrained, and so, by definition, the specific volume is constant. The specific volume at point B must, therefore, be the same as that at point A, and indeed v must remain constant for the whole test from A to B. The test path, therefore, remain in the shaded constant v plane ACDE. The point B represents

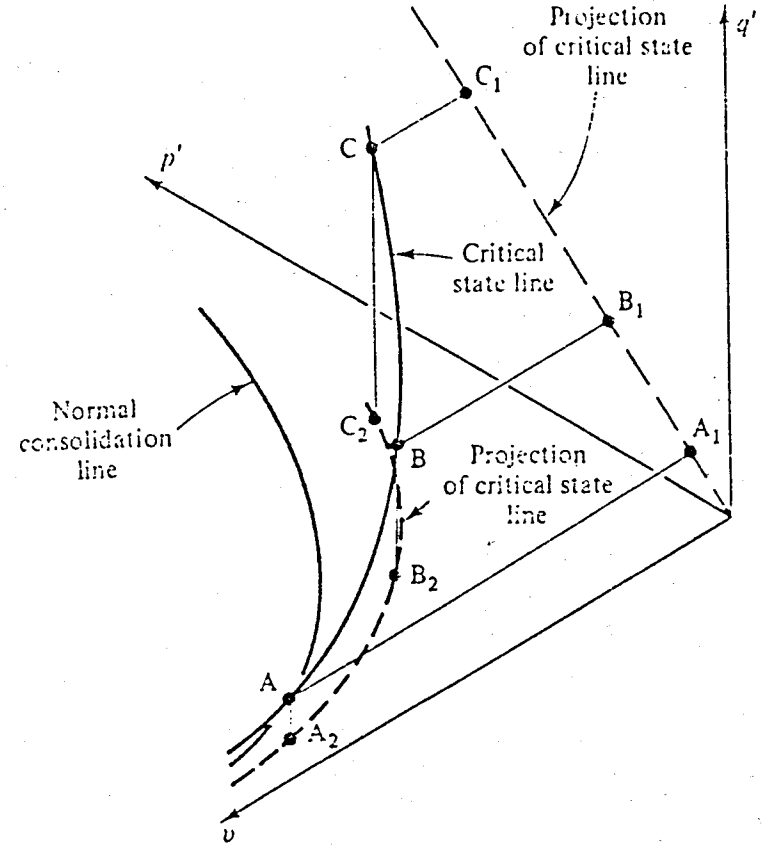

FIG.3.4 The Critical State Line in q':p':ν Space (After Roscoe, Schofield and Wroth, 1958)

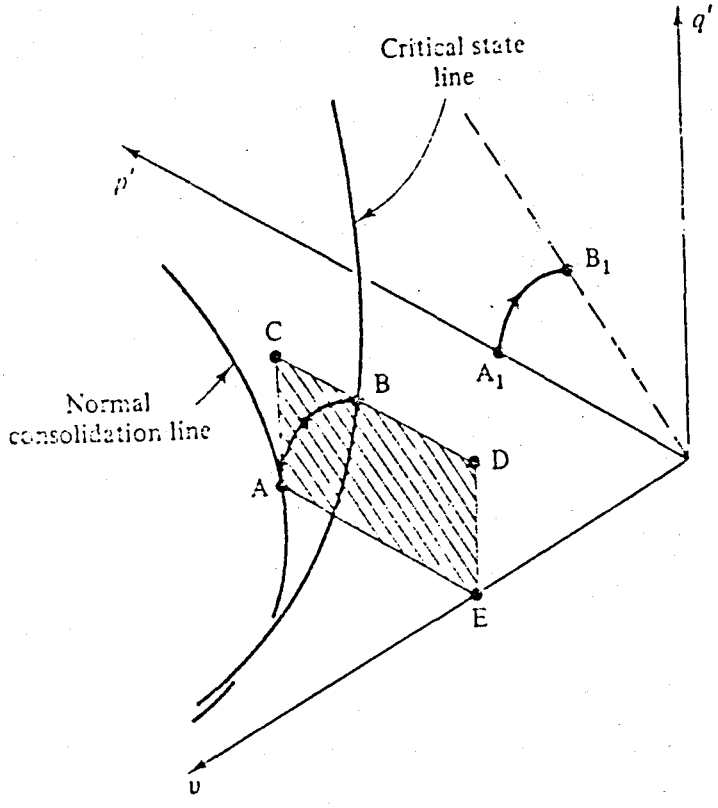

FIG.3.5 The Path Followed by an Undrained Test in q':p':ν Space
(After Schofield and Wroth, 1968)

the intersection of the undrained plane ACDE and the Critical State Line. The families of undrained planes are also illustrated in Fig. 3.6.

The test path for a standard drained triaxial compression test rises at a slope of 3 in q':p' space from the initial value p_0' of mean normal effective stress at q'=0. The sample may compress and so the specific volume changes. The plane in which drained tests lie is therefore parallel to the v axis and have a projection in q':p' space which is a straight line of slope 3; the drained plane ACB_1A_1 is shown shaded in Fig.3.7. The initial state of the sample on the Normal Consolidation Line is shown as point A and the test path ends at failure on the Critical State Line at B. The projection of the test path is shown as A_1B_1 on the q':p' plane. The exact shape of the test path within the drained plane ACB_1A_1 will depend on the experimental relationship between volume change and increase of q' as the test proceeds. However, the path AB remain within the plane ACB_1A_1. The families of drained planes are seen in Fig. 3.8.

3.1.3 Roscoe Surface

It has been established that for a particular value of p_0', the relevant undrained or drained plane over which the test path moves as the sample progresses to failure may be constructed. Of course, there will be different drained or undrained planes for each different value of p_0'. Considering undrained and drained planes, in each case, the relevant test path from the Normal Consolidation Line to the Critical State Line is shown in Fig.3.5 and in Fig.3.7.

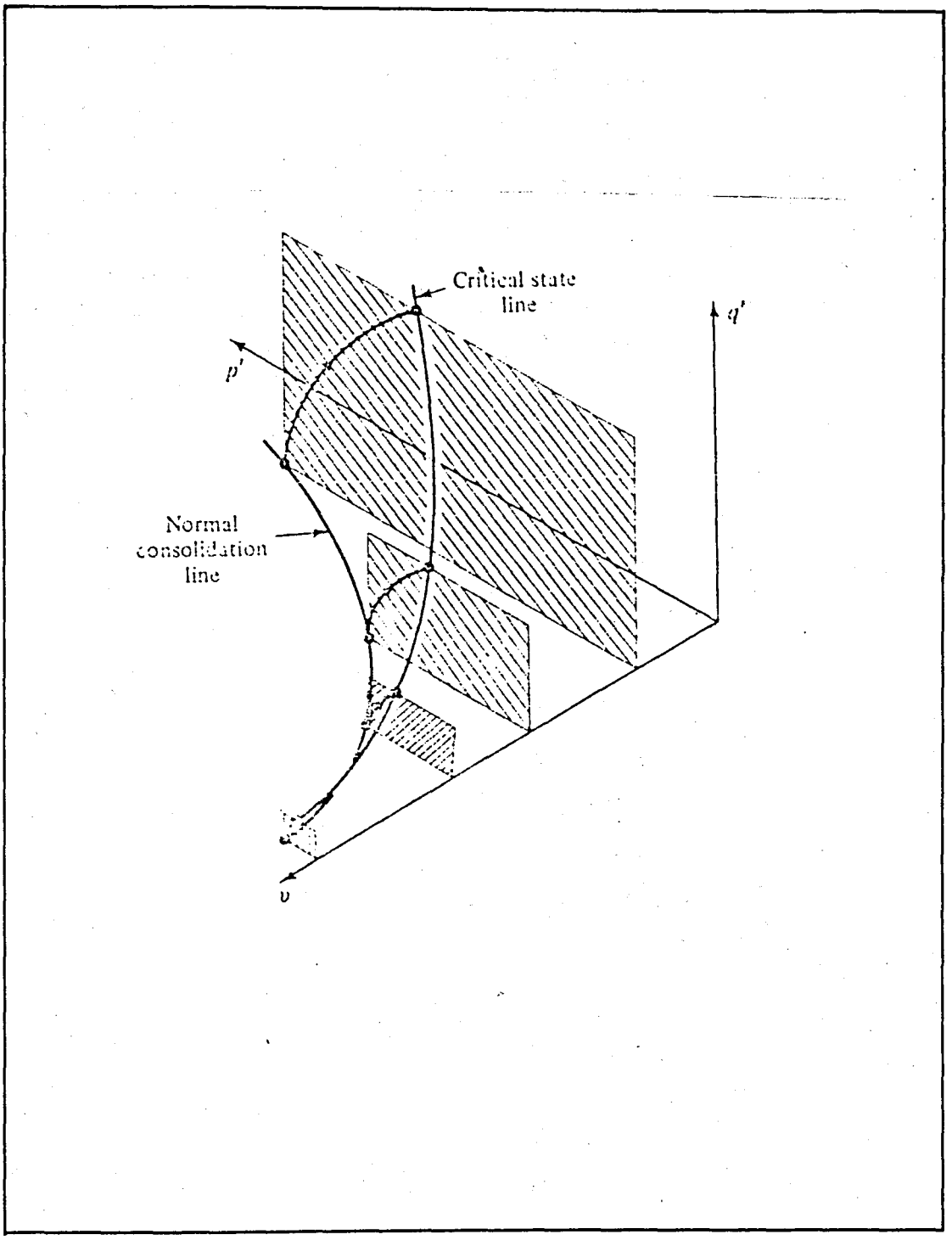

FIG.3.6 Four Undrained Planes in q':p': ν Space (After Atkinson and Bransby, 1978)

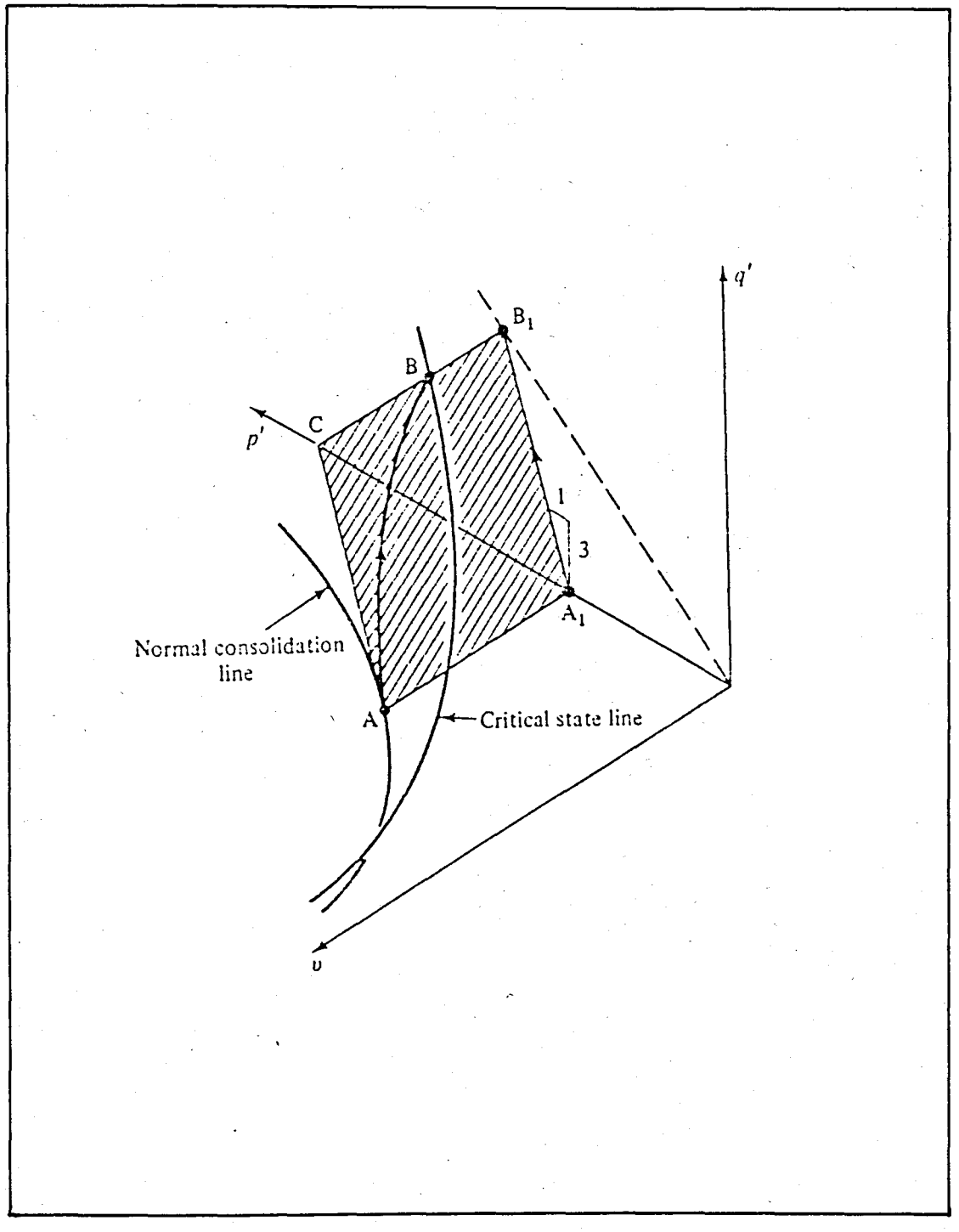

FIG.3.7 The Path Followed by a Drained Test in q':p':ν Space (After Roscoe, Schofield and Wroth, 1958)

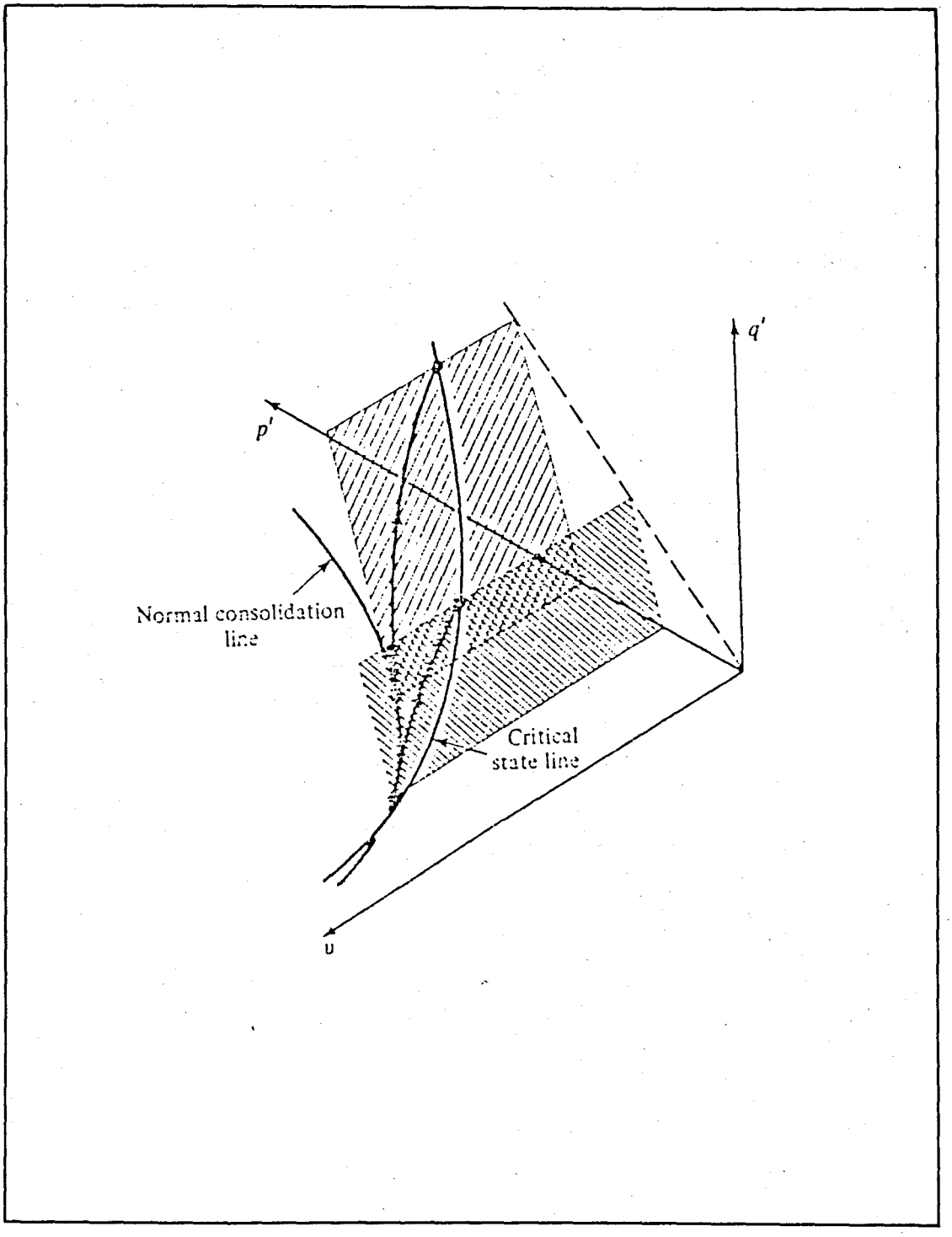

FIG. 3.8 Two Undrained Planes in q':p':ν Space (After Atkinson and Bransby, 1978)

Both the undrained tests and the drained tests seem to define a curved three dimensional surface linking the Normal Consolidation Line to the Critical State Line.

It is temting to ask if the families of undrained and drained on normally consolidated samples define the same three-dimensional surface in $q':p':\nu$ space. Clearly, it is reasonable that they should, for both drained and undrained tests start from the Normal Consolidation Line and finish at the Critical State Line. One way of checking whether the surface is unique is to investigate whether samples in the course of drained or undrained tests have the same specific volumes when they are subjected to the same effective stresses.

A more systematic procedure is to perform a series of drained tests on normally consolidated samples, and, from the specific volumes measured at different stages of the tests, construct a series of contours of constant ν in $q':p'$ space. To check whether there is a single surface in $q':p':\nu$ space for both drained and undrained tests will then be whether the two sets of contours (one from drained tests and one from undrained tests) are of the same shape and are consistent with one another, as shown in Fig. 3.9.

Hence, it can be concluded that the curved surface traced out in $q':p':\nu$ space by families of drained and undrained tests is identical for both families of tests. The same surface followed by all isotropically normally consolidated samples which are loaded by axial compression in the triaxial equipment is called the Roscoe surface.

The analogy between the Roscoe surface and normal consolidation line is the fact that the Normal Consolidation Line is the part of the

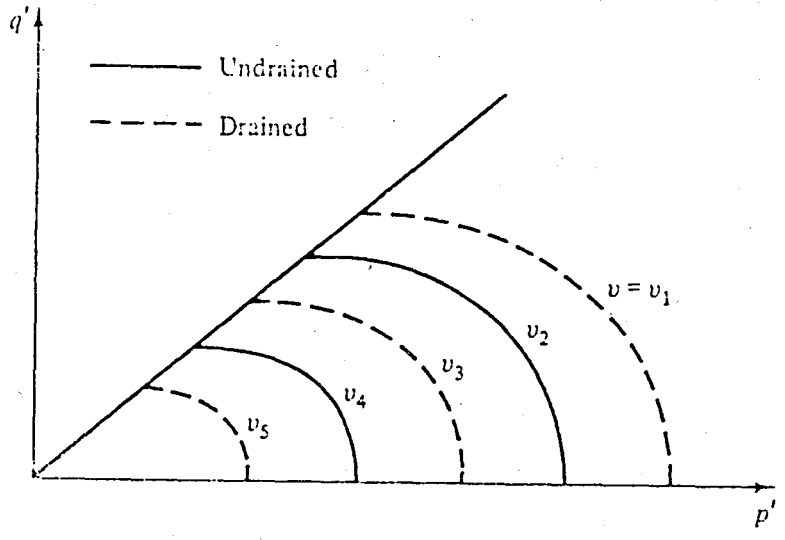

FIG.3.9 Contours of Constant ν from Drained and Undrained Tests (After Atkinson and Bransby, 1978)

Roscoe surface lying in the q'=0 plane. It may be thought of the Roscoe surface as a surface which separates states which samples can never achieve, as seen in Fig.3.10. The Roscoe surface is, therefore, a state boundary surface.

3.1.4 Hvorslev Surface

If the preconsolidation pressure p_c is larger than the in-situ overburden pressure, the soil has been subjected to a pressure at some time in the geologic past larger than the present pressure p_o, and this past pressure may have been due to:a greater amount of overburden which has been eroded away; drying and resulting shrinkage stresses; a change in the water table; a combination of drying and wetting in the presence of certain sodium, calcium, or magnesium salts particularly in uplifted marine deposits. In this case the soil is said to be overconsolidated, or preconsolidated (Bowles,1979).

The specimens which have been isotropically consolidated to some mean normal effective stress p and then allowed to swell isotropically to some lower mean normal stress p_o are considered to be overconsolidated samples, Fig.3.11. The overconsolidation ratio OCR is defined as P_{max}/P_o', and so normally consolidated samples have OCR=1.0 while OCR is large for heavily overconsolidated samples (Atkinson and Bransby, 1978).

In triaxial tests, when the deviator stress and effective mean normal stress is normalized with the initial effective mean normal stress P_{ei}', it is seen that data of both drained and undrained tests

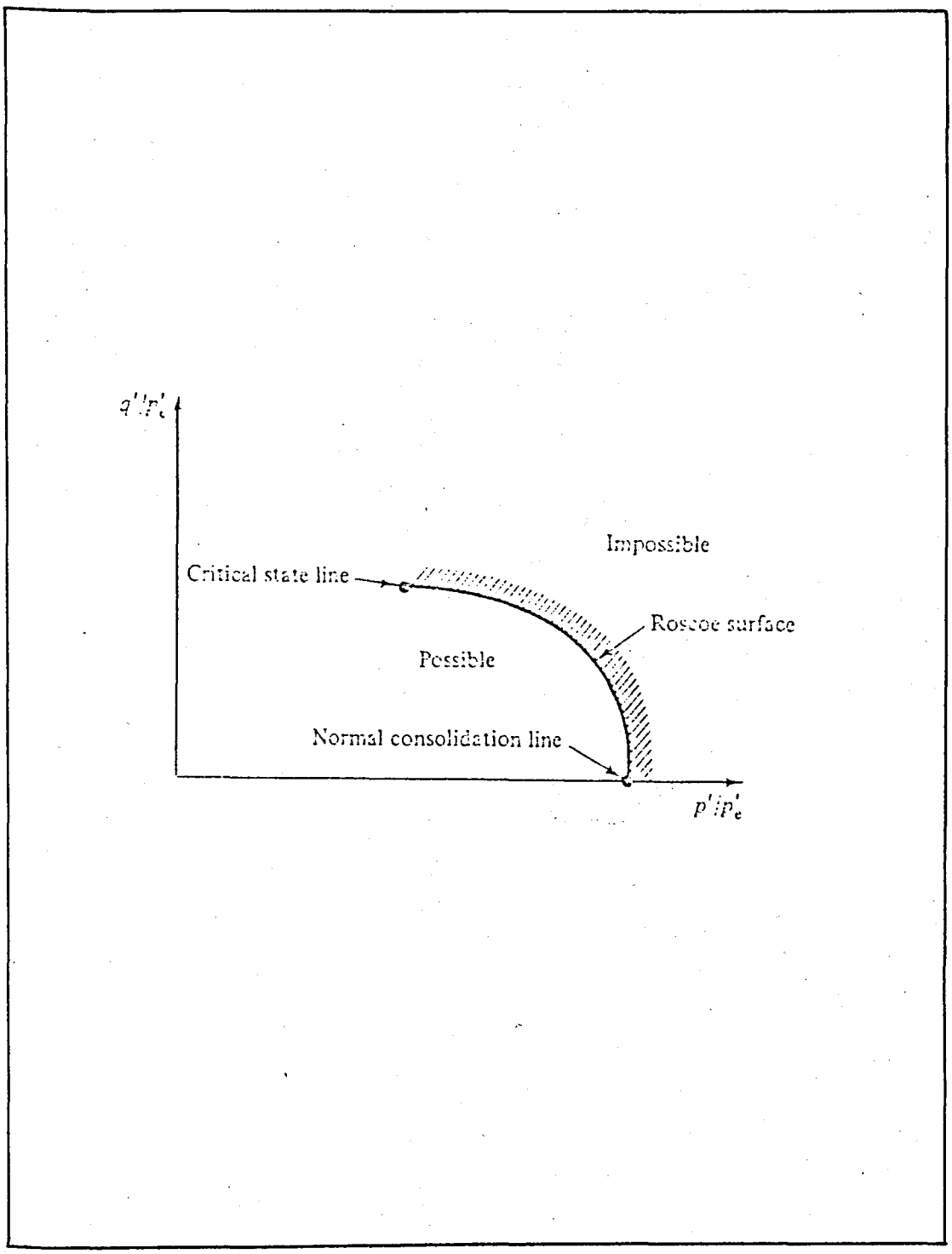

FIG.3.10 The Roscoe Surface as a State Boundary Surface (After Roscoe, Schofield and Wroth, 1958)

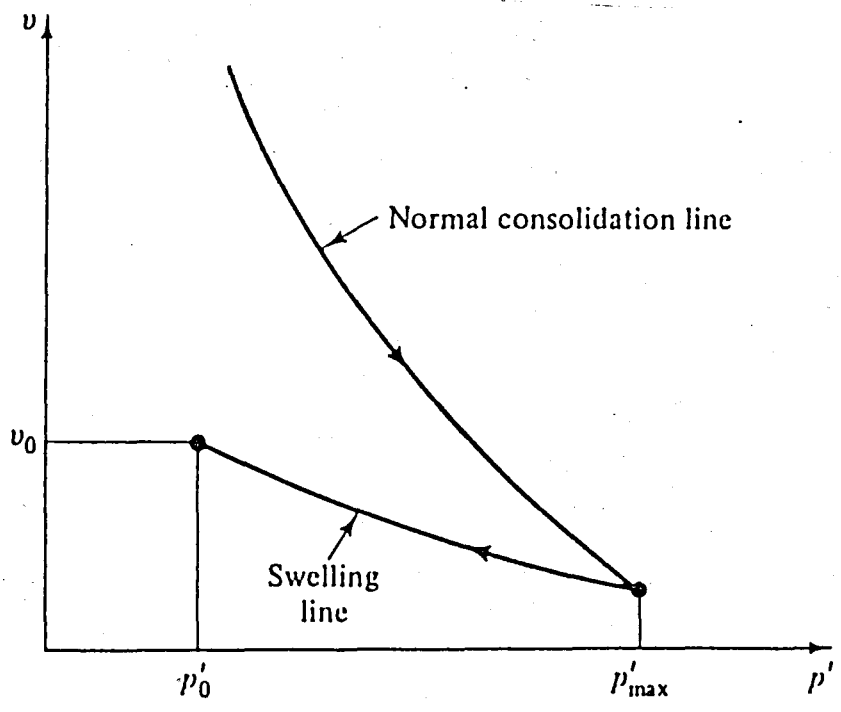

FIG.3.11. Compression and Swelling Lines

lie on a single line in q'/p'_{ei} : p'/p'_{ei} space, a seen in Fig. 3.12.

The significant feature of the surface with which Hvorslev was particularly concerned is that the shear strength of a specimen at failure is a function of both of the mean normal stress p', and of the specific volume ν of the specimen at failure. The specific volume appears in Fig. 3.13. through its influence on the equivalent stress p'_e, which depends directly on specific volume.

The equation of the Hvorslev surface is

$$q'/p'_{ei} = g + h\,(p'/p'_{ei}) \qquad \ldots(3.4)$$

in which g and h are soil constants as shown in Fig. 3.13.

The initial equivalent effective mean normal stress equation is

$$p'_{ei} = \exp\left|\,(N-\nu)/\lambda\,\right| \qquad \ldots(3.5)$$

Substituting Eq.(3.5) into (3.4), the following equation is obtained;

$$q' = g.\exp\left|\,(N-\nu)/\lambda\,\right| + h.p' \qquad \ldots(3.6)$$

The Hvorslev surface intersects the Critical State Line given by Eqs (3.1) and (3.2), substituting those equations into Eq.(3.6); it becomes

$$(M-h)p' = g.\exp\left|(N-\Gamma)/\lambda + \ln p'\right| \qquad \ldots(3.7)$$

$$g = (M-h) \exp | (\Gamma-N)/\lambda | \qquad \ldots (3.8)$$

Thus the equation of the Hvorslev surface is

$$q' = (M-h) \exp | (\Gamma-N)/\lambda | + h.p' \qquad \ldots (3.9)$$

The locus of failure points can be idealized as line AB, Fig. 3.13, and it is called as the Hvorslev surface. The equation (3.9) states that the deviator stress at failure of an overconsolidated specimen is made up of two components. The first component (h.p') is proportional to mean normal effective stress, and so may be thought of as being frictional by nature, while the second component ($|M-h| \exp |(\Gamma-\nu)/\lambda|$ depends only on the current specific volume, and the value of certain soil constant. The form of exponential term is such that the second component of strength increases as the specific volume of the specimen decreases.

Obviously, if the soil could sustain tensile effective stresses, the line corresponding to tensile failure would lie to the left of OA. The maximum value of q'/p' will be when axial stress σ_1' is large and confining pressure σ_3' is small. The highest value of q'/p' that could be observed would correspond to $\sigma_3'=0$. Therefore, for a triaxial compression test, it is clear that

$$q' = \sigma_1' \qquad \ldots (3.10)$$

$$p' = 1/3 \cdot \sigma_1' \qquad \ldots (3.11)$$

$$q'/p' = 3 \qquad \ldots (3.12)$$

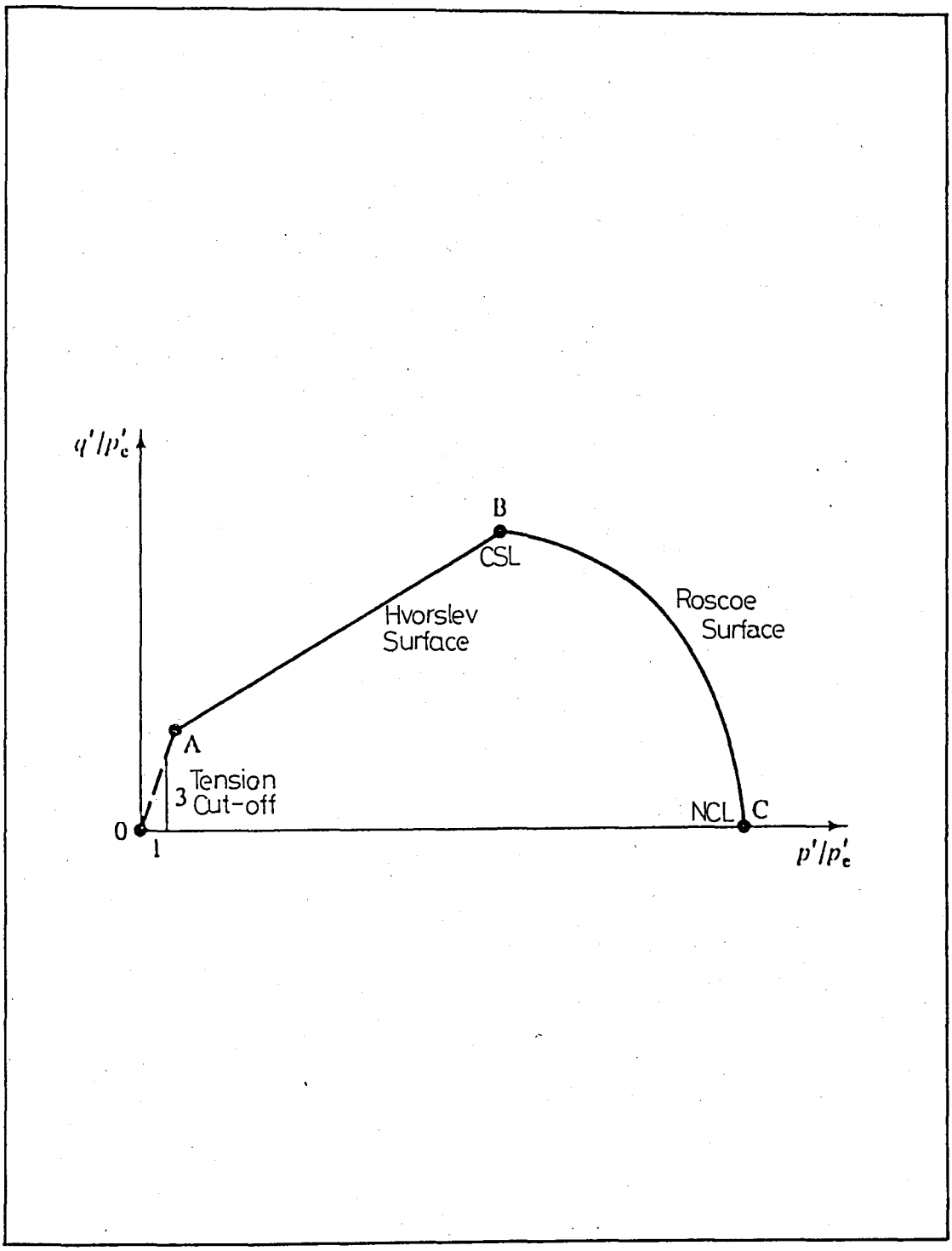

FIG.3.13 The Complete State Boundary Surface in q'/p'_{ei} : p'/p'_{ei} Space (After Atkinson and Bransby, 1978)

The locus is limited on its left-hand side by the line OA which has slope 3, corresponding to tensile failure, and on its right-hand side by the Critical State Line (B), and the Roscoe surface (BC).

3.2 SUMMARY

In this chapter, the critical state concept and the Critical State Line is explained. The complete state boundary surface,which consists of the Roscoe and Hvorslev surfaces, is mentioned. The following conclusions are deduced.

There exists a Critical State line in q':p':ν space in which all test paths from triaxial compression tests on isotropically normally consolidated samples terminate.

The test paths for both drained and undrained tests follow the same curved surface (the Roscoe surface) which links the Normal Consolidation Line with the Critical State Line in q':p':ν space.

The geometry of the Roscoe surface is such that all constant ν sections of the surface have the same shape but are different size. The sections may be scaled to a single normalized curve if the stresses are divided by the equivalent pressure, p_{ei}.

The Roscoe surface is a state boundary surface.

A state boundary surface, the Hvorslev surface, limits the states of overconsolidated specimens in q':p':ν space.

The complete state boundary surface, consisting of the Hvorsley surface, which meet at the Critical State Line, serves for drained and undrained tests on normally consolidated and overconsolidated samples, and, hence, unifies a wide range of behaviour.

IV. TESTING METHOD

4.1 INTRODUCTION

In this chapter, the details of the testing equipment, the material and preparation of samples in the experimental analysis are explained. Isotroprically consolidated-undrained tests are performed on the lime-stabilized Uskumru Clay by using the common MGI type triaxial compression apparatus. The purpose of the triaxial testing equipment is to confine the sample under all-round pressure and to provide a suitable way of applying the axial load to the sample with controlled strain. Pore-pressure is also measured due to consolidated-undrained type of triaxial tests.

4.2 TEST EQUIPMENT

4.2.1 Details of the Triaxial Cell

The form of the triaxial test used in this research is the cylindrical compression test; and the usual triaxial cell is utilized. The cell shown in Fig. 4.1. consists of three principal components- the base, which forms the pedestal on which the sample rests and incorporates the various pressure connections; the removable

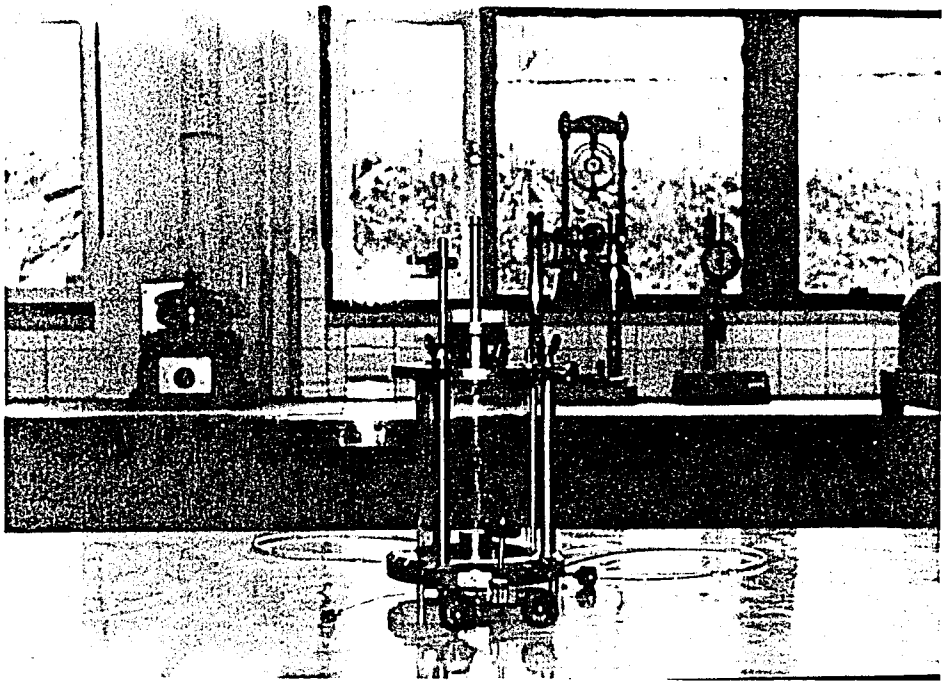

FIGURE 4.1 Triaxial Cell

cylinder and top cap, which enclose the sample and enable fluid pressure to be applied; and the loading ram, which applies the deviator stress to the sample.

The first connection at the base is to fill the cell with the fluid, usually water, in order to apply the all-round pressure. This connection also serves to empty the cell at the end of the test.

The second connection with the base of the sample provides drainage in a drained test, and for pore-pressure measurement in undrained or consolidated-undrained tests. Since the test type in this research is consolidated - undrained, the second connection is used for measuring pore-pressure.

The transparent perspex cylinder is used, which facilitates the setting up of the test and enables the mode of failure to be observed. The cylinder is permanently fitted between O-rings as seals; the only joint to be made during testing is between the lower brass collar and O-ring set in the base of the cell. For this the hand tightening of three wing nuts is sufficient.

The top cap, to which to cylinder is fixed, is a bronze casting and the central boss forms the bush through which the stainless-steel ram slides. An air release valve is fitted, and a short pillar to carry the arm for the axial strain indicator is screwed.

Porous filter stones prevent the fine soil particles from being washed out of the test specimen. The filter stones are boiled in water before each test to remove any soil particles imbedded in the pores.

The filter paper is wrapped around the testing specimen. The filter paper is slotted to minimize the restriction of the sample deformations. The purpose of the filter paper is to accelerate the consolidation of the sample during the test. Before wrapping, the filter paper is saturated to prevent absorption of moisture from the sample. The dimensions of the filter paper is seen in Fig. 4.2.

The sample is enclosed in a thin rubber membrane 12-15 cm in length. The membrane should apply the minimum restraint to the sample consistent with providing a reliable barrier to leakage. The rubber membrane is sealed against the smooth surface of the loading cap and of the pedestal by rubber O-rings under tension, sprung into place from the end of a metal tube. Since no water movement can take place through the membrane, the absorption or expulsion of water within the sample can only occur through the sample drainage-system. The diffusion through the rubber membrane is ordinarily negligible. The membrane should be as thin as possible in order to minimize pressure exerted on the sample as it expands.

4.2.2 Details of the Loading System

The loading system in this study is chosen to apply deviator stress with constant strain during the test.

For routine and for the more common research tests, the use of controlled rate of strain has many advantages and is generally accepted. The rate of strain at failure is accurately known and the influence of heological factors on the observed strength can therefore be taken into account. The shape of the stress-strain

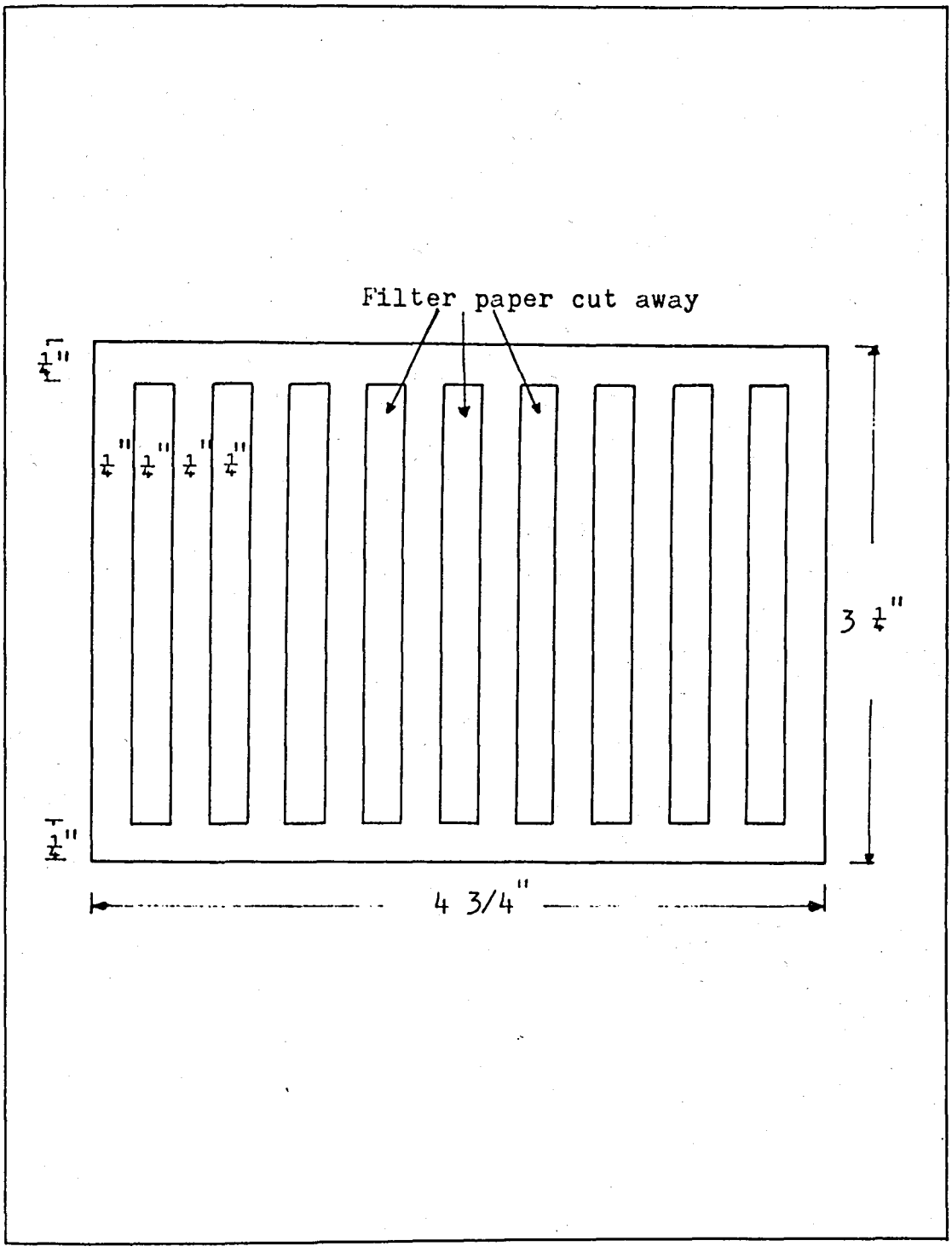

FIGURE 4.2 Side-Drain Papers

curve beyond the point of maximum stress can also be obsverved. The duration of the test can be predicted with reasonable accuracy, which, from the practical point of view, is important in planning the testing program. The rate of strain is adjusted by changing the gears in the loading apparatus. The gears listed in the Table 4.1 as A,C and E are always driving gears; the gears B,D and E are always driven gears. The rate of strain is chosen to be 0.0303 mm/min in the test.

An axial compressive force is applied to the ends of the test specimen by a constant rate of strain type loading press. The rate of strain can be varied depending on the type of material and the nature of the test. The axial force and vertical deformation are readable at all points throughout the operating range of the equipment.

The load is measured by a high-tensile steel proving ring placed between the top of the ram in the triaxial cell and the head of testing machine. The high tensile steel proving ring is equipped with a mechanical dial gauge for measuring the deformation of the ring. This dial gauge is normally graduated in divisions of 0.002 mm. The accuracy of the proving ring is ± 1 per cent of the measured force.

Axial strain is measured by 1.5 cm traved dial gauge calibrated in 1/100 cm in divisions. This is fixed to an arm clamped to the lower mounting of the proving ring. It is shown in Fig. 4.3.

Table 4.1. Gears Used for Adjusting the Loading Speed

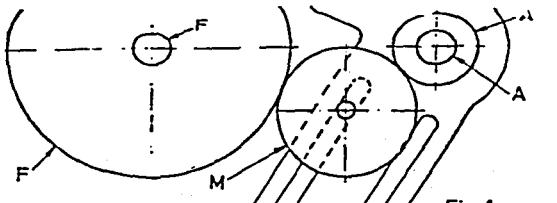

Fig. 1

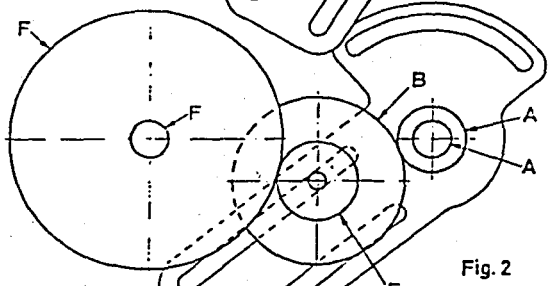

Fig. 2

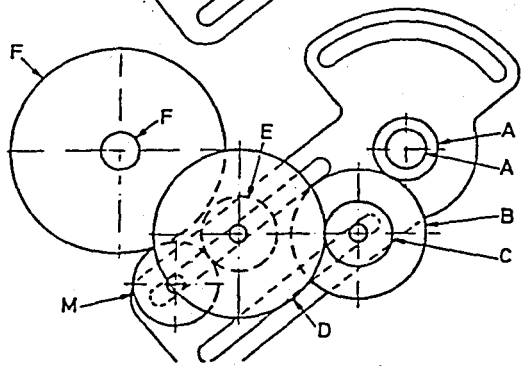

Day	Hour	Min.	Sec.	Fig.	M	A	B	C	D	E	F	$U=\frac{A\cdot C\cdot E}{B\cdot D\cdot F}$
		7	25	2		96	40			60	30	4,8
		11	50	2		96	50			63	40	3,024
		14	59	1	72	96					40	2,4
		22	42	1	40	96					60	1,6
		30	35	1	71	72					60	1,2
		44	50	1	71	60					72	0,8333
		55	26	2		82	50			40	96	0,6833
	1	16	28	1	82	24					47	0,511
	1	28	44	1	82	28					63	0,4449
	2	18	35	1	50	29					96	0,302
	4	39	15	2		24	72			50	96	0,1736
	5	36	22	2		28	63			33	96	0,15277
	9	16	23	2		24	63			28	96	0,1111
	23	43	5	3	32	24	46	24	60	25	72	0,07246
1	3	24	26	3	32	24	46	24	63	25	72	0,0690131
2	19	23	43	3	32	24	50	24	71	25	72	0,056338
3	16	5	43	3	32	24	46	24	60	25	96	0,054348
4	13	8	40	3	32	24	46	24	72	25	82	0,053022
4	16	7	16	3	32	24	60	24	72	25	63	0,05291
10	6	40	00	3	32	24	50	24	60	25	95	0,0500
11	22	49	18	3	32	24	47	24	72	28	96	0,0496454
14	16	22	52	3	32	25	50	24	71	28	96	0,04929577
21	1	27	52	3	32	24	50	24	72	25	82	0,04878049
513	21	20	00	3	32	24	63	24	72	72	72	0,047619

NB.

This table is based on the motor's speed without load. The speed will decrease with increasing load to a maximum of 7% at full load.

I/s Mossco Oslo. pat nr 78431

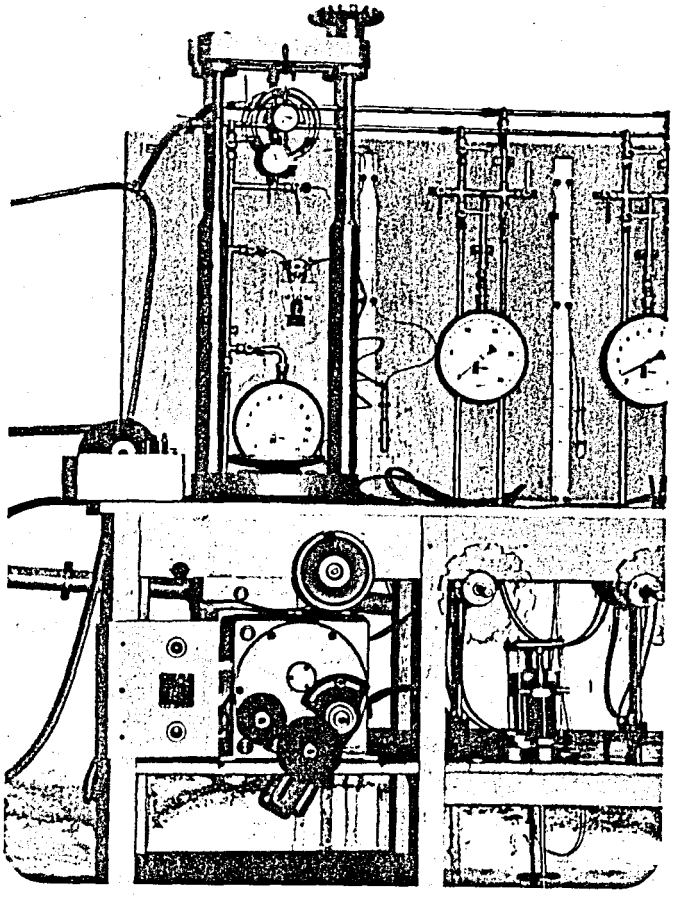

FIGURE 4.3 Loading Press and Gears

4.2.3 Details of Apparatus for Measuring Pore-Pressure

The equipment used to measure pore-pressure consists of a pore pressure instrument, a screw control, Bourdon gauge and mercury manomoter. These different units are connected with a copper pipe, with the exception of the connection between the pore-pressure instrument, the tube system and the sample, which is made up of 1/8" copper tubing and a short length of saran tubing.

In addition to being connected with the sample, the pore pressure assembly has a connection to tap water. The tap water connection is used when refilling the screw control or calibrating the manometer or pressure gauge.

The pore-pressure apparatus is in principle a "V" tube filled with mercury. One branch of the "V" is connected to the sample, the other end is coupled to the screw control, pressure gauge and manometre. By observing the mercury level in the branches of the "V" tube it is possible to detect a movement of the pore-water. By increasing or decreasing the back pressure on the mercury column with the screw control, the mercury level can be maintened at a constant elevation, thereby preventing any pore-water movement. The pressure required to hold the mercury column in position is, therefore, the pore pressure within the sample.

The diameter of the mercury column, in the branches of the "V", determines the accuracy to which the volume can be held constant; the smaller the diameter, the higher the degree of accuracy. However, for practical purposes in making the instrument, the diameter is limited to 1.3 mm.

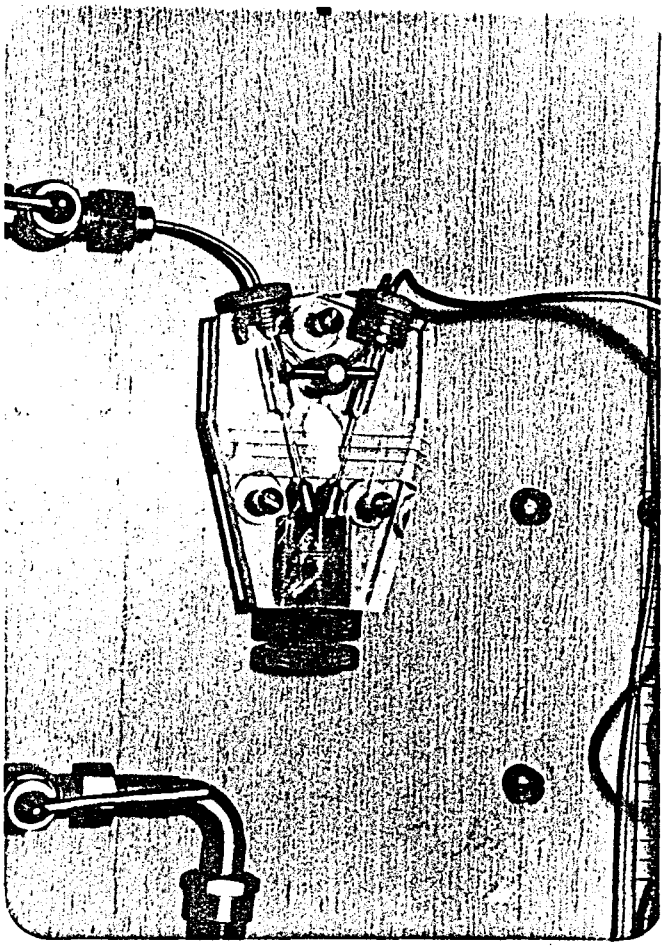

FIGURE 4.4 Pore-Pressure Measurement Apparatus

At the top of each small column is a section with a much larger diameter. The purpose of the larger diameter section is to act as small reservior to catch the mercury and to prevent it from flowing into the system in the event it should be accidentally blown out of the "V" tube. Since mercury will corrode brass and copper quickly, it should be kept out of the system.

If a wrong connection is made, blowing out of the mercury can be prevented by a "short circuit" in the "V" tube before the test storts. The short circuit can be done by a shut-off valve supplied with O-ring seals. The plastic body of the instrument serves as its housing. When the shut-off value is opened, Fig. 4.4, the column of the "V" tube are subjected to the same pressure; this is a convenient means of adjusting both mercury columns to the same elevation. A horizontal line across the two columns serves as a reference point for observing movement of the mercury during a test. While setting up a test, the tops of the mercury columns can be adjusted to these reference lines by turning the screw, at the bottom of the instrument, which will raise or lower both columns equally.

4.3 MATERIAL USED

The material used in thes research program is the Uskumru Clay. The index properties determined by the routine laboratory experiments are as follows

$w_{LL} = 0.85$

$w_{pL} = 0.30$

$w_{opt} = 0.31$

$G_s = 2.73$

To begin with, the material is mixed with sufficient water to prepare the triaxial test specimens having no lime. The water content chosen for the test specimens is nearly twice the optimum water content, w_{opt}.

Lime percentages are chosen as 5, 10 and 20 per cent respectively. For lime added clay specimens 5, 10 and 20 per cent lime is added to clay by the weight of total solid particles, i.e., 60 g lime is added to 540 g clay in order to obtain 10 per cent soil-lime mixture. To prepare such samples the lime and clay is first throughly mixed with sufficient water. After this, the clay-lime-water suspension is left for curing for a day for the purpose of dispersing water through clay particles.

Then, the mixture is placed to the triaxial specimen molds, with great care, having the diameter in the order of 3.6 cm and the height 10 cm. The samples are compacted in three layers with 25 stroke of wood hammer giving rise to the imbedded air in the pores to escape. After taking the samples out of the triaxial specimen molds, the edges of the specimen are cut by means of a wire saw in a craddle; its length determines the height of sample and its trimming edges assure that both ends of the sample are parallel. The diameter of the specimen is measured. Later, the samples are placed to the triaxial cell for the purpose of applying all-round confining pressures. The equipments used in the preparation of samples are seen in Fig. 4.5.

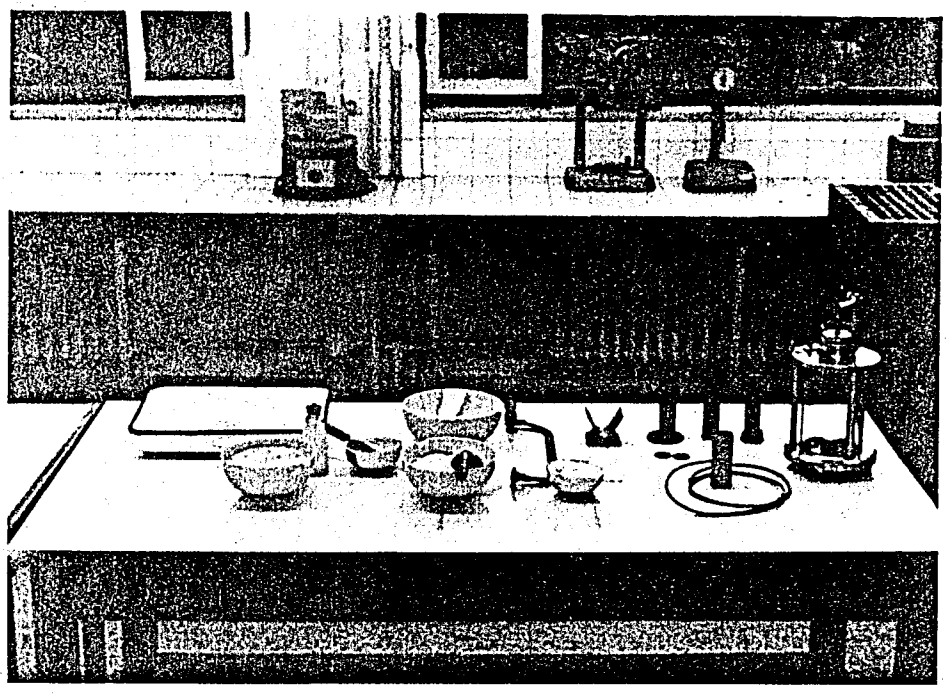

FIGURE 4.5 Sample Preparation Equipments

4.4 TESTING PROCEDURE

4.4.1 Placing The Specimen

The filter stone, which has previously been boiled in water, is placed directly on the pedestal of the base plate of the triaxial cell. Then the filter paper, having the diameter of 3.6 cm, is placed on the filter stone after saturating the filter paper. After this, the sample is placed directly from the cradle on to the filter paper. Basides handling the sample carefully, it is also important to prevent the formation of air bubbles on the end surfaces of the specimen. Later, the filter paper, the filter stone and the loading cap is placed on the sample, and the side-drain filter paper is wrapped neatly around the sample. The rubber membrane is placed on the mounting cylinder; after applying a slight suction to hold the membrane tihgt against the walls of the cylinder, the mounting cylinder, is placed over the sample and lowered, as seen in Fig. 4.6. By blowing the rubber tubing which will force the upper end of the membrane to slide over the loading cap. The fingers are used to push the bottom end of the membrane down over the pedestal. The mounting cylinder is removed and the membrane is smoothed out. Two O-ring are streched over the sample and rolled the lower O-ring to the end of the pedestal. The second O-ring is placed on the loading cap which rests on the test specimen. The transparent perspex cylinder is placed; when lowering the cell, the piston is held up so that it does not hit the sample. Three wing bolts are tightened in such a manner that the top and bottom plates are parallel. Then the piston is allowed to fall into the socket of

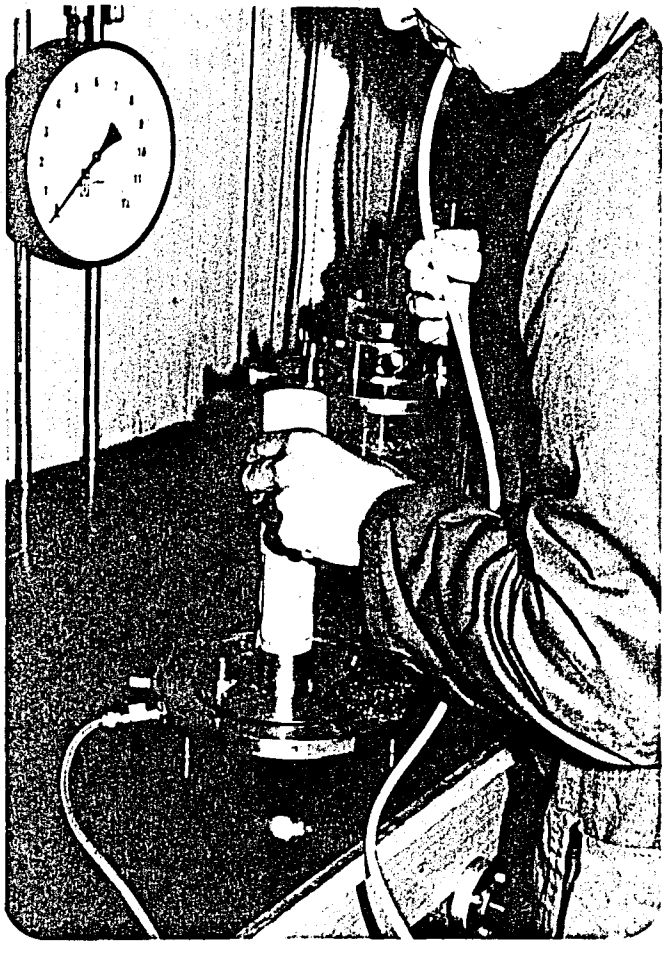

FIGURE 4.6 Placing the Specimen

the loading cap. The cell is filled with water after opening the valve to allow the entrapped air to escape.

4.4.2 Consolidation Process

The triaxial cell pressure is increased to the consolidation pressure. The consolidation pressure is the all-round fluid pressure acting on the test specimen during the experiment. And regularly the dissipated water from the sample is recorded through the use of a burette. When the water level in the burette is approximately constant, the consolidation process is terminated. The consolidation process in the triaxial compression apparatus is seen in Fig. 4.7. Consolidation pressures are chosen to be 2,0,2.5,3,0,3.5,4.0 and 5.0 kg/cm^2 respectively.

In twenty-four triaxial test samples, the drainage valve is not opened for a week; and later the valve is opened and dissipating water during consolidation is measured by means of the burette.

The three triaxial test specimens having 5,10 and 20 per cent lime are subjected exclusively to 3.0 kg/cm^2. The filter paper is not wrapped around the samples to give rise to the consolidation process to slow. The main purpose of this action is to observe the effect of no-drainage process for a week when consolidation pressure is in operation and then letting the drainage, and drainage process during whole consolidation process on the behaviour of artifically lime added soil-lime mixtures.

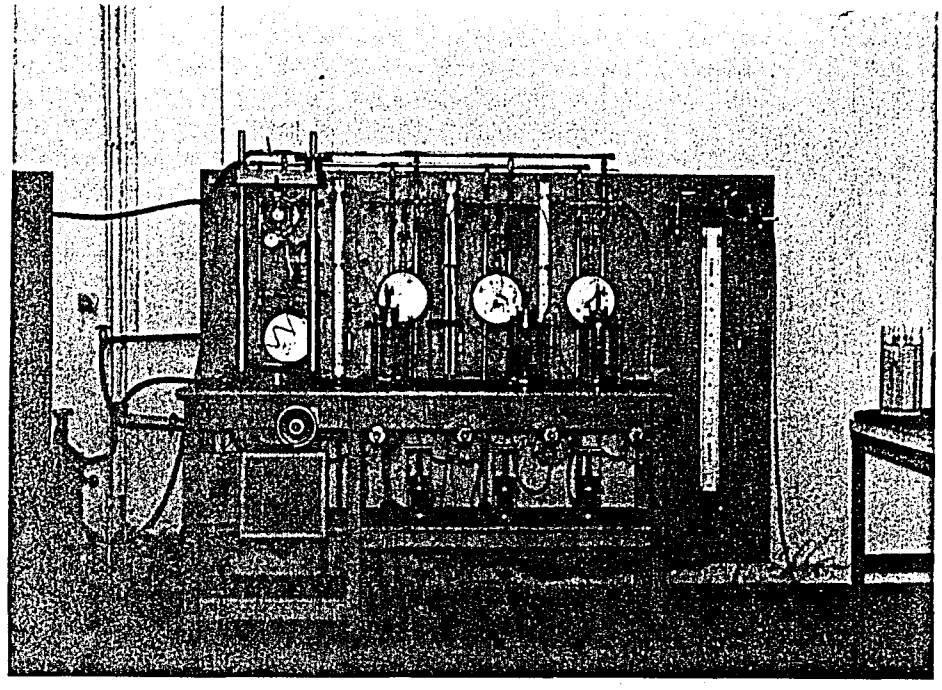

FIGURE 4.7 Consolidation Process in the Triaxial Apparatus

4.4.3 Placing the Triaxial Cell to the Loading Press

The loading table is lowered by hand and the cell placed on the table of the apparatus. The proving ring is connected to the yoke with rubber rings. The yoke is lowered until the lower end of the ring is almost in contact with the arm holding the piston, then the arm is removed and allowed the piston to slide upwards until it comes in contact with the prowing ring. The loading table is raised by using hand-wheel until the dial-gauge of the proving ring indicates that the piston is in contact with the sample. Before test is started, the dial gauge of the proving ring and another dial gauge to measure the axial deformation of the test specimen is adjusted to zero.

4.4.4 Loading and Removing the Sample

An axial compressive force is applied to the ends of the test specimen by a constant rate of strain type loading press, Fig. 4.8, the loading table is moved up with a constant rate by means of a gear drive unit. The rate of strain is 0.0303 mm/min. When axial force is applied, the pore-pressure readings are taken from the Bourdon gauge.

When the sample reaches failure condition, the pore-pressure valve is closed. The pressure in the triaxial cell,which is confining pressure, is decreased to zero. Water in the cell is emptied by opening cell pressure line. Upper part of the triaxial cell is removed. The O-rings at each end of the rubber membrane are taken out; then the membrane is taken out with care. The sample is removed from the loading pedestal. Removing of sample is seen in Fig. 4.9.

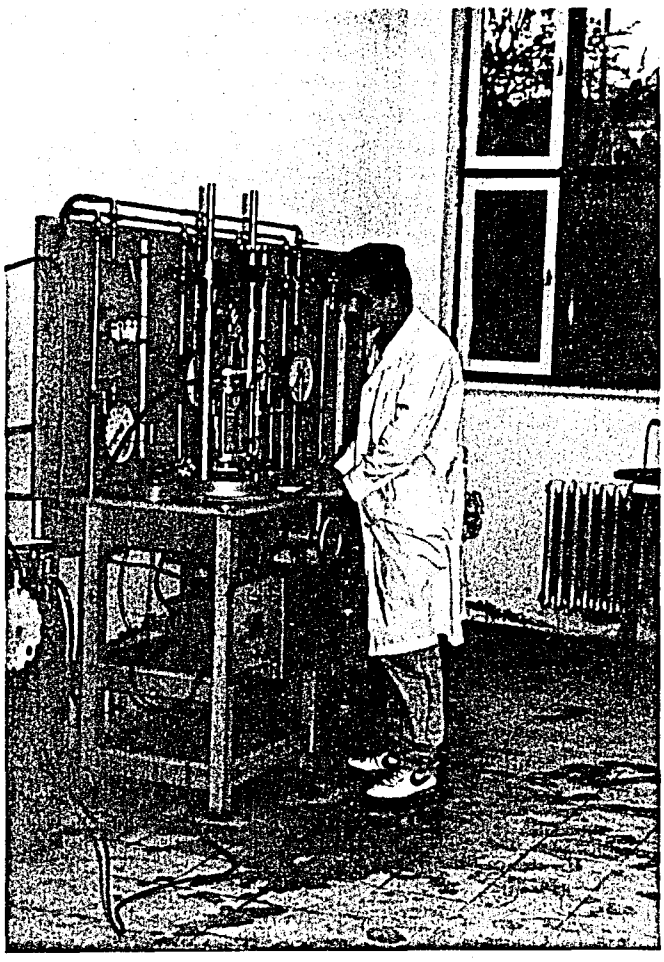

FIGURE 4.8 Loading the Specimen

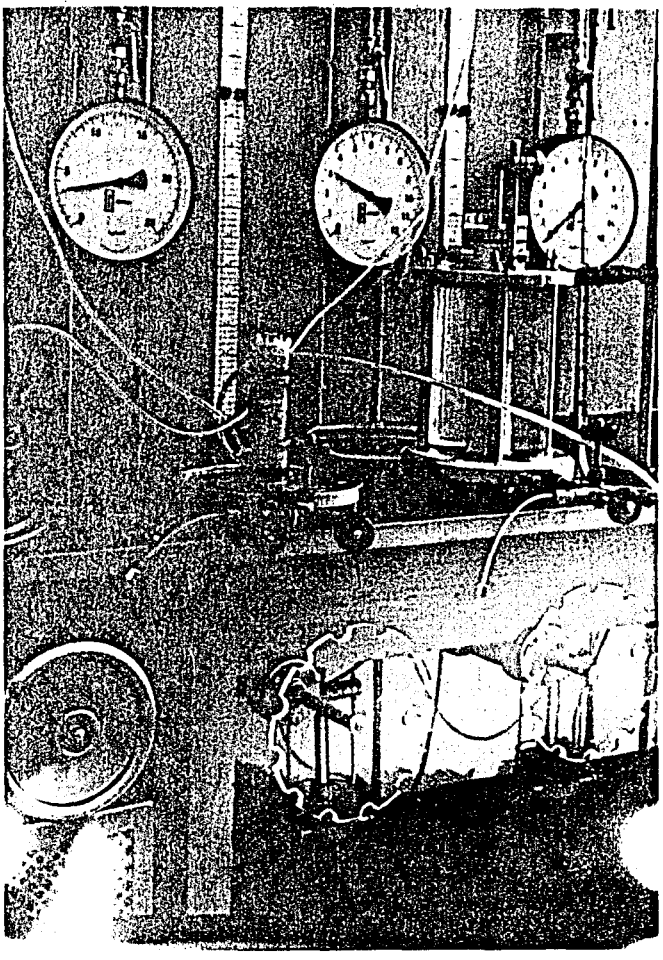

FIGURE 4.9 Removing the Specimen

4.5 SUMMARY

The details of the testing equipment, the material and sample preparation are presented in this chapter.

NGI type triaxial compression testing apparatus is used for conducting isotropically consolidated-undrained tests.

It is also possible to conduct consolidated-drained, unconsolidated-drained, and unconsolidated-undrained tests by using the same equipment.

The transparent perspex cylinder cell is used for observing the mode of failure.

Porous stone is placed to the bottom of the sample and the filter paper is wrapped around the test specimen to accelarate the consolidation process.

The loading system is chosen to apply deviator stress with constant strain during the test. The use of controlled strain has many advantages. The rate of strain at failure is accurately known and the influence of factors on the observed strength can be taken into consideration. The stress-strain curve shape can be observed beyond the point of failure stress. The rate of strain is chosen to be 0.0303 mm/min.

The load is measured by a steel proving ring dial gauge graduated in divisions of 0.002 mm.

Axial strain is measured by 1.5 cm traved dial gauge calibrated

in 1/100 cm in divisions.

The pore-pressure apparatus is in principle a "V" tube filled with mercury. It is possible to detect a movement of the pore-water by observing the mercury level in the branches of the "V" tube. The mercury level is maintened at a constant elevation; the pore-pressure required to hold the mercury column in horizontal position is the pore-pressure within the sample.

The soil-lime mixture triaxial test samples are prepared and different cell pressures are applied to them. The samples are sheared in the loading press and they are removed from the triaxial cell at the end of the test.

V. EVALUATION OF TEST RESULTS

5.1 INTRODUCTION

Experimental results obtained from the consolidated-undrained triaxial compression tests are presented, and the effect of lime content increase in soil-lime mixtures on deviator stress and pore-pressure is explained in this chapter. Deviator stress and effective mean normal stress relationship is mentioned. Pore-pressure and pore-pressure parameter vs. effective mean normal stress relationship, and pore-pressure vs. axial strain relationship is discussed. The effect of lime content on the Normal Consolidation and Critical State Lines is also mentioned.

5.1 Data Processing

Deviator stress is calculated by dividing the axial load increment, which is measured by means of a loading proving ring, to the average cross-sectional area of the specimen. The average

cross-sectional area is (Bishop and Henkel, 1962);

$$A' = A_o * (1-\varepsilon_v)/(1-\varepsilon_\alpha) \qquad ...(5.1)$$

in which A_o, ε_v and ε_α are initial cross-sectional area, volumetric strain and axial strain, respectively.

Since the change in volume is zero due to the type of consolidated - undrained tests, the average cross-sectional area depends only on axial strain. Therefore, the equation (5.1) becomes

$$A' = A_o * 1/(1-\varepsilon_\alpha) \qquad ...(5.2)$$

The axial load and vertical deformation are readable at all points throughout the operating range of equipment through the use of a proving ring and a dial gauge.

Pore pressure is measured by means of a Bourdon-gauge during the test procedure.

The deviator stress is calculated as

$$q = \sigma_1 - \sigma_3 = F/A' \qquad ...(5.3)$$

where F is the axial load and σ_1 is the axial stress. Hence, axial stress is

$$\sigma_1 = \sigma_3 + F/A' \qquad ...(5.4)$$

Total mean normal stress is

$$p = (\sigma_1+\sigma_2+\sigma_3)/3 \qquad ...(5.5)$$

Since $\sigma_2=\sigma_3$= cell pressure in the triaxial apparatus, total mean normal stress equation (5.5) becomes

$$p = (\sigma_1+2\sigma_3)/3 \qquad ...(5.6)$$

Substituting the equation (5.4) into the equation (5.6), the following one is obtained

$$p = \sigma_3+1/3\ (F/A') \qquad ...(5.7)$$

The effective mean normal stress is

$$p' = p-U \qquad ...(5.8)$$

in which U is the pore-pressure.

The effective deviator stress is equal to the total deviator stress;

$$q' = q \qquad ...(5.9)$$

Pore-pressure parameter A_p is calculated, assuming B=1.0 for saturated soils, by dividing pore-pressure to the deviator

stress (Skempton, 1954; Bishop, 1954; Skempton, 1960; Noorany and Seed, 1965);

$$A_p = U/q \qquad ...(5.10)$$

After those calculations, and usual corrections applied to every type of triaxial test, the following curves are plotted; $q:\varepsilon_\alpha$, $U:\varepsilon_\alpha$, $q':p'$, $q/p:\varepsilon_\alpha$, $q'/p':\varepsilon_\alpha$, $A_p:\varepsilon_\alpha$ $A_p:p'$, $q/P_{ei}:\varepsilon_\alpha$, $U/P_{ei}:\varepsilon_\alpha$ and $\nu:\ell np'$. The results of test data are presented in Appendix A.

5.1.2 Experimental Results

5.1.2.1 Effect of Lime Content on Deviator Stress and Pore Pressure

With the increase of lime in the soil-lime mixtures, there is a significant increase in the deviator stress at failure q_f for 5,10 and 20 per cent lime-added clay specimens. However, as it is seen in Fig.5.1, the strength of 20 per cent lime-added clay specimen is lesser than 5 and 10 per cent lime-added clay specimens; but the strength of 20 per cent lime-added clay sample is higher than the sample which is untreated with lime. In parallel to the increase in strength, moduli of elasticity for lime-treated soil specimens increase as well. If may be emhpasized that lime-stabilization improves the strength and moduli of elasticity of clayey soil especially when proper amount of lime is added. The curves of deviator stress vs. axial strain for each sample, lime-treated and untreated, are presented in Appendix B.

As it is seen from Fig. 5.1 and Table 5.1, in which failure state values are tabulated, the amount of pore-pressure increases for lime-treated clay specimens with reference to untreated clay. Pore-water pressures obtained at tests conducted on clay with 10 per cent lime content are higher than the pore water pressures that develop during the triaxial testing of clay with 5 per cent lime content. The value of pore water pressure measured on clays with 20 per cent lime content is in the same order as the clay containing 5 per cent lime.

5.1.2.2 Effect of Lime Content on q:p' Relationship

As mentioned in Section 5.1.2.1., the deviator stress at failure in lime-added clay specimens significantly increases when proper amount of lime is used. It is seen from the q:p' curves, Fig. 5.2, Fig.5.3, Fig.5.4 and Fig.5.5, that the lime-treated clay samples fail at a higher deviator stresses. The Critical State Line in q:p' space is a straight line which passes through the failure points of test specimens, and slope of the Critical State Line for lime-untreated clay samples is M=0.75, as seen in Fig.5.2. It is also seen in Fig. 5.2 that the samples isotropically normally consolidated to p=4.0 kg/cm^2 and p=5.0 kg/cm^2 fail before they reach the Critical State Line. It is supposed that when confining pressure is increased, the permeability of the specimen decreases; therefore relative increase of pore water pressure at the surrounding of the shear failure plane becomes more difficult

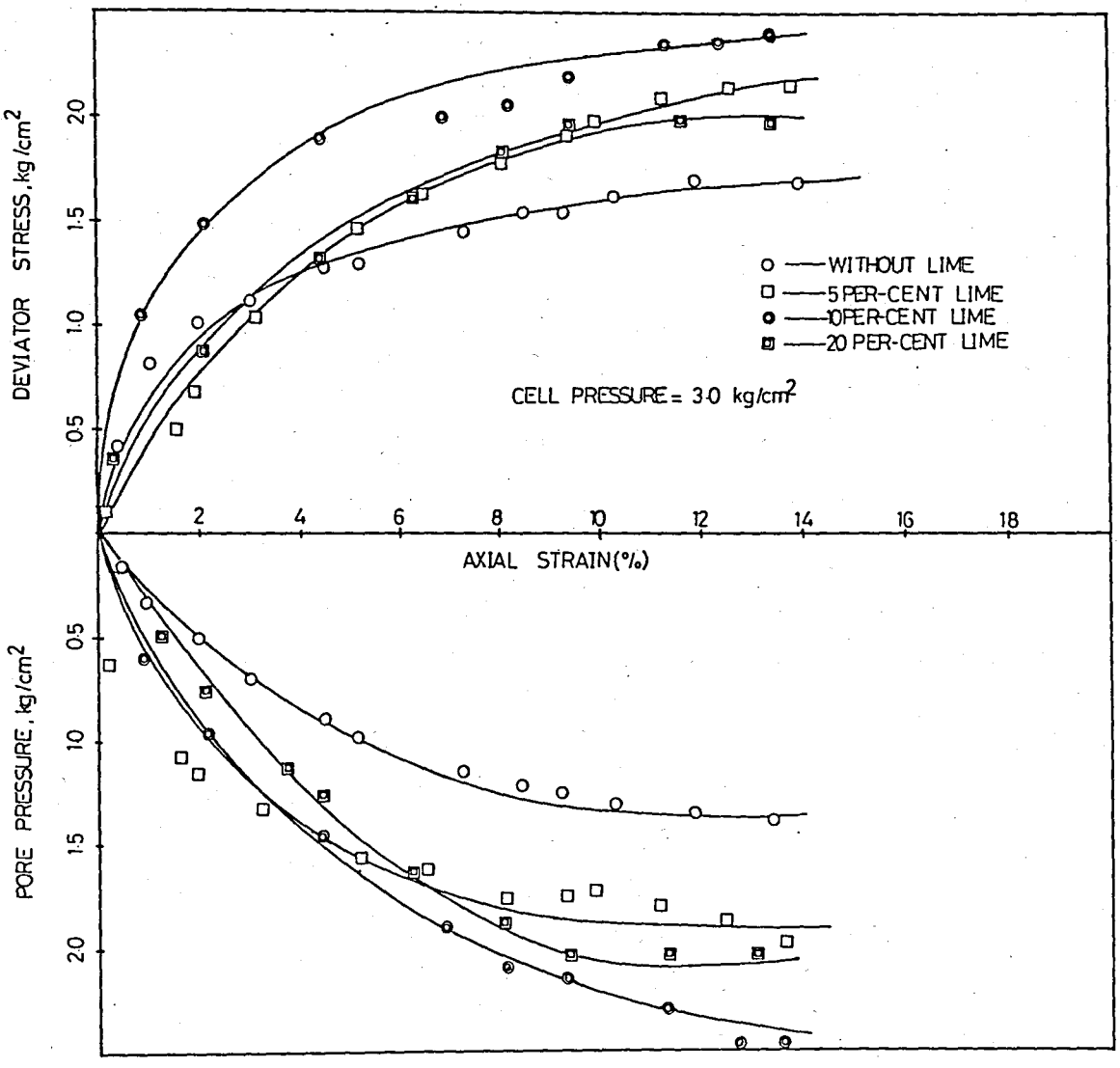

FIG. 5.1 Test Data (a) Deviator Stress q and Axial Strain ε_α and (b) Pore-pressure U and Axial Strain ε_α from Consolidated-Undrained Triaxial Test.

TABLE 5.1 Test Data of Failure Points Obtained from Isotropically Consolidated-Undrained Triaxial Tests.

Lime Per Cent	σ_c	q	U	σ_1	p	p'	q/p	q/p'	A_p	pei	q/pei	U/pei
%	kg/cm^2	kg/cm^2	kg/cm^2	kg/cm^2	kg/cm^2	kg/cm^2	-	-	-	kg/cm^2	-	-
-	2.0	1.302	1.05	3.302	2.434	1.384	0.534	0.940	0.806			
-	2.5	1.480	1.20	3.980	2.996	1.796	0.493	0.823	0.810			
-	3.0	1.690	1.35	4.690	3.566	2.216	0.473	0.762	0.798	3.20	0.506	0.406
-	3.5	1.880	1.50	5.380	4.130	2.630	0.455	0.714	0.797	3.40	0.552	0.441
-	4.0	2.062	1.65	6.062	4.675	3.055	0.433	0.663	0.800	3.70	0.557	0.445
-	5.0	2.300	1.85	7.300	5.766	3.916	0.398	0.587	0.804	4.50	0.511	0.411
5	2.0	1.860	1.95	3.860	2.622	0.672	0.709	2.765	1.048			
5	2.5	1.695	2.00	4.463	3.155	1.205	0.622	1.630	0.992			
5	3.0	2.000	2.15	5.000	3.663	1.513	0.546	1.321	1.075	2.70	0.740	0.796
5	3.5	2.170	2.30	5.670	4.223	1.923	0.513	1.127	1.059	3.15	0.688	0.730
5	4.0	2.23	2.40	6.230	4.743	2.343	0.470	0.951	1.076	4.70	0.474	0.510
5	5.0	2.530	2.65	7.530	5.841	3.191	0.433	0.792	1.047	6.10	0.414	0.434
10	2.0	2.320	2.50	4.320	2.771	0.271	0.837	8.530	1.077			
10	2.5	2.350	2.50	4.850	3.283	0.783	0.715	3.000	1.063			
10	3.0	2.400	2.55	5.400	3.801	1.251	0.631	1.917	1.062	2.45	0.979	1.040
10	3.5	2.430	2.60	5.930	4.309	1.709	0.563	1.421	1.069	3.05	0.796	0.852
10	4.0	2.490	2.60	6.490	4.829	2.229	0.515	1.117	1.044	5.15	0.483	0.504
10	5.0	2.480	2.65	7.279	5.759	3.109	0.395	0.732	1.162	6.10	0.406	0.434
20	2.0	1.850	1.90	3.850	2.615	0.715	0.707	2.586	1.027			
20	2.5	1.900	1.95	4.400	3.132	1.182	0.606	1.607	1.026			
20	3.0	2.000	2.05	5.000	3.667	1.617	0.545	1.236	1.025	2.65	0.724	0.735
20	3.5	1.950	2.00	5.450	4.148	2.148	0.470	0.907	1.025	2.95	0.661	0.667
20	4.0	2.037	2.10	6.037	4.678	2.578	0.435	0.789	1.030	5.15	0.395	0.407
20	5.0	2.075	2.15	7.075	5.691	3.541	0.364	0.585	1.036	6.90	0.300	0.311

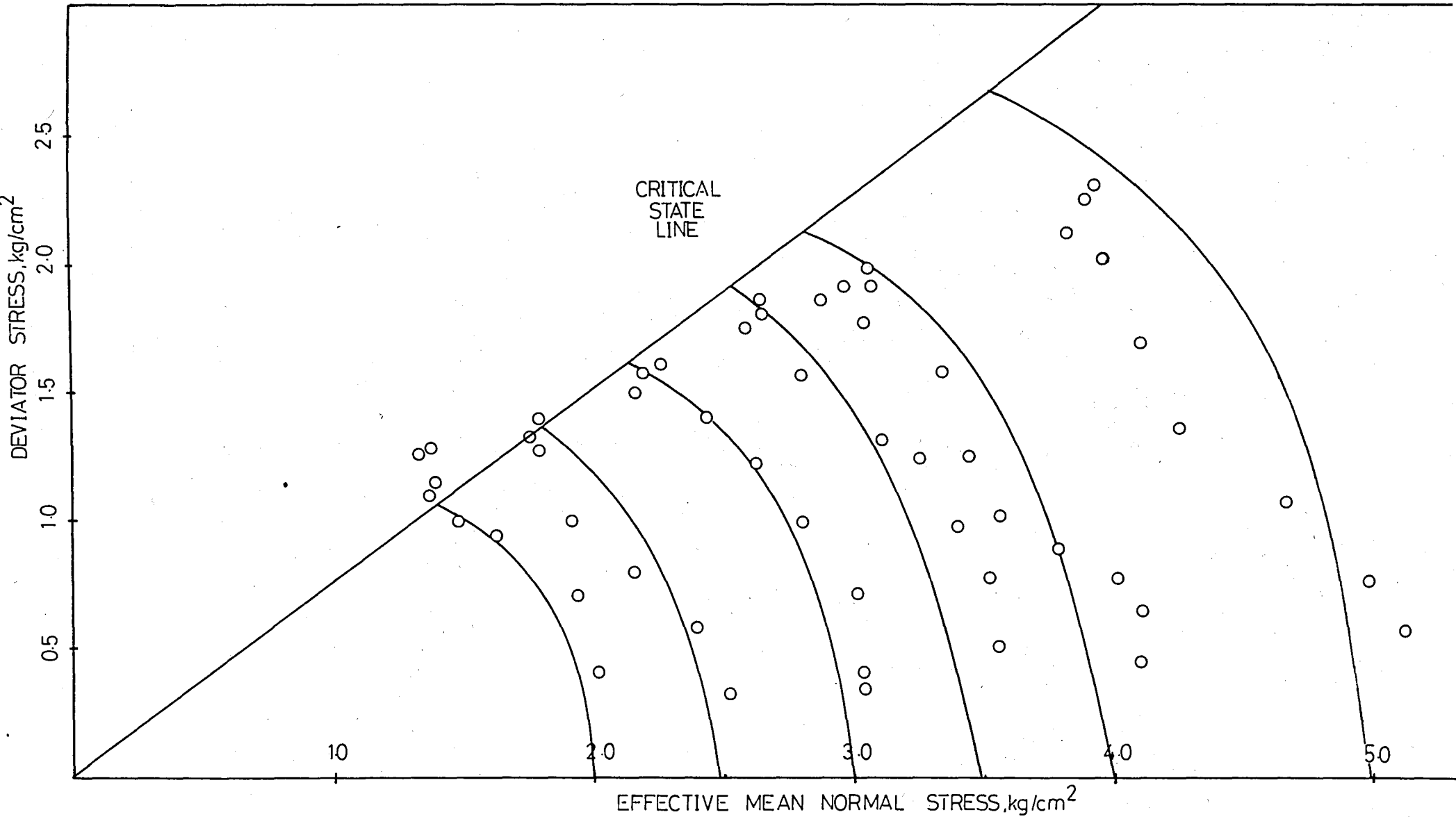

FIG.5.2 Stress Paths in q:p' Space for Consolidated-Undrained Triaxial Tests on Lime-Untreated Normally Consolidated Samples

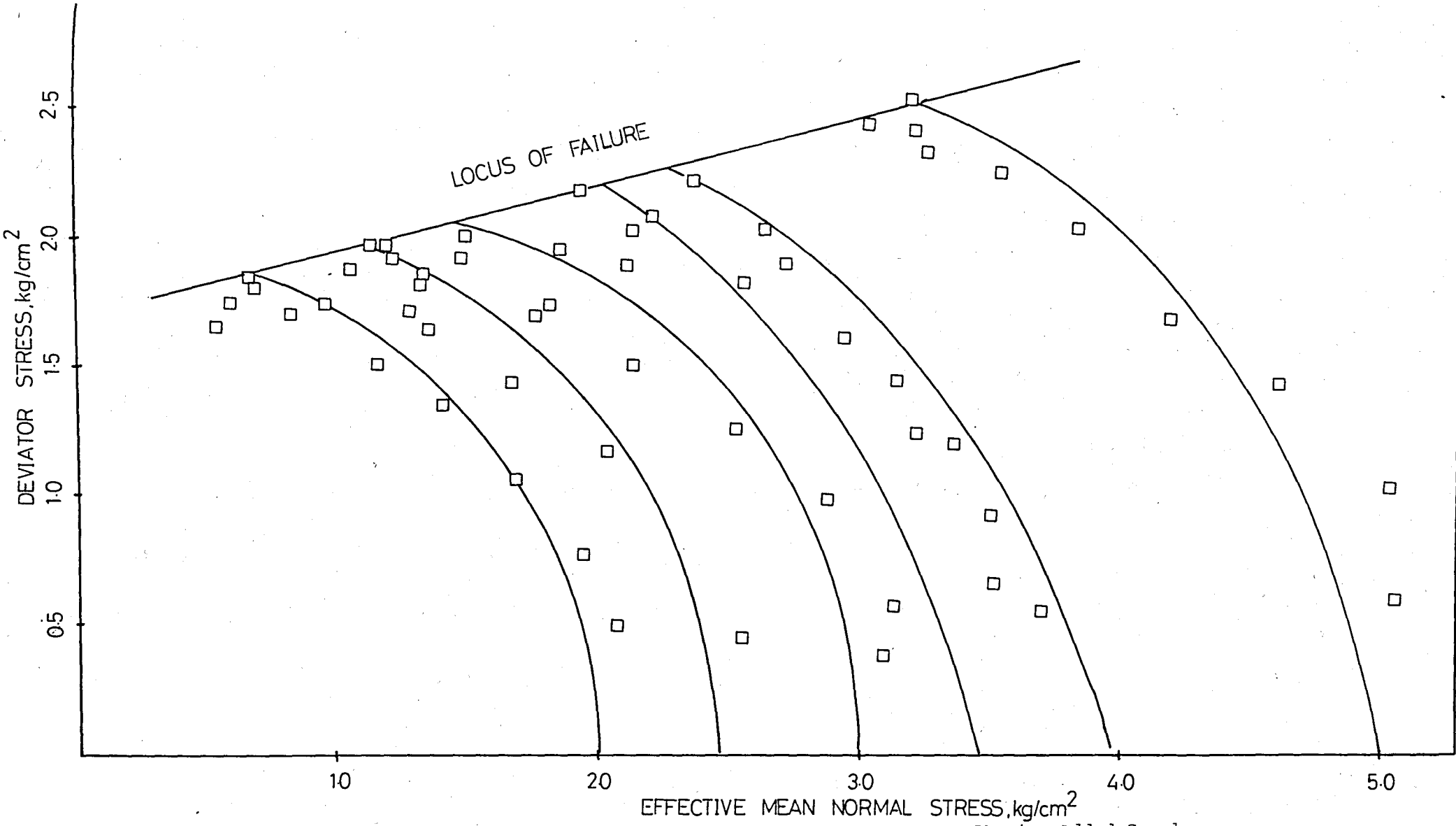

FIG.5.3 Stress Paths in q:p' Space for Consolidated-Undrained Triaxial Tests on 5% Lime-Added Samples

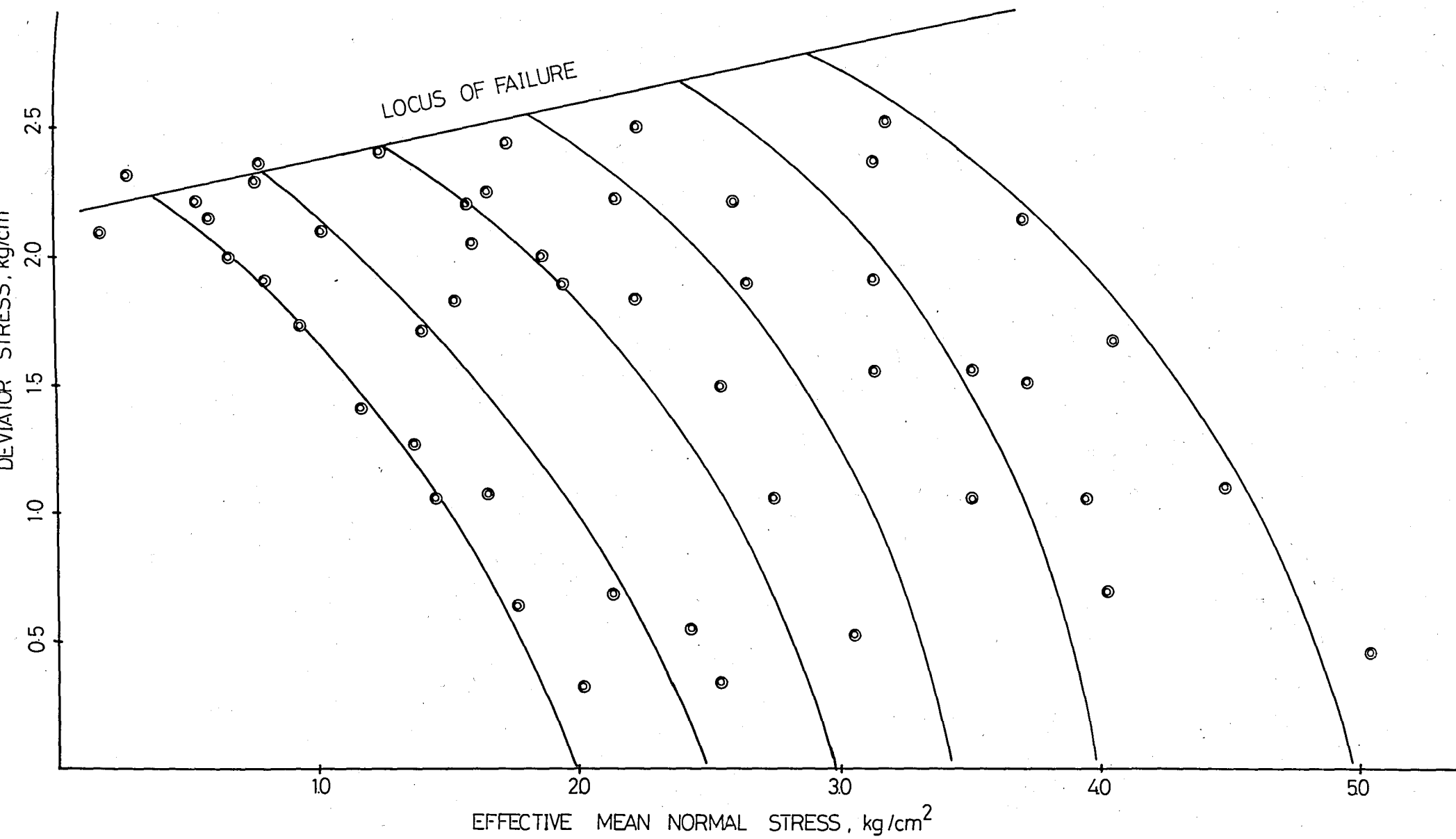

FIG.5.4 Stress Paths in q:p' Space for Consolidated-Undrained Triaxial Tests on 10% Lime-Added Samples

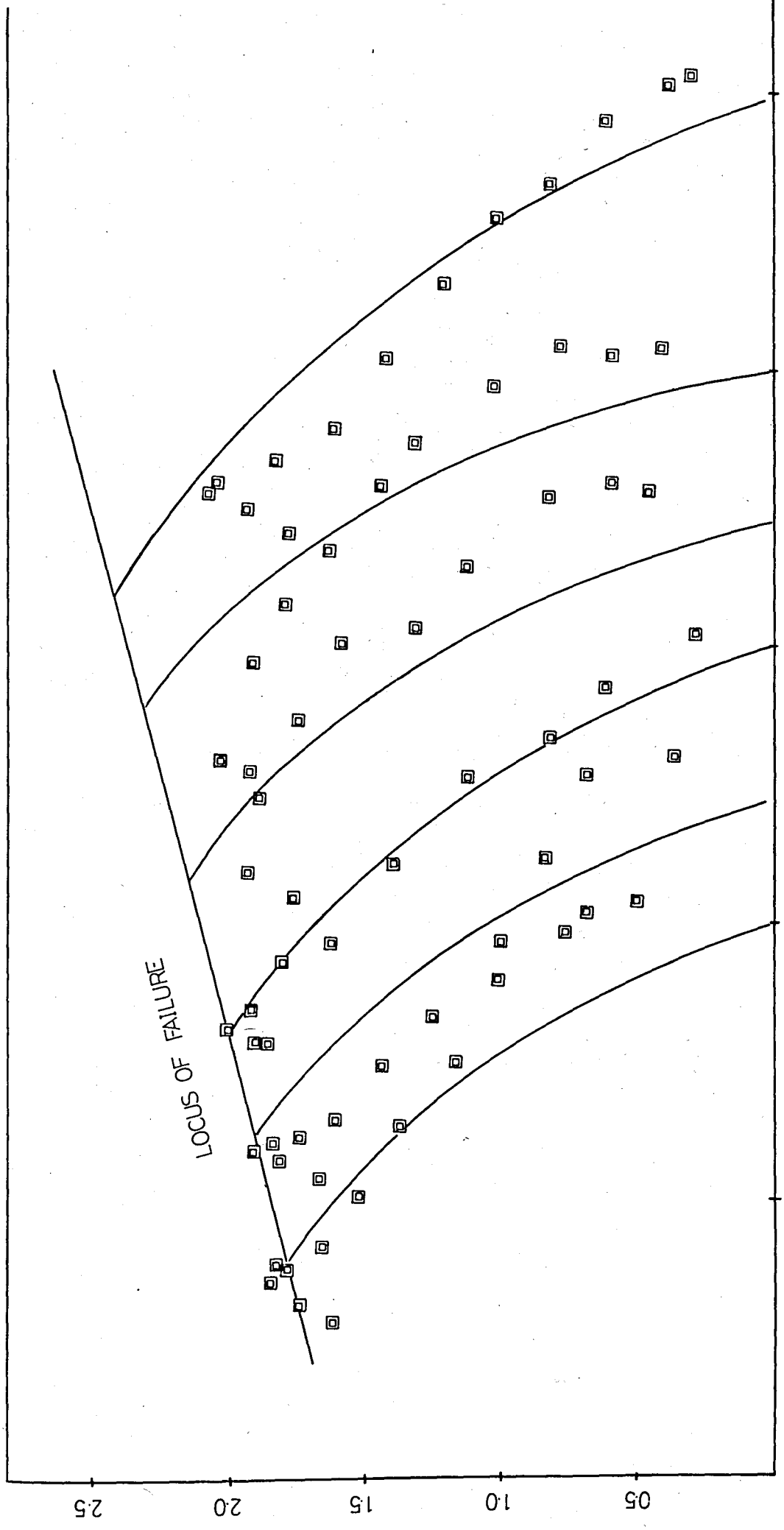

FIG.5.5 Stress Paths in q:p' Space for Consolidated-Undrained Triaxial Tests on 20% Lime-Aded Samples

to be measured accurately. Therefore, the stress paths of samples consolidated to high pressures seem not to be reaching the Critical State Line.

When a line is drawn in q:p' space through the failure points of lime-treated clay specimens, it is seen that this line has a different feature from the Critical State Line obtained from lime-untreated clay samples, and those lines are parallel to each other for 5,10 and 20 per cent lime-added clay samples. We will call this line the "Locus of Failure". The slope of the Locus of Failure is 0.25, and those surfaces intersects the vertical axis representing deviator stress q at different values, namely 1.68, 2.13 and 1.58 for 5,10 and 20 per cent lime-added clay specimens, respectively. It is seen that intersection value reaches its maximum value when 10 per cent lime is added.

It is seen from Fig. 5.2 that if a clay sample ,lime-untreated, is unconfined, i.e. p=0, than it would have no shear strength, i.e. q_f=0. On the other when investigating the stress paths of lime-added clay samples, Fig.5.3, Fig.5.4 and Fig.5.5, even if they are unconfined, they would possess a shear strength due to the fact that there have been cementation bonds between clay particles which arises from the pozzolanic chemical reaction of clay and lime. The cementation bonds between clay particles generated by lime need to be destructed before the sample fails, and therefore higher deviator stresses are needed to shear the clay to failure.

Hence, it may be emphasized that lime-stabilized clay samples, although they are tested under isotropically normally consolidated undrained conditions, may not be considered as normally consolidated samples.

5.1.2.3 Effect of lime Content on ν:p' Relationship

In a standard undrained triaxial compression test, the cell pressure is held constant, the axial stress on the specimen is increased, but drainage is not allowed to take place. Therefore the specific volume, ν= 1+e, is constant in an undrained test, and by definition, the test path followed by the isotropically consolidated sample is straight-forward in ν:ℓnp' space. The test path is then simply a line at constant ν from Normal Consolidation Line (NCL) to Critical State Line (CSL). In consequence, as the test proceeds, the sample responds to the changes of total stress, and the pore-pressure changes.

When drawing the Normal Consolidation Line and Critical State Line for lime-untreated clay samples, Fig.5.6 , it is seen that lime-untreated clay sample has the following basic soil parameters : N=2.856, Γ=2.747 and λ=0.293. The basic soil parameters are :

N = the value of specific volume ν corresponding to p' = 1.0 kg/cm^2 on Normal Consolidation Line.

Γ = the value of specific volume ν corresponding to

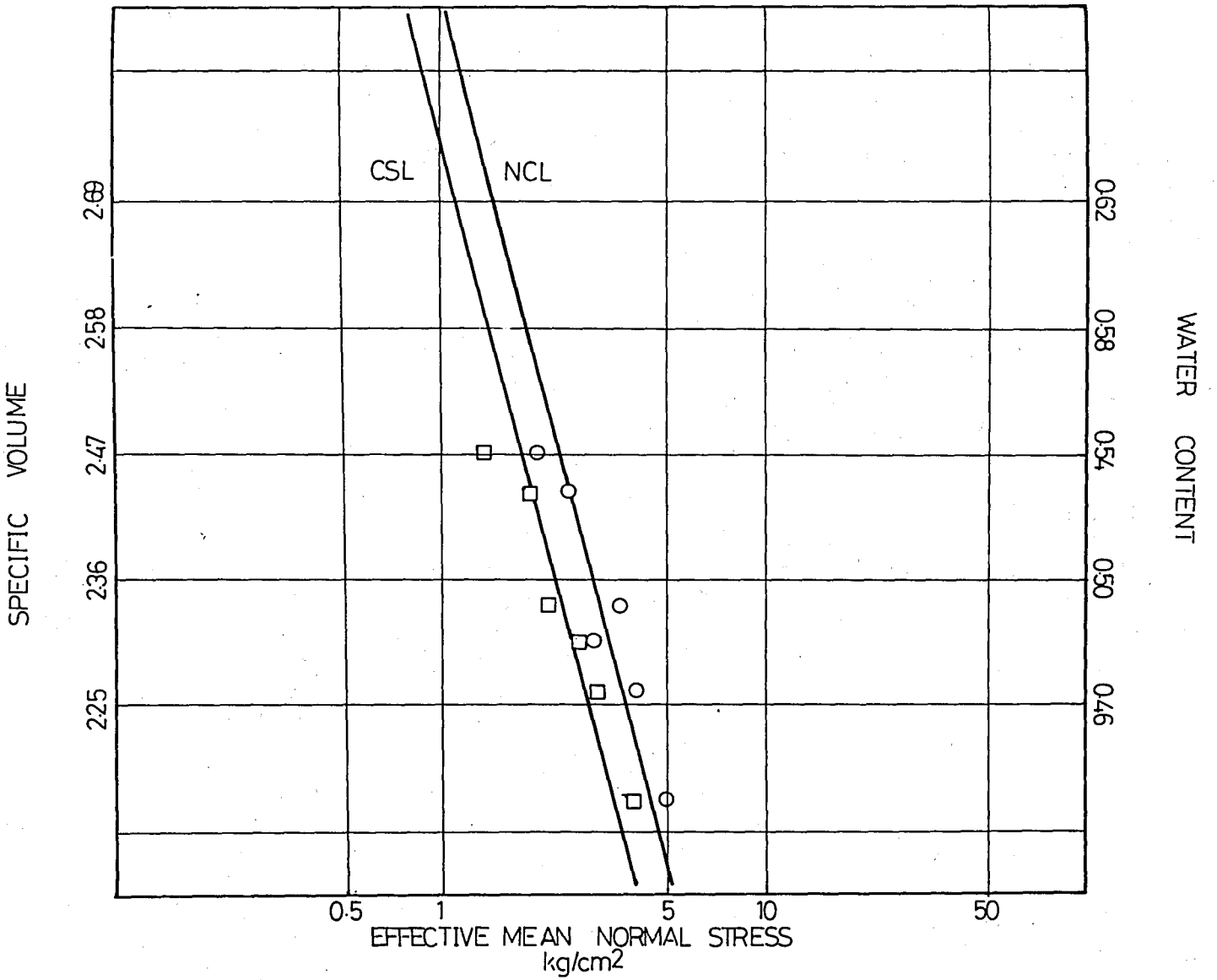

FIG.5.6 The Normal Consolidation and Critical State Lines for Consolidated-Undrained Triaxial Test on Lime-Un-treated Samples

$p' = 10\ kg/cm^2$ on Critical State Line.

λ = Slope of Normal Consolidation and Critical State Line in $v:\ell np'$ space.

On the other hand, when investigating the behaviour of lime-treated clay samples in $v:\ell np'$ space, Fig. 5.7 , Fig.5.8 and Fig.5.9 , it is clearly seen that failure values of lime-treated clay specimens follow a curved line instead of a straight line as in the case of lime-untreated clay samples. It can be stated that this curve is the projection of "Locus of Failure" on the $v:\ell np'$ space.

Therefore, it may be again emphasized that lime-stabilized clay samples, even though they are loaded under isotropically consolidated-undrained conditions, may not be regarded as normally consolidated samples.

5.1.2.4 Effect of Lime Content on U:p' Relationship

The characteristic shape of U:p' curves are illustrated in Fig.5.10, Fig.5.11,Fig.5.12 and Fig 5.13. As mentioned in Section 5.1.2.1, higher pore-pressures are observed in lime-stabilized clay specimens. When comparing the above mentioned figures, pore-pressure value at failure is maximum for 10 per cent lime-added clay specimen. It follows from the figures that there is not any significant behaviour difference between the curves of

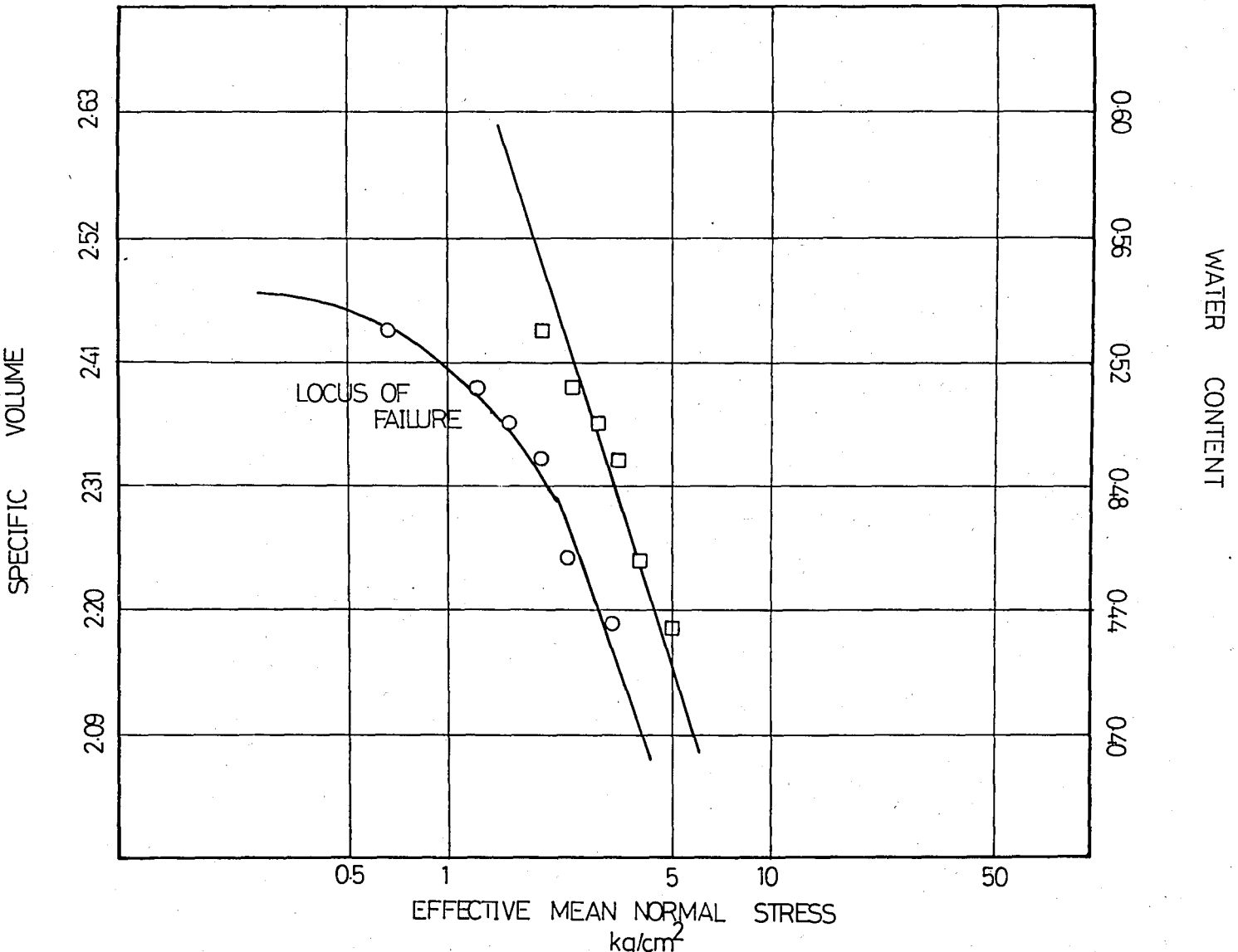

FIG.5.7 Normal Consolidation Line and Locus of Failure for Consolidated-Undrained Triaxial Test on 5% Lime-Added Samples

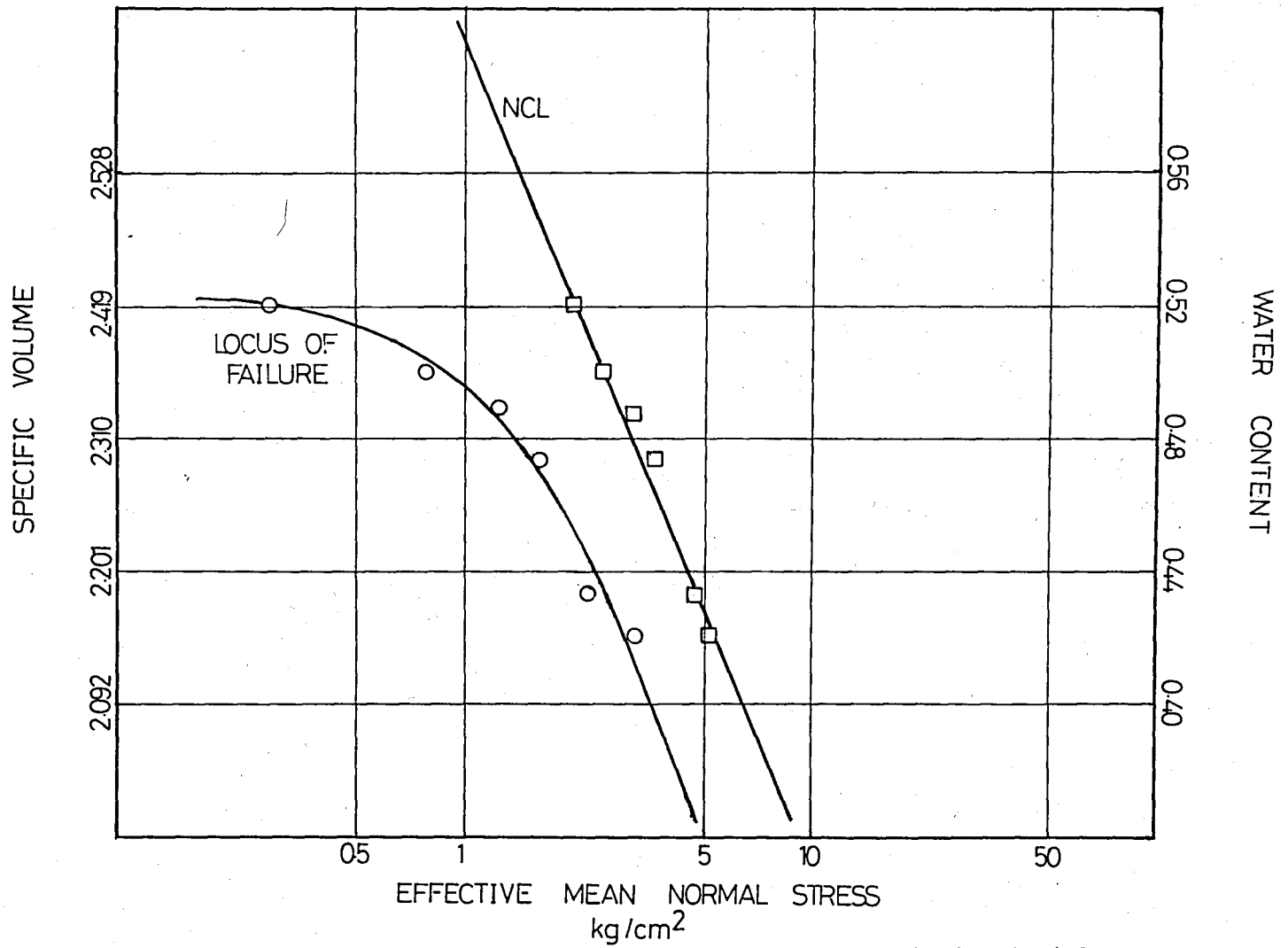

FIG.5.8 Stress Path in q:p' Space for Consolidated-Undrained Triaxial Test on 10 % Lime-Added Sample

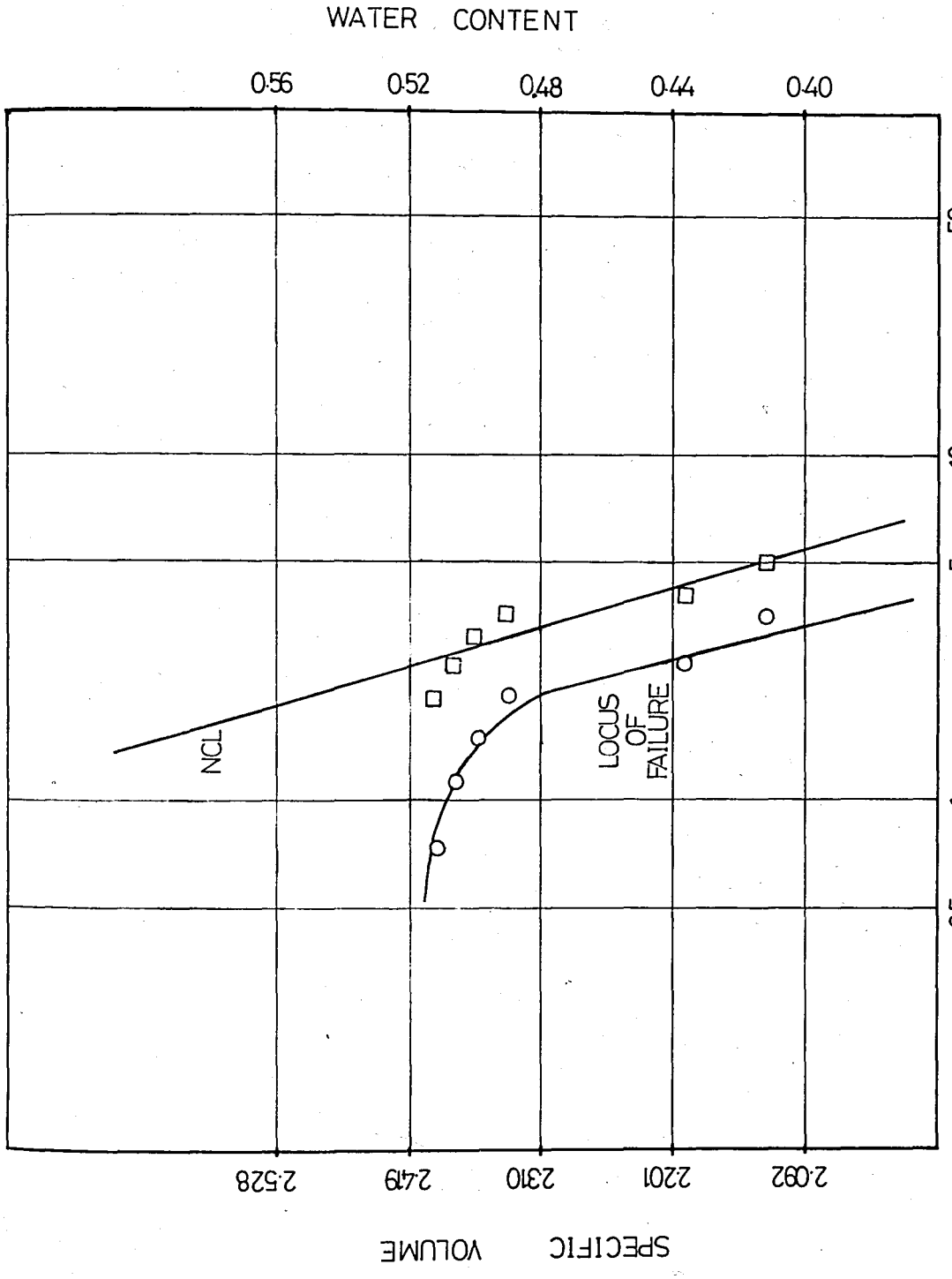

FIG.5.9. Normal Consolidation Line and Locus of Failure for Consolidated-Undrained Triaxial Test on 20% Lime-Added Samples

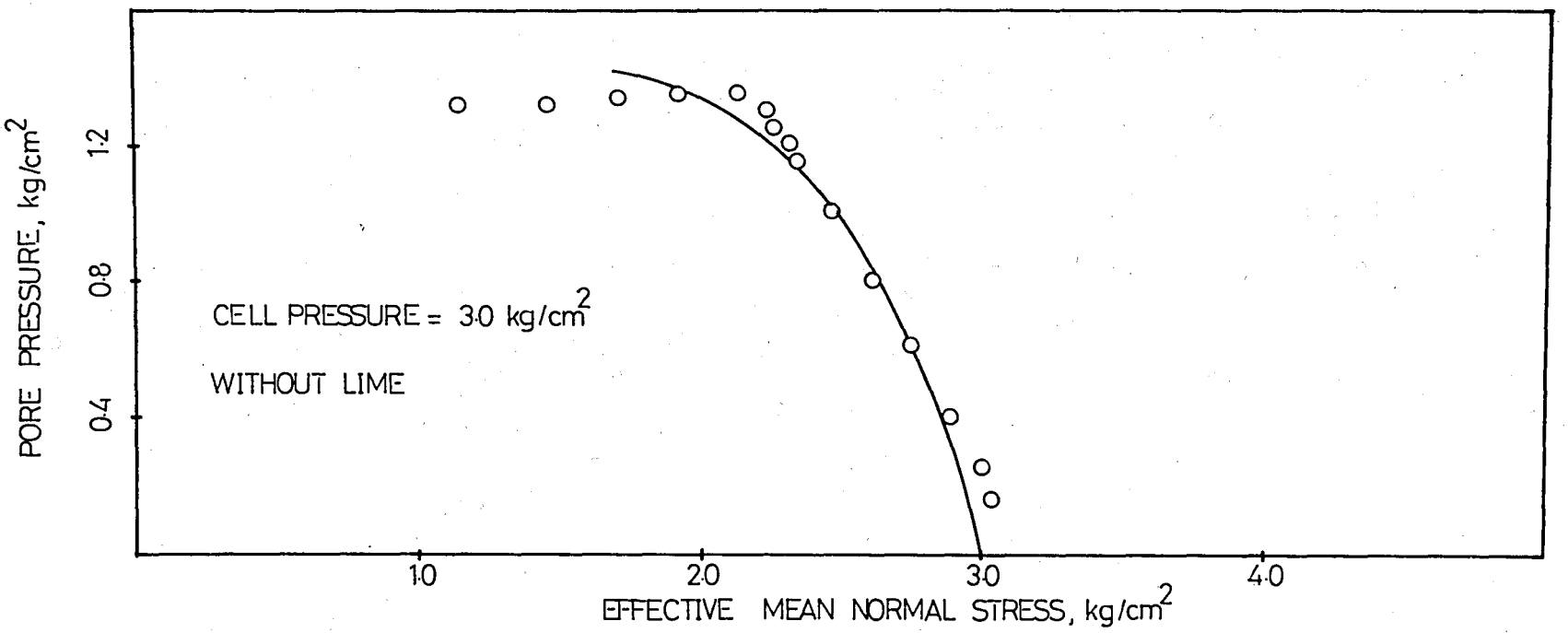

FIG.5.10 Test Data Pore-pressure U and Effective Mean Normal Stress p' from Consolidated-Undrained Triaxial Test

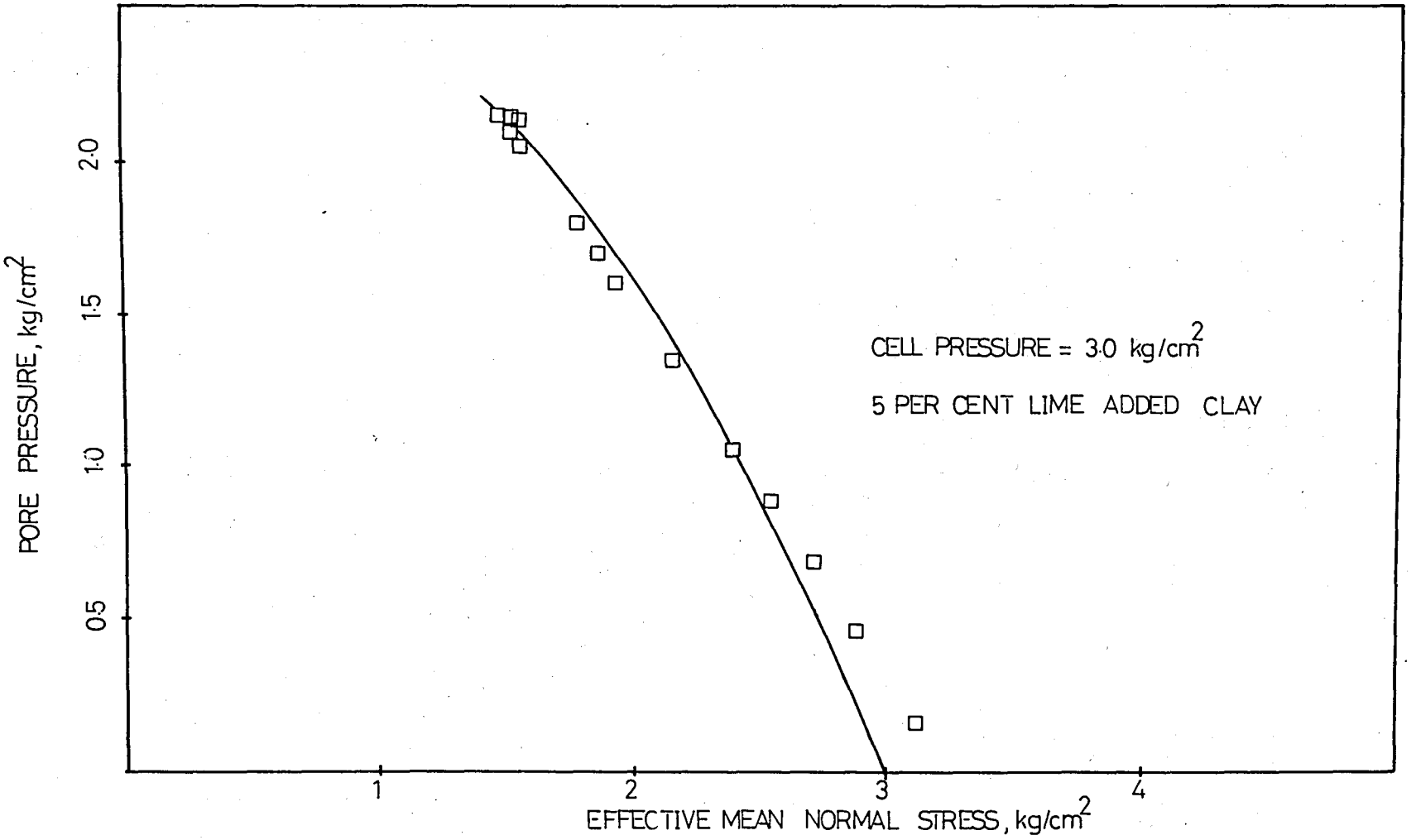

FIG. 5.11 Test Data Pore-pressure U and Effective Mean Normal Stress p' from Consolidated-Undrained Triaxial Test

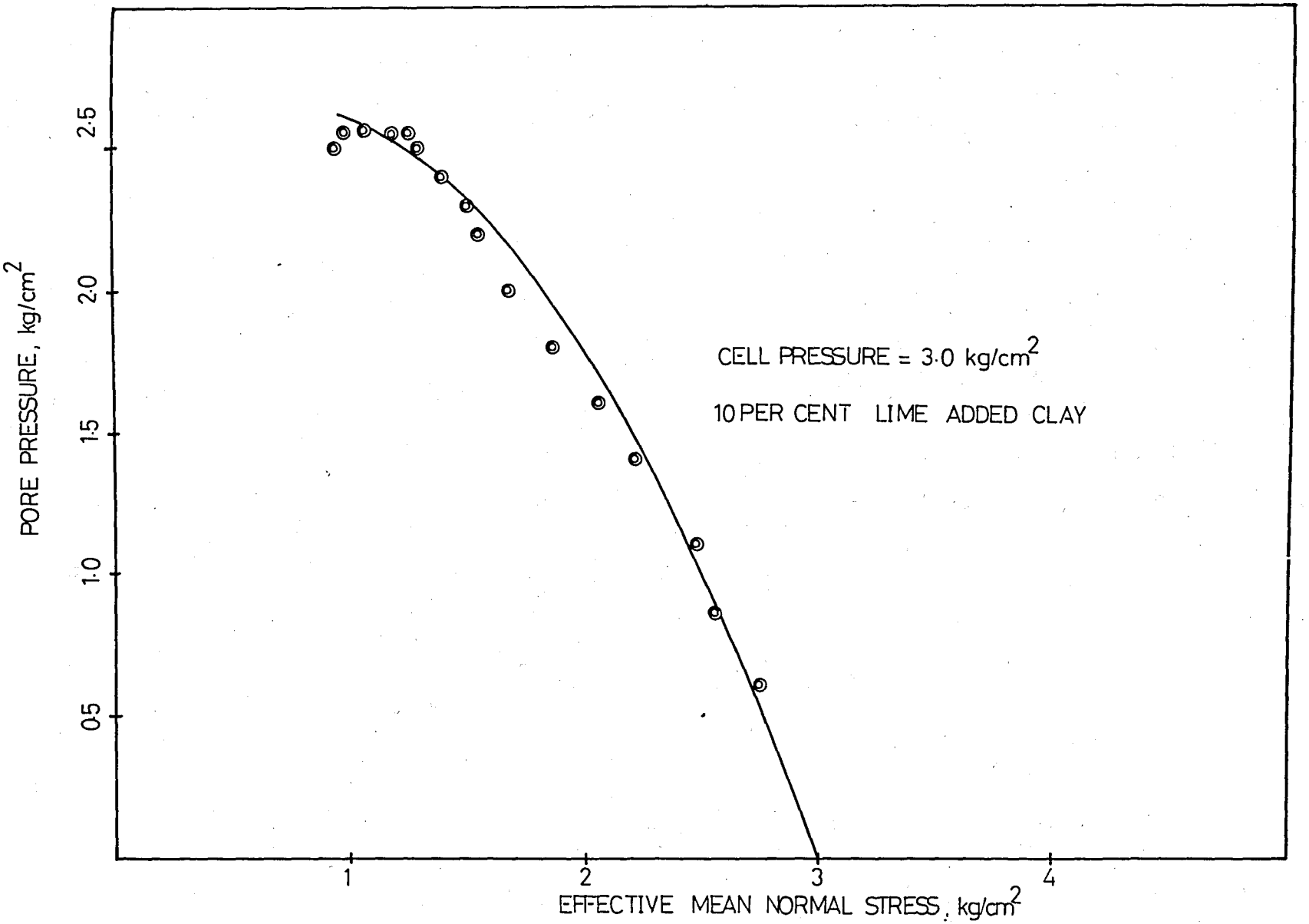

FIG.5.12 Test Data Pore-pressure U and Effective Mean Normal Stress p' from Consolidated-Undrained Triaxial Test

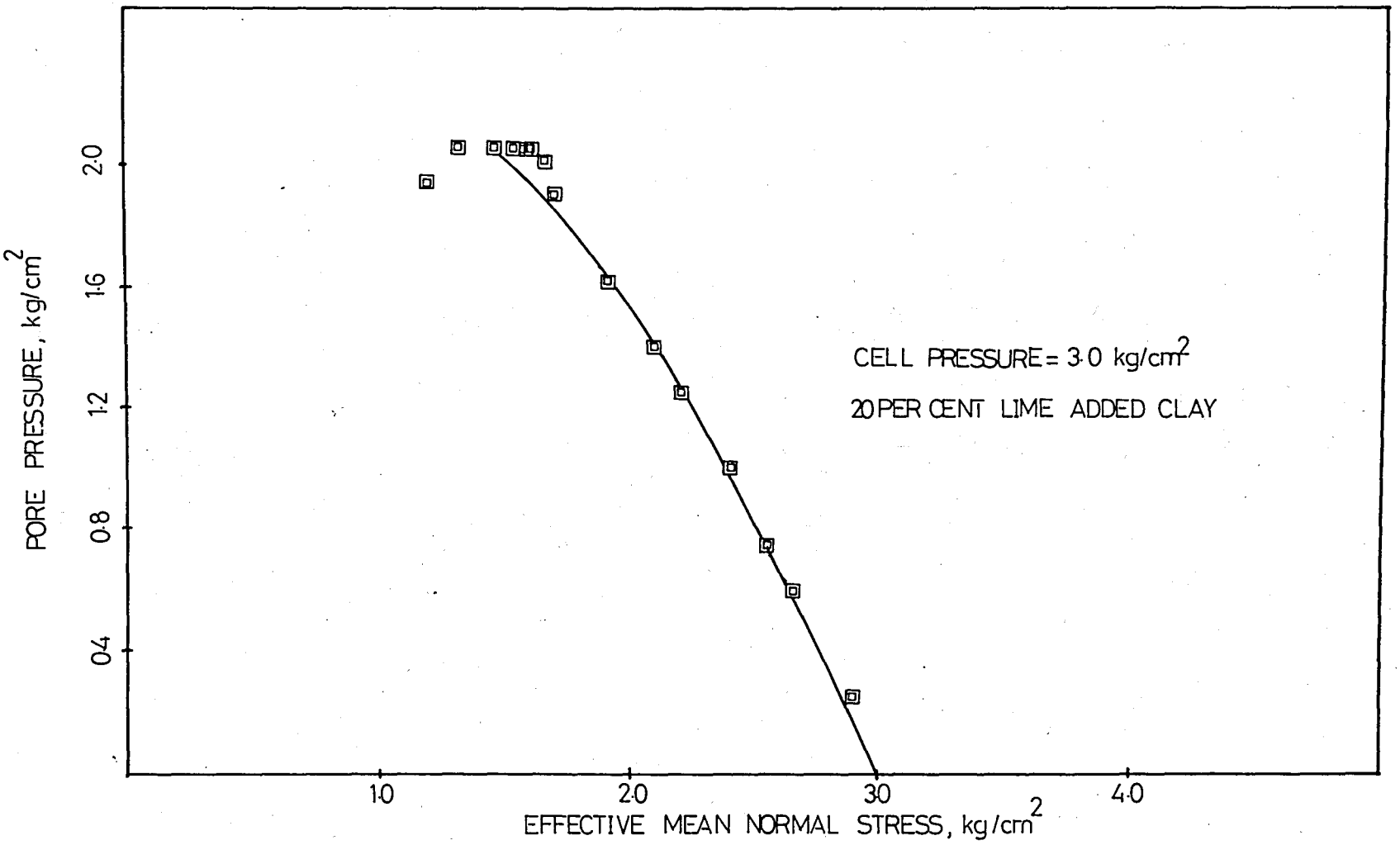

FIG.5.13 Test Data Pore-pressure U and Effective Mean Normal Stress p' from Consolidated-Undrained Triaxial Test

U:p' for lime-treated and untreated clay samples. The curves of U:p' for each test sample are seen in Appendix C.

5.1.2.5 Effect of Lime Content on $A_p:\varepsilon_\alpha$ and $A_p:p'$ Relationship

The characteristic shape of $A_p:\varepsilon_\alpha$ curves for lime-treated and untreated clay specimens are sketched in Fig. 5.14 and Fig.5.15. As seen in Table 5.1., pore-pressure parameter A_p at failure has a mean value of 0.802 for lime untreated clay specimens, and has a mean value of 1.052 for lime-treated clay specimens. The curves of $A_p:p'$ are also sketched in Fig.5.16 and Fig.5.17. It is seen from $A_p:\varepsilon_\alpha$ and $A_p:p'$ curves that there is not any substantial behaviour difference for lime-added and non-added clay specimens. Appendix D and Appendix E include the curves of $A_p:\varepsilon_\alpha$ and $A_p:p'$ for each test sample, respectively.

5.1.2.6 Effect of Curing

As mentioned in Section 4.4.2, the drainage valve is not opened for a week for 18 lime-treated triaxial specimens. On the other hand, the drainage valve is kept open for three triaxial specimens having 5,10 and 20 per cent lime while cell pressure σ_c = 3.0 kg/cm^2 is applied. The effect of curing process on the behaviour of lime-treated clay samples can be summarized as follows:

A substantial difference in the deviator stress between two procedure is not observed, however modulus of elasticity for the

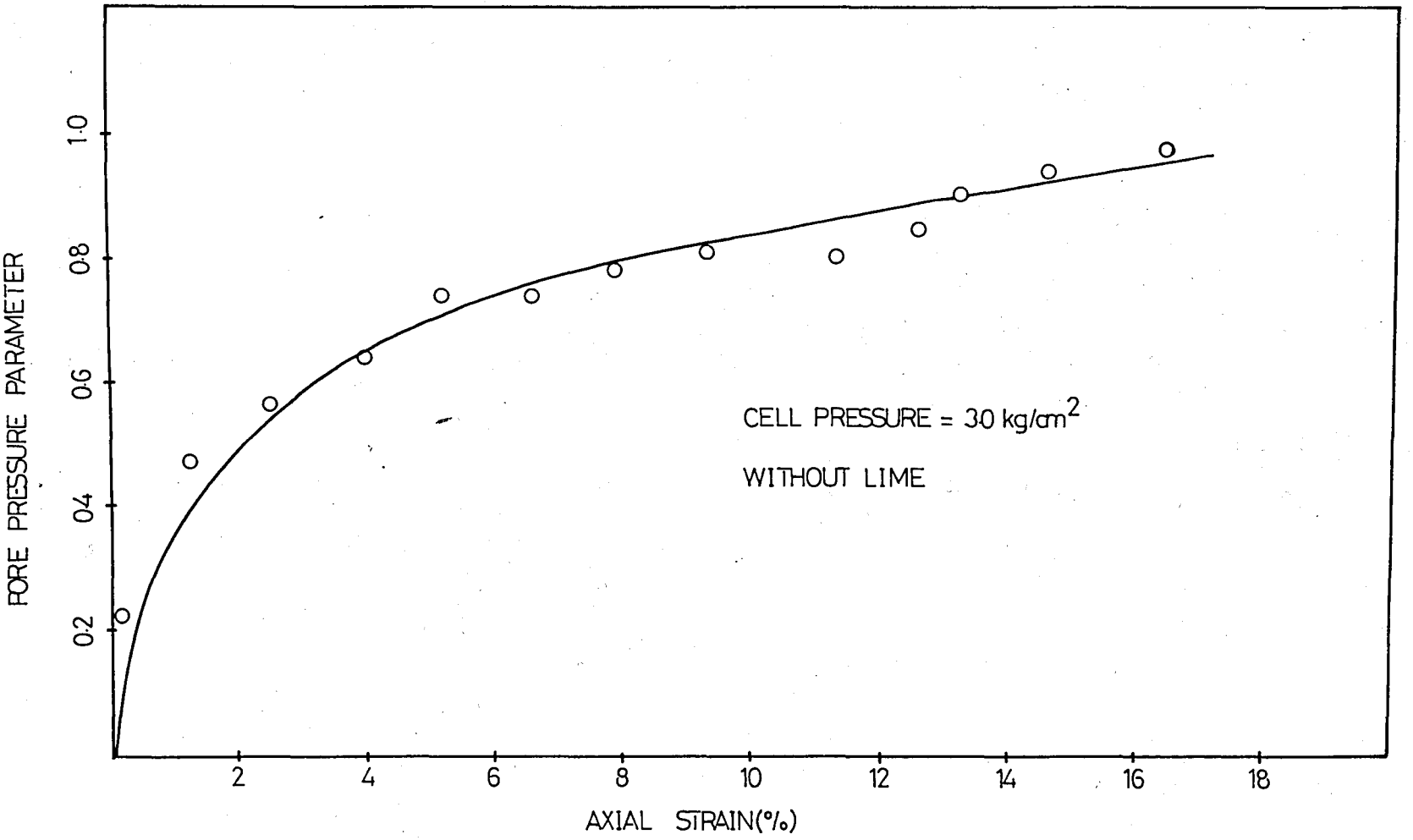

FIG.5.14 Relationship Between Pore-Pressure Parameter A_p and Axial Strain ε_α in Consolidated-Undrained Triaxial Test

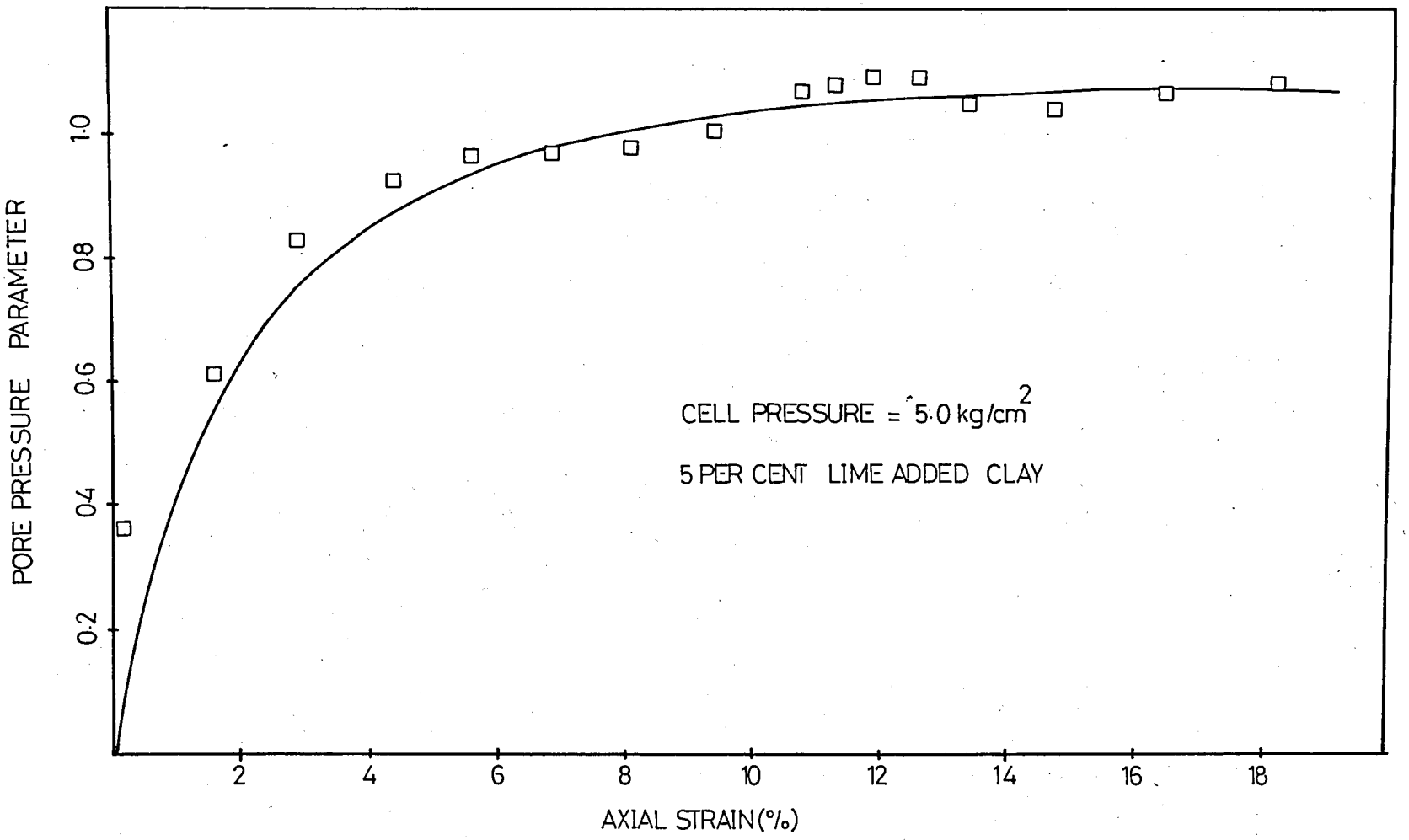

FIG.5.15 Relationship Between Pore-Pressure Parameter A_p and Axial Strain ε_α in Consolidated-Undrained Triaxial Test

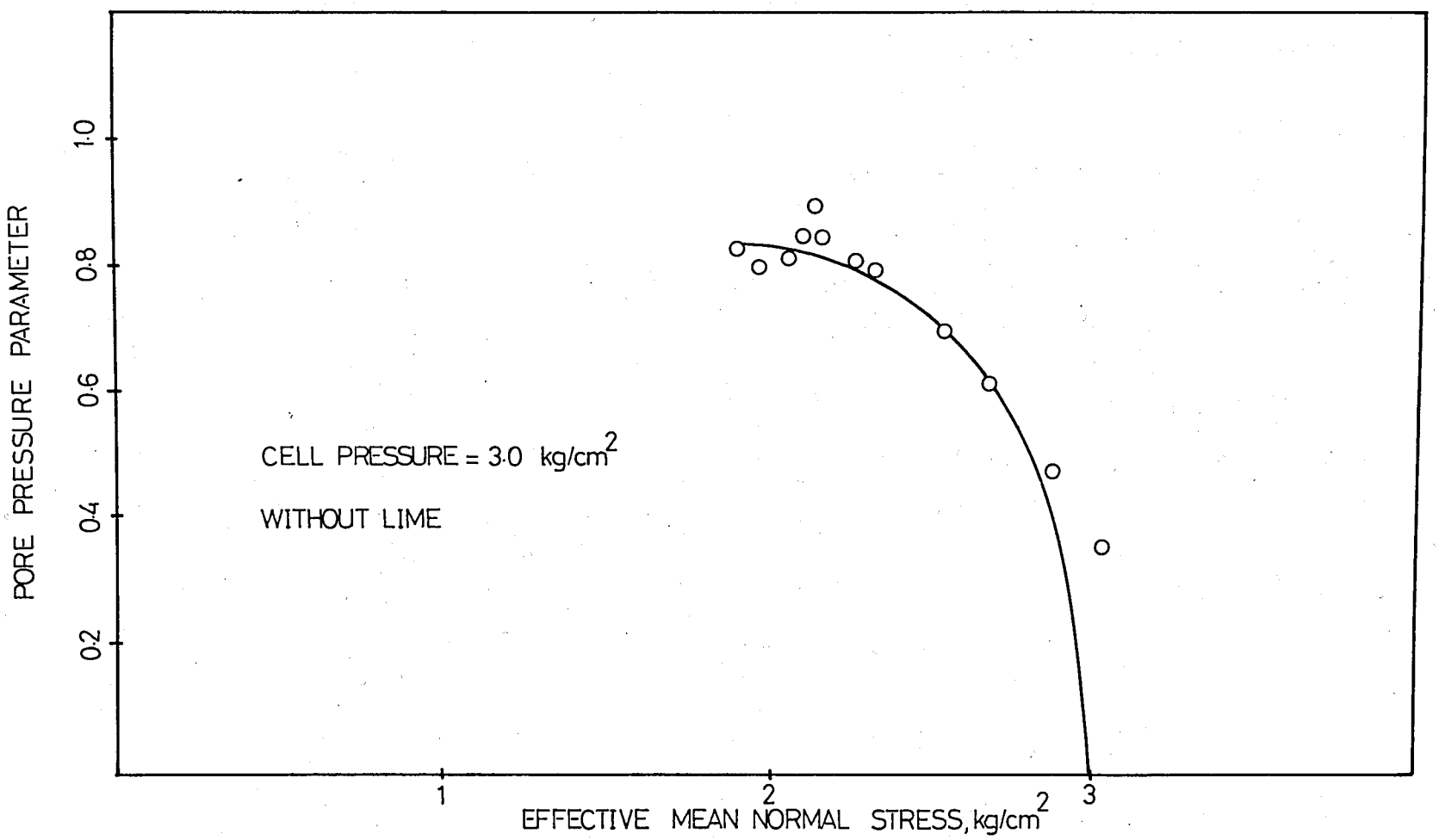

FIG.5.16 Test Data Pore-Pressure Parameter A_p and Effective Mean Normal Stress p' from Consolidated-Undrained Triaxial Test

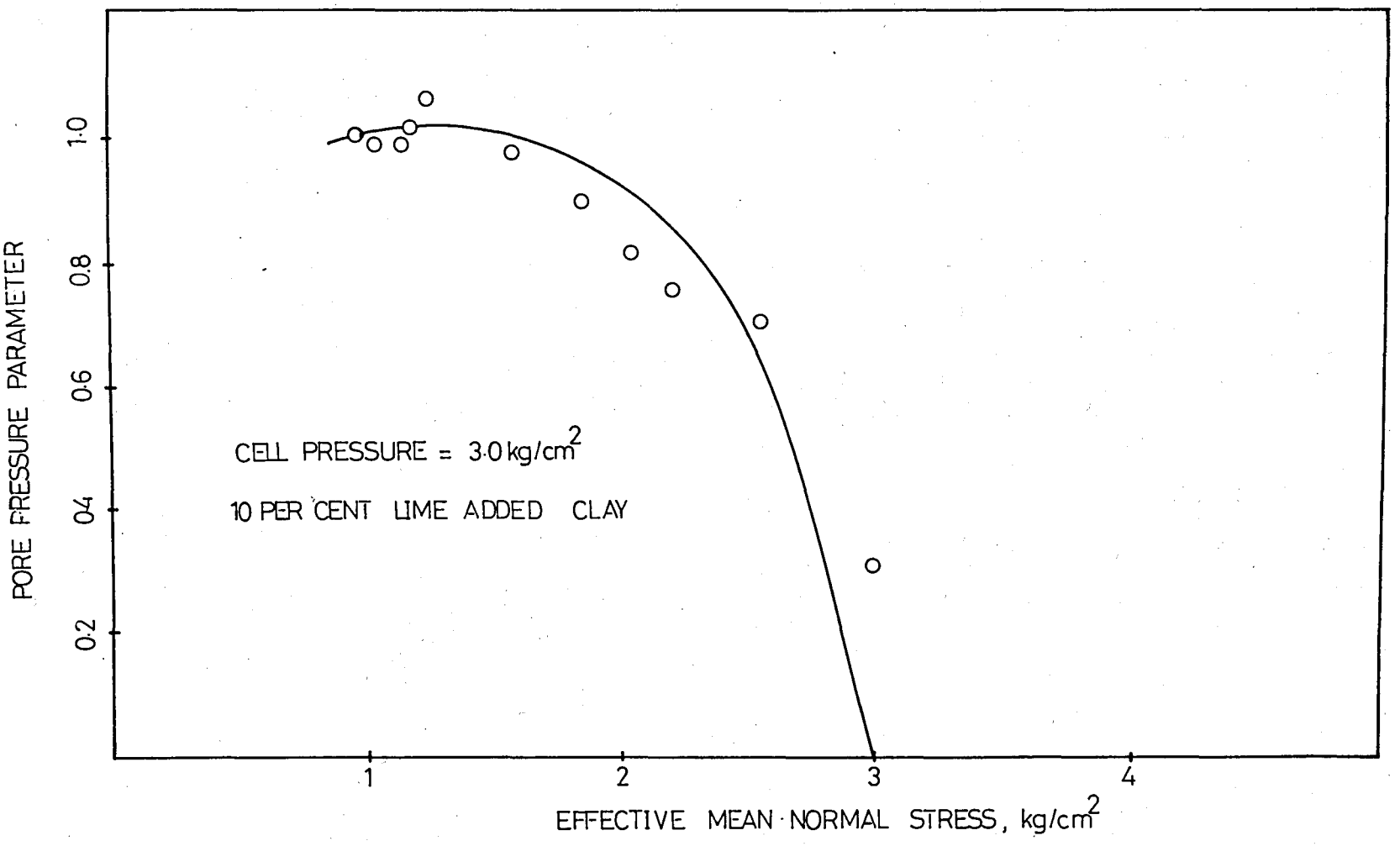

FIG 5.17 Test Data Pore-Pressure Parameter A_p and Effective Mean Normal Stress p' from Consolidated-Undrained Triaxial Test

samples, on which drainage is permitted, is higher; and those specimens fail at a smaller axial strain, this change is clearly seen when comparing Fig.5.18 and Fig.5.1.

In addition to that, the pore water pressure developed during the shear of cured specimens are less than the pore pressures obtained from triaxial tests conducted on un-cured samples. Therefore an increase in the effective mean normal stress p' is observed. Stress paths in q:p' space can also be seen in Fig. 5.19, Fig.5.20 and Fig.5.21. When the "Locus of Failure" lines obtained from un-cured specimens are drawn in the above mentioned figures, which were also drawn in Fig.5.3, Fig.5.4 and Fig.5.5, it is seen that the three cured samples fail as they reach the corresponding "Locus of Failure" lines.

The failure state values of specimens on which drainage is permitted are tabulated in Table 5.2. It is also seen that the total mean normal stress is not affected significantly.

It also follows from Table 5.2. that q/p' values of the specimens, on which drainage is permitted, decrease. Obviously, this is due to an increase in the effective mean normal stress.

The pore-pressure parameter A_p at failure is in the order of 0.80 for the cured specimens.

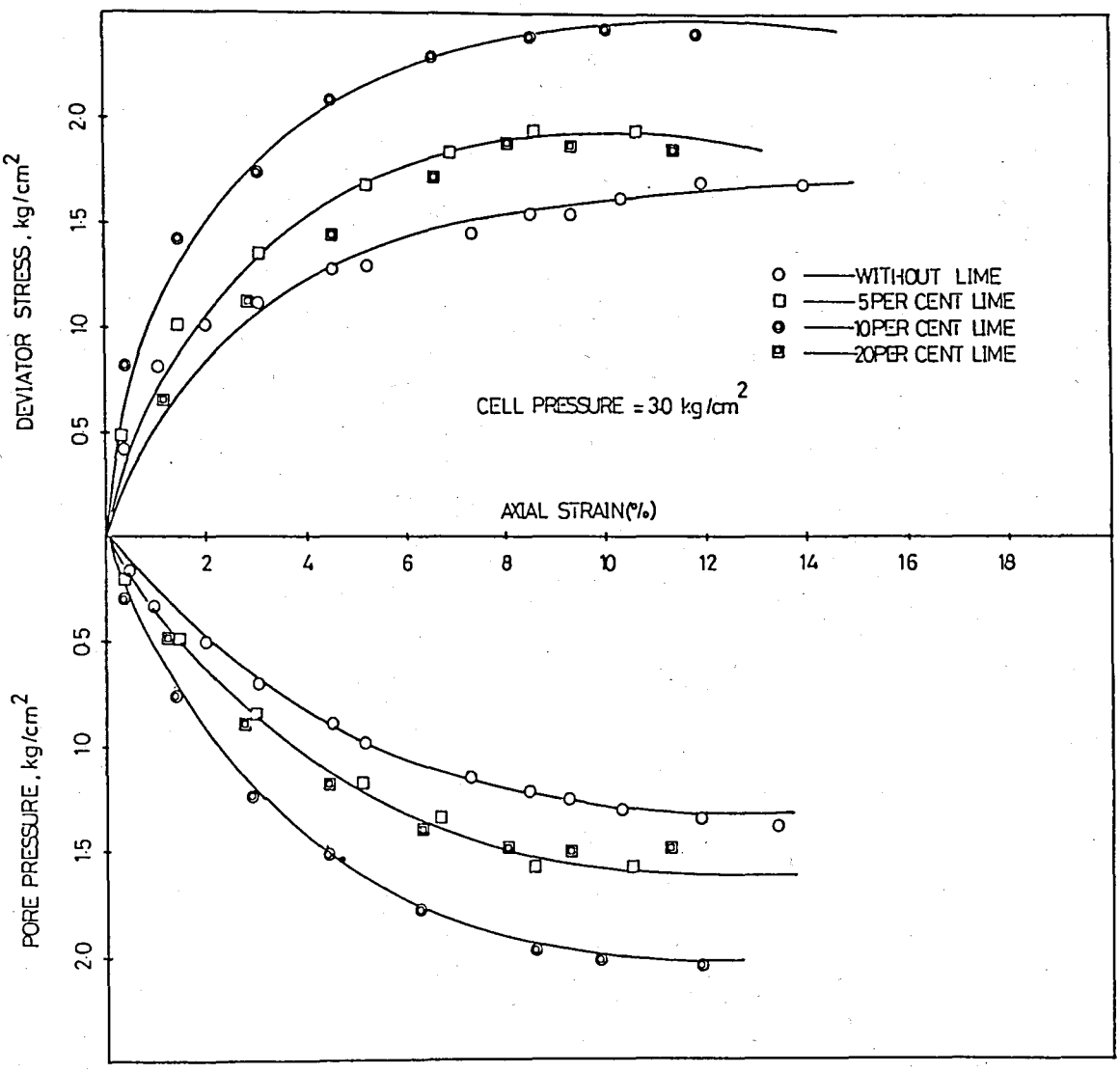

FIG.5.18 Test Data (a) Deviator Stress q and Axial Strain ε_α and (b) Pore-pressure U and Axial Strain ε_α from Consolidated-Un-drained Triaxial Test

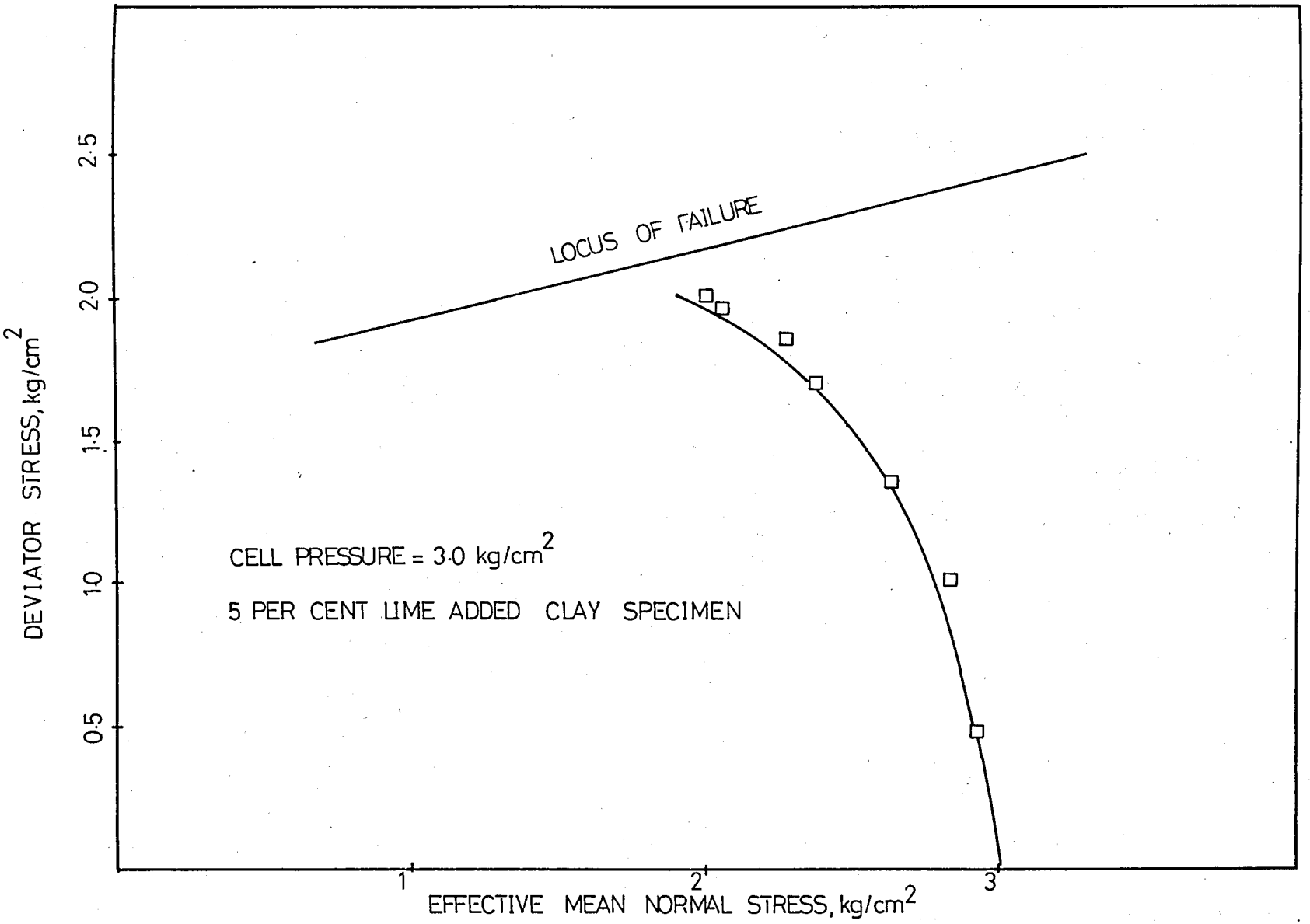

FIG.5.19 Stress Path in q:p' Space for Consolidated-Undrained Triaxial Test on 5% Lime-Added Sample

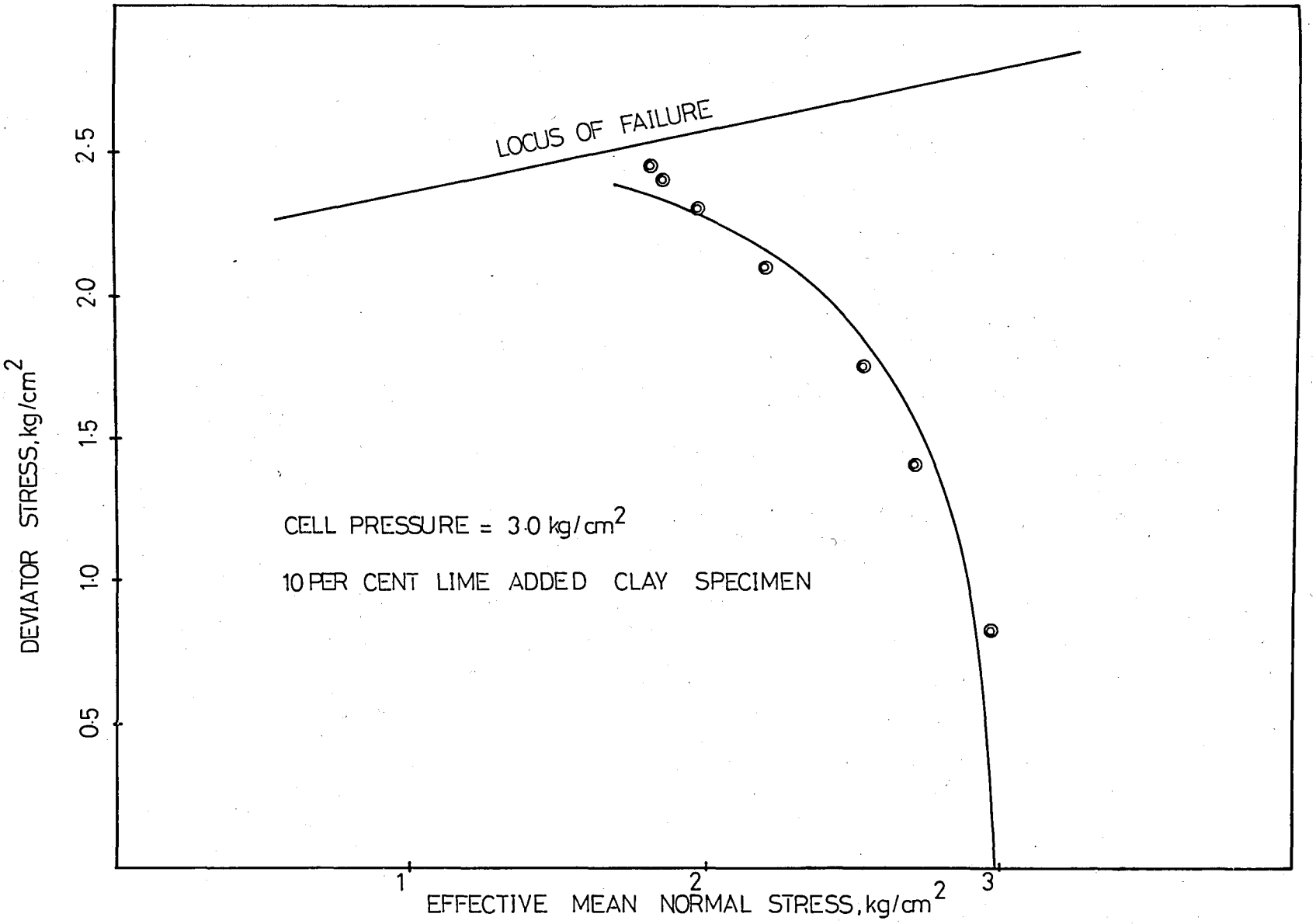

FIG.5.20 Stress Path in q:p' Space for Consolidated-Undrained Triaxial Test on 10% Lime-Added Sample

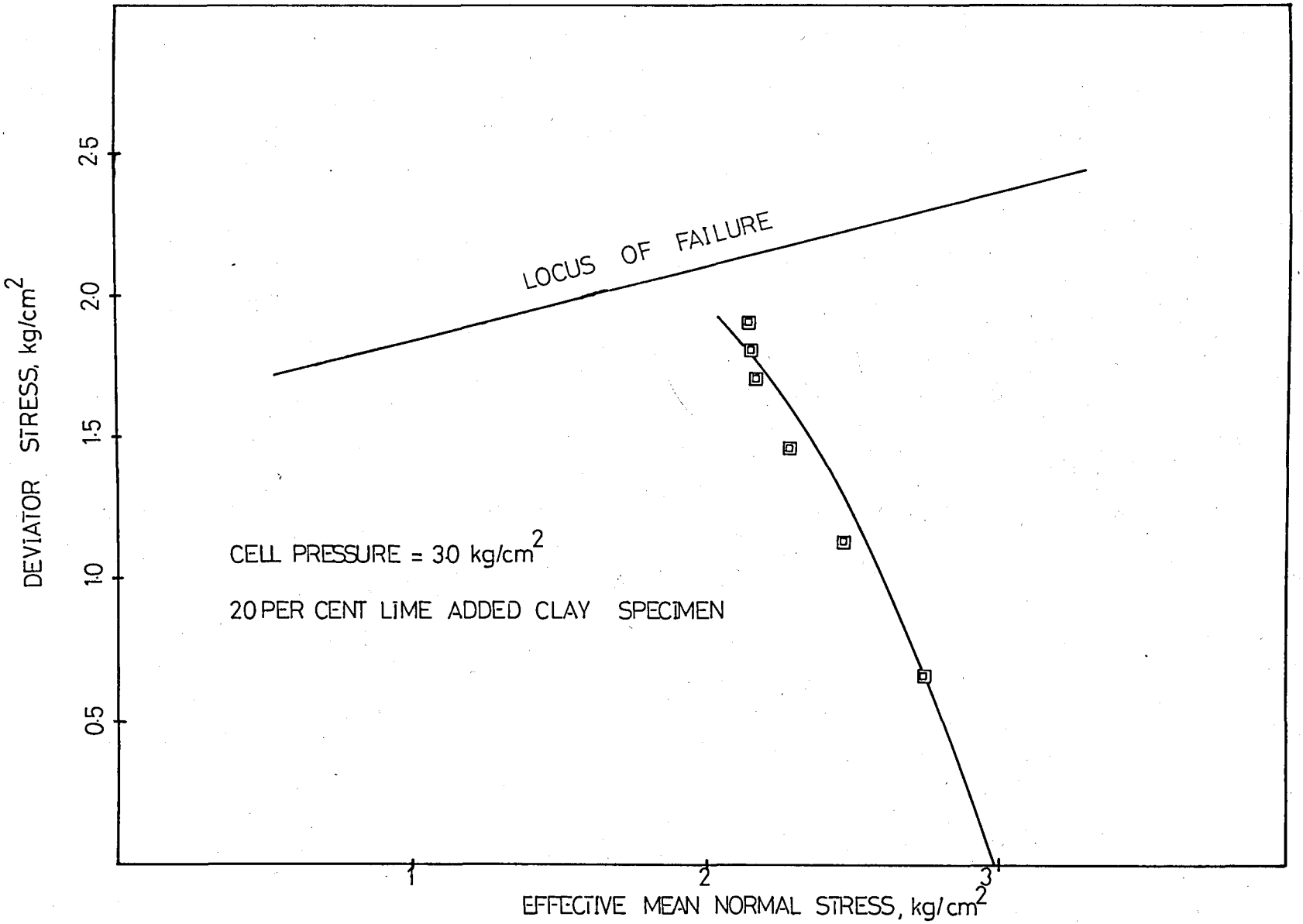

FIG.5.21 Stress Path in q:p' Space for Consolidated-Undrained Triaxial Test on 20% Lime-Added Sample

TABLE 5.2 Effect of Curing on Lime-treated Clay Specimens

Lime Content	q	σ_1	U	p	p'	q/p	q/p'	A_p	ε_f
%	kg/cm^2	kg/cm^2	kg/cm^2	kg/cm^2	kg/cm^2	-	-	-	-
0	1.69	4.69	1.35	3.566	2.216	0.473	0.762	0.798	0.107
5	2.00	5.00	2.15	3.663	1.513	0.546	1.321	1.075	0.119
5	*1.95*	*4.95*	*1.60*	*3.650*	*2.050*	*0.534*	*0.951*	*0.820*	*0.085*
10	2.40	5.40	2.55	3.801	1.251	0.631	1.917	0.062	0.138
10	*2.45*	*5.45*	*2.00*	*3.816*	*1.816*	*0.642*	*1.349*	*0.816*	*0.088*
20	2.00	5.00	2.05	3.667	1.617	0.545	1.236	1.025	0.134
20	*1.90*	*4.90*	*1.50*	*3.633*	*2.133*	*0.522*	*0.890*	*3.798*	*0.079*

*Inclined number indicates the values of cured samples.

5.2 SUMMARY

In this chapter, the behaviour of lime-treated and untreated clay specimens is evaluated in the light of critical state theory by using the data obtained from the isotropically consolidated-undrained triaxial compression tests. The following conclusions are deduced from the results of tests conducted in this research :

There is a significant strength increase in lime-stabilized clay samples, and this increase in strength may be due to the pozzolanic reaction of lime with soil, producing a cementing effect.

The stress strain behaviour of clay samples under lood, both lime-treated and untreated, is nonlinear.

The pore-pressure change behaviour of clay samples are also found to be nonlinear and stress-dependent.

In the analyses of compacted lime-untreated clay samples in consolidated-undrained tests, confining pressure is found to be an important variable influencing the stress-strain behaviour and pore-pressure change properties; however it is not found to be an important variable in lime-stabilized clay samplesin the range of confining pressures applied to the specimens in this study.

From the analyses of stress paths in q:p' space and ν:ℓnp' space, it is seen that lime-stabilized clay samples, although they are tested under isotropically consolidated-undrained conditions, may not be considered as normally consolidated samples.

VI. CONCLUSIONS

In this experimental study, the behaviour of lime-stabilized clay is investigated. For this purpose, a series of isotropically consolidated-undrained triaxial compression tests are carried out on lime-treated and untreated clay samples. Lime, which is used as a stabilization material, is mixed with clayey soil, and lime percentages are chosen to be 5,10 and 20, respectively : Each group of specimens having 5,10 and 20 per cent lime, and specimens having no lime, are subjected to different confining pressures such as 2.0 kg/cm^2, 2.5 kg/cm^2, 3.0 kg/cm^2, 3.5 kg/cm^2, 4.0 kg/cm^2 and 5.0 kg/cm^2 in consolidation process. Effect of lime content on the mechanical properties of lime-treated clayey soil is evaluated from the viewpoint of Critical State Theory.

From previous studies and results of tests carried out in this research, the following conclusions are obtained :

1) The electrical forces acting between clay particles are most responsible for soil strength in compacted clay.

2) The addition of lime produces a high concentration of

calcium ions in the double layer around the clay particles, hence decreasing the attraction for water.

3) The strength characteristics of wet clay is improved when proper amount of lime is added. This improvement in strength may be due partly to the improvement in plastic properties of the clay and partly to the pozzolanic reaction of lime with soil, which produces a cemented material that increases the strength with time.

4) Lime-treated clayey soil, in general, have greater strength and higher modulus of elasticity than untreated soil. The stress-strain behaviour of both lime-treated and untreated clay is nonlinear.

5) The pore-pressure change behaviour of clay and lime-stabilized clay are also found to be nonlinear and stress-dependent.

6) From the analyses of compacted lime-untreated clay samples in consolidated-undrained tests, confining pressure is found to be an important variable influencing the stress-strain behaviour and pore-pressure change properties; however it is seen that confining pressure is not an important variable for lime-stabilized clay samples in the range of pressures applied tothe specimens in this study.

7) In the analyses of stress paths in q:p' space and ν:ℓnp' space for lime-treated clay cpecimens, it is seen that those specimens, although they are tested under isotropically consolidated-undrained

conditions, may not be considered as normally consolidated specimens.

8) The specimens fail when they reach a certain line in the space "Locus of Failure".

9) The projection of "Locus of Failure" on the q:p' surface is a straight line. The slope of it is constant, but the intersection point changes with relation to lime content.

10) The projection of "Locus of Failure" on the $v : \ell n p'$ space is a curved line. It tends to become parallel to the Normal Consolidation Line at high confining pressures. The greater horizontal distance of "Locus of Failure" from the Normal Consolidation Line at low confining pressures indicate higher pore water pressures being developed during tests.

REFERENCES

1. Allam, Mehter Mohamed, and Sridharan Asuri, "*Effect of Wetting and Drying on Shear Strength,*" Journal of the Geotechnical Engineering Division, ASCE, Vol.107, No.GT4, Proc.Paper 16178, April, 1981, pp.421-438

2. Atkinson, J.H., and Bransby, P.L., *"The Mechanics of Soils; An Introduction to Critical State Soil Mechanics,"* Mc Graw-Hill Book Co., London, 1978.

3. Bishop, A.W., *"The Use of Pore Pressure Coefficients in Practice,"* Geotechnique, Vol.4, No.4, December, 1954, pp. 147-152.

4. Bishop, W.Alan, and Henker, D.J., *The Measurement of Soil Properties in the Triaxial Test,"* Edward Arnold Book Co., London, 1962.

5. Bowles, E.Joseph, *Physical and Geotechnical Properties of Soils,"* Mc Graw-Hill Book Co., New York, 1979.

6. Diamond, S., and Kinter, B.Earl, *"Mechanism of Soil-Lime Stabilization; An Interpretive Review,"* Highway Research Record, No.92, 1965, pp.83-96

7. Eades, L. James, Nichols, F.P., and Grim, E. Ralph, *"Formation of New Minerals with Lime Stabilization as Proven by Field Experiments in Virginia,"* Highway Research Board, Bull. 335, 1962, pp.31-39.

8. Hilt, G. Harrison, and Davidson, D.T., *Lime Fixation in Clayey Soils,* Highway Research Board, Bull. 262, 1960, pp. 20-32.

9. Jumikis, A.R., *"Soils Mechanics,"* D. Van Nostrand Book Co, New York, 1962.

10. Ladd, C.C., Moh, Z.C., and Lambe, T.W., *Recent Soil-Lime Research at the Massachusetts Institute of Technology,"* Highway Research Board, Bull. 262, 1960, pp. 64-85.

11. Lambe, T.William, *"The Structure of Compacted Clay,"* Journal of the Soil Mechanics and Foundations Division, ASCE, Vol. 84, No.SM2, Paper 1654, May, 1958, pp. 1-34.

12. Lambe, T. Willam, *The Engineering Behaviour of Compacted Clay,"* Journal of the Soil Mechanics and Foundations Division, ASCE, Vol 84, No.SM2, Paper 1655, May, 1958, pp. 1-35.

13. Mitchell, K.James, *"Fundamental Aspects of Thixotropy in Soils,"* Journal of the Soil Mechanics and Foundations Division, ASCE, Vol. 86, No. SM3, June, 1960, pp. 19-52.

14. Moh, Z. Chieh, *Soil Stabilization with Cement and Lime Additives,"* Journal of the Soil Mechanics and Foundations Division, ASCE, Vol.88, No. SM6, December, 1962, pp. 81-105.

15. Moh, Z. Chieh, *"Reactions of Soil Minerals with Cement and Chemicals,"*

Highway Research Record, No. 86, 1964, pp. 39-61.

16. Mohamed, A. Jan, and Walker, D. Richard, *"Effect of Lime, Moisture and Compaction on a Clay Soil,"* Highway Research Record, No. 29, 1963, pp. 1-13.

17. Noorany, I, and Seed, H. Bolton, *"In-Situ Strength Characteristics of Soft Clays,"* Journal of the Soil Mechanics and Foundations Division, ASCE, Vol. 91, No. SM2, March, 1965, pp. 49-80.

18. Parry, R.H.G., *"Triaxial Compression and Extension Tests on Remoulded Saturated Clay,"* Geotechnique, Vol. 10, 1960, pp.166-180.

19. Roscoe, K.H., Schofield, A.N., and Wroth, C.P., *"On the Yielding of Soils,"* Geotechnique, Vol. 8, No.1, March, 1958, pp.22-53.

20. Schofield, A., and Wroth, P., *"Critical State Soil Mechanics,"* McGraw-Hill Book, Co., London, 1968.

21. Scott, F. Ronald, *"Principles of Soil Mechanics,"* Addison-Wesley Publishing Co., Massachusetts, 1963.

22. Seed, H.B., and Chan, C.K., *Structure and Strength Characteristics of Compacted Clays,"* Journal of the Soil Mechanics and Foundations Division, ASCE, Vol, 85, No. SM5, October, 1959, pp. 87-128.

23. Seed, H.B., Mitchell, J.K., and Chan, C.K., *"The Strength of Compacted Cohesive Soils,"* Proceedings of Research Conference on Shear Strength of Cohesive Soils, Boulder, Colorado, ASCE, 1960, pp. 877-964.

24. Skempton, A.W., *"Pore Pressure Coefficients A and B,"* Geotechnique

Vol.4, No. 4, December, 1954, pp. 143-147.

25. Skempton, A.W., *"Correspondence on 'The Pore-Pressure Coefficient in Saturated Soils',"* Geotechnique, Vol. 10, No. 4, December, 1960, pp. 186-187.

26. Thompson, R. Marshall, *"Shear Strength and Elastic Properties of Lime-Soil Mixtures,"* Highway Research Record, No.139, 1966, pp. 1-14.

27. Thompson, R. Marshall, *"Factors Influencing the Plasticity and Strength of Lime-Soil Mixtures,"* University of Illinois Bulletin, Vol. 64,No.100, April, 1967, pp. 1-19.

28. Wang, W.H. Jerry, Mateos, M., and Davidson, T. Donald, *Comparative Effects of Hydraulic, Calcitic and Dolomitic Limes and Cement in Soil Stabilization,"* Highway Research Record, No.29, 1963, pp. 42-54.

APPENDICES

APPENDIX A

TEST DATA

TABLE A.1.1 Results of Isotropically Consolidated-Undained Triaxial Test

(Cell Pressure = 2.0 kg/cm^2)

F	ε_α	A'	q	σ_1	U	p	p'	q/p	q'/p'	A_p
kg	-	cm^2	kg/cm^2	kg/cm^2	kg/cm^2	kg/cm^2	kg/cm^2	-	-	-
4.716	$1.31*10^{-3}$	11.350	0.415	2.415	0.10	2.138	2.038	0.194	0.203	0.240
6.757	$1.97*10^{-3}$	11.357	0.594	2.954	0.13	2.198	2.068	0.287	0.287	0.210
8.163	$3.94*10^{-3}$	11.380	0.717	2.717	0.32	2.239	1.919	0.373	0.373	0.446
9.070	$7.89*10^{-3}$	11.425	0.793	2.793	0.60	2.264	1.664	0.350	0.476	0.756
10.432	0.015	11.517	0.905	2.905	0.65	2.301	1.651	0.393	0.548	0.718
10.929	0.019	11.563	0.945	2.945	0.69	2.315	1.625	0.408	0.581	0.730
11.564	0.030	11.689	0.989	2.989	0.86	2.329	1.469	0.424	0.673	0.869
12.017	0.039	11.980	1.018	3.018	0.86	2.339	1.479	0.435	0.688	0.844
12.698	0.052	11.965	1.061	3.061	0.95	2.353	1.424	0.450	0.745	0.895
13.559	0.061	12.082	1.122	3.122	0.95	2.374	1.424	0.472	0.787	0.846
13.605	0.065	12.133	1.121	3.121	0.95	2.373	1.423	0.472	0.787	0.847
13.695	0.070	12.193	1.123	3.123	0.98	2.374	1.394	0.473	0.805	0.872
13.922	0.075	12.254	1.136	3.136	1.00	2.378	1.378	0.477	0.824	0.880
14.375	0.078	12.307	1.168	3.168	1.00	2.389	1.389	0.488	0.840	0.856
14.602	0.086	12.413	1.176	3.176	1.00	2.392	1.392	0.491	0.844	0.850
15.195	0.096	12.530	1.212	3.212	1.02	2.404	1.384	0.504	0.875	0.841
15.872	0.103	12.650	1.254	3.254	1.03	2.418	1.388	0.518	0.903	0.821
16.601	0.110	12.743	1.302	3.302	1.05	2.434	1.384	0.534	0.94	0.806
16.556	0.117	12.838	1.289	3.289	1.05	2.429	1.379	0.530	0.934	0.814
16.556	0.122	12.915	1.281	3.281	1.05	2.427	1.377	0.527	0.93	0.819
16.556	0.128	13.013	1.272	3.272	1.05	2.424	1.374	0.524	0.925	0.825

TABLE A.1.2 Results of Isotropically Consolidated-Undrained Triaxial Test

(Cell Pressure = 2.5 kg/cm^2)

F	ε_α	A'	q	σ_1	U	p	p'	q/p	q'/p'	A_p
3.855	$1.84*10^{-3}$	11.356	0.339	2.839	0.10	2.613	2.513	0.129	0.138	0.294
5.125	$5.26*10^{-3}$	11.395	0.449	2.949	0.15	2.650	2.500	0.169	0.179	0.334
6.758	0.013	11.486	0.558	3.088	0.30	2.696	2.396	0.218	0.245	0.510
7.711	0.017	11.531	0.668	3.168	0.45	2.722	2.272	0.245	0.294	0.673
8.618	0.024	11.618	0.741	3.241	0.60	2.747	2.147	0.269	0.345	0.809
9.480	0.030	11.689	0.811	3.311	0.62	2.770	2.150	0.292	0.377	0.764
9.978	0.035	11.752	0.849	3.349	0.65	2.783	2.133	0.305	0.398	0.765
10.432	0.039	11.801	0.883	3.383	0.75	2.794	2.044	0.316	0.431	0.849
10.976	0.044	11.858	0.925	3.425	0.85	2.808	1.958	0.329	0.472	0.918
11.929	0.053	12.001	0.994	3.494	0.87	2.831	1.961	0.351	0.506	0.875
12.654	0.060	12.065	1.041	3.541	0.92	0.847	1.927	0.365	0.540	0.883
13.380	0.069	12.176	1.098	3.598	0.95	2.866	1.916	0.383	0.572	0.865
13.607	0.073	12.237	1.111	3.611	1.00	2.870	1.870	0.387	0.593	0.900
14.061	0.078	12.307	1.142	3.642	1.05	2.88	1.830	0.396	0.623	0.919
14.514	0.085	12.395	1.170	3.670	1.10	2.890	1.790	0.404	0.653	0.940
15.195	0.092	12.485	1.217	3.717	1.12	2.905	1.785	0.418	0.681	0.920
15.512	0.101	12.613	1.229	3.729	1.15	2.909	1.759	0.422	0.698	0.935
16.238	0.111	12.762	1.272	3.772	1.15	2.924	1.774	0.435	0.716	0.904
16.601	0.119	12.867	1.290	3.790	1.15	2.930	1.780	0.440	0.724	0.891
17.686	0.125	12.950	1.360	3.860	1.18	2.955	1.775	0.460	0.766	0.867
18.143	0.131	13.052	1.390	3.890	1.18	2.963	1.783	0.469	0.779	0.848
18.593	0.138	13.152	1.410	3.910	1.19	2.971	1.781	0.474	0.791	0.843
19.050	0.140	13.180	1.440	3.940	1.20	2.981	1.781	0.483	0.808	0.833
19.954	0.153	13.397	1.480	3.980	1.20	2.996	1.796	0.493	0.823	0.810
18.143	0.161	13.520	1.340	3.840	1.20	2.947	1.747	0.454	0.767	0.895

TABLE A.1.4 Results of Isotropically Consolidated-Undrained Triaxial Test
(Cell Pressure = 3.5 kg/cm^2)

F	ε_α	A'	q	σ_1	U	p	p'	q/p	q'/p'	A_p	q/pei	U/Pei
kg	-	cm^2	kg/cm^2	kg/cm^2	kg/cm^2	kg/cm^2	kg/cm^2	-	-	-	-	-
5.215	$1.26*10^{-3}$	10.447	0.499	3.999	0.10	3.666	3.566	0.136	0.140	0.20	0.146	0.029
8.163	$6.31*10^{-3}$	10.500	0.777	4.277	0.22	3.759	3.539	0.206	0.219	0.283	0.228	0.064
10.339	0.017	10.614	0.974	4.474	0.42	3.824	3.404	0.254	0.286	0.431	0.286	0.123
11.246	0.021	10.662	1.054	4.554	0.45	3.851	3.401	0.273	0.309	0.426	0.310	0.132
12.017	0.027	10.732	1.119	4.619	0.52	3.873	3.353	0.288	0.333	0.464	0.329	0.152
12.698	0.031	10.774	1.178	4.678	0.65	3.892	3.242	0.302	0.363	0.551	0.346	0.191
14.285	0.042	10.894	1.311	4.811	0.78	3.937	3.157	0.332	0.415	0.594	0.385	0.229
14.738	0.046	10.945	1.346	4.846	0.85	3.948	3.098	0.340	0.434	0.631	0.395	0.250
15.600	0.054	11.040	1.413	4.913	1.00	3.971	2.971	0.355	0.475	0.707	0.415	0.294
16.507	0.063	11.137	1.482	4.982	1.10	3.994	2.894	0.371	0.512	0.742	0.435	0.323
17.686	0.073	11.266	1.569	5.069	1.22	4.023	2.803	0.390	0.559	0.777	0.461	0.358
18.143	0.080	11.343	1.600	5.100	1.32	4.033	2.713	0.396	0.589	0.825	0.470	0.388
18.593	0.085	11.413	1.629	5.129	1.35	4.043	2.693	0.402	0.604	0.828	0.479	0.397
19.228	0.093	11.509	1.670	5.170	1.35	4.056	2.706	0.411	0.616	0.808	0.491	0.397
20.316	0.099	11.581	1.754	5.254	1.40	4.084	2.684	0.429	0.653	0.798	0.515	0.411
20.543	0.102	11.630	1.766	5.266	1.40	4.088	2.688	0.431	0.656	0.792	0.519	0.411
21.087	0.109	11.721	1.800	5.300	1.45	4.099	2.649	0.439	0.679	0.805	0.529	0.426
21.677	0.118	11.830	1.830	5.330	1.45	4.110	2.660	0.445	0.687	0.792	0.538	0.426
21.649	0.126	11.941	1.838	5.338	1.50	4.105	2.605	0.447	0.705	0.816	0.540	0.441
22.440	0.132	12.020	1.860	5.360	1.50	4.122	2.622	0.451	0.709	0.806	0.547	0.441
22.900	0.139	12.110	1.880	5.380	1.50	4.130	2.630	0.455	0.714	0.797	0.552	0.441
21.667	0.145	12.200	1.770	5.270	1.50	4.092	2.595	0.432	0.682	0.847	0.520	0.441

TABLE A.1.5 Results of Isotropically Consolidated-Undrained Triaxial Test

(Cell Pressure = 4.0 kg/cm^2)

F	ε_α	A'	q	σ_1	U	p	p'	q/p	q'/p'	Ap	q/pei	U/pei
kg	-	cm^2	kg/cm^2	kg/cm^2	kg/cm^2	kg/cm^2	kg/cm^2	-	-	-	-	-
4.081	$6.41*10^{-4}$	9.517	0.428	4.428	0.05	4.14	4.092	0.103	0.104	0.116	0.115	0.013
5.669	$1.28*10^{-3}$	9.523	0.595	4.595	0.10	4.198	4.098	0.141	0.145	0.168	0.160	0.027
6.757	$2.56*10^{-3}$	9.535	0.708	4.708	0.20	4.236	4.036	0.167	0.175	0.282	0.191	0.054
7.632	$3.85*10^{-3}$	9.547	0.799	4.799	0.28	4.266	3.986	0.187	0.200	0.350	0.215	0.075
8.888	$7.70*10^{-3}$	9.584	0.927	4.927	0.55	4.309	3.759	0.215	0.246	0.593	0.250	0.148
10.432	0.012	9.634	1.082	5.082	0.90	4.360	3.460	0.248	0.267	0.831	0.292	0.243
11.428	0.016	9.672	1.181	5.181	0.95	4.393	3.440	0.268	0.342	0.804	0.319	0.256
12.335	0.020	9.710	1.270	5.270	1.05	4.423	3.373	0.287	0.376	0.826	0.343	0.283
12.698	0.025	9.761	1.300	5.300	1.22	4.433	3.213	0.293	0.404	0.938	0.351	0.329
14.375	0.033	9.839	1.461	5.461	1.30	4.487	3.187	0.325	0.458	0.889	0.394	0.351
15.195	0.038	9.886	1.537	5.537	1.40	4.512	3.112	0.340	0.493	0.910	0.415	0.378
15.645	0.042	9.931	1.575	5.575	1.42	4.525	3.105	0.348	0.507	0.901	0.425	0.383
16.601	0.048	9.998	1.660	5.660	1.50	4.553	3.053	0.364	0.543	0.903	0.448	0.405
17.233	0.053	10.050	1.714	5.714	1.50	4.571	3.071	0.374	0.558	0.875	0.463	0.405
17.641	0.059	10.100	1.746	5.746	1.50	4.582	3.082	0.381	0.566	0.859	0.471	0.405
18.321	0.066	10.190	1.797	5.797	1.52	4.599	3.079	0.390	0.583	0.845	0.485	0.410
18.593	0.070	10.230	1.817	5.817	1.57	4.605	3.035	0.394	0.598	0.864	0.491	0.424
19.273	0.077	10.300	1.871	5.871	1.57	4.623	3.053	0.404	0.612	0.839	0.505	0.424
19.591	0.082	10.362	1.890	5.890	1.60	4.630	3.030	0.408	0.623	0.846	0.510	0.432
20.490	0.089	10.450	1.960	5.960	1.60	4.653	3.053	0.421	0.641	0.816	0.540	0.432
21.087	0.094	10.500	2.000	6.000	1.62	4.669	3.049	0.428	0.655	0.810	0.540	0.437
21.450	0.100	10.569	2.020	6.020	1.62	4.676	3.056	0.431	0.660	0.801	0.545	0.437
21.541	0.105	10.629	2.026	6.026	1.62	4.675	3.055	0.433	0.663	0.800	0.547	0.437
22.131	0.112	10.722	2.062	6.062	1.65	4.687	3.037	0.439	0.678	0.800	0.557	0.445

TABLE A.1.6 Results of Isotropically Consolidated-Undrained Triaxial Test
(Cell Pressure = 5.0 kg/cm^2)

F	ε_α	A'	q	σ_1	U	p	p'	q/p	q'/p'	A_p	q/pei	U/pei
kg	-	cm^2	kg/cm^2	kg/cm^2	kg/cm^2	kg/cm^2	kg/cm^2	-	-	-	-	-
6.394	$3.91*10^{-3}$	11.380	0.561	5.561	0.05	5.187	5.137	0.108	0.109	0.089	0.124	0.011
10.929	$7.89*10^{-3}$	11.425	0.956	5.956	0.70	5.138	4.618	0.179	0.207	0.732	0.212	0.155
13.060	0.013	11.486	1.137	6.137	0.82	5.379	4.559	0.211	0.249	0.721	0.252	0.182
14.058	0.017	11.531	1.219	6.219	0.95	5.406	4.456	0.225	0.273	0.779	0.270	0.211
15.464	0.023	11.610	1.331	6.331	1.20	5.443	4.242	0.244	0.313	0.901	0.295	0.266
16.688	0.030	11.689	1.427	6.427	1.30	5.475	4.175	0.260	0.341	0.911	0.317	0.288
18.140	0.039	11.801	1.537	6.537	1.35	5.512	4.162	0.278	0.369	0.878	0.341	0.300
19.273	0.047	11.900	1.619	6.619	1.40	5.539	4.139	0.292	0.391	0.864	0.359	0.311
20.400	0.056	12.015	1.697	6.697	1.50	5.565	4.065	0.304	0.417	0.883	0.377	0.333
21.541	0.063	12.100	1.780	6.780	1.50	5.593	4.093	0.318	0.434	0.842	0.395	0.333
22.220	0.069	12.185	1.823	6.823	1.50	5.607	4.107	0.325	0.443	0.822	0.405	0.333
23.808	0.076	12.271	1.940	6.940	1.55	5.646	4.096	0.343	0.473	0.798	0.431	0.344
24.035	0.082	12.359	1.944	6.944	1.55	5.648	4.098	0.344	0.474	0.797	0.432	0.344
24.579	0.089	12.449	1.974	6.974	1.62	5.658	4.038	0.348	0.488	0.820	0.438	0.360
24.942	0.096	12.539	1.989	6.989	1.67	5.663	3.993	0.351	0.498	0.839	0.442	0.371
25.396	0.102	12.631	2.010	7.010	1.70	5.670	3.970	0.354	0.506	0.845	0.446	0.377
26.303	0.109	12.725	2.067	7.067	1.75	5.689	3.939	0.363	0.524	0.846	0.459	0.388
26.801	0.115	12.819	2.090	7.090	1.80	5.696	3.896	0.366	0.536	0.861	0.464	0.400
28.117	0.122	12.915	2.177	7.177	1.80	5.725	3.925	0.380	0.554	0.826	0.483	0.400
30.157	0.135	13.112	2.300	7.300	1.85	5.766	3.916	0.398	0.587	0.804	0.511	0.411

TABLE A.2.1 Results of Isotropically Consolidated-Undrained Triaxial Test for Clay Having 5 per cent lime (Cell Pressure = 2.0 kg/cm^2)

F	ϵ_α	A'	q	σ_1	U	p	p'	q/p	q'/p'	A_p
kg	-	cm^2	kg/cm^2	kg/cm^2	kg/cm^2	kg/cm^2	kg/cm^2	-	-	-
5.215	$1.26*10^{-3}$	10.412	0.5	2.5	0.10	2.166	2.066	0.230	0.241	0.20
8.163	$6.30*10^{-3}$	10.471	0.779	2.779	0.32	2.259	1.939	0.344	0.401	0.41
10.432	0.016	10.575	0.986	2.986	0.60	2.328	1.728	0.423	0.570	0.608
11.428	0.021	10.629	1.075	3.075	0.68	2.358	1.678	0.455	0.640	0.632
11.929	0.027	10.694	1.115	3.115	0.75	2.371	1.621	0.470	0.687	0.672
12.698	0.031	10.738	1.182	3.182	0.82	2.394	1.574	0.493	0.750	0.693
14.285	0.037	10.805	1.322	3.322	0.95	2.440	1.490	0.541	0.886	0.718
14.738	0.044	10.884	1.354	3.354	1.05	2.451	1.401	0.552	0.966	0.775
15.645	0.050	10.953	1.428	3.428	1.25	2.476	1.226	0.576	1.164	0.875
16.688	0.056	11.023	1.513	3.513	1.35	2.504	1.154	0.604	1.310	0.892
17.686	0.069	11.177	1.582	3.582	1.45	2.527	1.077	0.626	1.468	0.916
18.143	0.075	11.249	1.612	3.612	1.55	2.537	0.987	0.635	1.632	0.961
18.593	0.081	11.323	1.642	3.642	1.60	2.547	0.947	0.644	1.733	0.974
19.050	0.088	11.410	1.669	3.669	1.67	2.556	0.886	0.652	1.882	1.000
19.591	0.094	11.485	1.705	3.705	1.75	2.568	0.818	0.663	2.084	1.026
20.316	0.100	11.562	1.757	3.757	1.80	2.585	0.785	0.679	2.236	1.024
20.543	0.107	11.652	1.763	3.763	1.82	2.587	0.767	0.681	2.296	1.032
21.087	0.113	11.738	1.796	3.796	1.85	2.598	0.748	0.691	2.398	1.030
21.450	0.119	11.811	1.816	3.816	1.87	2.605	0.735	0.697	2.470	1.029
21.677	0.123	11.865	1.826	3.826	1.90	2.608	0.708	0.700	2.575	1.040
21.768	0.129	11.959	1.820	3.820	1.92	2.606	0.686	0.698	2.650	1.054
22.440	0.134	12.016	1.860	3.860	1.95	2.622	0.672	0.709	2.765	1.048

TABLE A.2.2 Results of Isotropically Consolidated-Undrained Triaxial Test for Clay Having 5 per cent lime (Cell Pressure = 2.5 kg/cm^2)

F	ε_α	A'	q	σ_1	U	p	p'	q/p	q'/p'	A_p
kg	-	cm^2	kg/cm^2	kg/cm^2	kg/cm^2	kg/cm^2	kg/cm^2	-	-	-
4.760	$1.26*10^{-3}$	10.476	0.454	2.954	0.10	2.651	2.551	0.171	0.177	0.220
6.212	$2.52*10^{-3}$	10.489	0.592	3.092	0.30	2.697	2.397	0.219	0.246	0.506
8.616	$6.30*10^{-3}$	10.529	0.818	3.318	0.40	2.772	2.372	0.295	0.344	0.488
10.430	0.012	10.596	0.984	3.484	0.55	2.828	2.278	0.347	0.431	0.558
12.470	0.018	10.664	1.690	3.569	0.85	2.889	2.090	0.404	0.573	0.727
13.380	0.025	10.731	1.246	3.746	1.00	2.915	1.915	0.427	0.650	0.802
14.285	0.031	10.797	1.323	3.823	1.20	2.941	1.741	0.449	0.759	0.907
15.640	0.037	10.865	1.439	3.939	1.30	2.979	1.679	0.483	0.856	0.903
16.550	0.044	10.944	1.512	4.012	1.40	3.000	1.600	0.504	0.942	0.925
17.686	0.050	11.013	1.605	4.105	1.55	3.035	1.485	0.528	1.080	0.965
18.143	0.054	11.062	1.640	4.140	1.65	3.046	1.396	0.538	1.174	1.000
19.050	0.060	11.137	1.710	4.210	1.70	3.070	1.370	0.557	1.248	0.994
20.316	0.068	11.227	1.809	4.309	1.77	3.103	1.333	0.582	1.356	0.978
21.087	0.073	11.288	1.868	4.368	1.85	3.122	1.272	0.598	1.468	0.990
21.677	0.079	11.365	1.907	4.407	1.88	3.135	1.255	0.608	1.518	0.985
21.949	0.088	11.472	1.913	4.413	1.92	3.137	1.217	0.609	1.570	1.000
22.170	0.034	11.555	1.918	4.418	1.95	3.139	1.189	0.611	1.612	1.016
22.850	0.100	11.625	1.965	4.465	1.95	3.155	1.205	0.622	1.630	0.992
23.000	0.107	11.716	1.963	4.463	2.00	3.154	1.154	0.622	1.700	1.018

TABLE A.2.3 Results of Isotropically Consolidated-Undrained Triaxial Test for Clay Having 5 per cent lime (Cell Pressure = 3.0 kg/cm^2)

F	ϵ_α	A'	q	σ_1	U	p	p'	q/p	q'/p'	A_p	q/pei	U/pei
kg	-	cm^2	kg/cm^2	kg/cm^2	kg/cm^2	kg/cm^2	kg/cm^2	-	-	-	-	-
3.855	$6.30*10^{-4}$	10.469	0.368	3.368	0.02	3.120	3.100	0.117	0.118	0.054	0.136	$7.4*10^{-3}$
5.896	$1.26*10^{-3}$	10.476	0.562	3.562	0.05	3.187	3.137	0.176	0.179	0.088	0.208	0.018
6.757	$2.52*10^{-3}$	10.489	0.644	3.644	0.10	3.214	3.114	0.200	0.206	0.155	0.238	0.037
7.711	$3.78*10^{-3}$	10.502	0.734	3.734	0.15	3.244	3.094	0.226	0.237	0.204	0.271	0.055
10.432	0.012	10.596	0.984	3.984	0.45	3.328	2.878	0.295	0.341	0.457	0.364	0.167
11.428	0.016	10.633	1.074	4.074	0.52	3.358	2.838	0.319	0.378	0.484	0.397	0.192
12.335	0.020	10.676	1.155	4.155	0.68	3.385	2.705	0.341	0.426	0.588	0.427	0.251
13.380	0.025	10.731	1.246	4.246	0.88	3.415	2.535	0.364	0.491	0.706	0.461	0.325
14.285	0.031	10.817	1.320	4.320	1.05	3.440	2.390	0.383	0.520	0.795	0.488	0.388
15.645	0.041	10.910	1.434	4.434	1.25	3.478	2.228	0.412	0.643	0.871	0.531	0.462
16.556	0.047	10.989	1.506	4.506	1.35	3.582	2.152	0.430	0.699	0.896	0.557	0.500
17.233	0.052	11.048	1.550	4.550	1.45	3.519	2.069	0.440	0.748	0.935	0.574	0.537
17.686	0.058	11.107	1.590	4.590	1.60	3.530	1.930	0.450	0.823	1.000	0.588	0.592
18.143	0.065	11.197	1.620	4.620	1.62	3.540	1.920	0.457	0.843	1.000	0.600	0.600
18.593	0.069	11.242	1.643	4.643	1.70	3.551	1.851	0.462	0.887	1.030	0.608	0.629
19.591	0.075	11.311	1.732	4.732	1.75	3.577	1.827	0.484	0.947	1.010	0.641	0.648
20.316	0.081	11.385	1.780	4.780	1.80	3.594	1.794	0.495	0.992	0.391	0.659	0.666
21.087	0.107	11.716	1.800	4.800	2.05	3.600	1.550	0.500	1.161	1.138	0.666	0.759
21.677	0.113	11.795	1.830	4.830	2.10	3.612	1.512	0.506	1.209	1.147	0.677	0.777
21.949	0.117	11.849	1.850	4.850	2.10	3.617	1.517	0.511	1.219	1.130	0.685	0.777
22.440	0.119	11.876	1.890	4.890	2.12	3.629	1.509	0.520	1.251	1.121	0.700	0.785
22.901	0.126	11.971	1.910	4.910	2.15	3.637	1.487	0.527	1.284	1.125	0.707	0.796
23.350	0.131	12.042	1.940	4.940	2.15	3.646	1.496	0.532	1.296	1.108	0.718	0.796
23.940	0.134	12.090	1.980	4.980	2.15	3.660	1.510	0.540	1.311	1.085	0.733	0.796
24.170	0.138	12.138	2.000	5.000	2.15	3.663	1.513	0.546	1.321	1.075	0.740	0.796

TABLE A.2.4 Results of Isotropically Consolidated-Undrained Triaxial Test for Clay Having 5 per cent Lime (Cell Pressure = 3.5 kg/cm^2)

F	ε_α	A'	q	σ_1	U	p	p'	q/p	q'/p'	A_p	q/pei	U/pei
kg	-	cm^2	kg/cm^2	kg/cm^2	kg/cm^2	kg/cm^2	kg/cm^2	kg/cm^2	-	-	-	-
6.757	3.78*10^{-3}	10.559	0.640	4.140	0.20	3.713	3.513	0.172	0.182	0.312	0.203	0.063
9.520	6.30*10^{-3}	10.586	0.900	4.400	0.30	3.800	3.500	0.236	0.257	0.333	0.285	0.095
10.976	8.82*10^{-3}	10.613	1.030	4.530	0.40	3.844	3.444	0.267	0.300	0.388	0.326	0.126
11.929	0.01	10.627	1.122	4.622	0.45	3.874	3.424	0.284	0.327	0.401	0.356	0.142
12.698	0.012	10.654	1.191	4.691	0.55	3.897	3.347	0.305	0.355	0.461	0.378	0.174
14.285	0.016	10.691	1.336	4.836	0.65	3.945	3.295	0.338	0.405	0.486	0.424	0.206
14.738	0.020	10.736	1.372	4.872	0.75	3.957	3.207	0.346	0.427	0.546	0.435	0.238
15.464	0.025	10.789	1.433	4.933	0.85	3.977	3.127	0.360	0.458	0.593	0.454	0.269
16.688	0.030	10.848	1.538	5.038	1.00	4.012	3.012	0.383	0.510	0.650	0.488	0.317
17.686	0.037	10.924	1.619	5.119	1.15	4.039	2 889	0.400	0.560	0.710	0.513	0.365
18.140	0.044	11.000	1.649	5.149	1.25	4.049	2.800	0.407	0.588	0.758	0.523	0.396
18.820	0.050	11.070	1.700	5.200	1.35	4.066	2.716	0.418	0.625	0.794	0.539	0.428
19.050	0.056	11.144	1.709	5.209	1.40	4.069	2.669	0.420	0.640	0.819	0.542	0.444
19.590	0.063	11.227	1.744	5.244	1.50	4.081	2.581	0.427	0.675	0.860	0.553	0.476
20.316	0.069	11.300	1.797	5.297	1.55	4.099	2.549	0.438	0.704	0.862	0.570	0.492
21.677	0.075	11.372	1.906	5.406	1.62	4.135	2.515	0.460	0.757	0.850	0.605	0.514
21.949	0.081	11.447	1.917	5.417	1.70	4.139	2.439	0.463	0.785	0.886	0.608	0.539
22.440	0.098	11.662	1.924	5.424	2.05	4.141	2.091	0.464	0.920	1.065	0.610	0.650
23.000	0.103	11.733	1.960	5.460	2.10	4.153	2.053	0.471	0.954	1.071	0.622	0.666
23.580	0.113	11.860	1.988	5.488	2.20	4.162	1.962	0.477	1.012	1.106	0.631	0.698
24.035	0.119	11.951	2.010	5.501	2.25	4.170	1.920	0.482	1.046	1.119	0.638	0.714
24.480	0.126	12.038	2.030	5.503	2.30	4.177	1.877	0.485	1.081	1.133	0.644	0.730
24.940	0.129	12.090	2.060	5.506	2.30	4.187	1.887	0.491	1.091	1.116	0.653	0.730
26.520	0.138	12.214	2.170	5.670	2.30	4.223	1.923	0.513	1.127	1.059	0.688	0.730
24.940	0.145	12.304	2.020	5.520	2.30	4.175	1.875	0.483	1.076	1.138	0.641	0.730
24.030	0.151	12.390	1.939	5.439	2.30	4.146	1.846	0.467	1.050	1.186	0.615	0.730

TABLE A.2.5 Results of Isotropically Consolidated-Undrained Triaxial Test for Clay Having 5 per cent Lime (Cell Pressure = 4.0 kg/cm^2)

F	ϵ_α	A'	q	σ_1	U	p	p'	q/p	q'/p'	A_p	q/pei	U/pei
kg	-	cm^2	kg/cm^2	kg/cm^2	kg/cm^2	kg/cm^2	kg/cm^2	-	-	-	-	-
2.490	$1.26*10^{-3}$	10.583	0.235	4.235	0.05	4.078	4.028	0.057	0.058	0.212	0.050	0.010
5.830	$8.82*10^{-3}$	10.613	0.550	4.550	0.50	4.183	3.683	0.131	0.149	0.909	0.117	0.106
9.190	0.016	10.691	0.860	4.860	0.80	4.286	3.486	0.200	0.246	0.930	0.182	0.170
10.432	0.021	10.745	0.970	4.970	0.90	4.323	3.423	0.224	0.283	0.927	0.206	0.191
13.270	0.029	10.834	1.225	5.225	1.20	4.408	3.208	0.277	0.381	0.979	0.260	0.255
15.645	0.037	10.924	1.432	5.432	1.40	4.477	3.077	0.319	0.465	0.977	0.304	0.297
18.260	0.050	11.070	1.650	5.650	1.65	4.549	2.899	0.362	0.568	1.000	0.351	0.351
19.591	0.056	11.144	1.757	5.757	1.85	4.585	2.735	0.383	0.642	1.052	0.373	0.393
21.110	0.066	11.263	1.875	5.875	1.95	4.624	2.674	0.405	0.700	1.040	0.398	0.414
21.949	0.075	11.372	1.930	5.930	2.00	4.643	2.643	0.415	0.730	1.036	0.410	0.425
23.250	0.084	11.484	2.020	6.020	2.05	4.674	2.624	0.432	0.769	1.014	0.429	0.436
23.440	0.092	11.585	2.023	6.023	2.20	4.674	2.474	0.432	0.817	1.087	0.430	0.468
24.035	0.097	11.650	2.060	6.060	2.20	4.687	2.487	0.439	0.828	1.067	0.438	0.468
24.420	0.104	11.741	2.080	6.080	2.25	4.693	2.443	0.443	0.851	1.081	0.442	0.478
24.820	0.110	11.820	2.100	6.100	2.25	4.699	2.449	0.446	0.857	1.071	0.446	0.478
25.350	0.118	11.927	2.120	6.120	2.30	4.708	2.408	0.450	0.880	1.084	0.451	0.489
25.580	0.126	12.038	2.125	6.125	2.35	4.708	2.358	0.451	0.901	1.105	0.452	0.500
27.420	0.145	12.300	2.230	6.230	2.40	4.743	2.343	0.470	0.951	1.076	0.474	0.510

TABLE A.2.6 Results of Isotropically Consolidated-Undrained Triaxial Test for Clay Having 5 per cent Lime (Cell Pressure = 5.0 kg/cm^2)

F	ε_α	A'	q	σ_1	U	p	p'	q/p	q'/p'	A_p	q/pei	U/pei
kg	-	cm^2	kg/cm^2	kg/cm^2	kg/cm^2	kg/cm^2	kg/cm^2	-	-	-	-	-
2.49	$6.30*10^{-3}$	10.412	0.239	5.239	0.10	5.079	4.979	0.047	0.047	0.418	0.039	0.016
7.256	$1.26*10^{-3}$	10.419	0.696	5.696	0.25	5.232	4.982	0.133	0.139	0.359	0.114	0.040
10.976	$3.78*10^{-3}$	10.445	1.050	6.050	0.35	5.350	5.000	0.196	0.209	0.333	0.172	0.057
13.370	$9.45*10^{-3}$	10.505	1.272	6.272	0.50	5.424	4.924	0.234	0.258	0.393	0.208	0.081
14.285	0.012	10.538	1.355	6.355	0.65	5.451	4.801	0.248	0.282	0.479	0.222	0.106
14.738	0.016	10.579	1.393	6.393	0.85	5.464	4.614	0.254	0.301	0.610	0.228	0.139
16.552	0.022	10.647	1.554	6.554	1.10	5.518	4.418	0.281	0.351	0.707	0.254	0.180
18.140	0.029	10.716	1.692	6.692	1.40	5.564	4.164	0.304	0.406	0.827	0.277	0.229
19.050	0.035	10.786	1.766	6.766	1.75	5.588	3.838	0.316	0.460	0.990	0.289	0.286
20.634	0.044	10.884	1.895	6.895	1.75	5.631	3.881	0.336	0.488	0.923	0.310	0.286
21.949	0.050	10.953	2.000	7.000	1.85	5.667	3.817	0.352	0.523	0.925	0.327	0.303
23.000	0.056	11.023	2.080	7.080	2.00	5.695	3.695	0.365	0.562	0.961	0.340	0.327
24.040	0.063	11.106	2.160	7.160	2.00	5.721	3.721	0.377	0.580	0.925	0.354	0.327
24.940	0.069	11.177	2.230	7.230	2.15	5.743	3.593	0.388	0.620	0.964	0.365	0.352
25.486	0.075	11.249	2.260	7.260	2.20	5.755	3.555	0.392	0.635	0.973	0.370	0.360
27.070	0.081	11.323	2.300	7.300	2.25	5.767	3.517	0.398	0.653	0.978	0.377	0.368
26.530	0.088	11.410	2.320	7.320	2.30	5.775	3.475	0.401	0.667	0.991	0.380	0.377
26.980	0.094	11.485	2.340	7.340	2.35	5.783	3.433	0.404	0.681	1.004	0.383	0.385
27.210	0.100	11.562	2.350	7.350	2.40	5.784	3.384	0.406	0.694	1.021	0.385	0.393
27.250	0.107	11.652	2.340	7.340	2.50	5.779	3.279	0.404	0.713	1.068	0.383	0.409
27.890	0.113	11.738	2.370	7.370	2.55	5.792	3.242	0.409	0.731	1.075	0.388	0.418
28.340	0.119	11.822	2.390	7.390	2.60	5.799	3.199	0.412	0.747	0.087	0.391	0.426
28.790	0.126	11.906	2.420	7.420	2.62	5.806	3.186	0.416	0.759	1.082	0.396	0.429
29.380	0.129	11.959	2.450	7.450	2.64	5.818	3.178	0.421	0.830	1.077	0.401	0.432
30.380	0.134	12.029	2.530	7.530	2.65	5.841	3.191	9.433	0.792	1.047	0.414	0.434

TABLE A.3.1 Results of Isotropically Consolidated-Undrained Triaxial Test for Clay Having 10 per cent Lime (Cell Pressure = 2.0 kg/cm^2)

F	ε_α	A'	q	σ_1	U	p	p'	q/p	q'/p'	A_p
kg	-	cm^2	kg/cm^2	kg/cm^2	kg/cm^2	kg/cm^2	kg/cm^2	-	-	-
3.401	$1.26*10^{-3}$	10.476	0.324	2.324	0.15	2.108	2.008	0.153	0.161	0.462
6.800	$8.82*10^{-3}$	10.556	0.644	2.644	0.45	2.214	1.764	0.290	0.364	0.698
9.520	0.016	10.633	0.895	2.895	0.75	2.298	1.548	0.389	0.578	0.837
11.420	0.021	10.687	1.069	3.069	0.90	2.356	1.456	0.453	0.734	0.841
15.192	0.037	10.775	1.410	3.410	1.30	2.469	1.169	0.571	1.205	0.921
16.100	0.041	10.910	1.475	3.475	1.40	2.491	1.091	0.592	1.350	0.949
17.233	0.046	10.967	1.571	3.571	1.50	2.523	1.023	0.622	1.534	0.954
18.140	0.054	11.060	1.640	3.640	1.60	2.546	0.946	0.644	1.732	0.975
19.228	0.059	11.119	1.729	3.729	1.65	2.576	0.926	0.671	1.866	0.954
20.180	0.066	11.202	1.800	3.800	1.75	2.600	0.850	0.692	2.116	0.972
21.080	0.071	11.262	1.871	3.871	1.75	2.623	0.873	0.713	2.140	0.935
21.949	0.079	11.360	1.932	3.932	1.85	2.644	0.794	0.730	2.433	0.957
23.350	0.084	11.422	2.040	4.040	1.90	2.681	0.781	0.760	2.610	0.931
24.030	0.093	11.535	2.083	4.083	2.00	2.694	0.694	0.773	3.000	0.960
24.940	0.097	11.586	2.152	4.152	2.15	2.717	0.567	0.792	3.791	0.999
25.849	0.104	11.677	2.210	4.210	2.20	2.737	0.537	0.807	4.108	0.995
26.300	0.109	11.742	2.240	4.240	2.24	2.746	0.496	0.815	4.510	1.004
26.530	0.113	11.795	2.249	4.249	2.30	2.749	0.449	0.818	5.000	1.022
26.620	0.118	11.862	2.244	4.244	2.40	2.748	0.348	0.816	6.447	1.069
26.980	0.126	11.971	2.253	4.253	2.45	2.751	0.301	0.818	7.478	1.087
27.390	0.132	12.054	2.270	4.270	2.48	2.757	0.277	0.823	8.182	1.092
27.890	0.134	12.081	2.300	4.300	2.48	2.769	0.289	0.830	7.943	1.078
28.110	0.142	12.201	2.304	4.304	2.50	2.767	0.267	0.832	8.597	1.085
28.340	0.145	12.237	2.320	4.320	2.50	2.771	0.271	0.837	8.530	1.077

TABLE A.3.2 Results of Isotropically Consolidated-Undrained Triaxial Test for Clay Having 10 per cent Lime (Cell Pressure = 2.5 kg/cm^2)

F	ε_α	A'	q	σ_1	U	p	p'	q/p	q'/p'	A_p
kg	-	cm^2	kg/cm^2	kg/cm^2	kg/cm^2	kg/cm^2	kg/cm^2	kg/cm^2	-	-
2.89	$1.26*10^{-3}$	10.533	0.275	2.775	0.20	2.591	2.391	0.106	0.114	0.727
7.25	$2.52*10^{-3}$	10.546	0.688	3.188	0.60	2.729	2.129	0.252	0.323	0.872
11.45	0.012	10.654	1.075	3.575	1.20	2.858	1.658	0.376	0.648	1.116
13.57	0.016	10.691	1.270	3.770	1.55	2.923	1.373	0.434	0.924	1.220
15.19	0.021	10.745	1.413	3.913	1.92	2.971	1.051	0.475	1.344	1.358
17.23	0.029	10.834	1.590	4.090	2.05	3.030	0.980	0.524	1.622	1.289
18.94	0.034	10.890	1.740	2.240	2.15	3.079	0.929	0.565	1.872	1.235
19.52	0.041	10.969	1.780	4.280	2.20	3.093	0.893	0.575	1.992	1.235
21.70	0.050	11.073	1.960	4.460	2.38	3.153	0.773	0.621	2.534	1.214
21.94	0.054	11.120	1.973	4.473	2.38	3.157	0.777	0.624	2.537	1.206
22.13	0.059	11.179	1.979	4.479	2.45	3.159	0.709	0.626	2.787	1.237
22.67	0.075	11.372	2.100	4.600	2.50	3.164	0.664	0.663	3.160	1.190
22.90	0.079	11.422	2.000	4.500	2.50	3.168	0.668	0.631	2.992	1.250
23.12	0.095	11.624	1.980	4.480	2.50	3.162	0.662	0.626	2.986	1.262
23.35	0.098	11.662	2.000	4.500	2.50	3.167	0.667	0.631	2.996	1.250
23.88	0.100	11.688	2.270	4.770	2.50	3.181	0.681	0.713	3.333	1.101
26.80	0.105	11.754	2.280	4.780	2.50	3.260	0.760	0.700	3.000	1.096
27.11	0.109	11.806	2.300	4.800	2.50	3.265	0.765	0.704	3.000	1.086
27.87	0.113	11.860	2.350	4.850	2.50	3.283	0.783	0.715	3.000	1.063

TABLE A.3.3 Results of Isotropically Consolidated-Undrained Triaxial Test for Clay Having 10 per cent Lime (Cell Pressure = 3.0 kg/cm^2)

F	ϵ_α	A'	q	σ_1	U	p	p'	q/p	q'/p'	A_p	q/pei	U/pei
kg	-	cm^2	kg/cm^2	kg/cm^2	kg/cm^2	kg/cm^2	kg/cm^2	-	-	-	-	-
3.40	$1.26*10^{-3}$	10.533	0.32	3.32	0.10	3.107	3.007	0.103	0.107	0.310	0.131	0.040
11.14	$8.82*10^{-3}$	10.613	1.05	4.05	0.60	3.349	2.749	0.313	0.381	0.571	0.428	0.244
12.92	0.016	10.691	1.20	4.20	0.85	3.402	2.552	0.352	0.470	0.708	0.489	0.346
16.10	0.021	10.745	1.49	4.49	0.95	3.499	2.549	0.425	0.584	0.637	0.608	0.387
18.63	0.029	10.834	1.72	4.72	1.10	3.572	2.472	0.481	0.695	0.639	0.702	0.448
20.18	0.037	10.924	1.84	4.84	1.40	3.615	2.215	0.508	0.830	0.760	0.751	0.571
21.08	0.044	11.004	1.91	4.91	1.45	3.638	2.188	0.525	0.872	0.759	0.779	0.591
21.59	0.050	11.073	1.95	4.95	1.60	3.649	2.049	0.534	0.951	0.820	0.795	0.653
22.22	0.056	11.144	1.99	4.99	1.70	3.664	1.964	0.543	1.012	0.854	0.812	0.693
22.45	0.063	11.227	2.00	5.00	1.80	3.666	1.866	0.545	1.071	0.900	0.816	0.734
22.60	0.069	11.300	2.00	5.00	1.90	3.666	1.766	0.545	1.132	0.950	0.816	0.775
23.00	0.075	11.372	2.01	5.01	2.00	3.674	1.674	0.547	1.200	0.995	0.820	0.816
23.67	0.081	11.447	2.06	5.06	2.10	3.689	1.589	0.558	1.296	1.019	0.840	0.857
24.35	0.088	11.530	2.11	5.11	2.10	3.703	1.603	0.569	1.315	0.995	0.861	0.857
25.57	0.094	11.610	2.20	5.20	2.15	3.734	1.584	0.589	1.388	0.977	0.897	0.877
26.29	0.100	11.688	2.25	5.25	2.20	3.749	1.549	0.600	1.451	0.977	0.918	0.897
26.98	0.107	11.780	2.29	5.29	2.25	3.763	1.513	0.608	1.513	0.982	0.934	0.918
27.38	0.109	11.806	2.32	5.32	2.25	3.773	1.523	0.614	1.523	0.969	0.946	0.918
28.11	0.113	11.860	2.37	5.37	2.30	3.790	1.490	0.625	1.590	0.970	0.967	0.938
28.29	0.119	11.940	2.37	5.37	2.40	3.789	1.389	0.625	1.705	1.012	0.967	0.979
28.27	0.126	12.030	2.37	5.37	2.45	3.783	1.333	0.626	1.777	1.033	0.967	1.000
28.79	0.132	12.120	2.37	5.37	2.50	3.791	1.291	0.625	1.834	1.054	0.967	1.020
29.25	0.134	12.160	2.40	5.40	2.55	3.801	1.251	0.631	1.917	1.062	0.979	1.040

TABLE A.3.4 Results of Isotropically Consolidated - Undrained Triaxial Test for Clay Having 10 per cent Lime (Cell Pressure = 3.5 kg/cm^2)

F	ϵ_α	A'	q	σ_1	U	p	p'	q/p	q'/p'	A_p	q/pei	U/pei
kg	-	cm^2	kg/cm^2	kg/cm^2	kg/cm^2	kg/cm^2	kg/cm^2	-	-	-	-	-
2.490	$6.30*10^{-4}$	10.526	0.236	3.736	0.10	3.578	3.478	0.065	0.067	0.423	0.077	0.032
7.256	$1.26*10^{-3}$	10.533	0.688	4.188	0.25	3.729	3.479	0.184	0.197	0.363	0.225	0.081
10.976	$3.78*10^{-3}$	10.559	1.039	4.539	0.35	3.846	3.496	0.270	0.297	0.336	0.340	0.114
13.370	$9.45*10^{-3}$	10.620	1.258	4.758	0.55	3.919	3.369	0.321	0.373	0.437	0.412	0.180
14.510	0.012	10.654	1.360	4.860	0.75	3.953	3.203	0.344	0.424	0.551	0.445	0.245
16.507	0.018	10.712	1.540	5.040	0.90	4.013	3.113	0.383	0.494	0.584	0.504	0.295
18.143	0.025	10.789	1.681	5.181	1.25	4.060	2.810	0.414	0.598	0.743	0.551	0.409
19.228	0.031	10.856	1.771	5.271	1.45	4.090	2.640	0.433	0.670	0.818	0.580	0.475
20.720	0.037	10.924	1.896	5.396	1.50	4.132	2.632	0.458	0.720	0.791	0.621	0.491
21.813	0.044	11.000	1.983	5.483	1.65	4.160	2.510	0.476	0.789	0.832	0.650	0.540
22.900	0.050	11.070	2.068	5.568	1.75	4.189	2.439	0.493	0.847	0.846	0.678	0.573
23.670	0.056	11.144	2.120	5.620	1.90	4.208	2.308	0.503	0.918	0.896	0.695	0.622
24.260	0.063	11.227	2.160	5.660	1.90	4.220	2.320	0.511	0.930	0.879	0.708	0.622
24.919	0.069	11.300	2.205	5.705	2.10	4.235	2.135	0.520	1.032	0.952	0.722	0.688
25.486	0.075	11.372	2.240	5.740	2.10	4.247	2.147	0.527	1.043	0.937	0.734	0.688
25.849	0.081	11.447	2.258	5.758	2.10	4.252	2.152	0.531	1.048	0.930	0.740	0.688
26.300	0.088	11.535	2.280	5.780	2.30	4.260	1.960	0.535	1.163	0.008	0.747	0.754
26.520	0.094	11.618	2.280	5.780	2.35	4.260	1.910	0.535	1.193	1.030	0.747	0.770
26.750	0.100	11.688	2.288	5.788	2.40	4.262	1.862	0.536	1.228	1.048	0.750	0.786
26.980	0.107	11.780	2.290	5.790	2.40	4.263	1.863	0.537	1.228	1.048	0.750	0.786
27.250	0.113	11.860	2.290	5.790	2.45	4.265	1.815	0.536	1.261	1.069	0.750	0.803
27.890	0.119	11.940	2.330	5.830	2.50	4.278	1.778	0.544	1.310	1.072	0.763	0.819
28.340	0.126	12.030	2.350	5.850	2.50	4.285	1.785	0.548	1.316	1.063	0.770	0.819
28.790	0.128	12.070	2.380	5.880	2.55	4.295	1.745	0.554	1.363	1.071	0.780	0.836
29.380	0.131	12.100	2.430	5.930	2.60	4.309	1.709	0.563	1.421	1.069	0.796	0.852
27.890	0.145	12.300	2.260	5.760	2.60	4.255	1.655	0.531	1.465	1.150	0.740	0.852

TABLE A.3.5 Results of Isotropically Consolidated-Undrained Triaxial Test for Clay Having 10 per cent Lime (Cell Pressure = 4.0 kg/cm^2)

F	ε_α	A'	q	σ_1	U	p	p'	q/p	q'/p'	A_p	q/pei	U/pei
kg	-	cm^2	kg/cm^2	kg/cm^2	kg/cm^2	kg/cm^2	kg/cm^2	-	-	-	-	-
2.490	$6.30*10^{-4}$	10.469	0.237	4.237	0.10	4.079	3.979	0.058	0.059	0.421	0.046	0.019
7.256	$1.26*10^{-3}$	10.476	0.692	4.692	0.20	4.230	4.030	0.163	0.171	0.289	0.134	0.038
10.976	$3.78*10^{-3}$	10.502	1.045	5.045	0.40	4.348	3.948	0.240	0.264	0.382	0.202	0.077
13.370	$9.45*10^{-3}$	10.562	1.265	5.265	0.60	4.421	3.821	0.286	0.330	0.474	0.245	0.116
14.510	0.012	10.596	1.369	5.369	0.85	4.456	3.606	3.307	0.379	0.620	0.265	0.165
16.507	0.016	10.637	1.551	5.551	1.00	4.517	3.517	0.343	0.440	0.644	0.301	0.194
18.140	0.023	10.719	1.692	5.692	1.20	4.564	3.364	0.370	0.502	0.709	0.328	0.233
19.228	0.030	10.789	1.782	5.782	1.40	4.594	3.194	0.387	0.557	0.785	0.346	0.271
20.720	0.036	10.860	1.907	5.907	1.50	4.635	3.135	0.411	0.608	0.786	0.370	0.291
21.813	0.045	10.960	1.990	5.990	1.75	4.663	2.913	0.426	0.683	0.879	0.386	0.339
22.900	0.051	11.033	2.075	6.075	1.90	4.691	2.791	0.442	0.743	0.915	0.402	0.368
23.670	0.058	11.107	2.131	6.131	2.00	4.710	2.710	0.452	0.786	0.938	0.413	0.388
24.260	0.065	11.197	2.166	6.166	2.10	4.722	2.622	0.458	0.826	0.969	0.420	0.407
24.940	0.073	11.288	2.209	6.209	2.15	4.736	2.586	0.466	0.854	0.973	0.428	0.417
25.486	0.080	11.381	2.239	6.239	2.20	4.746	2.546	0.471	0.879	0.982	0.434	0.427
25.849	0.088	11.746	2.252	6.252	2.30	4.750	2.450	0.474	0.918	1.021	0.437	0.446
26.300	0.093	11.539	2.279	6.279	2.40	4.759	2.359	0.478	0.965	1.053	0.442	0.466
26.520	0.099	11.620	2.282	6.282	2.40	4.760	2.360	0.479	0.966	1.051	0.443	0.466
27.390	0.104	11.686	2.343	6.343	2.40	4.781	2.381	0.490	0.983	1.024	0.454	0.466
27.430	0.110	11.769	2.330	6.330	2.45	4.776	2.326	0.487	1.001	1.051	0.452	0.475
27.890	0.118	11.870	2.340	6.340	2.50	4.783	2.283	0.489	1.024	1.068	0.454	0.485
28.340	0.126	11.971	2.360	6.360	2.60	4.789	2.189	0.492	1.078	1.101	0.458	0.504
28.790	0.132	12.059	2.380	6.380	2.60	4.795	2.195	0.496	1.084	1.092	0.462	0.504
29.930	0.134	12.094	2.470	6.470	2.60	4.824	2.224	0.512	1.110	1.052	0.479	0.504
30.150	0.138	12.148	2.482	6.482	2.60	4.827	2.227	0.514	1.114	1.057	0.481	0.504
30.380	0.142	12.201	2.490	6.490	2.60	4.829	2.229	0.515	1.117	1.044	0.483	0.504

TABLE A.3.6 Results of Isotropically Consolidated-Undrained Triaxial Test for Clay Having 10 per cent Lime (Cell Pressure = 5.0 kg/cm^2)

F	ε_α	A'	q	σ_1	U	p	p'	q/p	q'/p'	A_p	q/pei	U/pei
kg	-	cm^2	kg/cm^2	kg/cm^2	kg/cm^2	kg/cm^2	kg/cm^2	-	-	-	-	-
3.401	$1.26*10^{-3}$	10.476	0.324	5.324	0.10	5.108	5.008	0.063	0.064	0.308	0.053	0.016
5.660	$3.78*10^{-3}$	10.502	0.538	5.538	0.25	5.179	4.929	0.103	0.109	0.464	0.088	0.040
8.164	$8.82*10^{-3}$	10.556	0.773	5.773	0.50	5.257	4.757	0.147	0.162	0.646	0.126	0.081
9.520	0.012	10.596	0.898	5.898	0.70	5.299	4.599	0.169	0.195	0.779	0.147	0.114
11.420	0.018	10.654	1.071	6.071	0.90	5.357	4.457	0.199	0.240	0.840	0.175	0.147
13.370	0.025	10.731	1.245	6.245	1.10	5.415	4.315	0.229	0.288	0.883	0.204	0.180
15.192	0.031	10.797	1.407	6.407	1.30	5.469	4.169	0.257	0.337	0.923	0.230	0.213
16.550	0.037	10.865	1.523	6.523	1.50	5.507	4.007	0.276	0.380	0.984	0.249	0.245
18.360	0.044	10.944	1.677	6.677	1.60	5.559	3.959	0.301	0.423	0.954	0.274	0.262
20.271	0.050	11.010	1.841	6.841	1.70	5.613	3.913	0.327	0.470	0.923	0.301	0.278
21.677	0.056	11.083	1.955	6.955	1.90	5.651	3.751	0.345	0.521	0.971	0.320	0.311
23.350	0.065	11.190	2.086	7.086	2.05	5.695	3.645	0.366	0.572	0.982	0.341	0.336
25.390	0.078	11.348	2.230	7.230	2.20	5.745	3.545	0.388	0.628	0.986	0.365	0.360
25.849	0.085	11.444	2.258	7.258	2.35	5.752	3.402	0.392	0.663	1.040	0.370	0.385
26.620	0.093	11.535	2.307	7.307	2.42	5.769	3.349	0.399	0.688	1.048	0.378	0.396
27.250	0.100	11.625	2.344	7.344	2.50	5.781	3.281	0.405	0.714	1.066	0.384	0.409
27.890	0.105	11.690	2.385	7.385	2.55	5.795	3.245	0.411	0.734	1.069	0.390	0.418
27.980	0.113	11.795	2.370	7.370	2.60	5.790	3.190	0.409	0.742	1.097	0.388	0.426
28.340	0.119	11.876	2.380	7.380	2.65	5.795	3.145	0.410	0.756	1.113	0.390	0.434
28.790	0.126	11.970	2.400	7.400	2.65	5.801	3.151	0.413	0.761	1.104	0.393	0.434
29.250	0.129	12.020	2.430	7.430	2.65	5.811	3.161	0.418	0.768	1.090	0.398	0.434
29.930	0.132	12.050	2.480	7.480	2.65	5.827	3.177	0.425	0.780	1.068	0.406	0.434
28.790	0.138	12.148	2.369	7.369	2.65	5.789	3.139	0.409	0.754	1.118	0.388	0.434
27.890	0.145	12.237	2.279	7.279	2.65	5.759	3.109	0.395	0.732	1.162	0.373	0.434

TABLE A.4.1 Results of Isotropically Consolidated-Undrained Triaxial Test for Clay Having 20 per cent Lime (Cell Pressure = 2.0 kg/cm^2)

F kg	ε_α -	A' cm^2	q kg/cm^2	σ_1 kg/cm^2	U kg/cm^2	p kg/cm^2	p' kg/cm^2	q/p -	q'/p' -	A_p -
5.215	$1.26*10^{-3}$	10.476	0.497	2.497	0.10	2.165	2.065	0.229	0.240	0.201
7.256	$3.78*10^{-3}$	10.502	0.690	2.690	0.20	2.230	2.030	0.309	0.339	0.289
8.163	$6.30*10^{-3}$	10.529	0.775	2.775	0.30	2.258	1.958	0.343	0.395	0.387
8.800	$8.82*10^{-3}$	10.556	0.833	2.833	0.35	2.277	1.927	0.365	0.432	0.420
10.339	0.017	10.643	0.971	2.971	0.55	2.323	1.773	0.417	0.547	0.566
10.838	0.018	10.654	1.017	3.017	0.55	2.339	1.789	0.434	0.568	0.540
12.017	0.027	10.753	1.117	3.117	0.85	2.372	1.522	0.470	0.733	0.760
12.698	0.031	10.797	1.176	3.176	0.90	2.392	1.492	0.491	0.788	0.765
13.695	0.037	10.865	1.260	3.260	1.00	2.420	1.420	0.520	0.887	0.793
14.285	0.042	10.921	1.308	3.308	1.10	2.436	1.336	0.536	0.979	0.840
15.192	0.050	11.013	1.379	3.379	1.20	2.459	1.259	0.560	1.094	0.870
16.099	0.059	11.119	1.447	3.447	1.40	2.482	1.082	0.582	1.336	0.967
17.233	0.068	11.226	1.535	3.535	1.50	2.511	1.011	0.611	1.517	0.977
17.686	0.073	11.286	1.567	3.567	1.55	2.522	0.972	0.621	1.612	0.989
18.143	0.080	11.372	1.595	3.595	1.60	2.531	0.931	0.630	1.713	1.003
18.593	0.085	11.434	1.626	3.626	1.65	2.542	0.892	0.639	1.832	1.014
19.228	0.093	11.535	1.666	3.666	1.72	2.555	0.835	0.652	1.993	1.032
20.316	0.098	11.600	1.751	3.751	1.75	2.583	0.833	0.677	2.100	0.999
21.087	0.107	11.716	1.800	3.800	1.85	2.600	0.750	0.692	2.400	1.027
21.677	0.113	11.802	1.830	3.830	1.85	2.612	0.762	0.700	2.400	1.010
21.940	0.119	11.887	1.850	3.850	1.90	2.615	0.715	0.707	2.586	1.027

TABLE A.4.2 Results of Isotropically Consolidated-Undrained Triaxial Test for Clay Having 20 per cent Lime

(Cell Pressure = 2.5 kg/cm^2)

F	ε_α	A'	q	σ_1	U	p	p'	q/p	q'/p'	A_p
kg	-	cm^2	kg/cm^2	kg/cm^2	kg/cm^2	kg/cm^2	kg/cm^2	-	-	-
5.215	$1.26*10^{-3}$	10.533	0.495	2.995	0.05	2.500	2.450	0.198	0.202	0.101
7.256	$3.78*10^{-3}$	10.559	0.687	3.187	0.20	2.729	2.529	0.251	0.271	0.291
8.163	$7.56*10^{-3}$	10.600	0.770	3.270	0.40	2.756	2.356	0.279	0.326	0.519
8.800	0.012	10.654	0.825	3.325	0.55	2.775	2.225	0.297	0.370	0.667
10.339	0.018	10.712	0.965	3.465	0.70	2.821	2.121	0.342	0.454	0.725
10.838	0.025	10.789	1.000	3.500	0.90	2.834	1.934	0.352	0.516	0.900
12.017	0.031	10.856	1.100	3.600	1.05	2.868	1.818	0.383	0.604	0.954
12.698	0.037	10.924	1.162	3.662	1.15	2.887	1.734	0.402	0.670	0.989
13.695	0.044	11.000	1.245	3.745	1.25	2.915	1.665	0.427	0.747	1.004
14.285	0.050	11.070	1.290	3.790	1.35	2.930	1.580	0.440	0.816	1.046
14.738	0.054	11.120	1.325	3.825	1.40	2.941	1.541	0.450	0.859	1.056
15.192	0.056	11.144	1.363	3.863	1.40	2.954	1.554	0.461	0.876	1.027
16.100	0.063	11.227	1.434	3.934	1.50	2.978	1.478	0.481	0.970	1.046
17.686	0.075	11.372	1.555	4.055	1.63	3.018	1.388	0.515	1.119	1.048
18.593	0.088	11.535	1.611	4.111	1.75	3.037	1.287	0.530	2.251	1.086
19.228	0.097	11.650	1.650	4.150	1.80	3.050	1.250	0.540	1.319	1.090
20.316	0.104	11.741	1.730	4.230	1.85	3.076	1.226	0.562	1.410	1.069
21.087	0.113	11.860	1.770	4.270	1.88	3.092	1.212	0.572	1.459	1.062
21.949	0.119	11.951	1.830	4.330	1.90	3.112	1.212	0.588	1.509	1.038
22.440	0.126	12.038	1.860	4.360	1.90	3.121	1.221	0.595	1.522	1.021
23.000	0.132	12.125	1.900	4.400	1.95	3.132	1.182	0.606	1.607	1.026
22.130	0.138	12.214	1.810	4.310	1.95	3.103	1.153	0.583	1.568	1.077

A.4.3 Results of Isotropically Consolidated-Undrained Triaxial Test for Clay Having 20 per cent Lime (Cell Pressure = 3.0 kg/cm^2)

F	ε_α	A'	q	σ_1	U	p	p'	q/p	q'/p'	A_p	q/p_{ei}	U/p_{ei}
kg	-	cm^2	kg/cm^2	kg/cm^2	kg/cm^2	kg/cm^2	kg/cm2	-	-	-	-	-
2.948	$126*10^{-3}$	10.476	0.281	3.281	0.05	3.093	3.043	0.090	0.092	0.177	0.106	0.018
3.855	$3.15*10^{-3}$	10.496	0.367	3.367	0.15	3.122	2.972	0.114	0.123	0.408	0.138	0.056
4.989	$5.04*10^{-3}$	10.516	0.474	3.474	0.25	3.158	2.908	0.150	0.162	0.527	0.178	0.094
6.439	$7.56*10^{-3}$	10.542	0.610	3.610	0.35	3.203	2.853	1.190	0.213	0.573	0.230	0.132
7.665	0.012	10.596	0.723	3.723	0.50	3.241	2.741	0.223	0.263	0.691	0.272	0.188
8.639	0.016	10.633	0.812	3.812	0.60	3.270	2.670	0.248	0.304	0.738	0.306	0.226
9.525	0.021	10.687	0.891	3.891	0.75	3.297	2.547	0.270	0.349	0.841	0.336	0.283
12.017	0.025	10.731	1.119	4.119	0.85	3.373	2.523	0.331	0.443	0.759	0.422	0.320
13.060	0.031	10.797	1.209	4.209	1.00	3.403	2.403	0.355	0.503	0.827	0.456	0.377
13.627	0.037	10.865	1.254	4.254	1.15	3.418	2.268	3.366	0.552	0.317	0.473	0.433
15.192	0.044	10.944	1.388	4.388	1.25	3.462	2.212	0.400	0.627	0.900	0.523	0.471
16.507	0.050	11.013	1.498	4.498	1.40	3.521	2.121	0.425	0.706	0.934	0.565	0.528
17.233	0.056	11.083	1.554	4.554	1.50	3.518	2.018	0.441	0.769	0.965	0.586	0.566
18.143	0.063	11.166	1.624	4.624	1.62	3.541	1.921	0.458	0.845	0.997	0.612	0.611
19.050	0.069	11.238	1.695	4.695	1.75	3.565	1.815	0.475	0.933	1.032	0.639	0.660
20.271	0.075	11.311	1.792	4.792	1.75	3.597	1.847	3.498	0.970	0.976	0.676	0.660
21.087	0.081	11.385	1.852	4.852	1.90	3.617	1.717	0.512	1.078	1.025	0.698	0.716
22.080	0.088	11.472	1.920	4.920	1.95	3.641	1.691	0.527	1.135	1.015	0.724	0.735
23.128	0.094	11.555	2.000	5.000	2.05	3.667	1.617	0.545	1.236	1.025	0.754	0.773
22.130	0.100	11.625	1.900	4.900	2.05	3.634	1.584	0.522	1.199	1.078	0.716	0.773
21.810	0.107	11.716	1.860	4.860	2.05	3.620	1.570	0.513	1.184	1.102	0.701	0.773

TABLE A.4.4 Results of Isotropically Consolidated-Undrained Triaxial Test for Clay Having 20 per cent Lime (Cell Pressure = 3.0 kg/cm^2)

F	ε_α	A'	q	σ_1	U	p	p'	q/p	q'/p'	A_p	q/Pei	U/Pei
kg	-	cm^2	kg/cm^2	kg/cm^2	kg/cm^2	kg/cm^2	kg/cm^2	-	-	-	-	-
4.760	$1.26*10^{-3}$	10.533	0.451	3.951	0.07	3.650	3.575	0.123	0.126	0.166	0.152	0.025
6.212	$2.52*10^{-3}$	10.546	0.589	4.089	0.10	3.696	3.596	0.159	0.163	0.169	0.199	0.033
8.616	$6.30*10^{-3}$	10.586	0.813	4.313	0.25	3.771	3.521	0.215	0.230	0.307	0.275	0.084
10.430	0.012	10.654	0.978	4.478	0.50	3.826	3.326	0.255	0.294	0.511	0.331	0.169
12.017	0.018	10.712	1.121	4.621	0.60	3.873	3.273	0.289	0.242	0.535	0.380	0.203
13.380	0.025	10.789	1.240	4.740	0.80	3.913	3.113	0.316	0.398	0.645	0.420	0.271
14.285	0.029	10.834	1.318	4.818	0.90	3.939	3.039	0.334	0.433	0.682	0.446	0.305
15.640	0.034	10.890	1.436	4.936	1.00	3.978	2.978	0.360	0.482	0.696	0.486	0.338
17.233	0.037	10.924	1.577	5.077	1.00	4.025	3.025	0.391	0.521	0.634	0.534	0.338
18.143	0.044	11.000	1.649	5.490	1.20	4.049	2.849	0.407	0.578	0.727	0.558	0.406
19.050	0.050	11.070	1.720	5.220	1.35	4.073	2.723	0.422	0.631	0.784	0.583	0.457
20.316	0.058	11.167	1.819	5.319	1.40	4.106	2.706	0.443	0.672	0.769	0.616	0.474
21.087	0.063	11.227	1.870	5.370	1.50	4.126	2.626	0.453	0.712	0.802	0.633	0.508
21.405	0.069	11.300	1.890	5.390	1.60	4.131	2.531	0.457	0.746	0.846	0.640	0.542
21.450	0.075	11.372	1.880	5.380	1.70	4.128	2.428	0.455	0.774	0.904	0.637	0.576
21.677	0.081	11.447	1.890	5.390	1.75	4.131	2.381	0.457	0.793	0.925	0.640	0.593
21.768	0.088	11.535	1.880	5.380	1.80	4.129	2.329	0.455	0.807	0.957	0.637	0.610
21.810	0.094	11.611	1.870	5.370	1.85	4.126	2.276	0.453	0.821	0.989	0.633	0.627
21.858	0.100	11.688	1.870	5.370	1.90	4.123	2.223	0.453	0.841	1.016	0.633	0.644
21.949	0.107	11.780	1.860	5.360	1.95	4.121	2.171	0.451	0.856	1.048	0.630	0.661
22.130	0.113	11.860	1.860	5.360	1.95	4.140	2.171	0.451	0.856	1.048	0.630	0.661
22.440	0.119	11.940	1.880	5.380	2.00	4.126	2.126	6.455	0.884	1.063	0.637	0.677
23.000	0.126	12.038	1.910	5.410	2.00	4.136	2.136	0.461	0.893	1.047	0.647	0.677
23.580	0.132	12.120	1.950	5.450	2.00	4.148	2.148	0.470	0.907	1.025	0.671	0.677
22.440	0.138	12.204	1.830	5.330	2.00	4.112	2.112	0.445	0.866	1.092	0.620	0.677
21.677	0.145	12.304	1.761	5.261	2.00	4.087	2.087	0.430	0.843	1.135	0.596	0.677

TABLE A.4.5 Results of Isotropically Consolidated-Undrained Triaxial Test for Clay Having 20 per cent Lime (Cell Pressure = 4.0 kg/cm^2)

F	ε_α	A'	q	σ_1	U	p	p'	q/p	q'/p'	A_p	q/pei	U/pei
kg	-	cm^2	kg/cm^2	kg/cm^2	kg/cm^2	kg/cm^2	kg/cm^2	-	-	-	-	-
4.308	$1.26*10^{-3}$	10.476	0.411	4.411	0.05	4.137	4.087	0.099	0.100	0.121	0.079	$9.7*10^{-3}$
6.212	$2.52*10^{-3}$	10.489	0.592	4.592	0.15	4.197	4.047	0.141	0.146	0.253	0.114	0.029
8.816	$6.40*10^{-3}$	10.529	0.818	4.818	0.20	4.272	4.072	0.191	0.200	0.244	0.158	0.038
10.976	0.012	10.596	1.035	5.035	0.40	4.345	3.945	0.238	0.262	0.386	0.200	0.077
12.017	0.018	10.654	1.127	5.127	0.55	4.375	3.825	0.257	0.294	0.488	0.218	0.106
14.285	0.025	10.731	1.331	5.331	0.75	4.443	3.693	0.290	0.360	0.563	0.258	0.145
15.600	0.031	10.797	1.444	5.444	0.90	4.481	3.581	0.322	0.403	0.623	0.280	0.174
16.779	0.037	10.865	1.544	5.544	1.10	4.514	3.414	0.342	0.452	0.712	0.299	0.213
17.913	0.044	10.944	1.636	5.636	1.20	4.545	3.345	0.359	0.489	0.733	0.317	0.233
18.820	0.050	11.013	1.708	5.708	1.40	4.569	3.169	0.373	0.538	0.819	0.331	0.271
19.954	0.056	11.083	1.800	5.800	1.45	4.600	3.150	0.391	0.571	0.805	0.349	0.281
21.087	0.063	11.166	1.888	5.888	1.60	4.629	3.029	0.407	0.623	0.847	0.366	0.310
21.541	0.069	11.238	1.916	5.916	1.70	4.638	2.938	0.413	0.651	0.887	0.372	0.330
22.312	0.075	11.311	1.972	5.972	1.75	4.657	2.907	0.423	0.678	0.887	0.382	0.339
22.901	0.081	11.385	2.010	6.010	1.85	4.670	2.820	0.430	0.712	0.920	0.390	0.359
23.350	0.088	11.472	2.020	6.020	1.90	4.678	2.778	0.431	0.727	0.940	0.392	0.368
23.580	0.094	11.550	2.028	6.028	2.00	4.680	2.680	0.433	0.756	0.986	0.393	0.388
23.670	0.102	11.661	2.029	6.029	2.05	4.676	2.626	0.433	0.772	1.010	0.393	0.398
23.940	0.107	11.716	2.030	6.030	2.05	4.681	2.631	0.433	0.771	1.009	0.394	0.398
24.170	0.118	11.870	2.037	6.037	2.10	4.678	2.578	0.435	0.789	1.030	0.395	0.407
23.940	0.126	11.971	2.000	6.000	2.10	4.666	2.566	0.428	0.779	1.050	0.388	0.407
23.350	0.132	12.059	1.936	5.936	2.10	4.645	2.545	0.416	0.760	1.084	0.375	0.407

TABLE A.4.6 Results of Isotropically Consolidated-Undrained Triaxial Test for Clay Having 20 per cent Lime (Cell Pressure = 5.0 kg/cm^2)

F	ε_α	A'	q	σ_1	U	p	p'	q/p	q'/p'	A_p	q/pei	U/pei
kg	-	cm^2	kg/cm^2	kg/cm^2	kg/cm^2	kg/cm^2	kg/cm^2	-	-	-	-	-
2.948	$6.30*10^{-4}$	10.412	0.283	5.283	0.05	5.094	5.044	0.055	0.056	0.176	0.041	$7.2*10^{-3}$
3.855	$1.26*10^{-3}$	10.419	0.369	5.369	0.10	5.123	5.023	0.072	0.073	0.271	0.053	0.014
4.989	$3.15*10^{-3}$	10.438	0.477	5.477	0.20	5.159	4.959	0.092	0.096	0.419	0.069	0.028
6.439	$7.56*10^{-3}$	10.485	0.614	5.614	0.30	5.204	4.904	0.117	0.125	0.488	0.088	0.043
7.665	0.011	10.521	0.728	5.728	0.45	5.242	4.792	0.138	0.151	0.618	0.105	0.065
8.639	0.014	10.559	0.818	5.818	0.60	5.272	4.672	0.155	0.175	0.733	0.118	0.086
9.525	0.020	10.620	0.896	5.896	0.70	5.298	4.598	0.169	0.194	0.781	0.129	0.101
10.838	0.025	10.675	1.015	6.015	0.80	5.338	4.538	0.190	0.223	0.788	0.147	0.115
12.017	0.030	10.730	1.119	6.119	0.95	5.373	4.423	0.208	0.252	0.848	0.162	0.137
13.060	0.036	10.800	1.209	6.209	1.10	5.403	4.303	0.223	0.280	0.909	0.175	0.159
13.627	0.041	10.857	1.255	6.255	1.20	5.418	4.218	0.231	0.297	0.956	0.181	0.173
15.192	0.053	10.995	1.381	6.381	1.40	5.460	4.060	0.252	0.340	1.013	0.200	0.202
15.872	0.058	11.054	1.435	6.435	1.45	5.478	4.028	0.261	0.356	1.010	0.207	0.210
16.507	0.063	11.106	1.486	6.486	1.55	5.495	3.945	0.270	0.376	1.043	0.215	0.224
17.233	0.068	11.166	1.543	6.543	1.70	5.514	3.814	0.279	0.404	1.101	0.223	0.246
18.143	0.074	11.242	1.613	6.613	1.75	5.537	3.787	0.291	0.425	1.084	0.233	0.253
19.050	0.080	11.319	1.683	6.683	1.80	5.561	3.761	0.302	0.447	1.069	0.243	0.260
20.271	0.087	11.397	1.778	6.778	1.90	5.592	3.692	0.317	0.481	1.068	0.257	0.275
21.087	0.093	11.476	1.837	6.837	1.95	5.612	3.662	0.327	0.501	1.061	0.266	0.282
21.994	0.097	11.533	1.907	6.907	2.00	5.635	3.635	0.338	0.524	1.048	0.276	0.289
23.128	0.105	11.630	1.988	6.988	2.07	5.662	3.587	0.351	0.554	1.043	0.288	0.300
24.040	0.113	11.738	2.048	7.048	2.10	5.682	3.582	0.360	0.571	1.025	0.296	0.304
24.489	0.118	11.805	2.075	7.075	2.15	5.691	3.541	0.364	0.585	1.036	0.300	0.311
24.040	0.122	11.856	2.020	7.020	2.15	5.675	3.525	0.355	0.572	1.064	0.292	0.311
23.128	0.126	11.907	1.940	6.940	2.15	5.647	3.497	0.380	0.554	1.108	0.281	0.311

APPENDIX B

$q : \varepsilon_\alpha$
$U : \varepsilon_\alpha$ CURVES

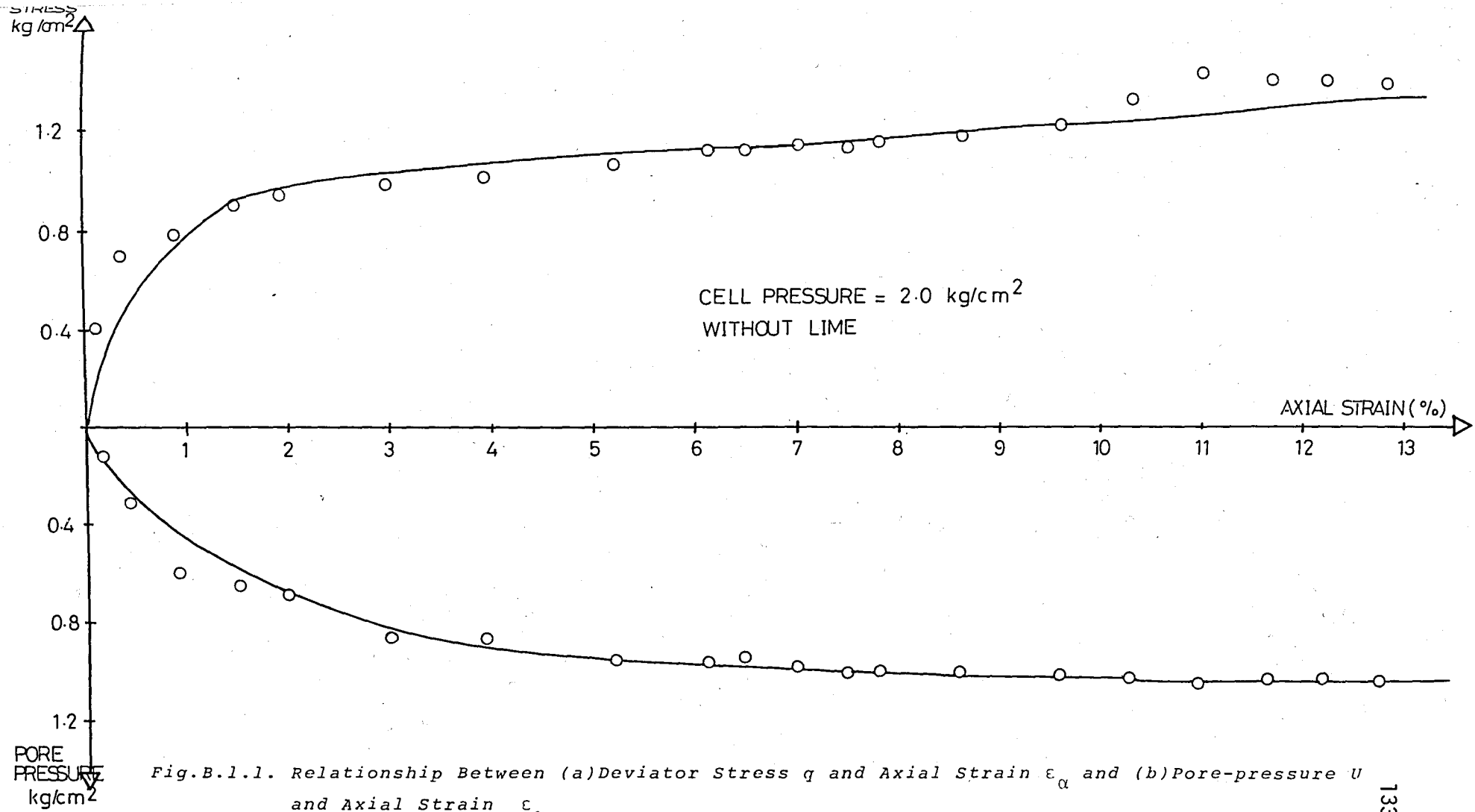

Fig.B.1.1. Relationship Between (a)Deviator Stress q and Axial Strain ε_α and (b)Pore-pressure U and Axial Strain ε_α

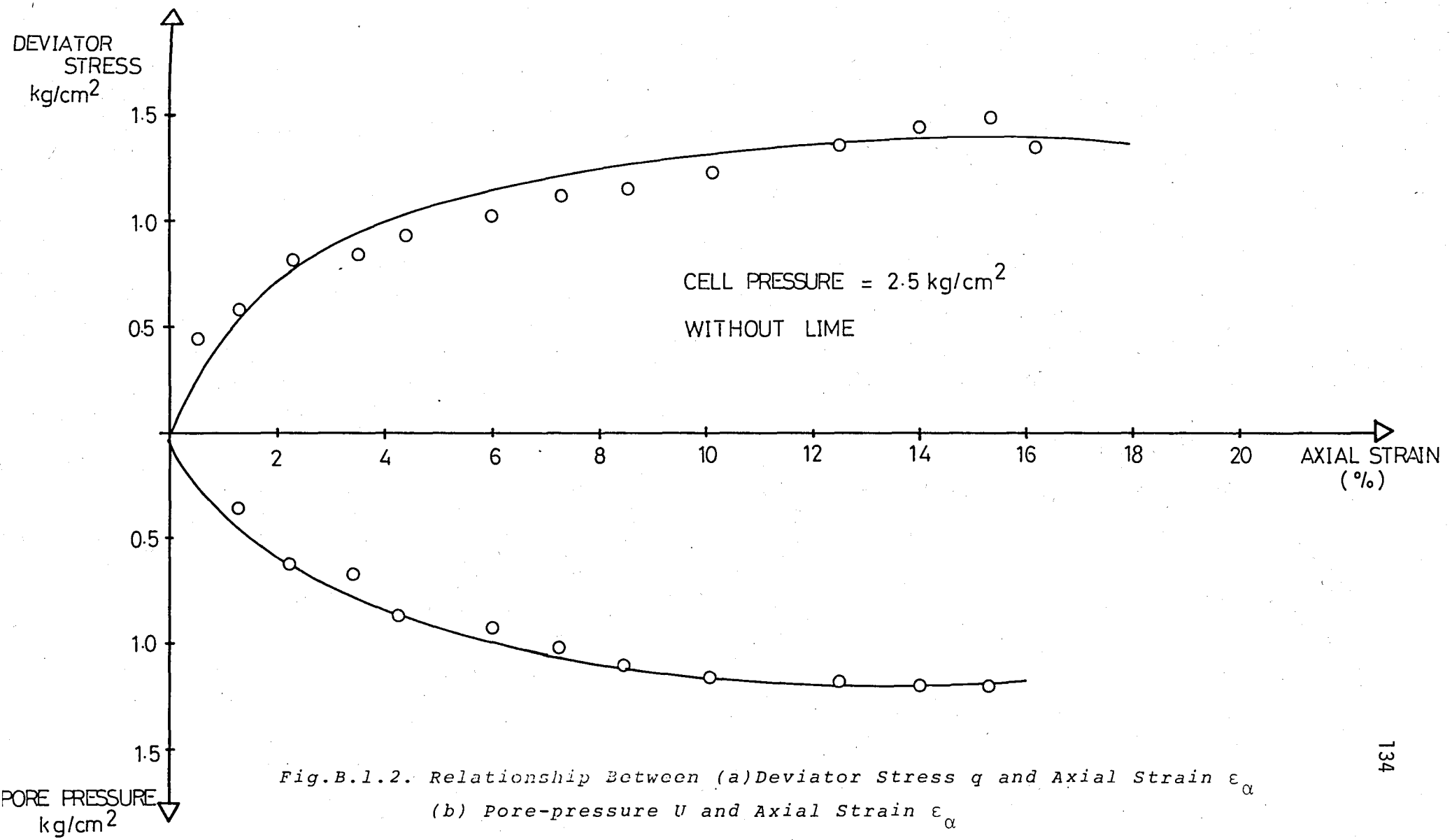

Fig.B.1.2. Relationship Between (a)Deviator Stress q and Axial Strain ε_α
(b) Pore-pressure U and Axial Strain ε_α

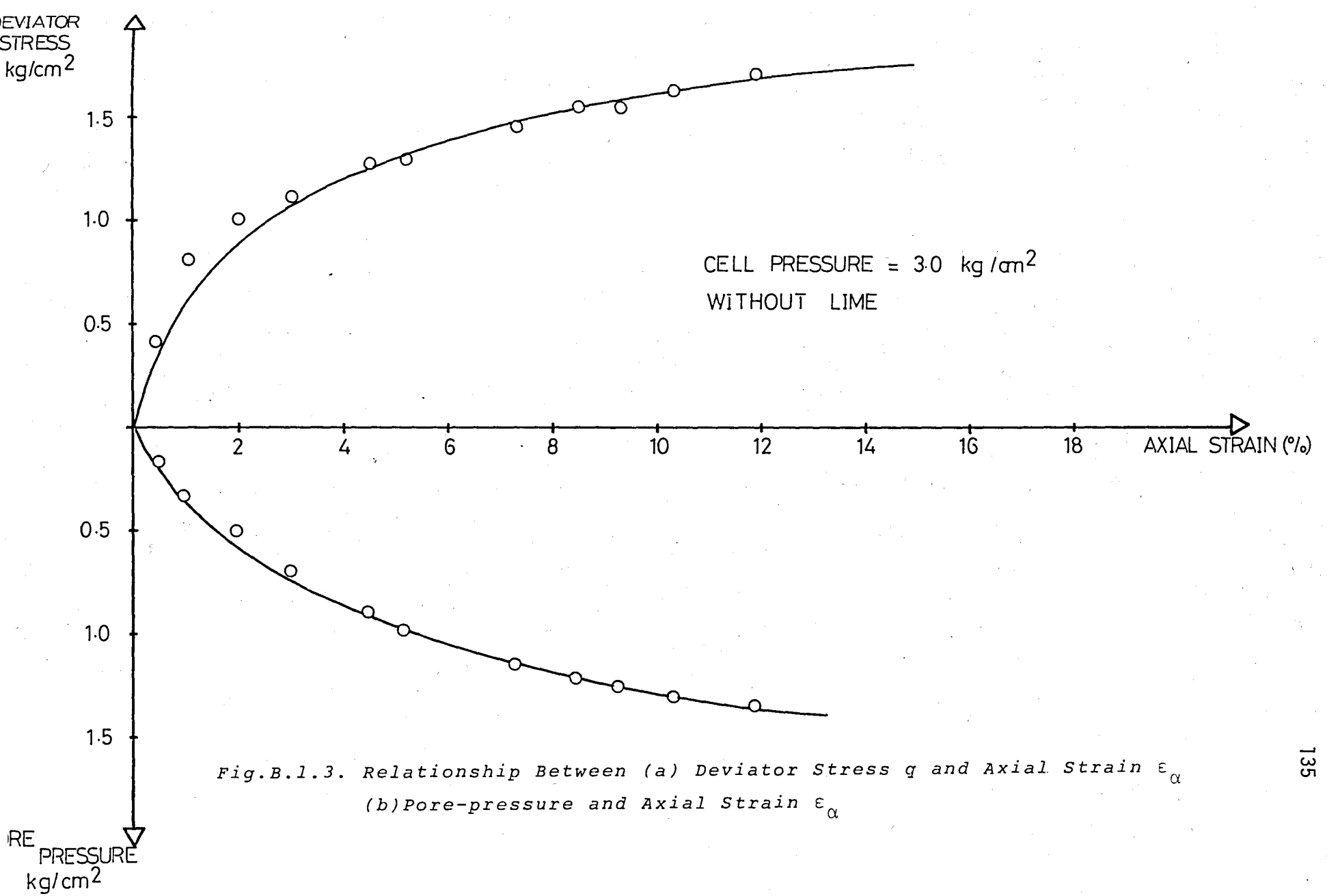

Fig.B.1.3. Relationship Between (a) Deviator Stress q and Axial Strain ε_α
(b)Pore-pressure and Axial Strain ε_α

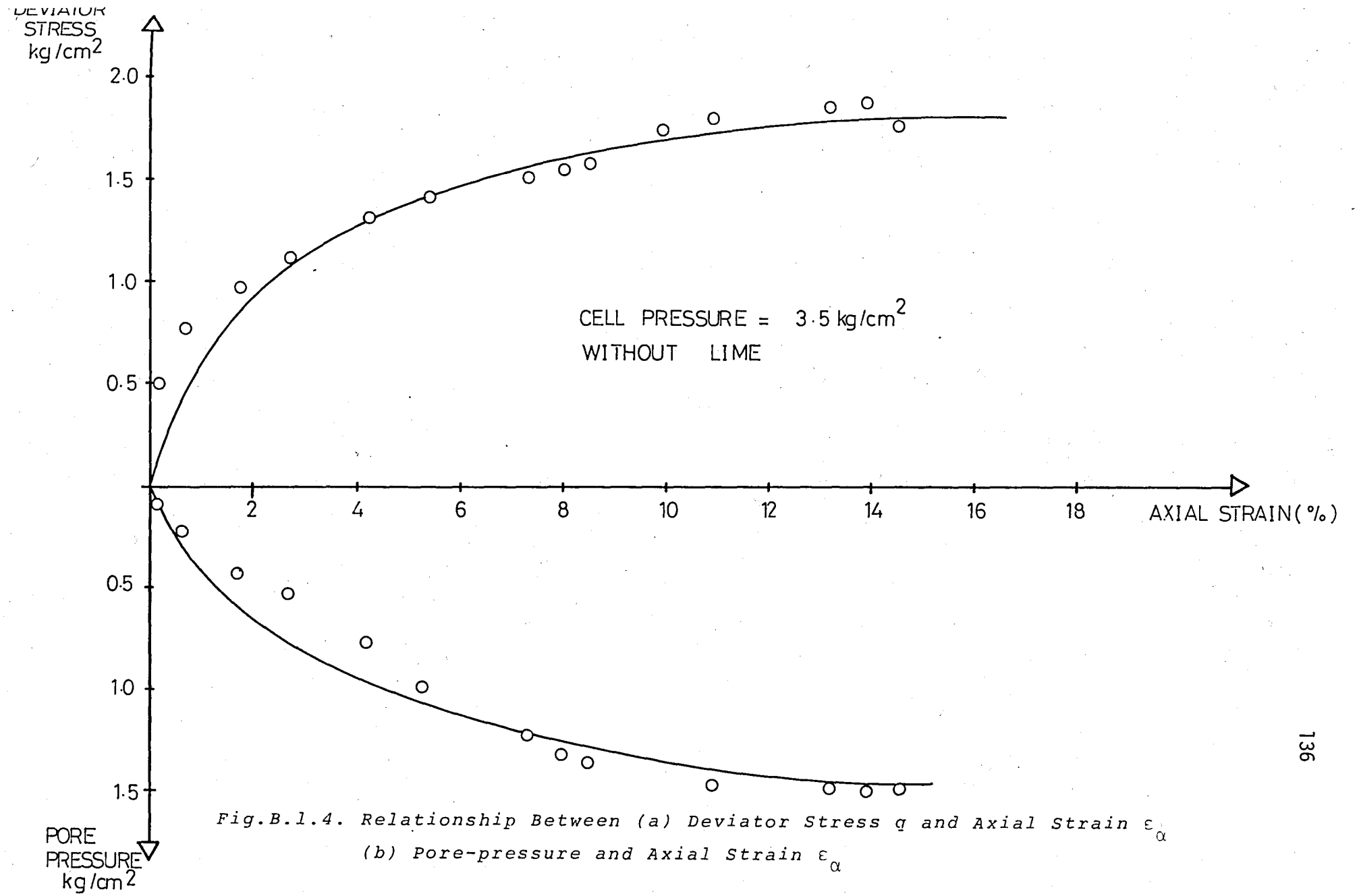

Fig.B.1.4. Relationship Between (a) Deviator Stress q and Axial Strain ε_α

(b) Pore-pressure and Axial Strain ε_α

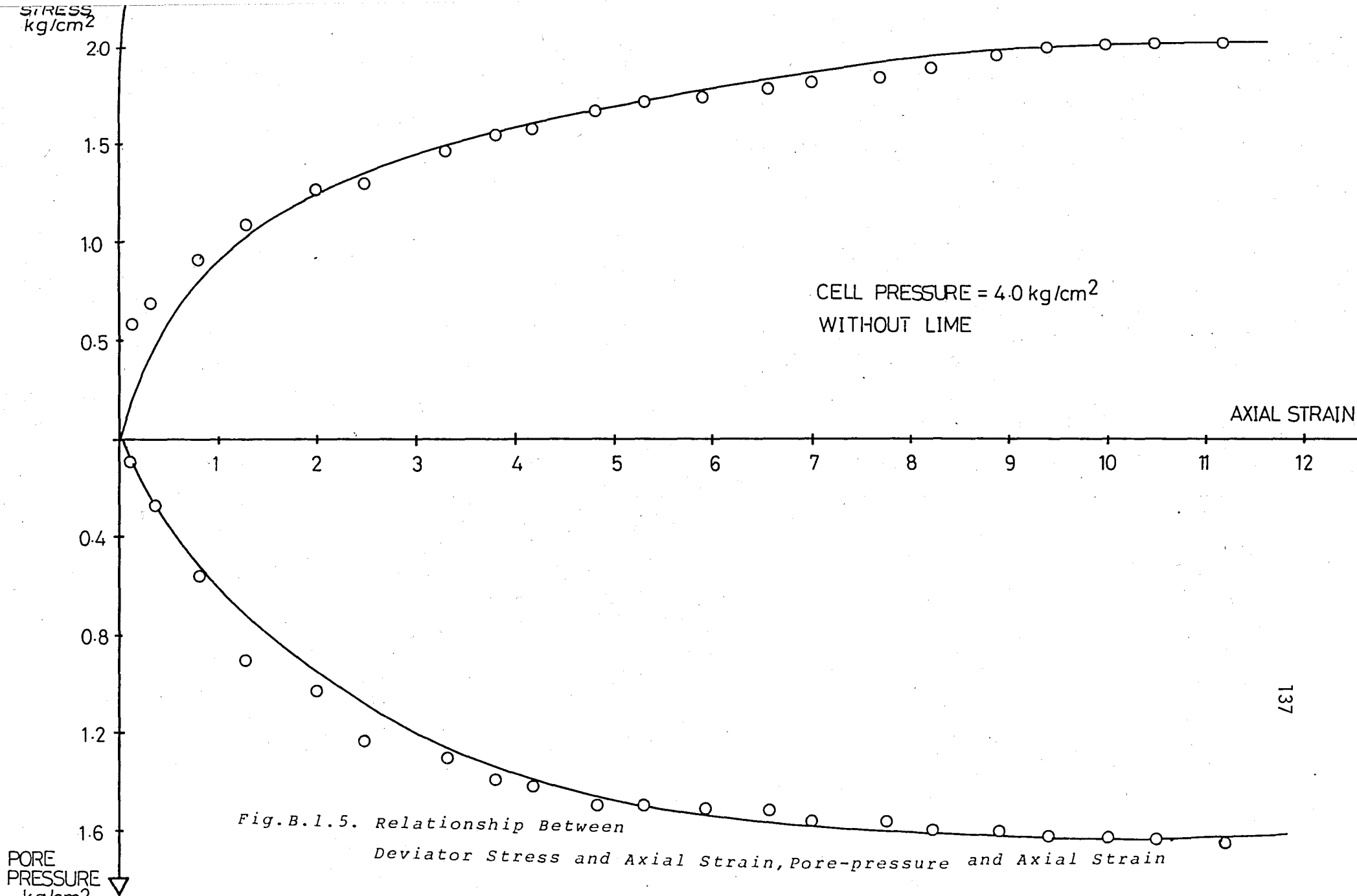

Fig.B.1.5. Relationship Between Deviator Stress and Axial Strain, Pore-pressure and Axial Strain

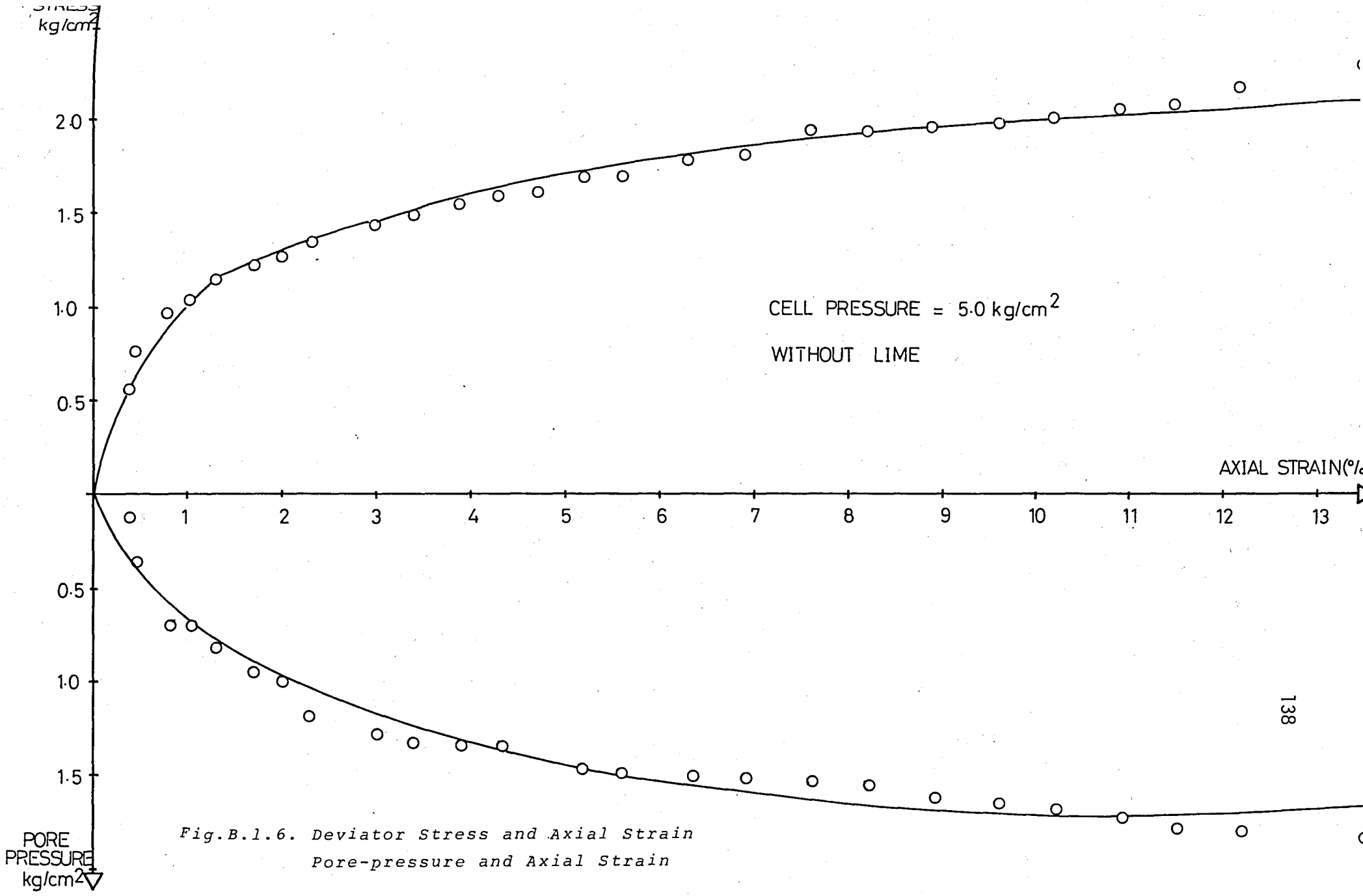

Fig.B.1.6. Deviator Stress and Axial Strain
Pore-pressure and Axial Strain

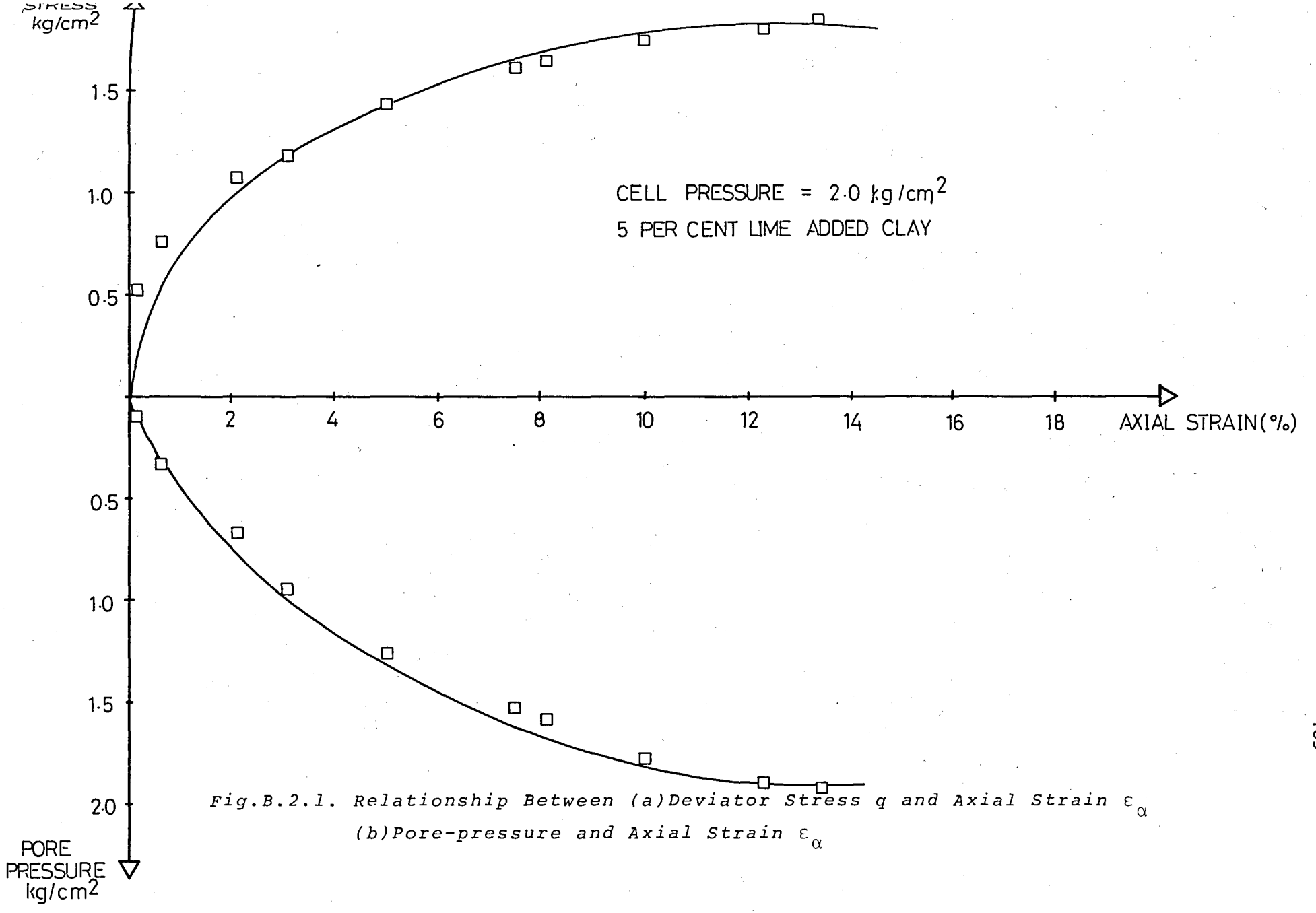

Fig.B.2.1. Relationship Between (a)Deviator Stress q and Axial Strain ε_α
(b)Pore-pressure and Axial Strain ε_α

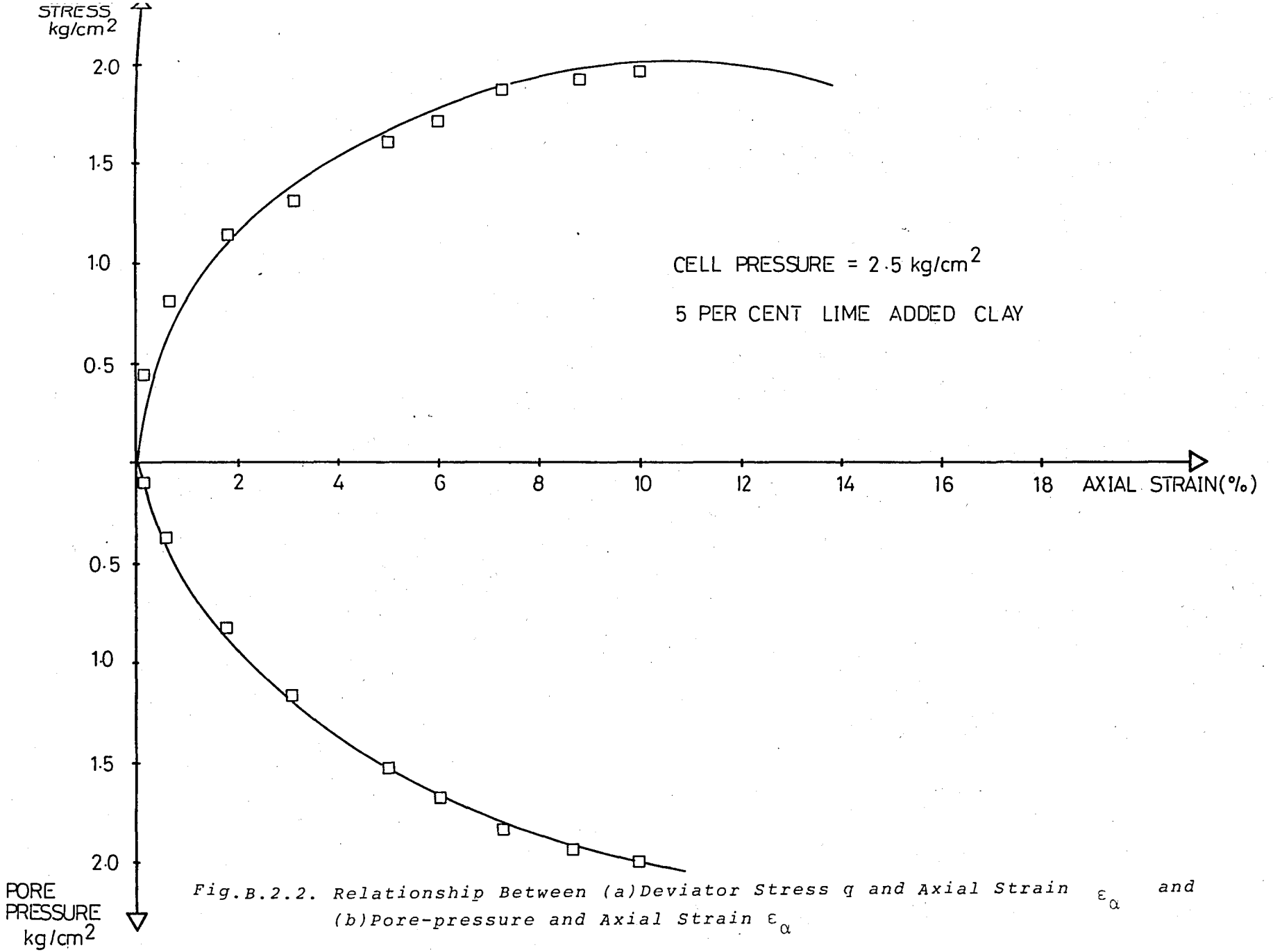

Fig.B.2.2. Relationship Between (a)Deviator Stress q and Axial Strain ε_α and (b)Pore-pressure and Axial Strain ε_α

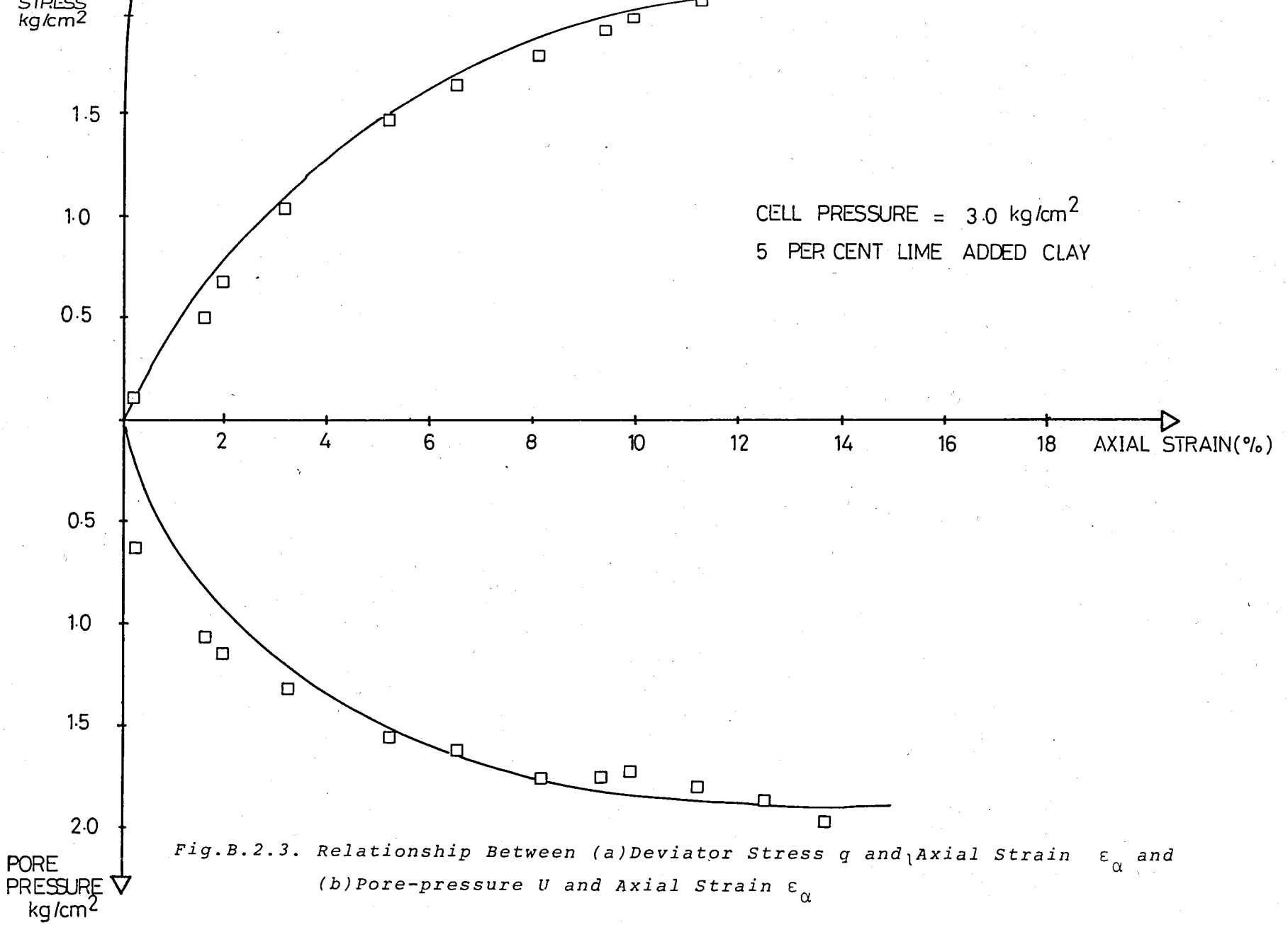

Fig.B.2.3. Relationship Between (a)Deviator Stress q and Axial Strain ε_α and (b)Pore-pressure U and Axial Strain ε_α

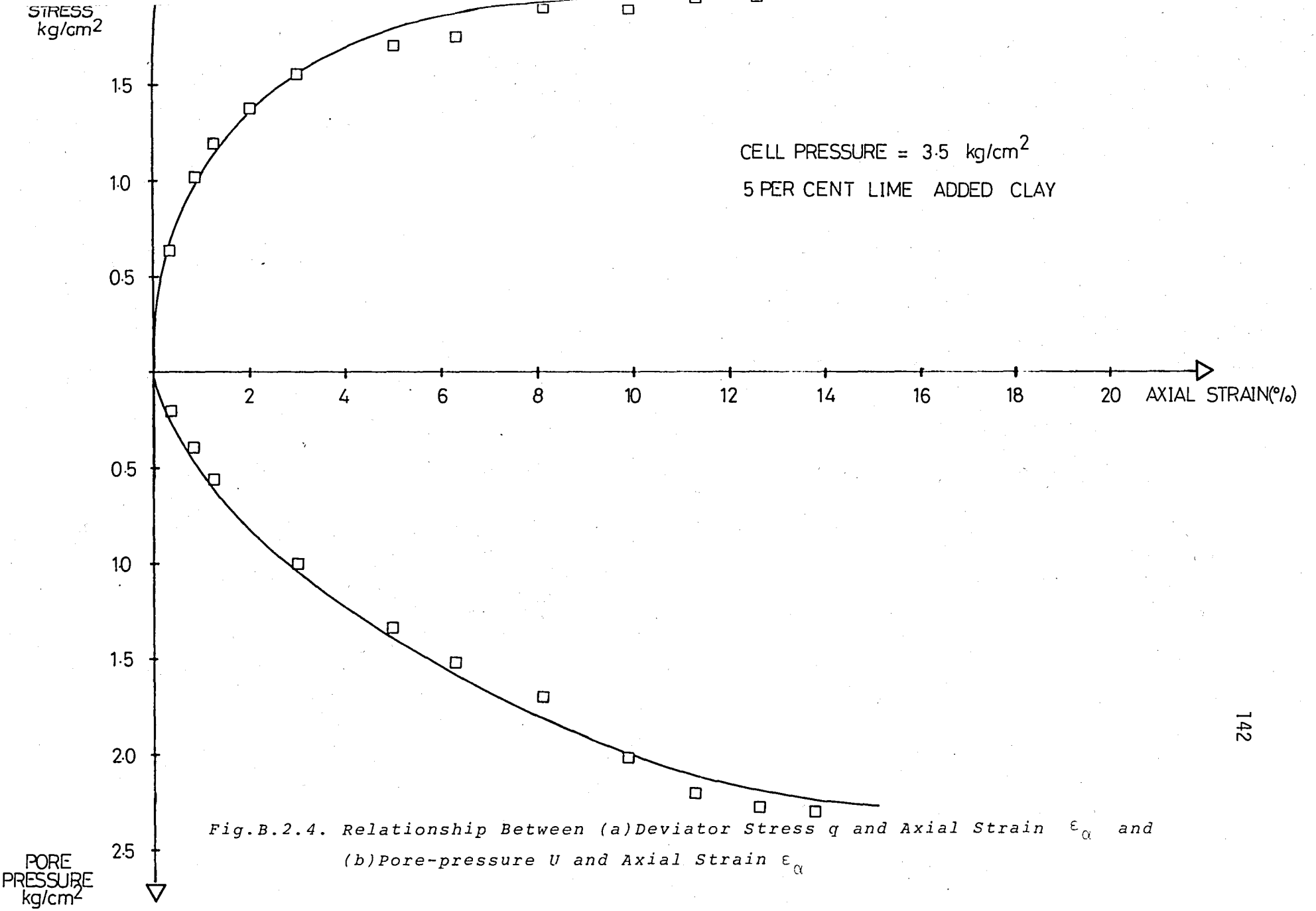

Fig.B.2.4. Relationship Between (a)Deviator Stress q and Axial Strain ε_α and (b)Pore-pressure U and Axial Strain ε_α

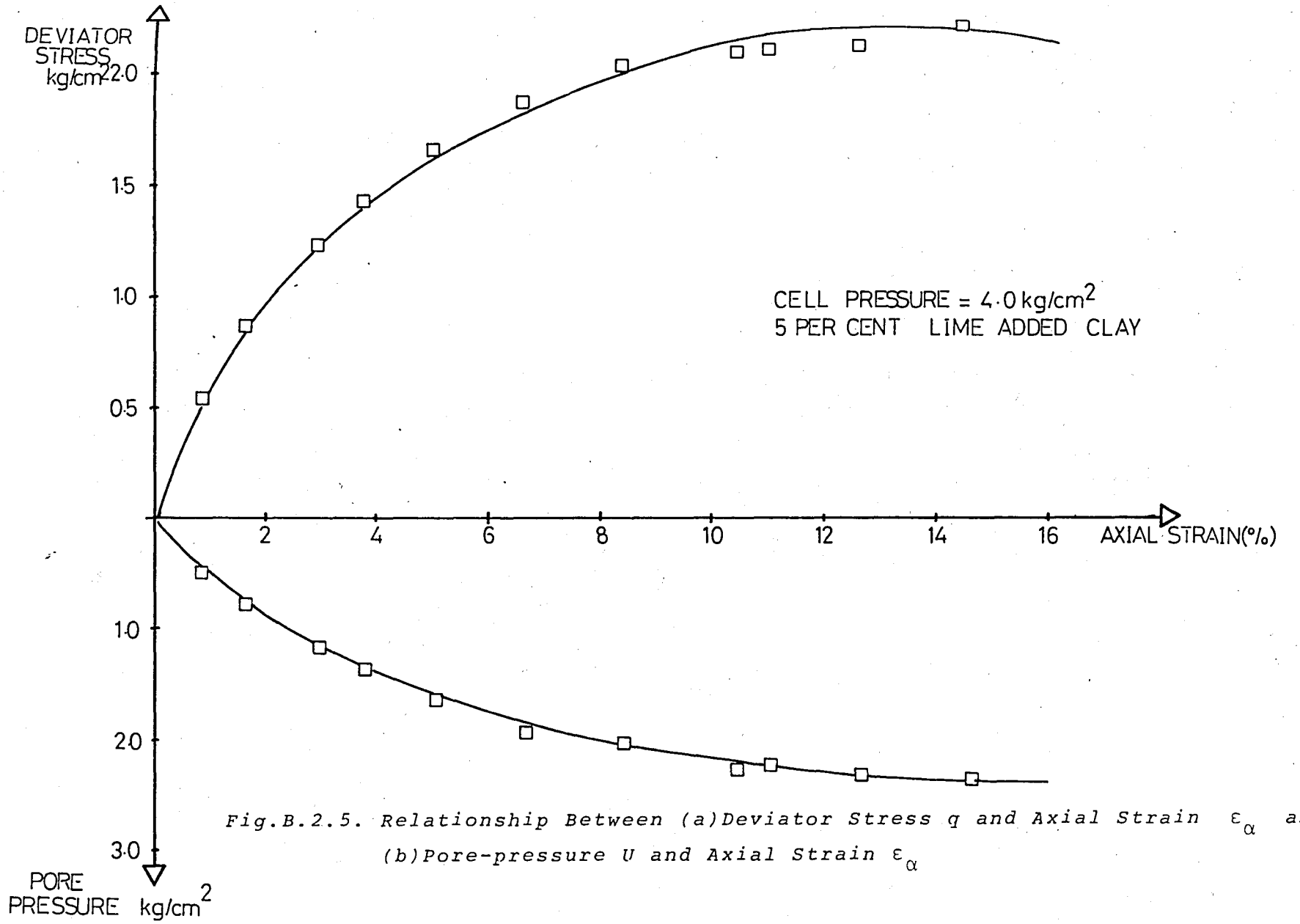

Fig.B.2.5. Relationship Between (a)Deviator Stress q and Axial Strain ε_α and (b)Pore-pressure U and Axial Strain ε_α

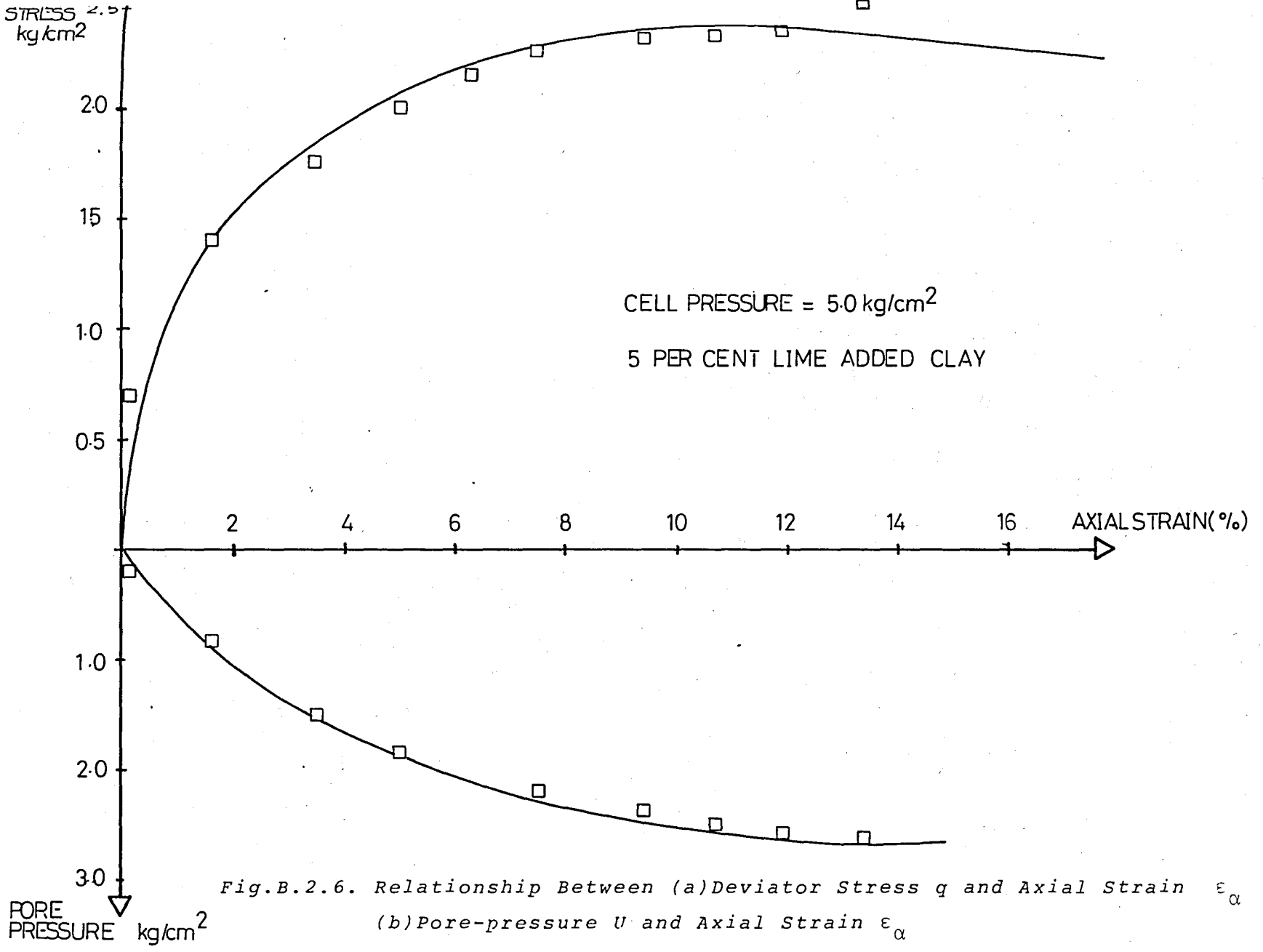

Fig.B.2.6. Relationship Between (a)Deviator Stress q and Axial Strain ε_α and (b)Pore-pressure U and Axial Strain ε_α

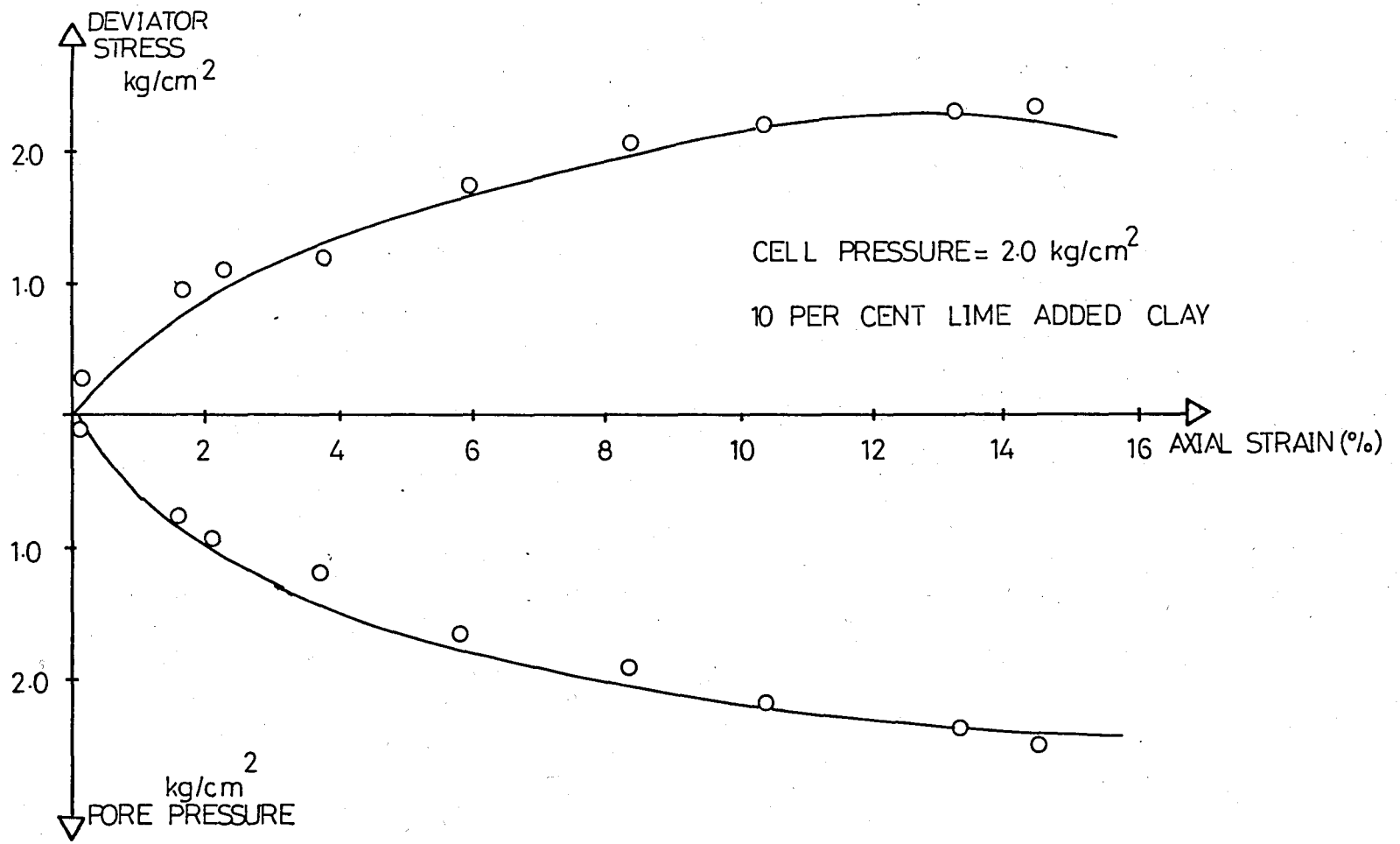

Fig.B.3.1. Relationship Between (a)Deviator Stress q and Axial Strain ε_α *and (b)Pore-pressure U and Axial Strain* ε_α

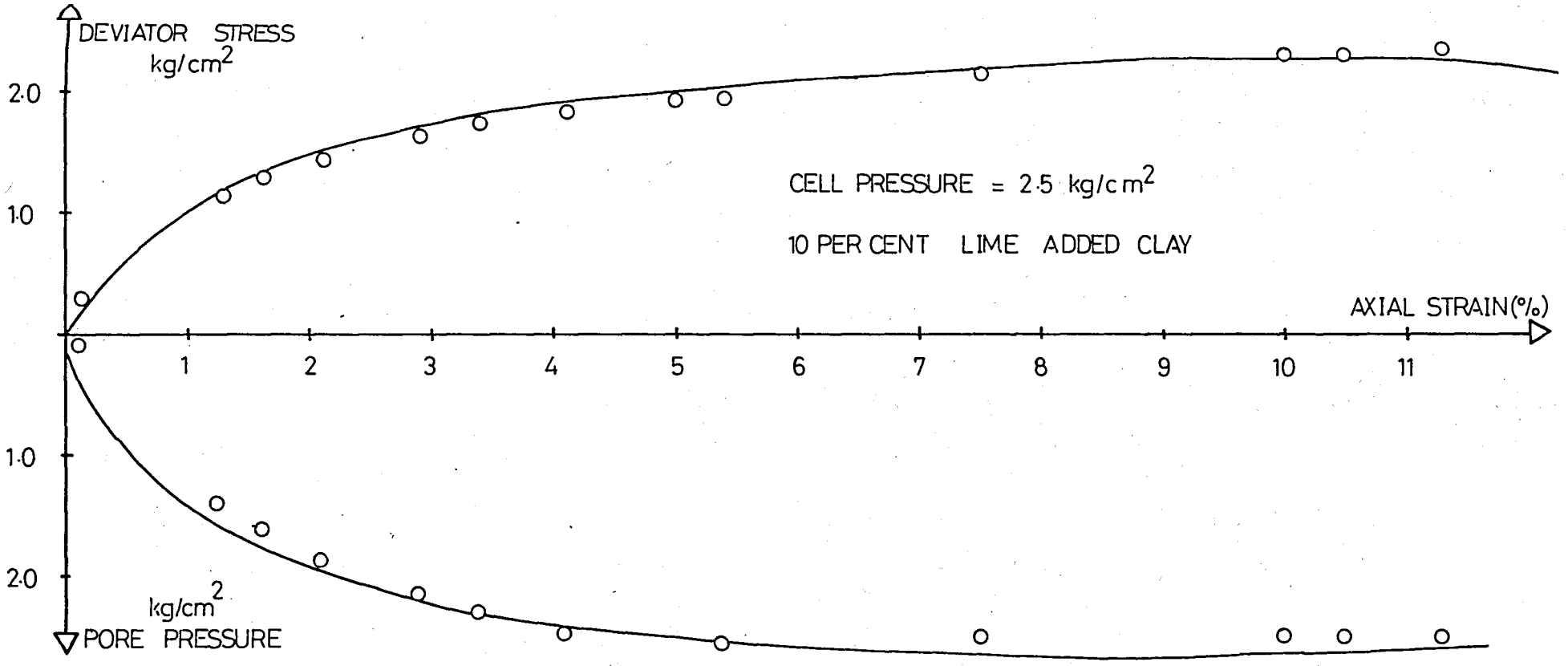

Fig.B.3.2. Relationship Between (a)Deviator Stress q and Axial Strain ε_α *and (b)Pore-pressure U and Axial Strain* ε_α

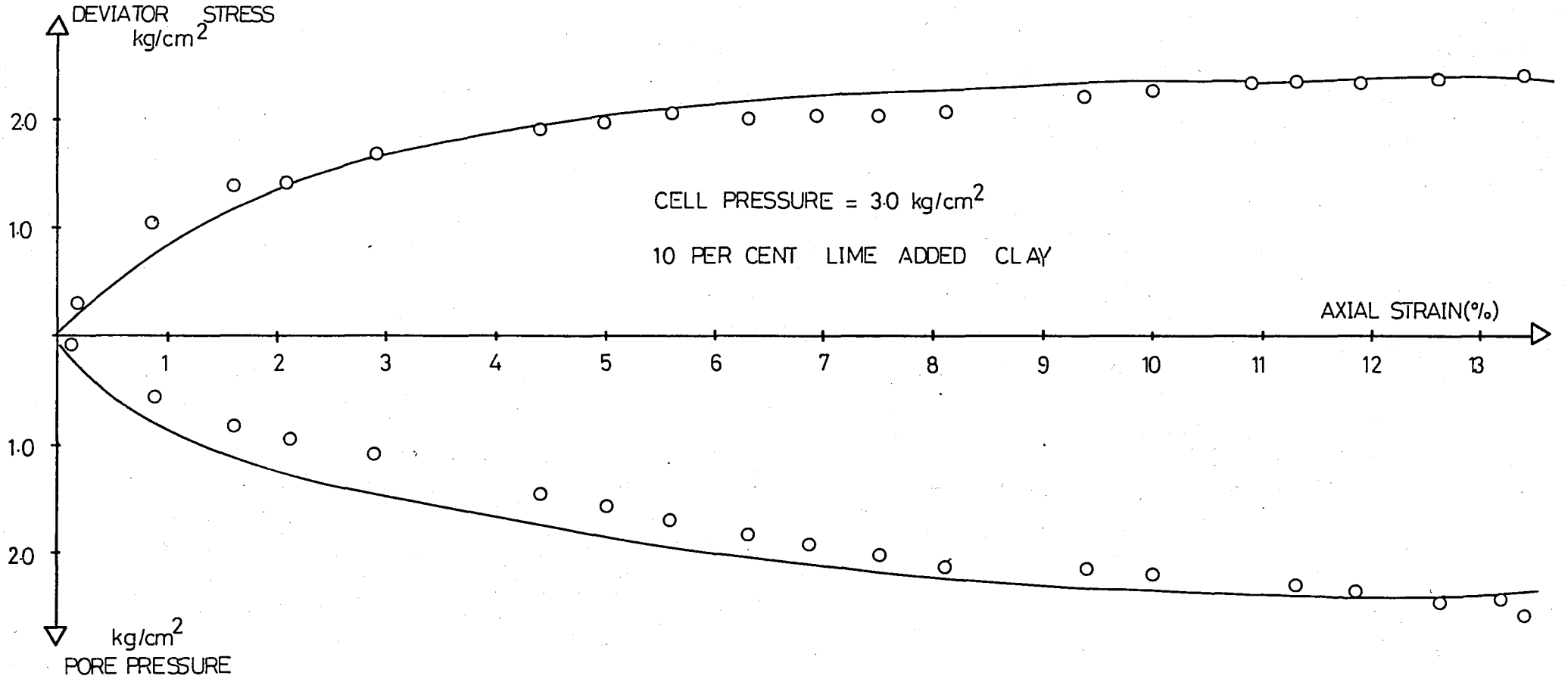

Fig.B.3.3. Relationship Between (a)Deviator Stress q and Axial Strain ε_α *and (b) Pore-pressure U and Axial Strain* ε_α

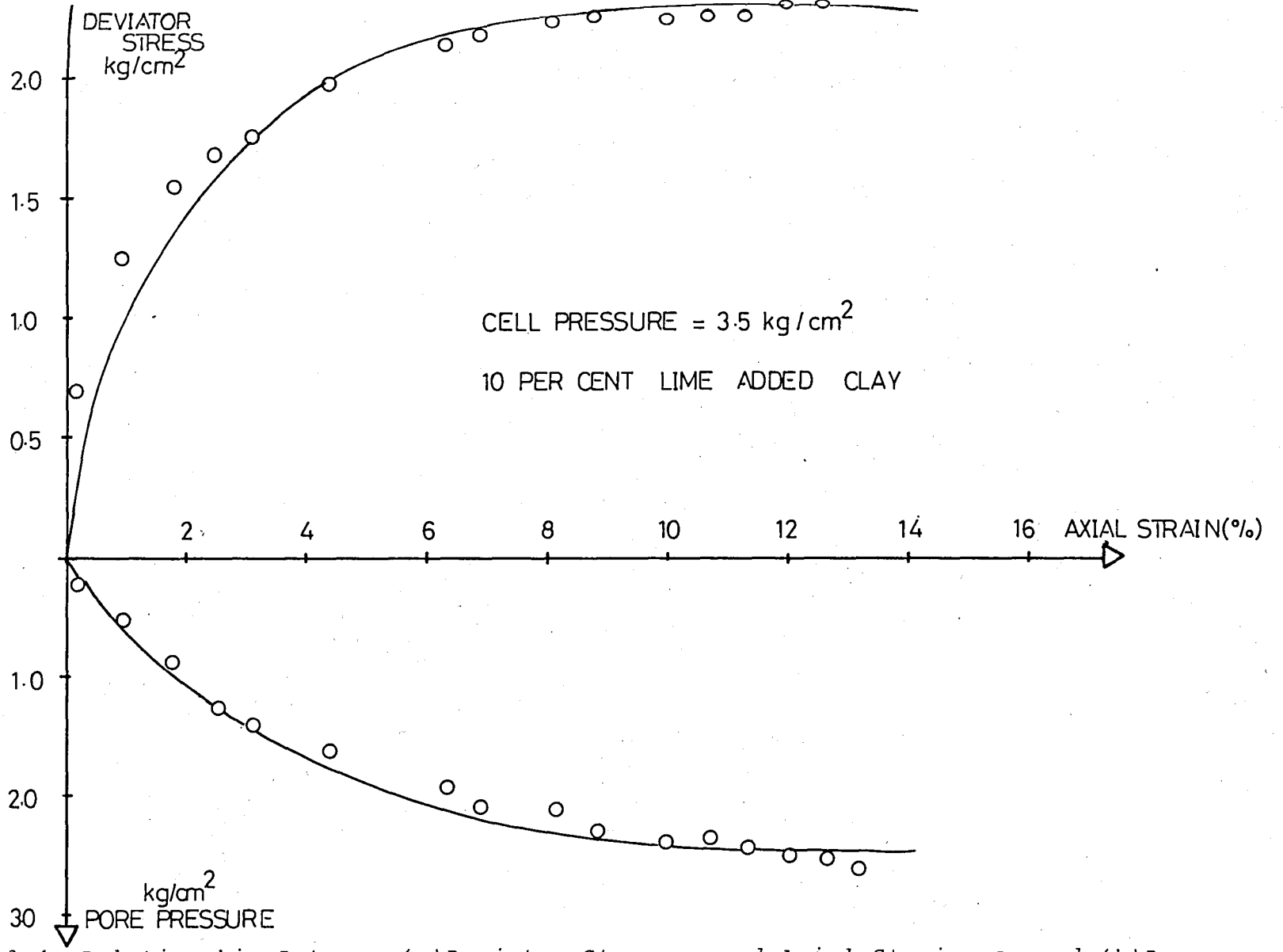

Fig.B.3.4. Relationship Between (a)Deviator Stress q and Axial Strain ε_α and (b)Pore-pressure U and Axial Strain ε_α

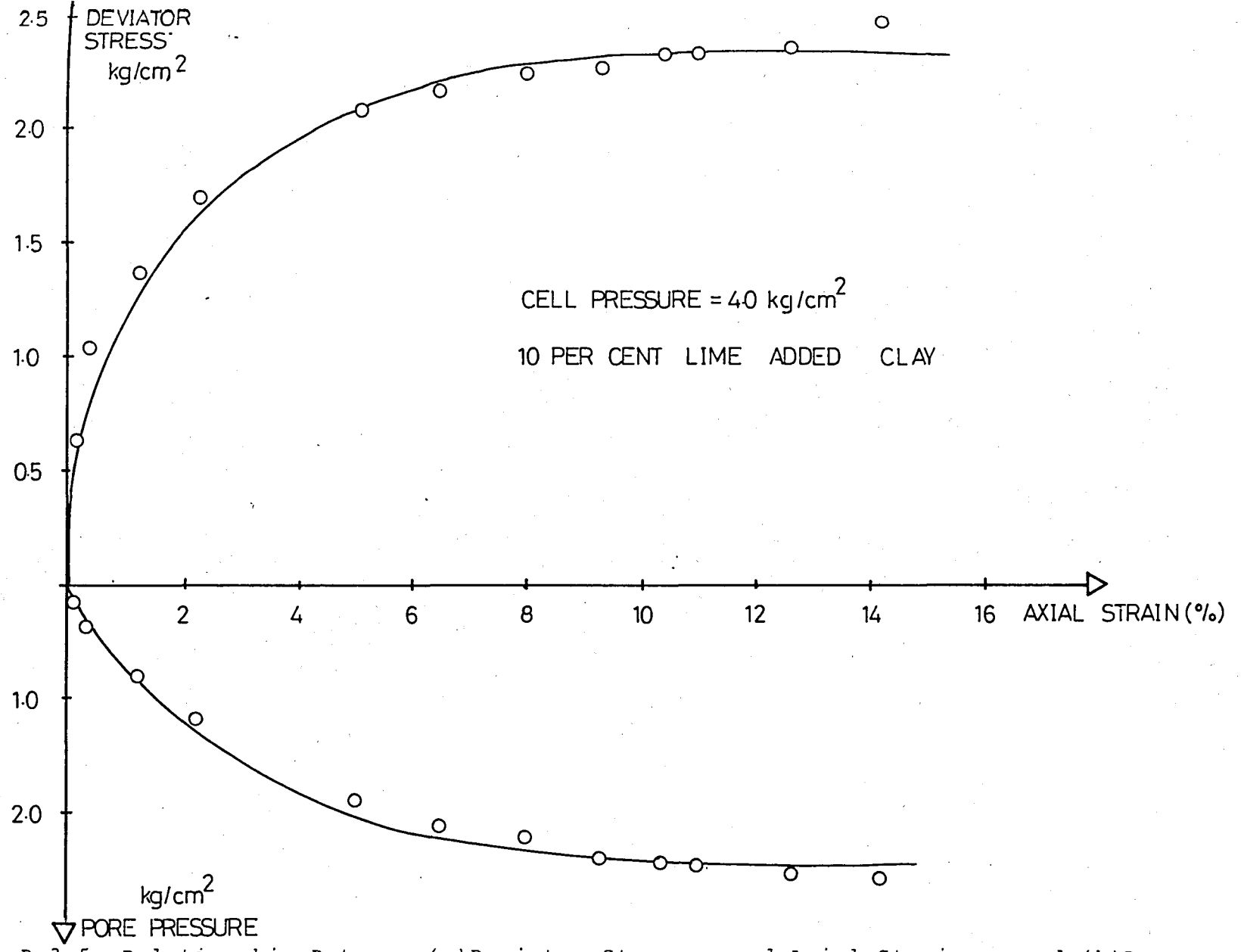

Fig.B.3.5. Relationship Between (a)Deviator Stress q and Axial Strain ε_α and (b)Pore-pressure U and Axial Strain ε_α

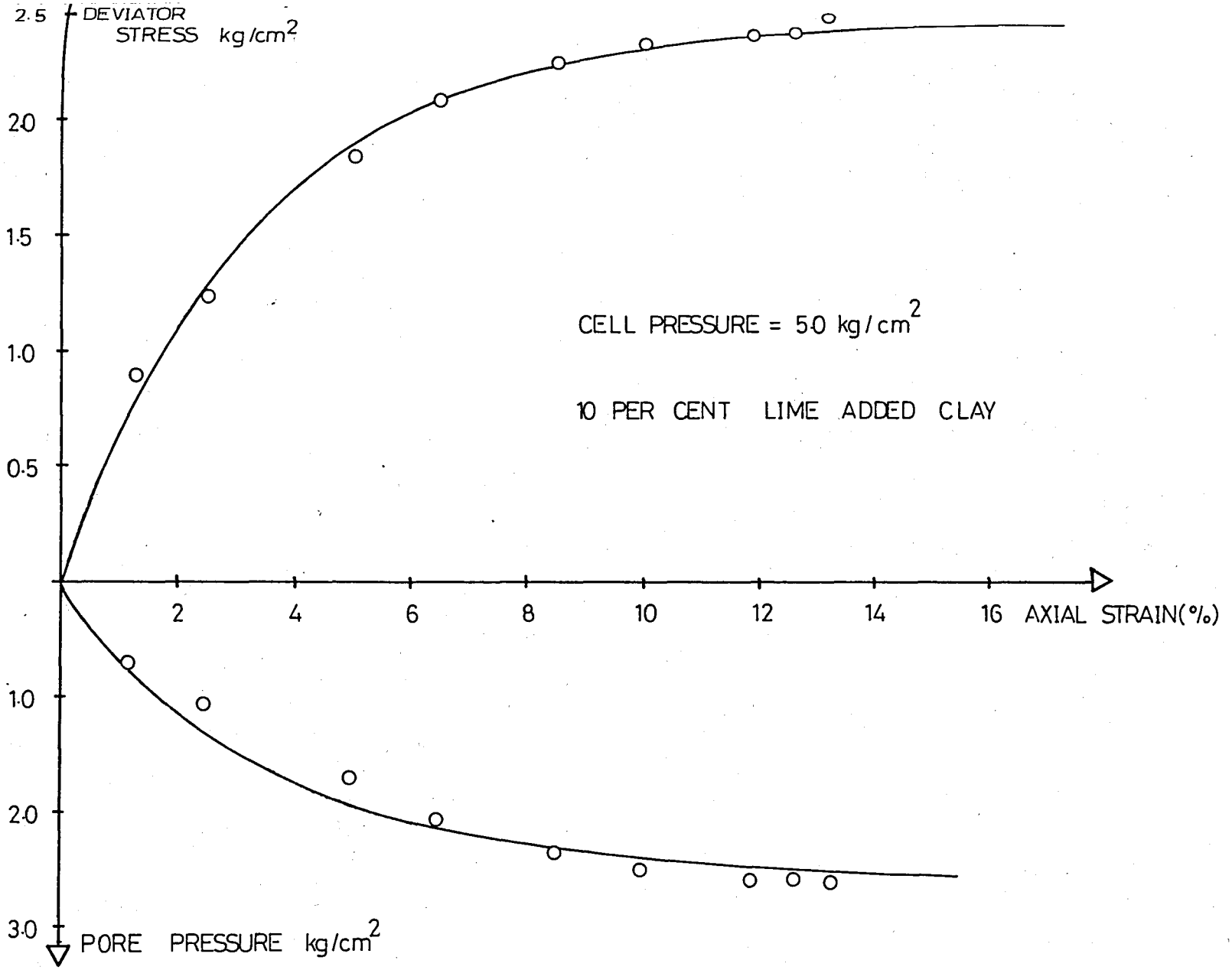

Fig.B.3.6. RelationshipBetween (a)Deviator Stress q and Axial Strain ε_α and (b)Pore-pressure U and Axial Strain ε_α

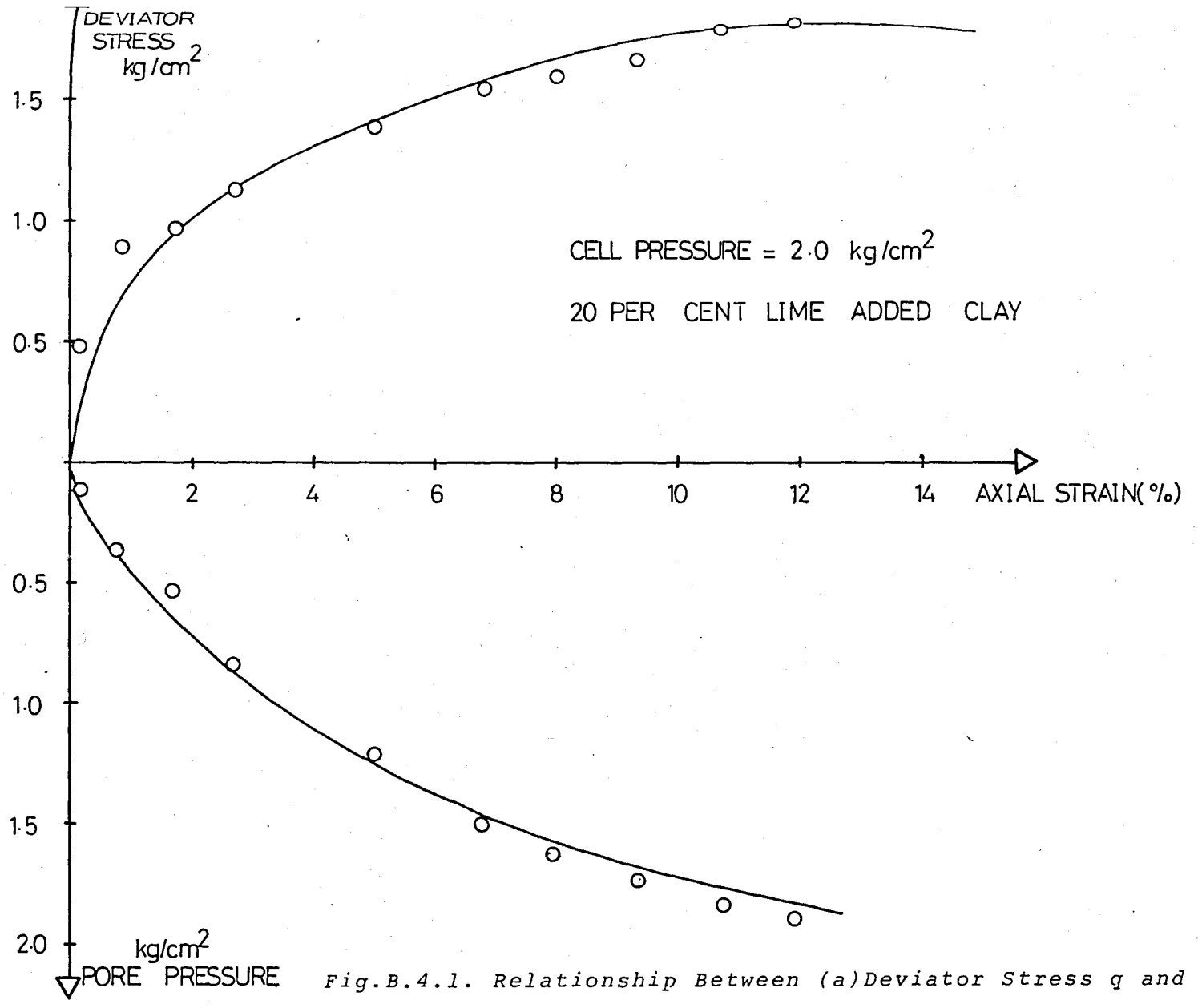

Fig.B.4.1. Relationship Between (a)Deviator Stress q and Axial Strain ε_α *and (b)Pore-pressure U and Axial Strain* ε_α

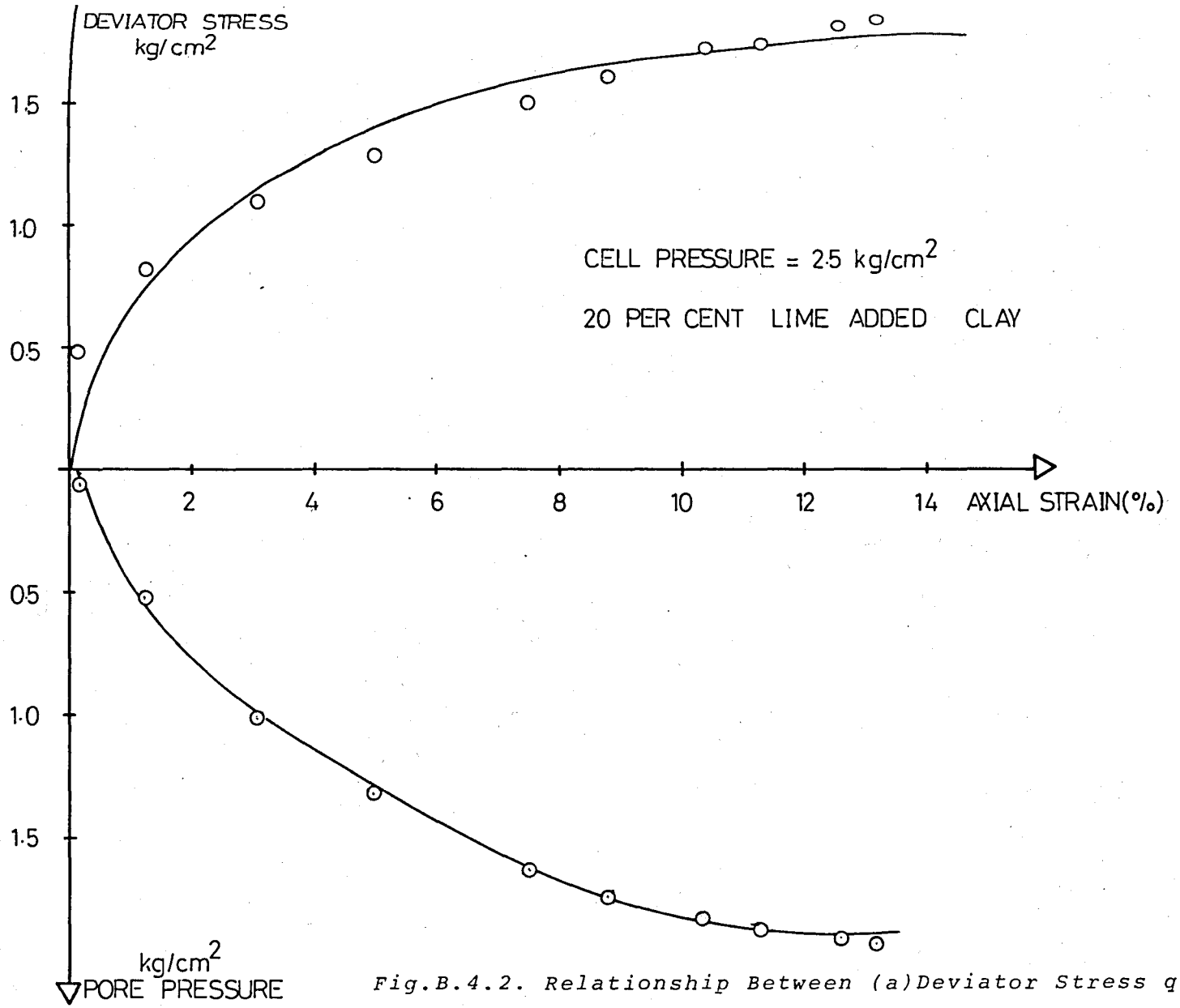

Fig.B.4.2. Relationship Between (a)Deviator Stress q and Axial Strain ε_α and (b)Pore-pressure U and Axial Strain ε_α

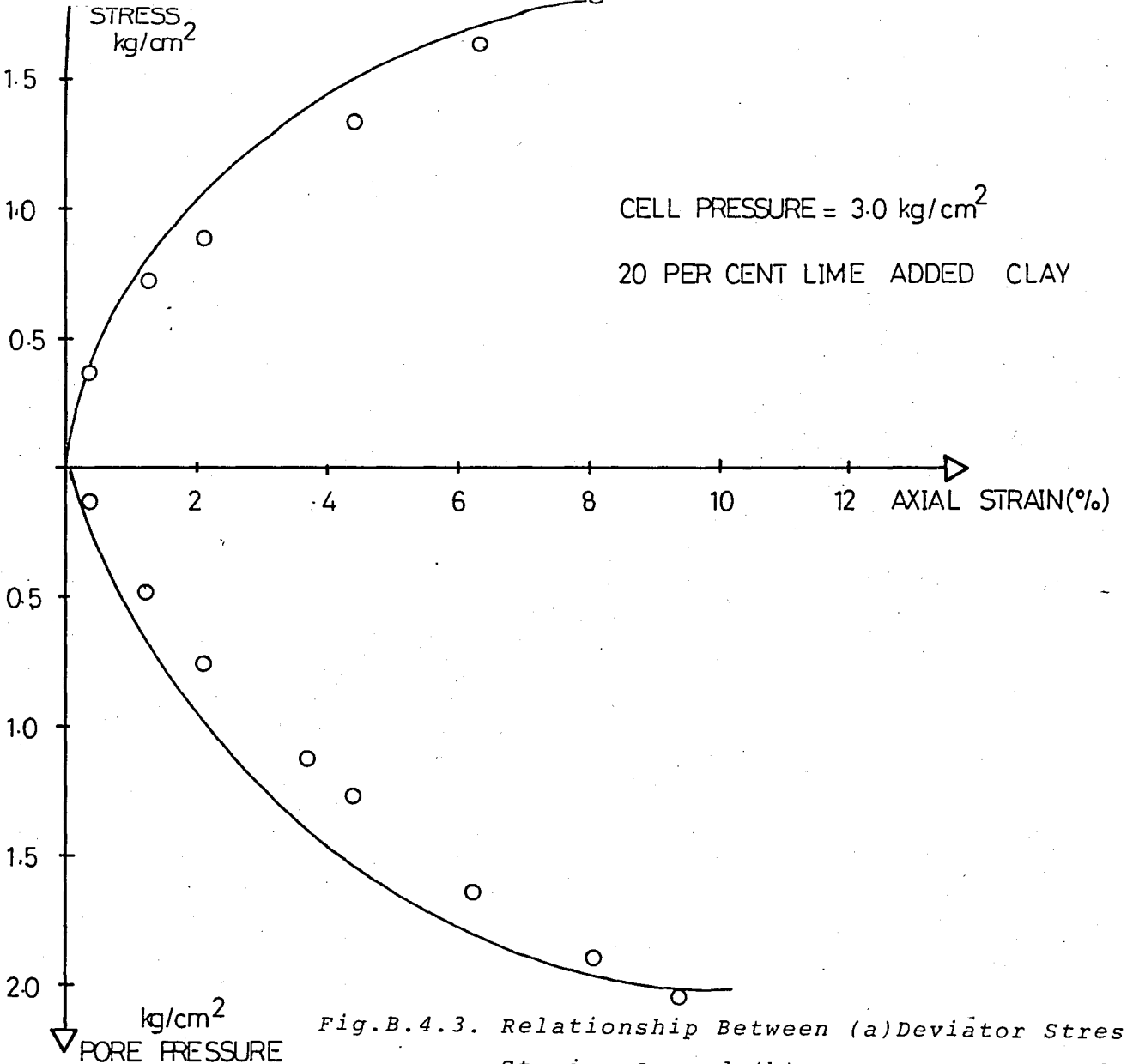

Fig.B.4.3. Relationship Between (a)Deviator Stress q and Axial Strain ε_α and (b)Pore-pressure U and Axial Strain ε_α

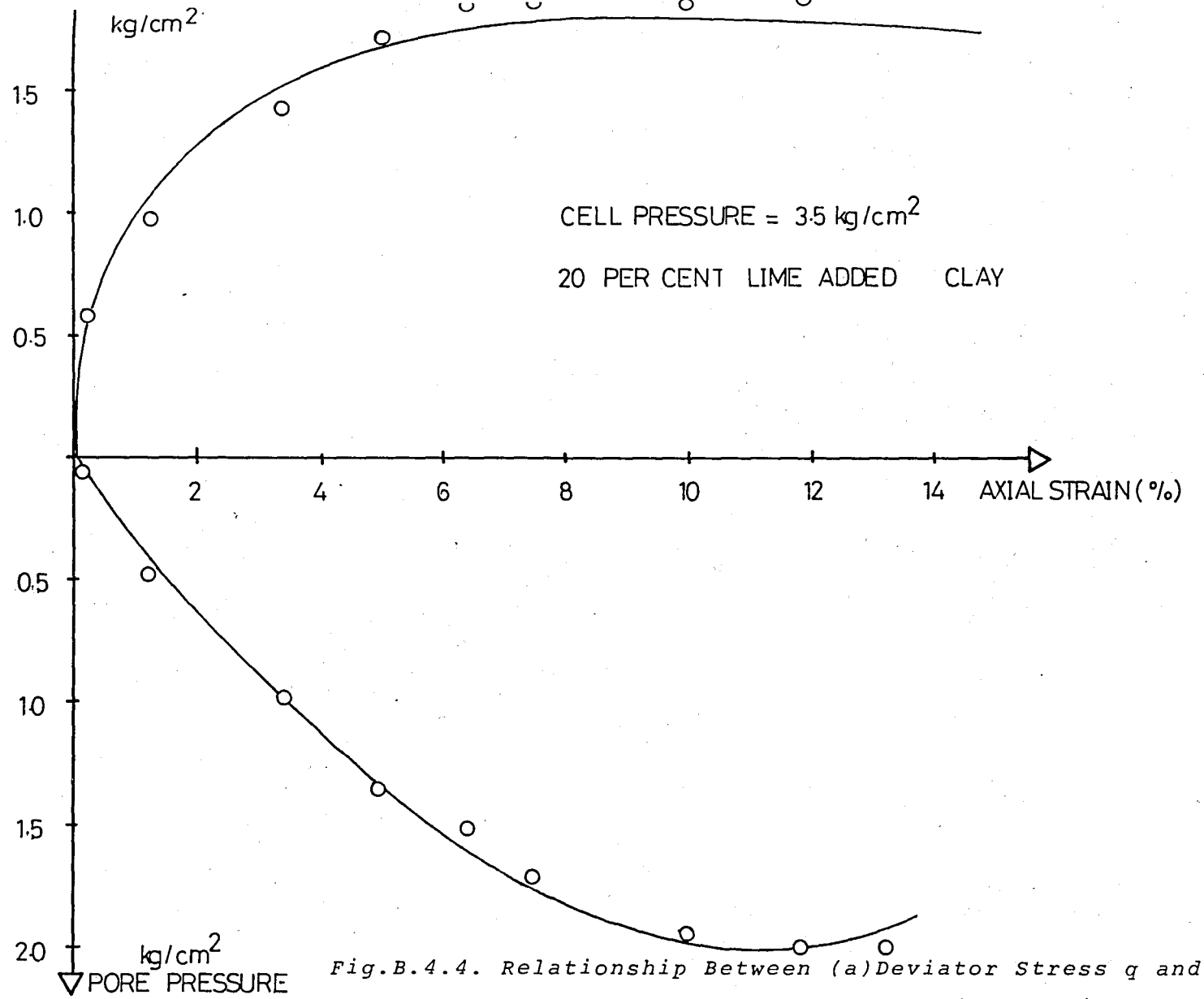

Fig.B.4.4. Relationship Between (a)Deviator Stress q and Axial Strain ε_α and (b)Pore-pressure U and Axial Strain ε_α

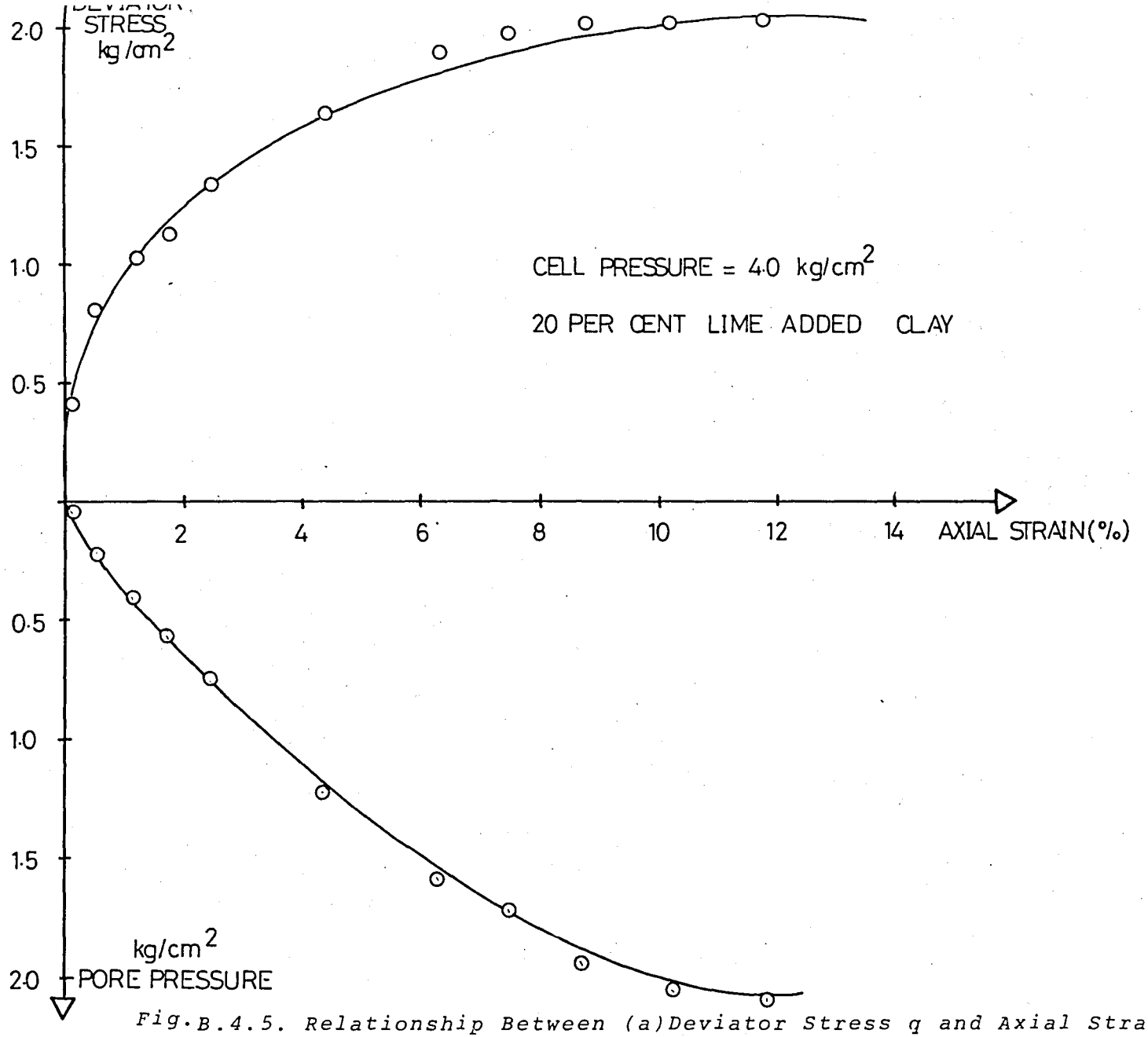

Fig. B.4.5. Relationship Between (a)Deviator Stress q and Axial Strain ε_α and (b)Pore-pressure U and Axial Strain ε_α

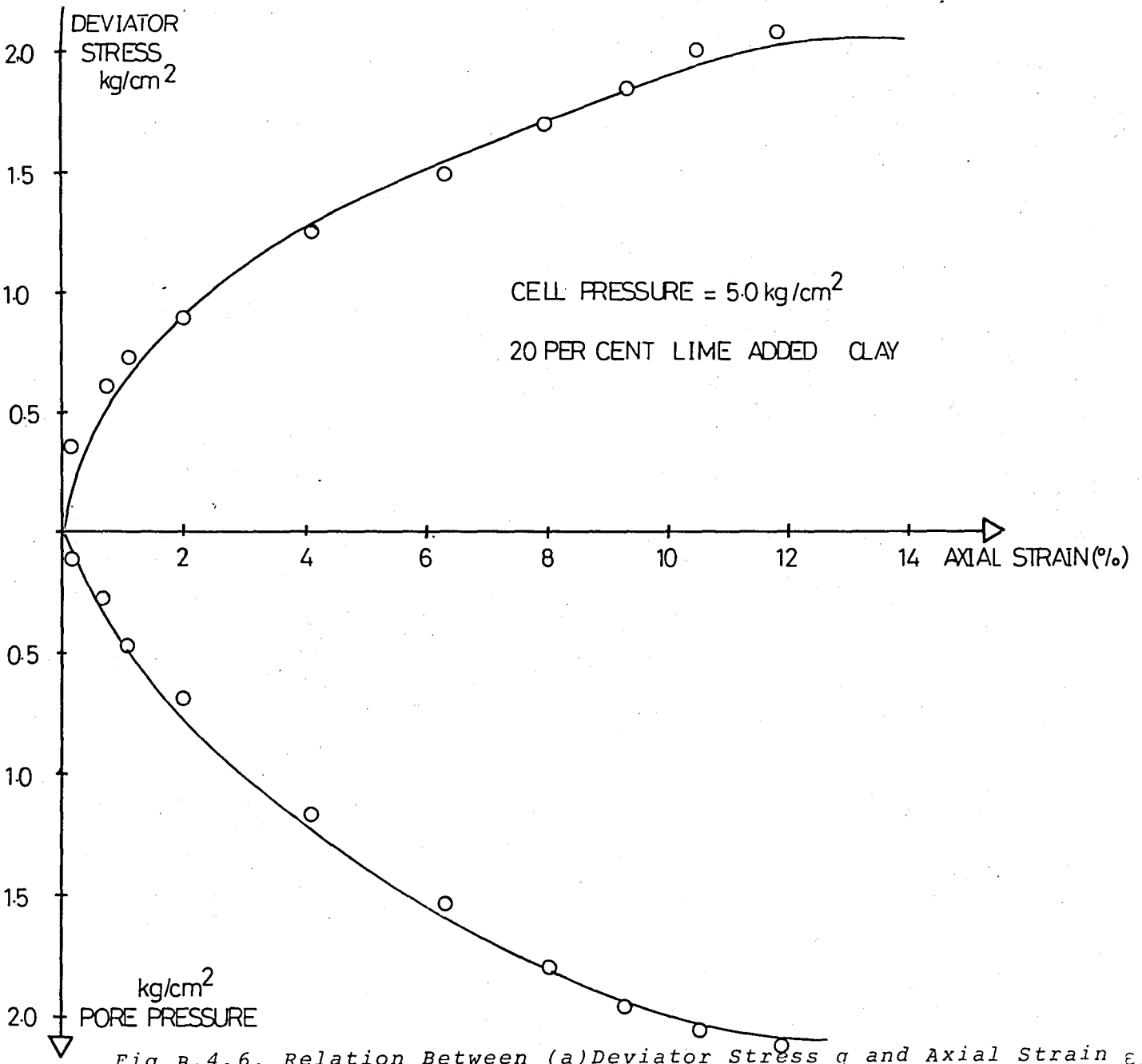

Fig.B.4.6. Relation Between (a)Deviator Stress q and Axial Strain ε_α and (b)Pore-pressure U and Axial Strain ε_α

APPENDIX C

U : p' CURVES

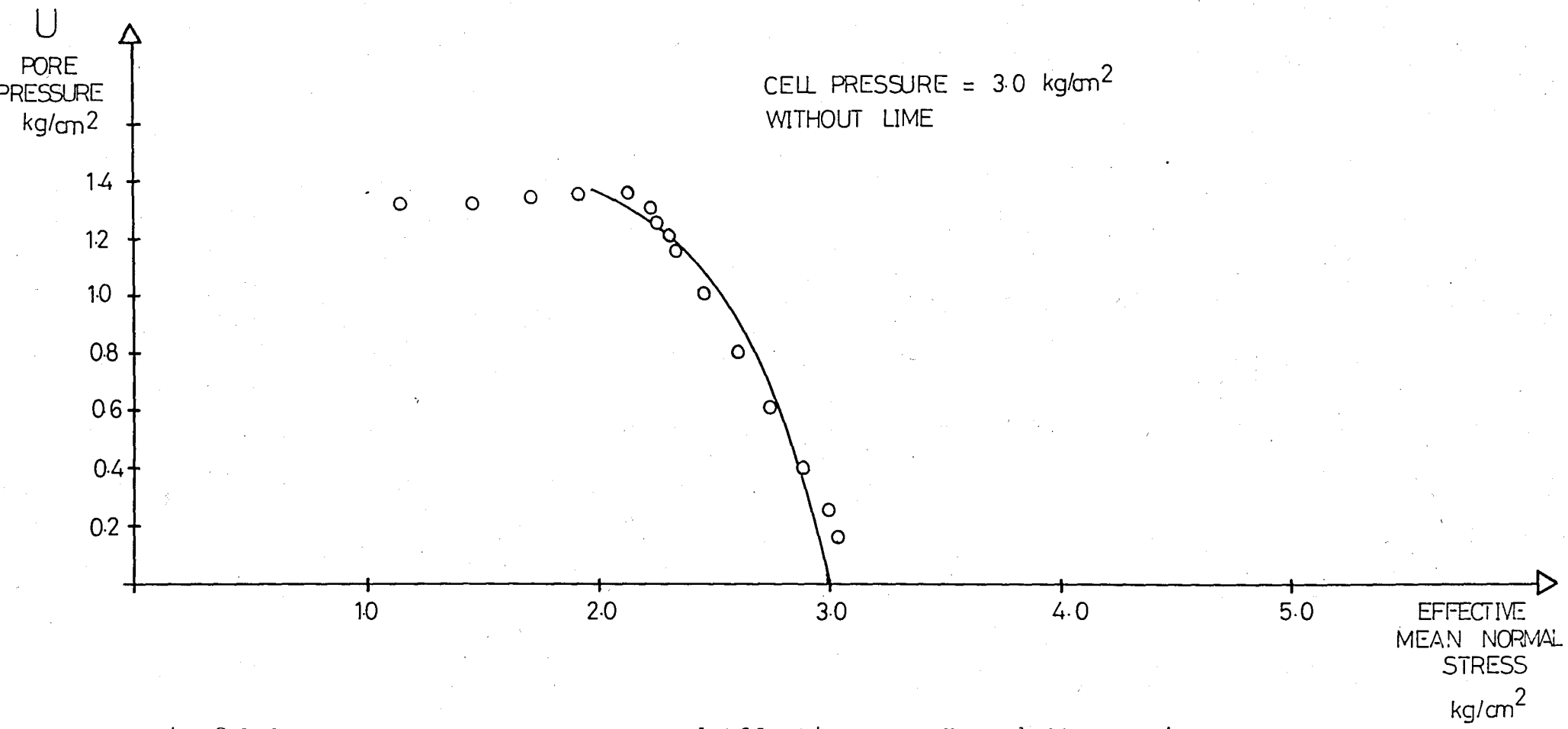

Fig. C 1.1. Test Data Pore-pressure and Effective Mean Normal Stress p'

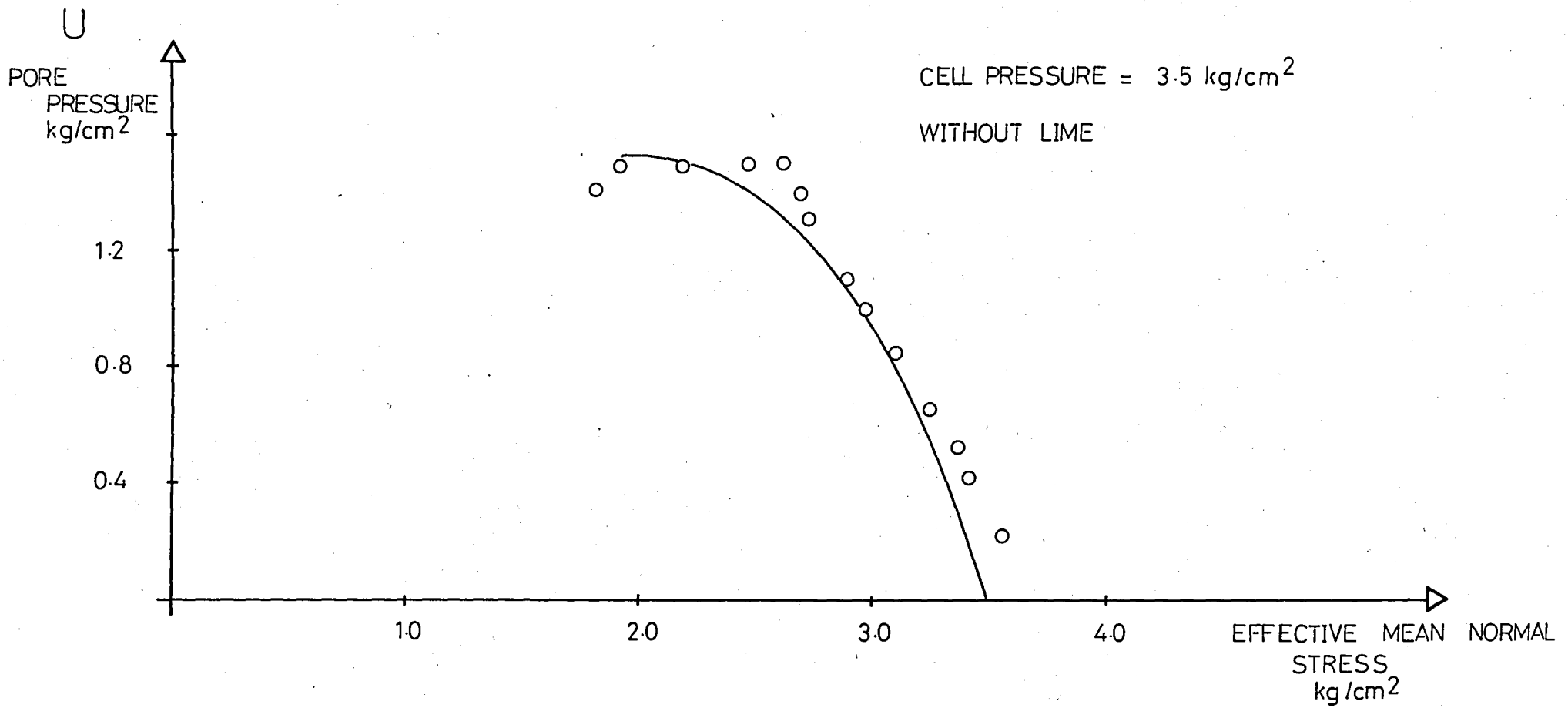

Fig.C 1.2. Test Data Pore-pressure U and Effective Mean Normal Stress p'

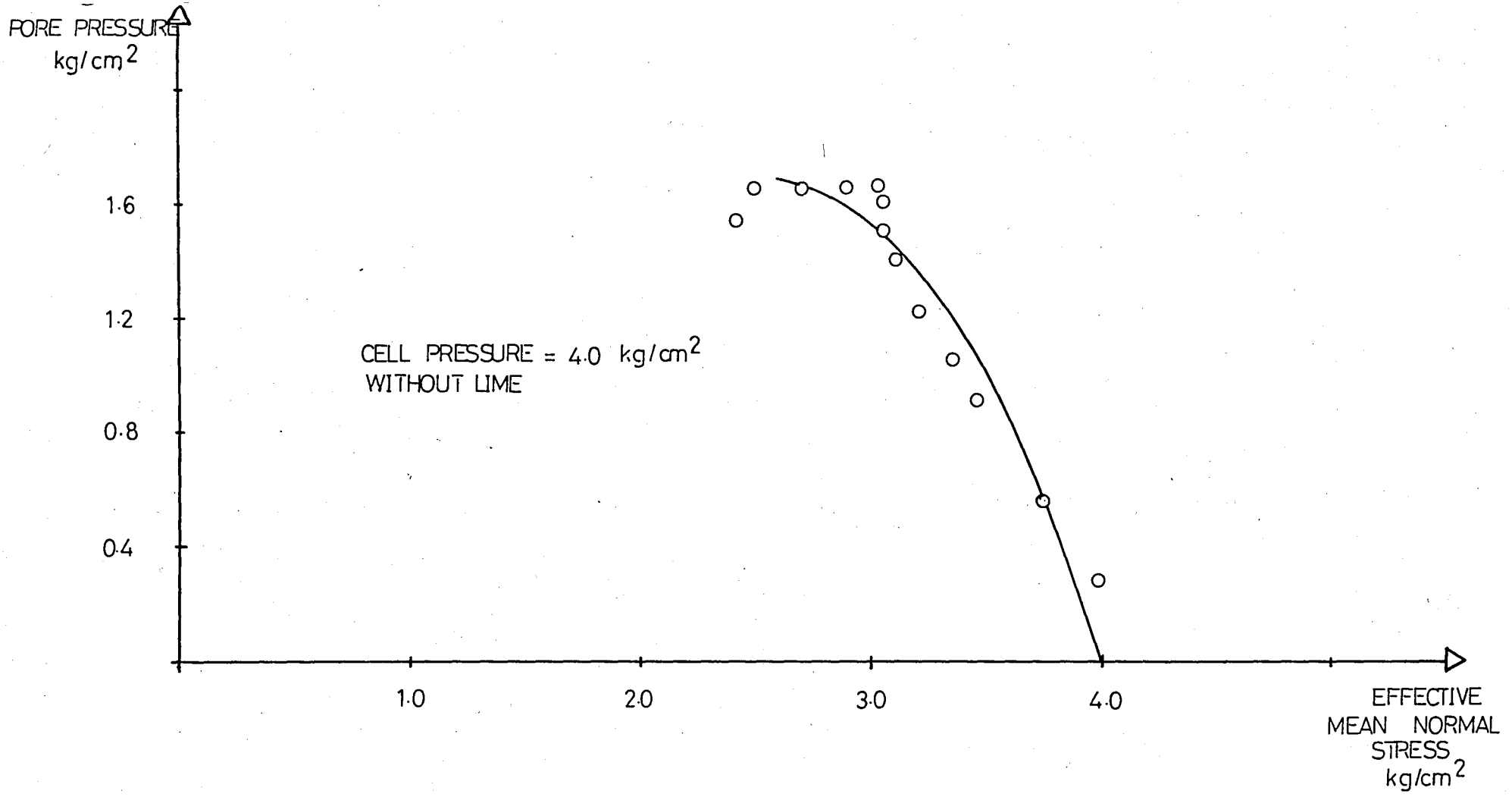

Fig.C 1.3. Test Data Pore-pressure U and Effective Mean Normal Stress p'

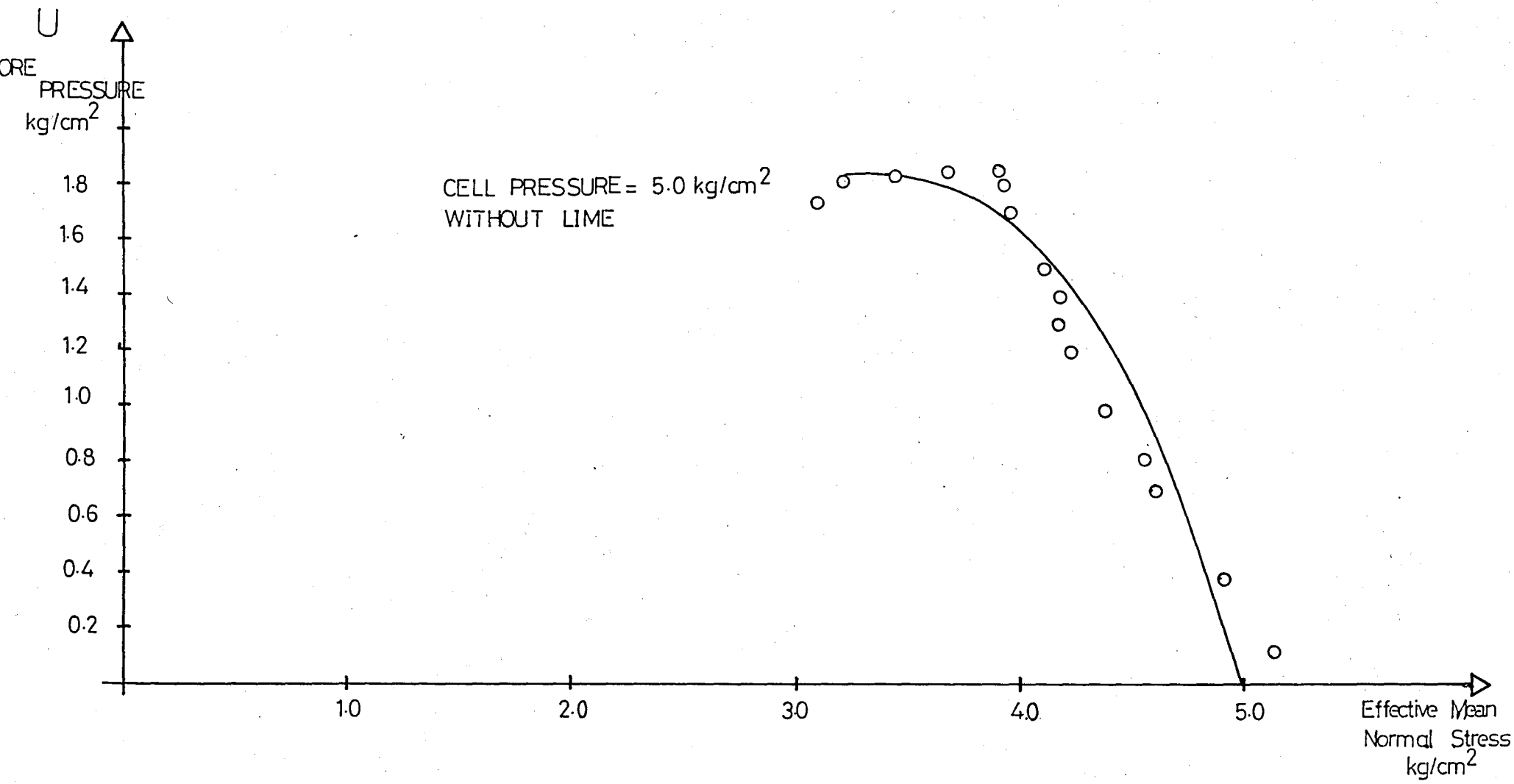

Fig. C 1.4. Test Data Pore-pressure U and Effective Mean Normal Stress p'

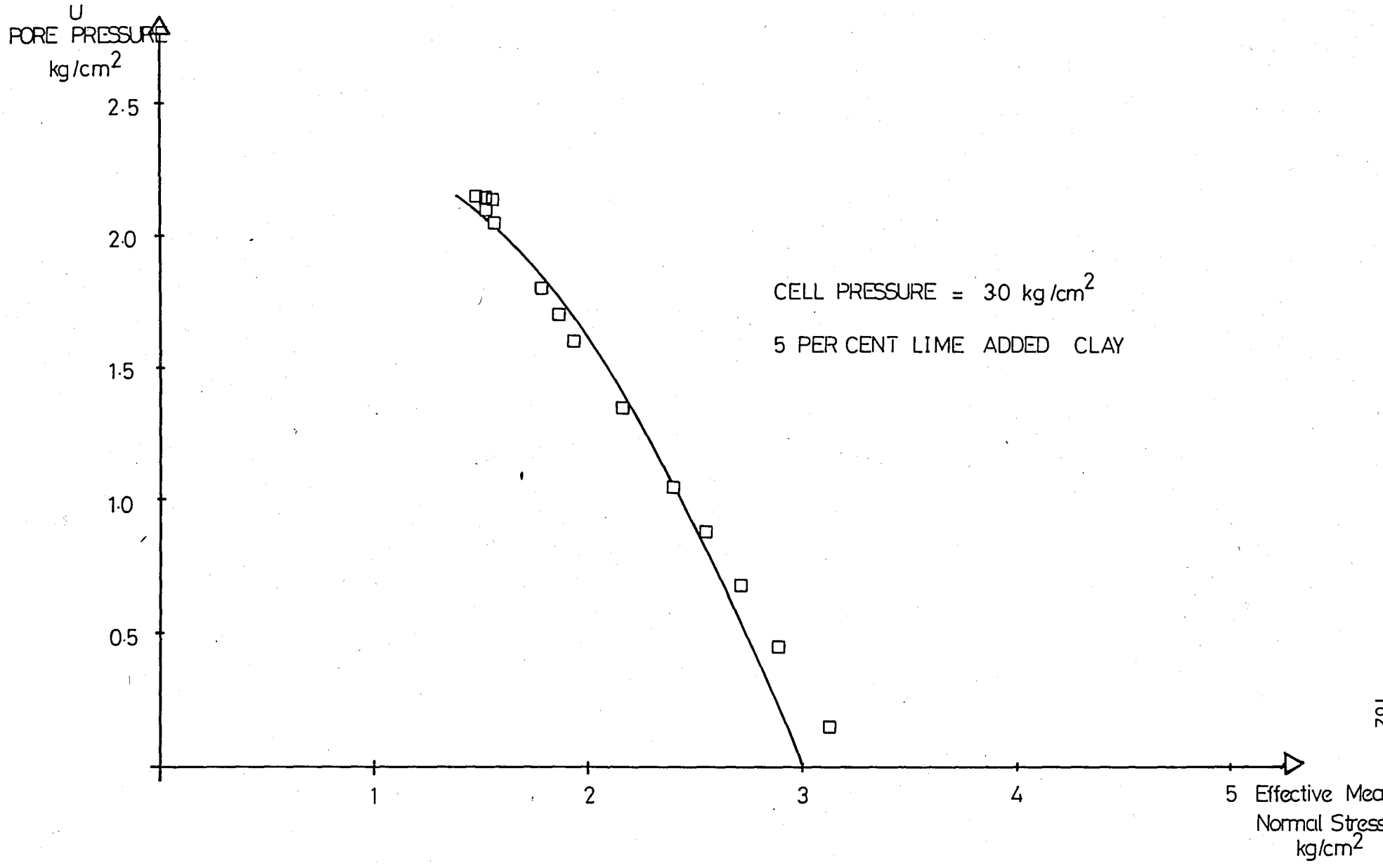

Fig C.2.1. Test Data Pore-pressure U and Effective Mean Normal Stress p'

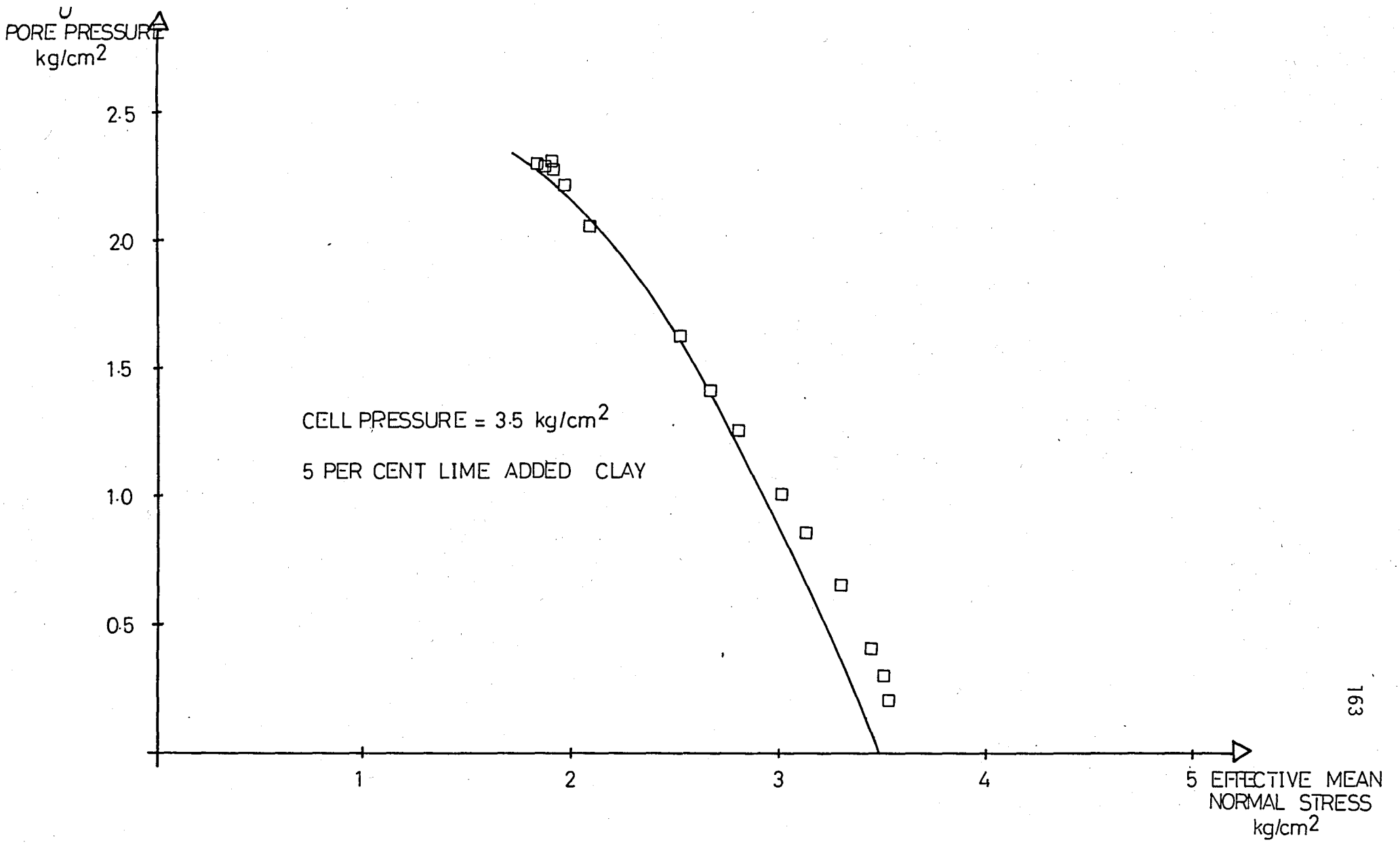

Fig. C 2.2. Test Data Pore-pressure U and Effective Mean Normal Stress p'

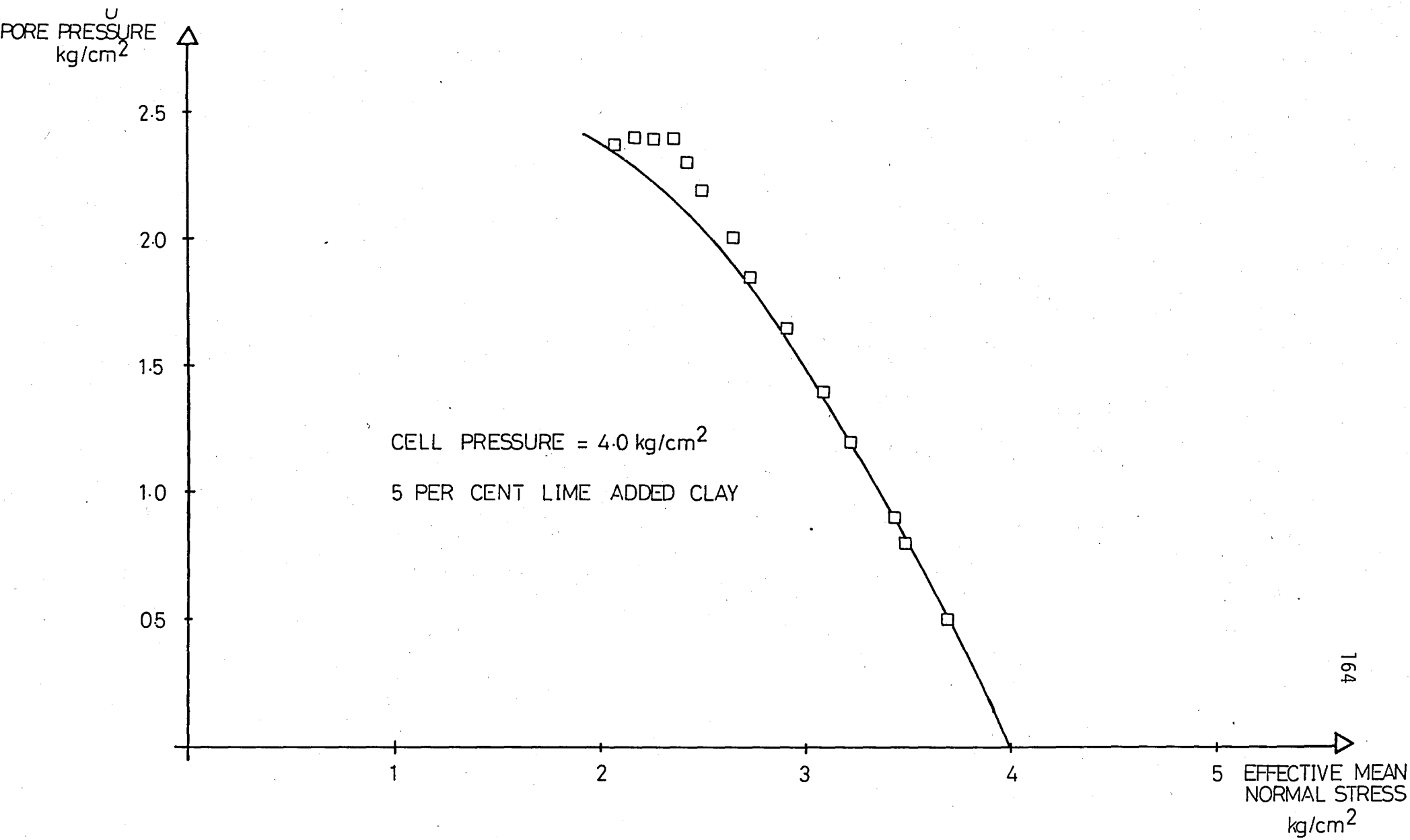

Fig C.2.3. Test Data Pore-pressure U and Effective Mean Normal Stress p'

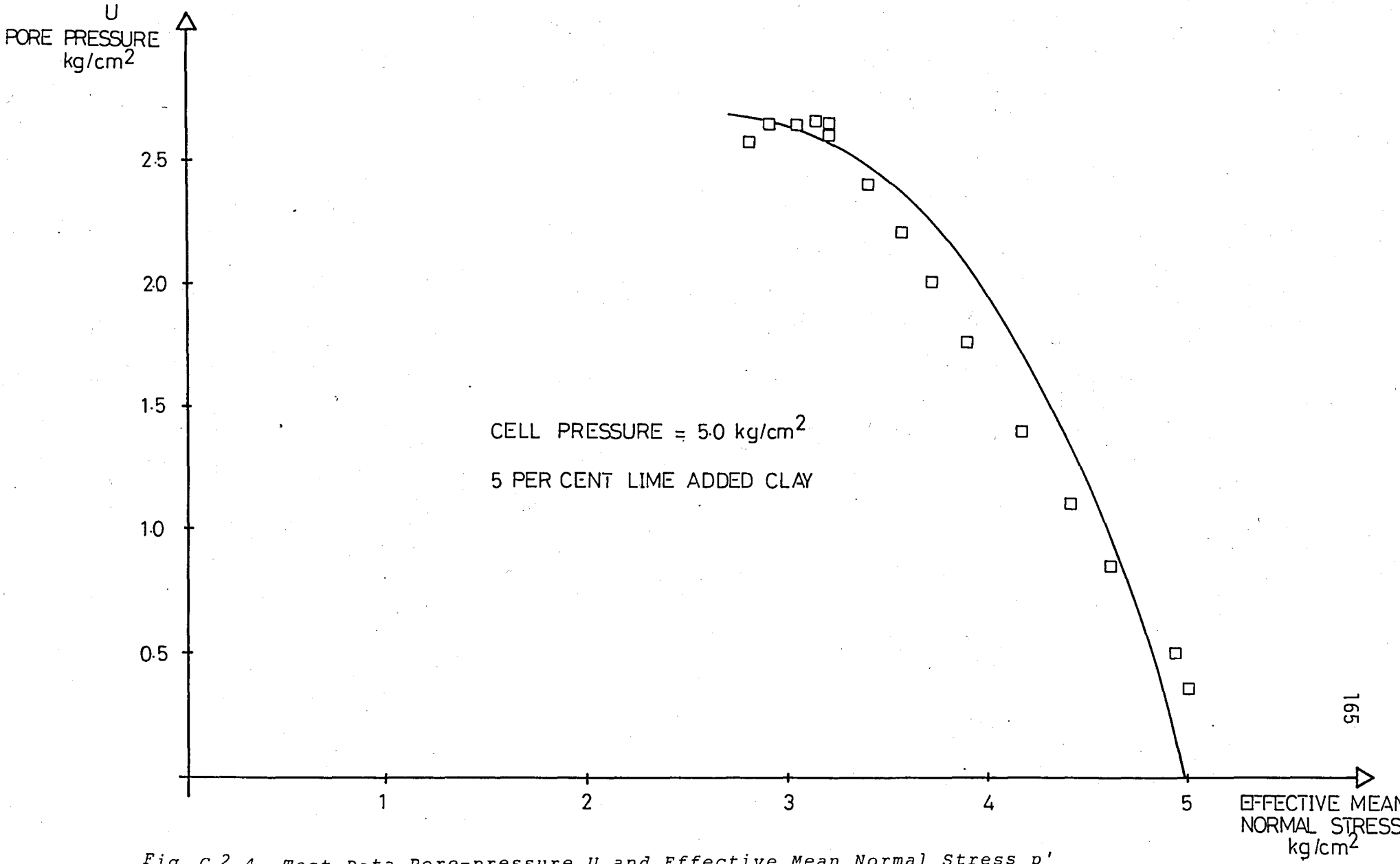

Fig. C.2.4. Test Data Pore-pressure U and Effective Mean Normal Stress p'

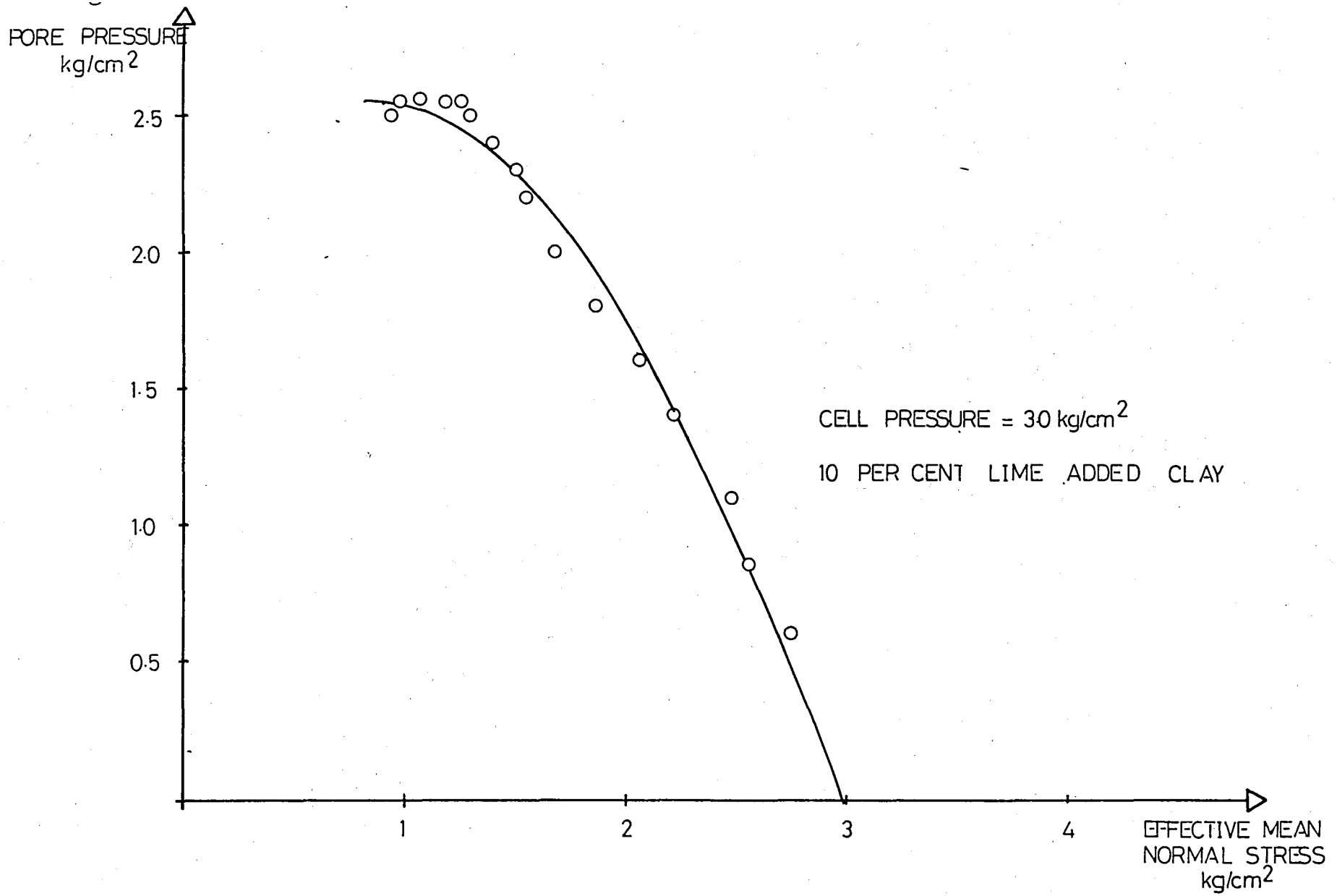

Fig.C 3.1. Test Data Pore-pressure U and Effective Mean Normal Stress p'

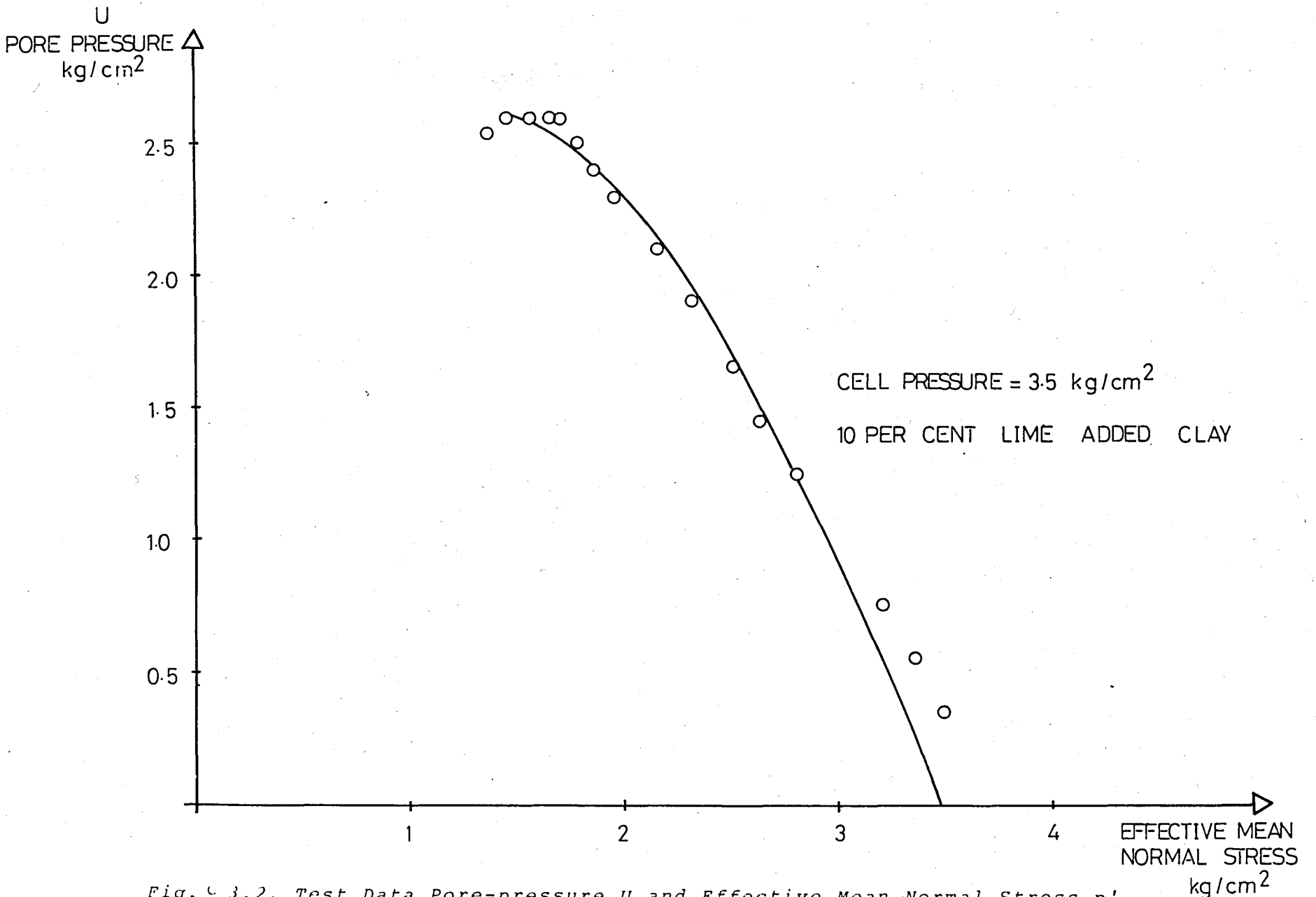

Fig. 3.2. Test Data Pore-pressure U and Effective Mean Normal Stress p'

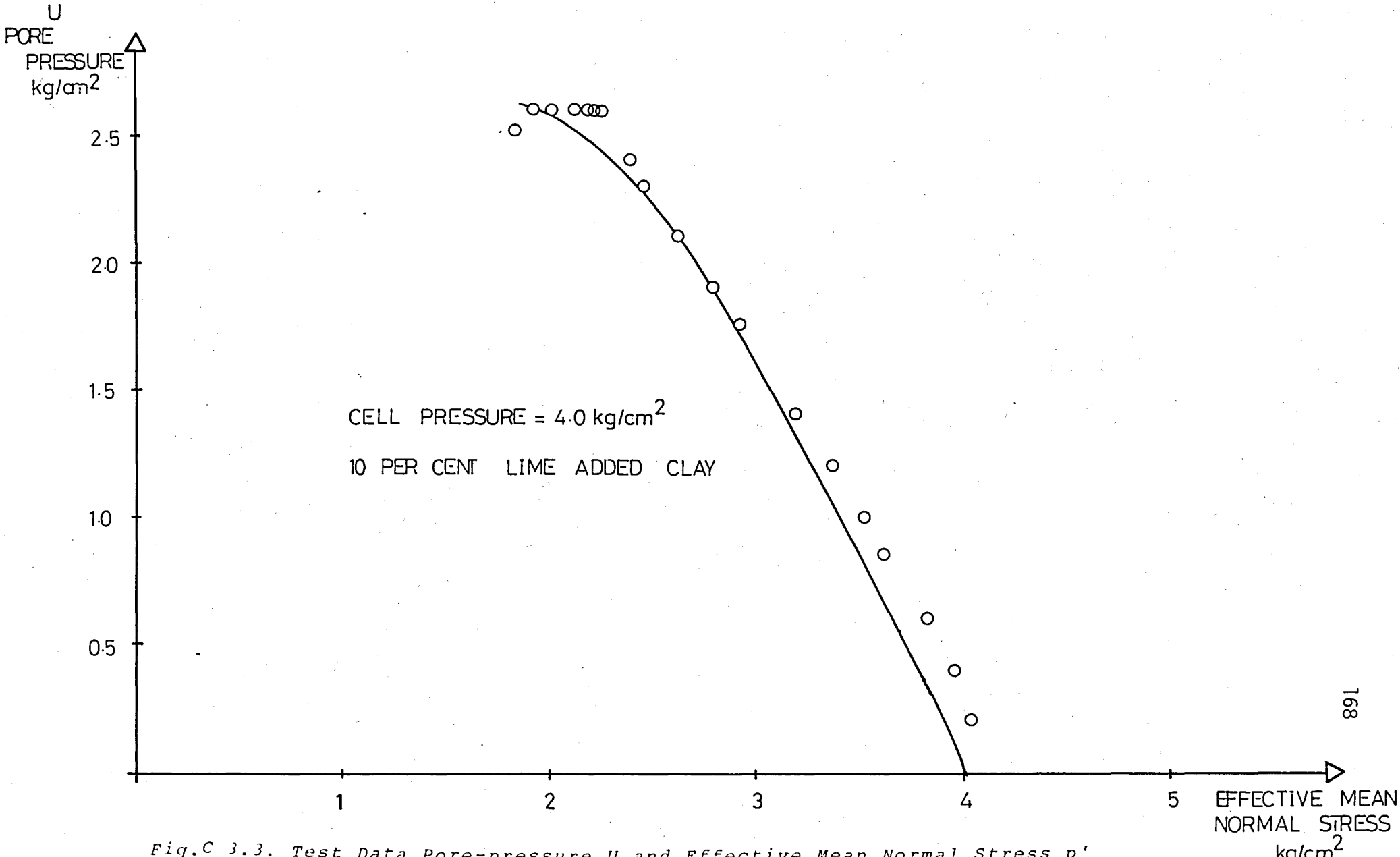

Fig.C 3.3. Test Data Pore-pressure U and Effective Mean Normal Stress p'

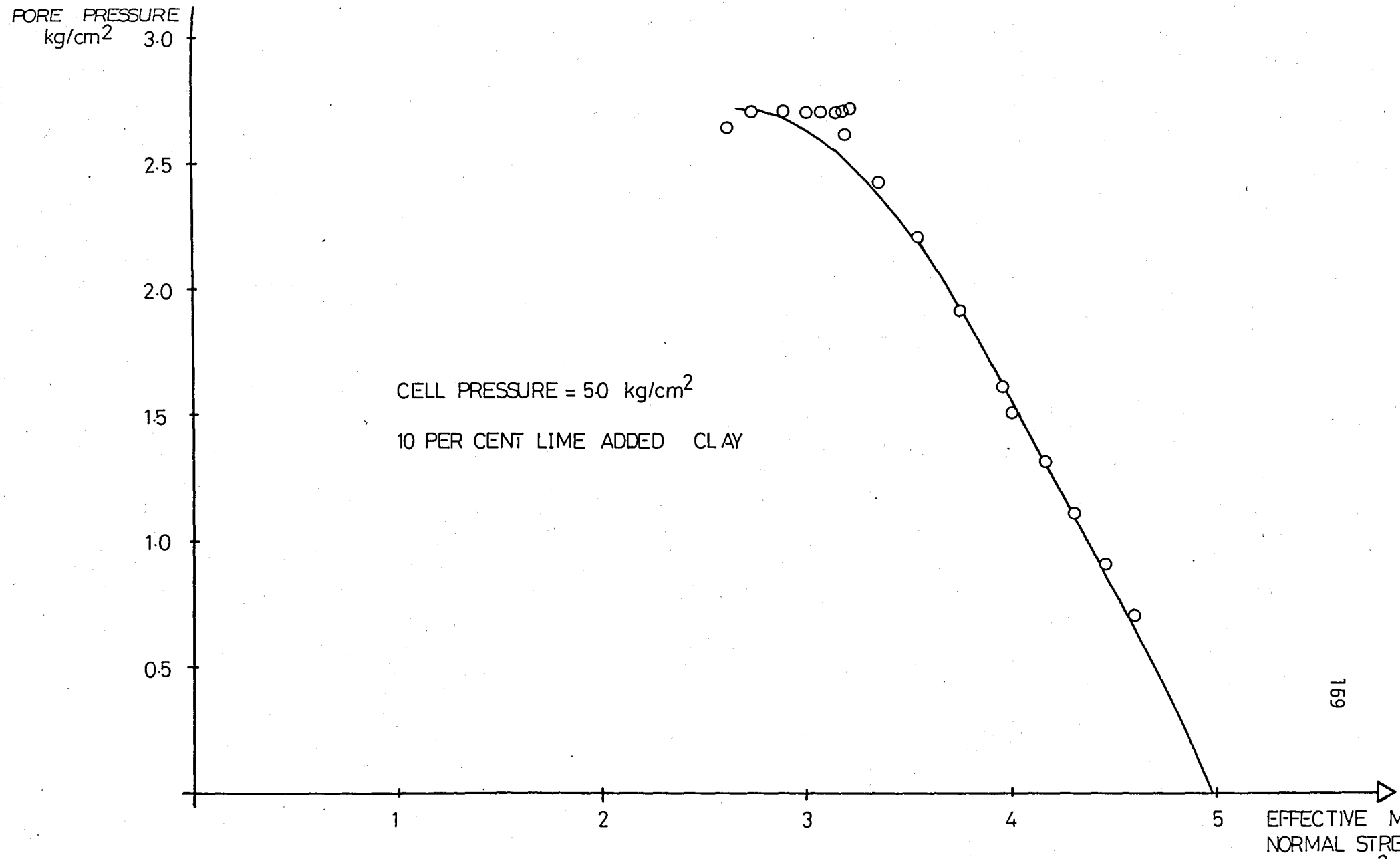

Fig.C 3.4. Test Data Pore-pressure U and Effective Mean Normal Stress p'

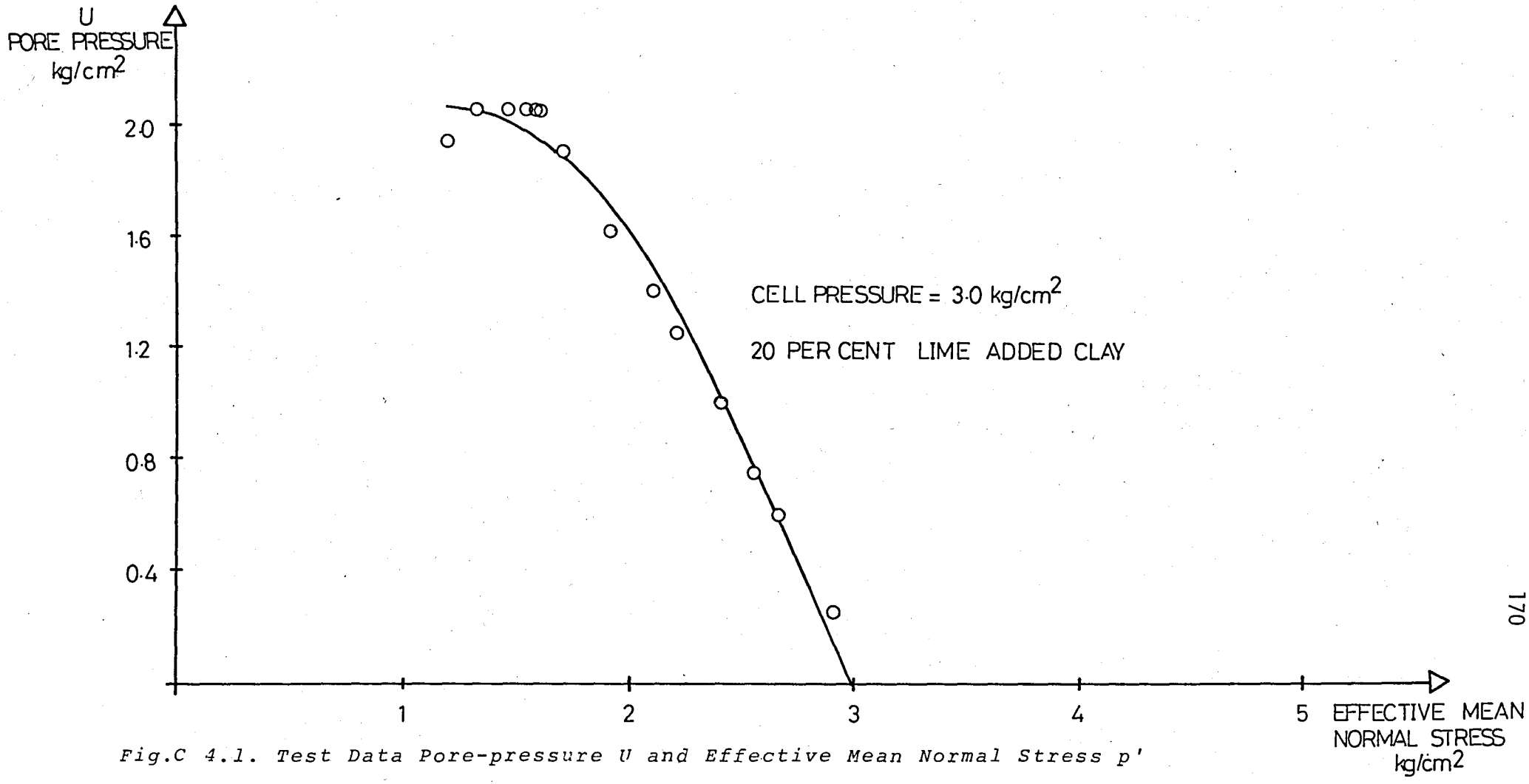

Fig.C 4.1. Test Data Pore-pressure U and Effective Mean Normal Stress p'

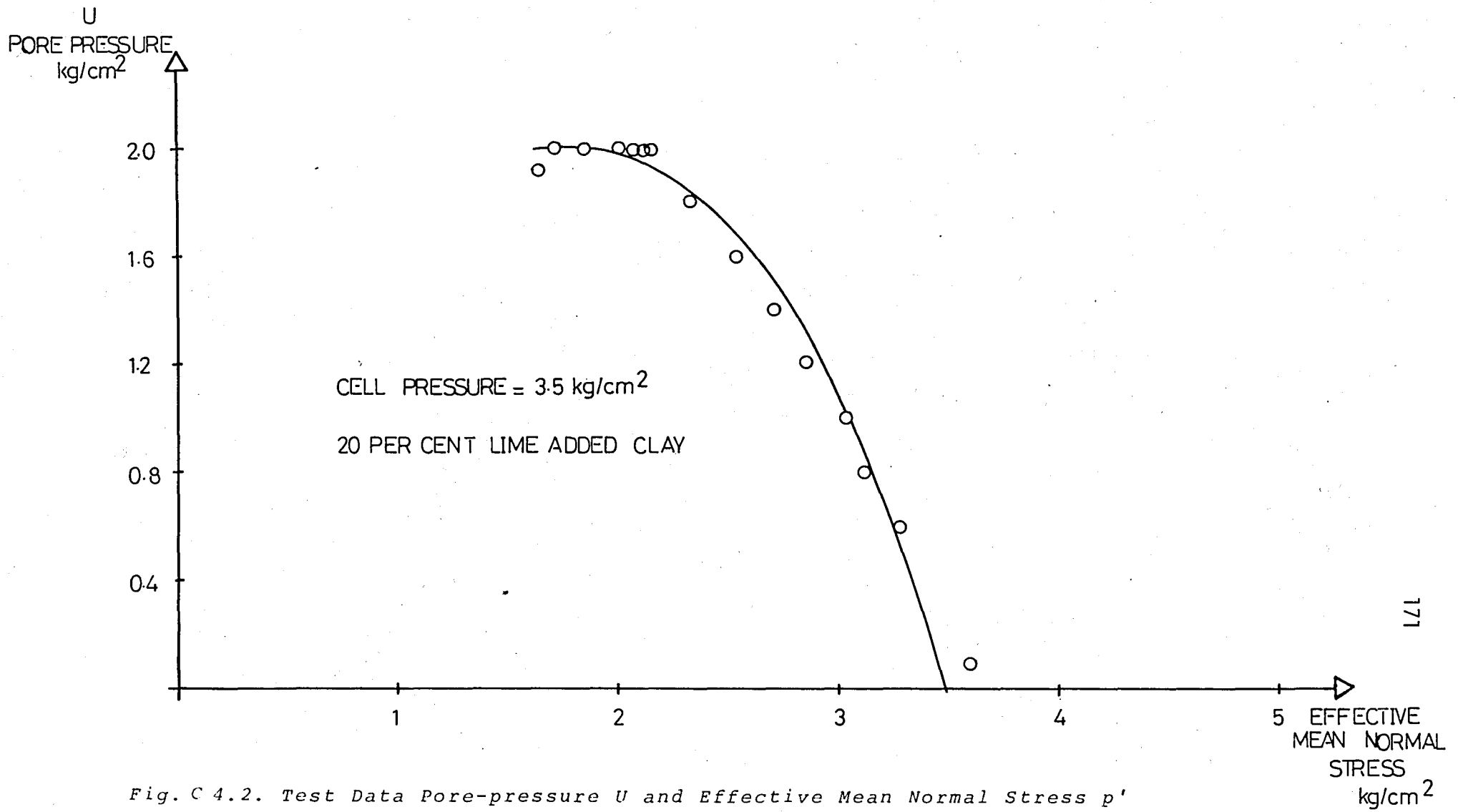

Fig. C 4.2. Test Data Pore-pressure U and Effective Mean Normal Stress p'

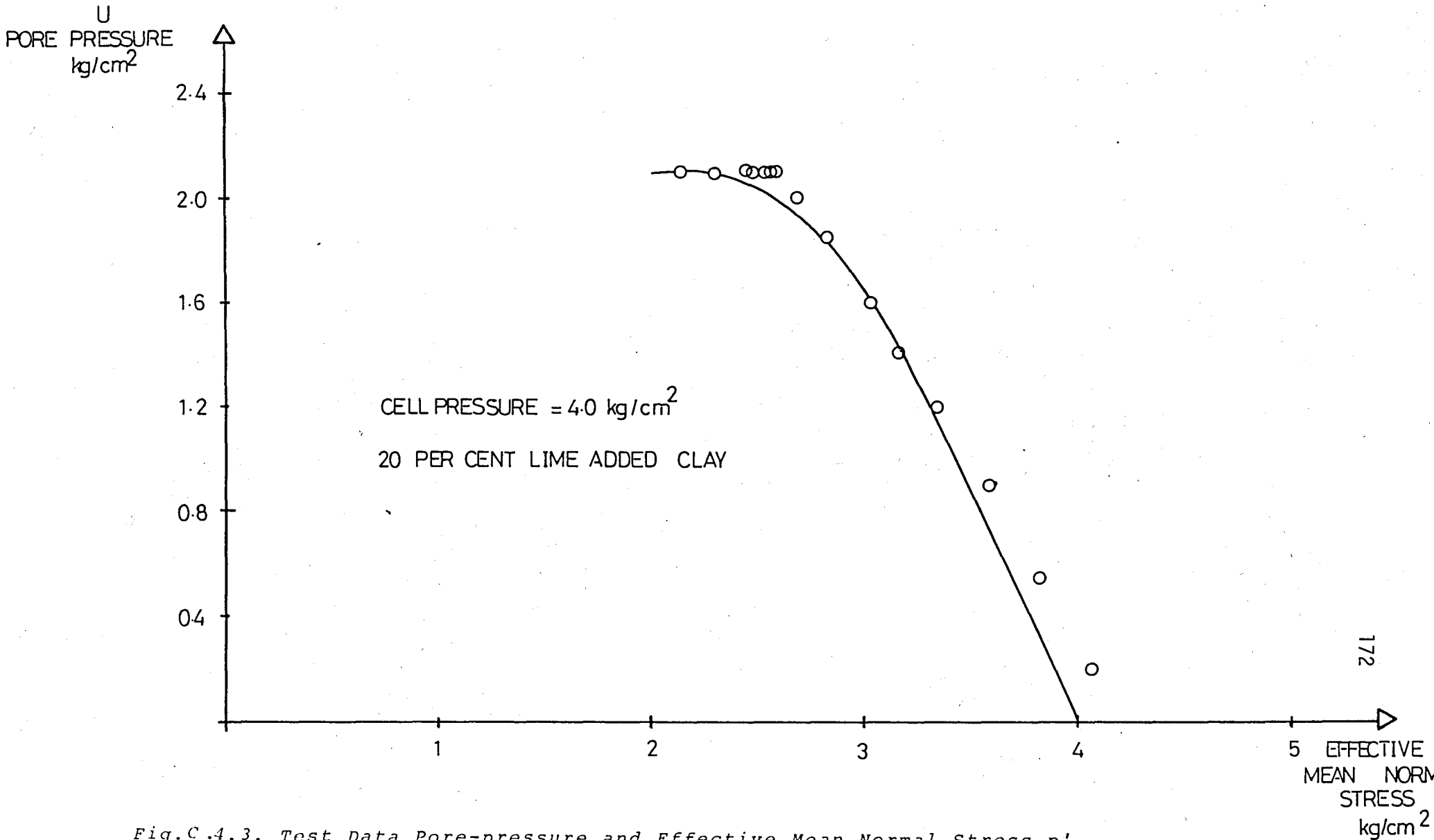

Fig.C.4.3. Test Data Pore-pressure and Effective Mean Normal Stress p'

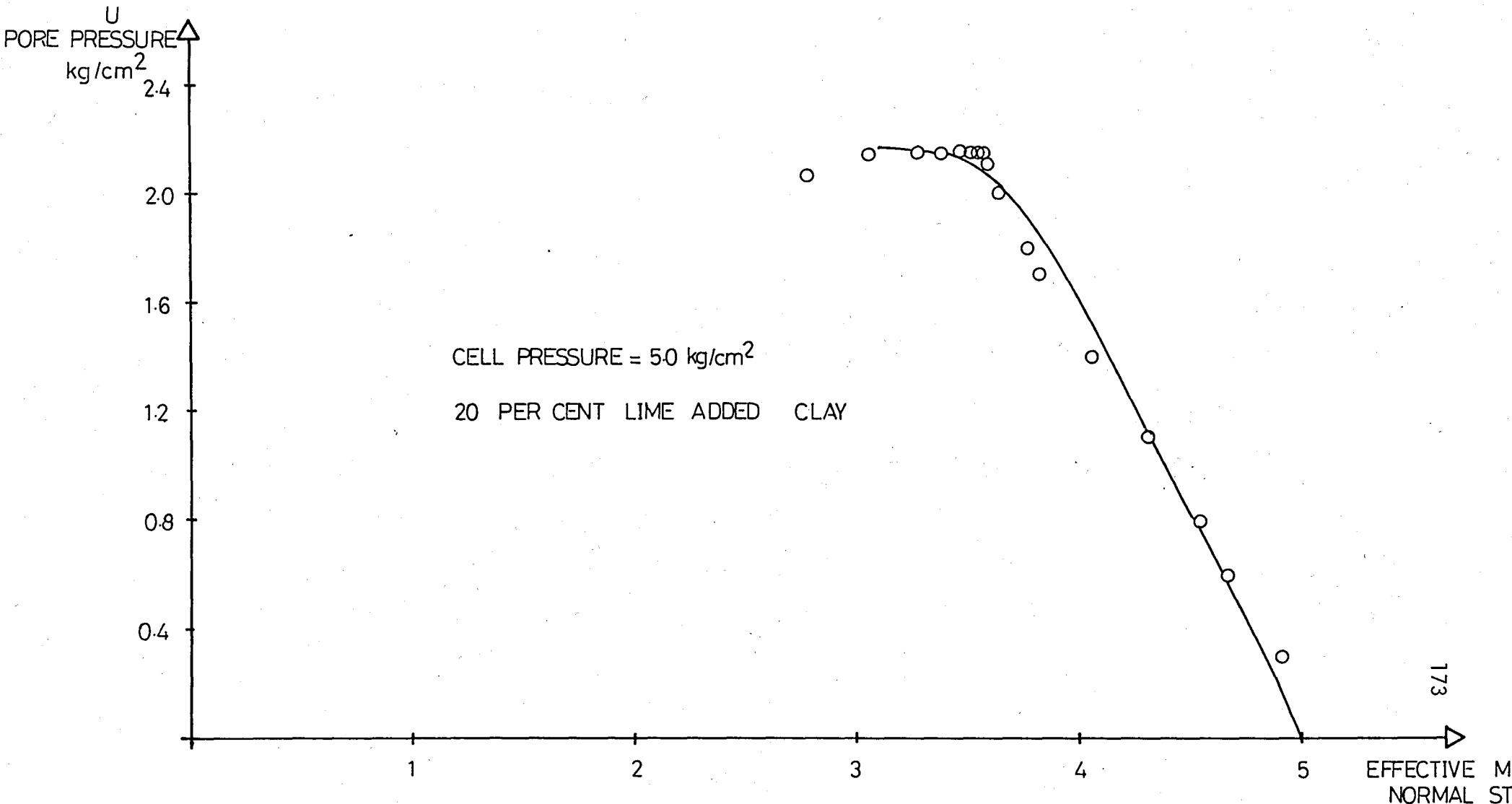

Fig.C.4.4. Test Data Pore-pressure U and Effective Mean Normal Stress p'

APPENDIX D

$A_p : \varepsilon_\alpha$ CURVES

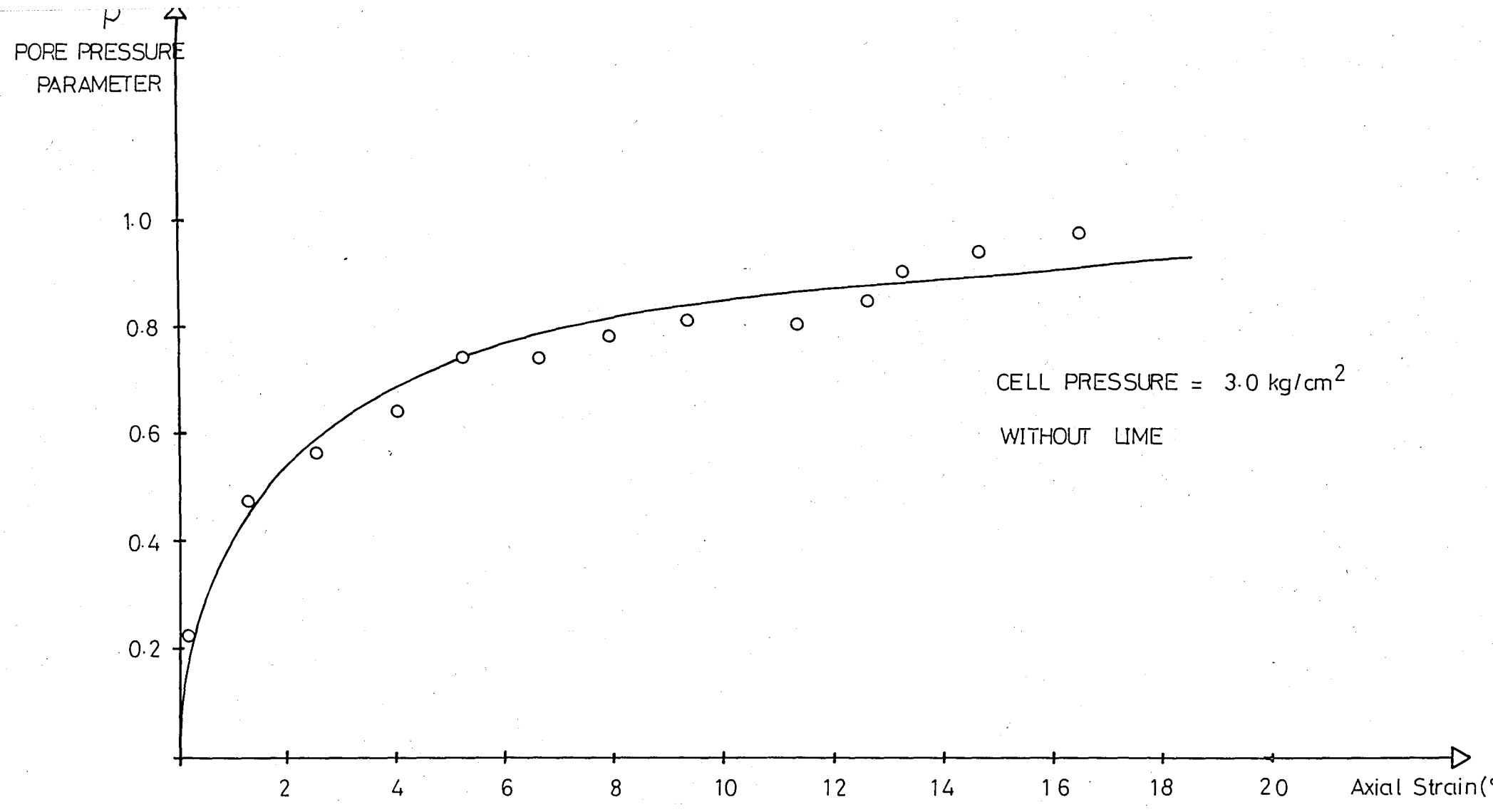

Fig. D 1.1. Relationship Between Pore-pressure Parameter A_p and Axial Strain ε_a

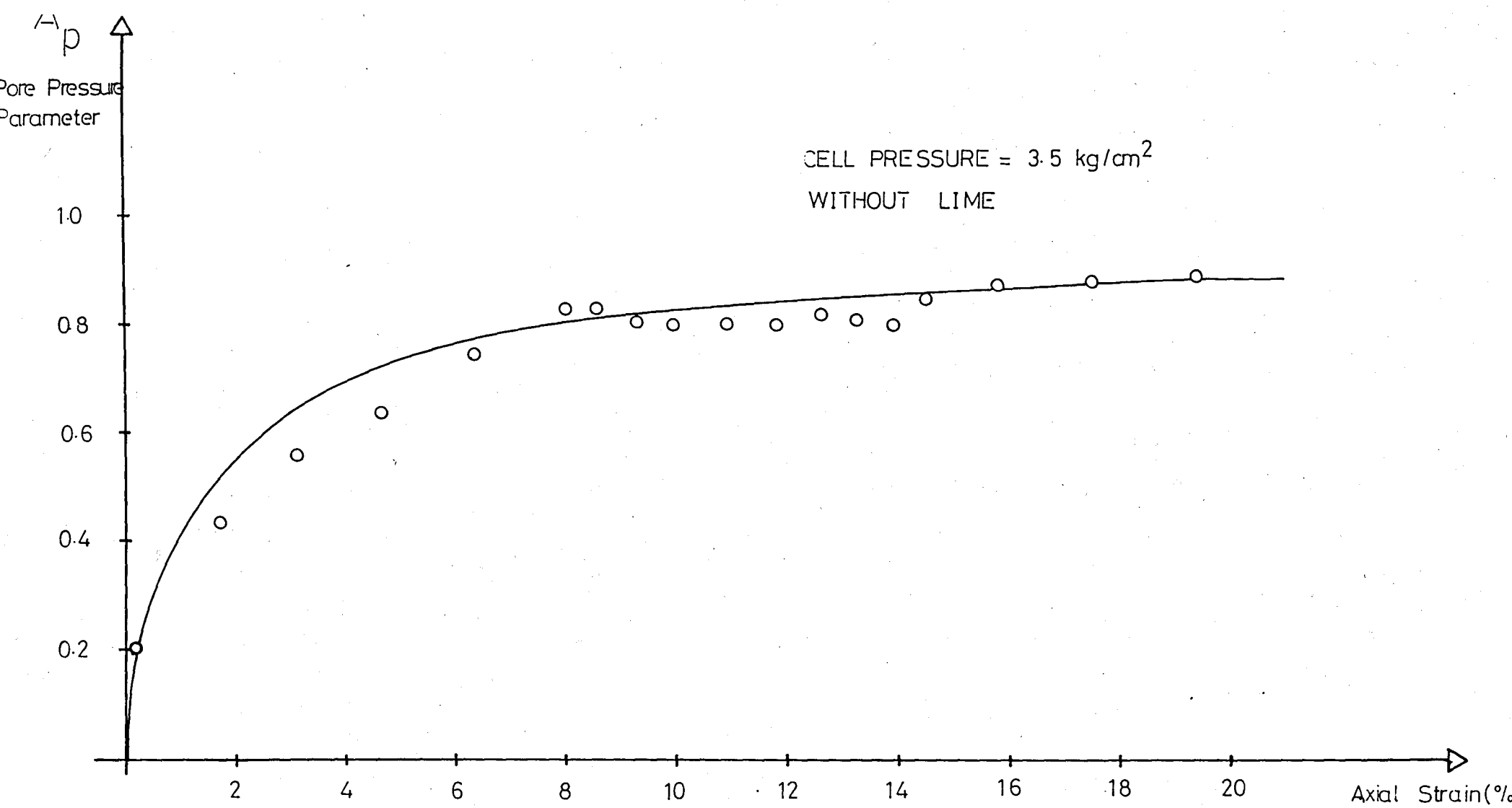

Fig. 11.2. Relationship Between Pore-pressure Parameter A_p and Axial Strain ε_a

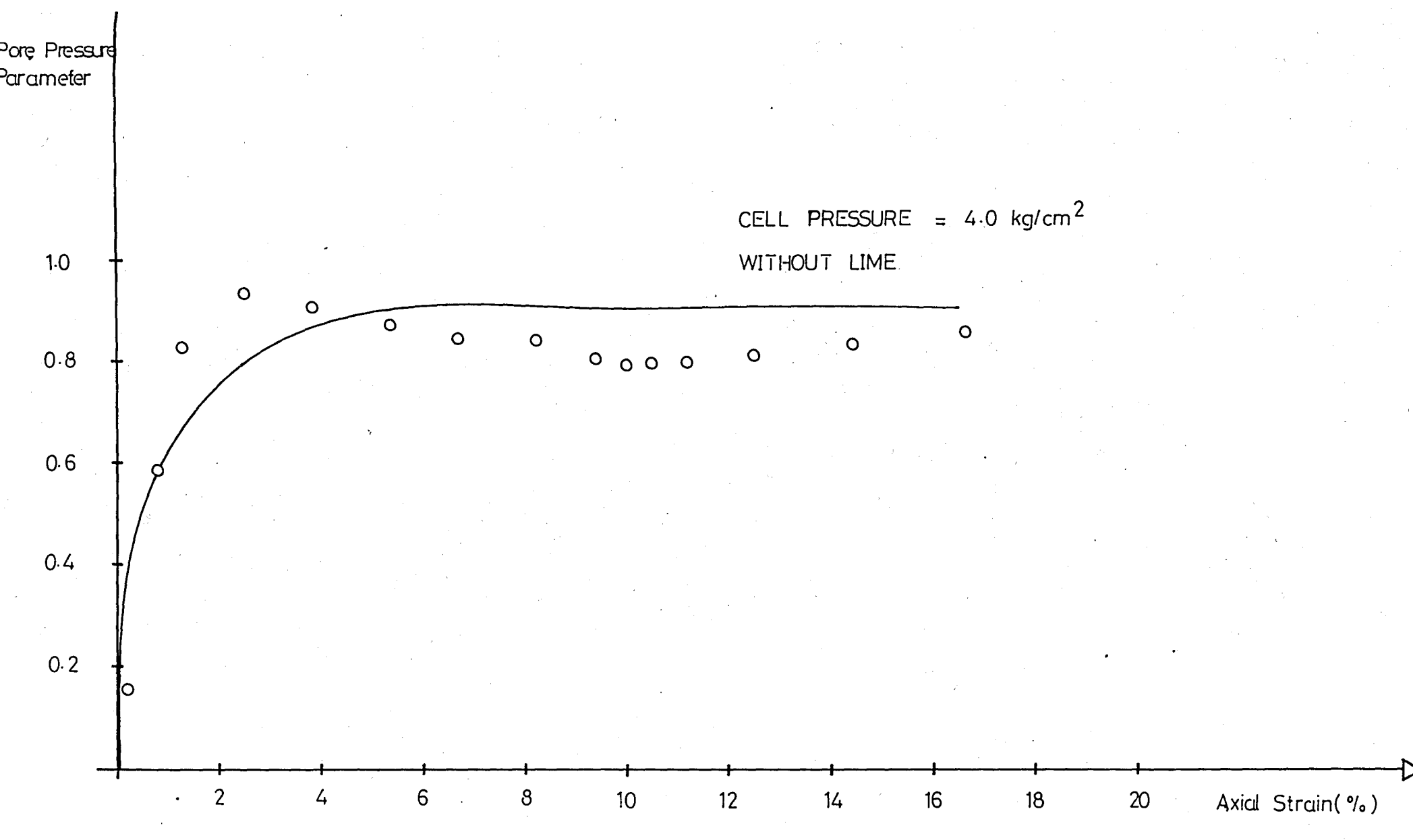

Fig. D.1.3. Relationship Between Pore-pressure Parameter A_p and Axial Strain ε_a

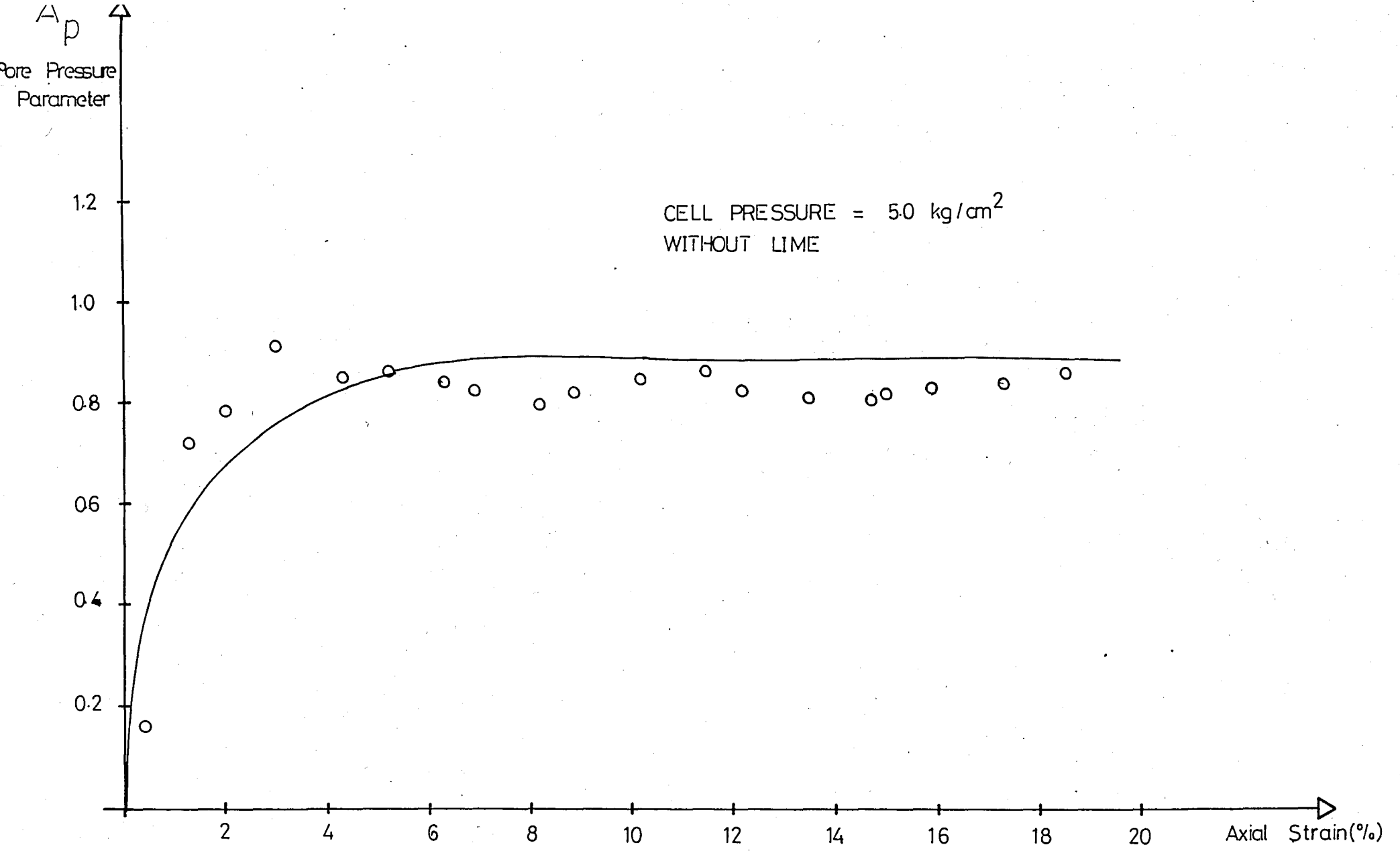

Fig.D.1.4. Relationship Between Pore-pressure Parameter A_p and Axial Strain ε_a

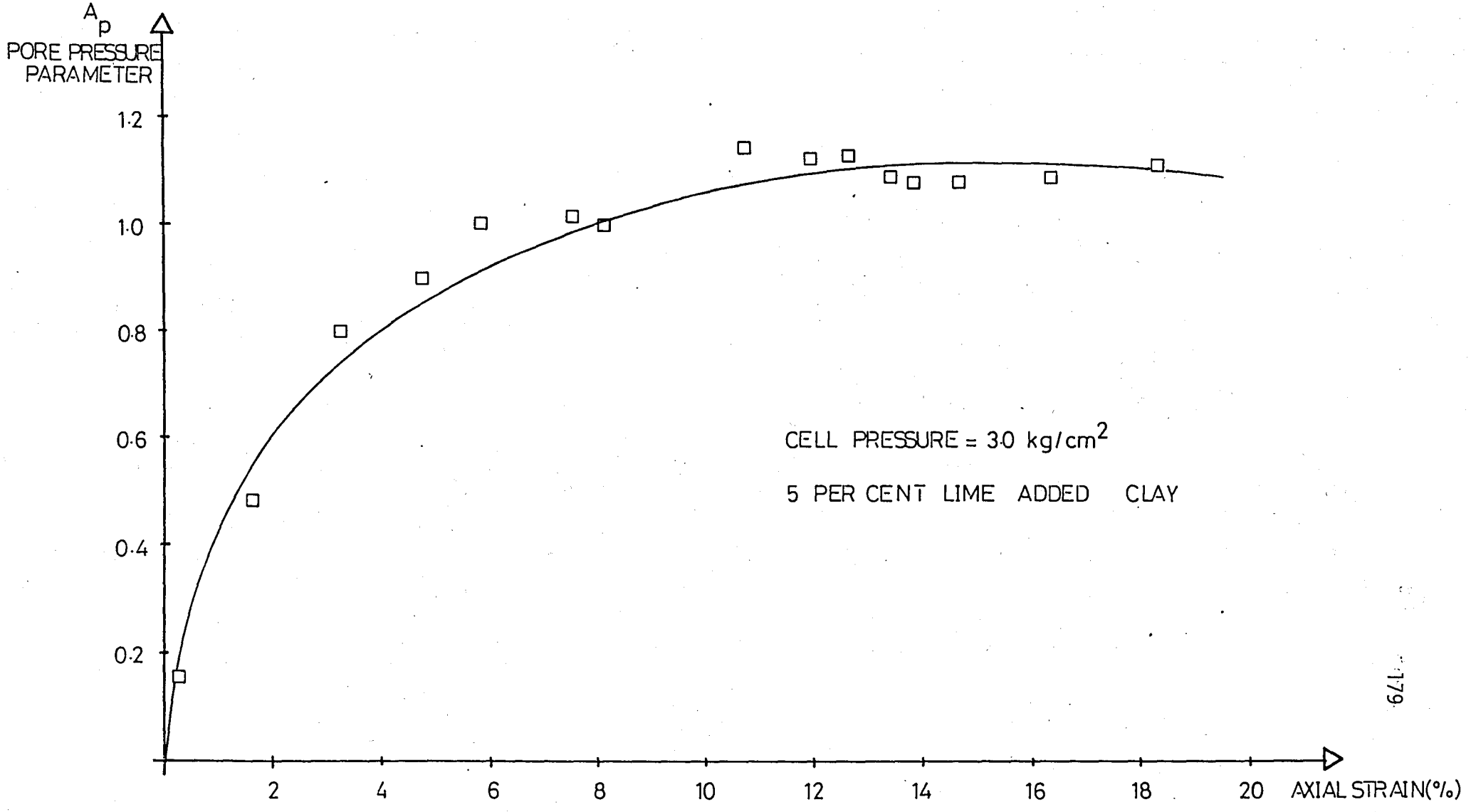

Fig. D 2.1. Relationship Between Pore-pressure Parameter A_p and Axial Strain ε_α

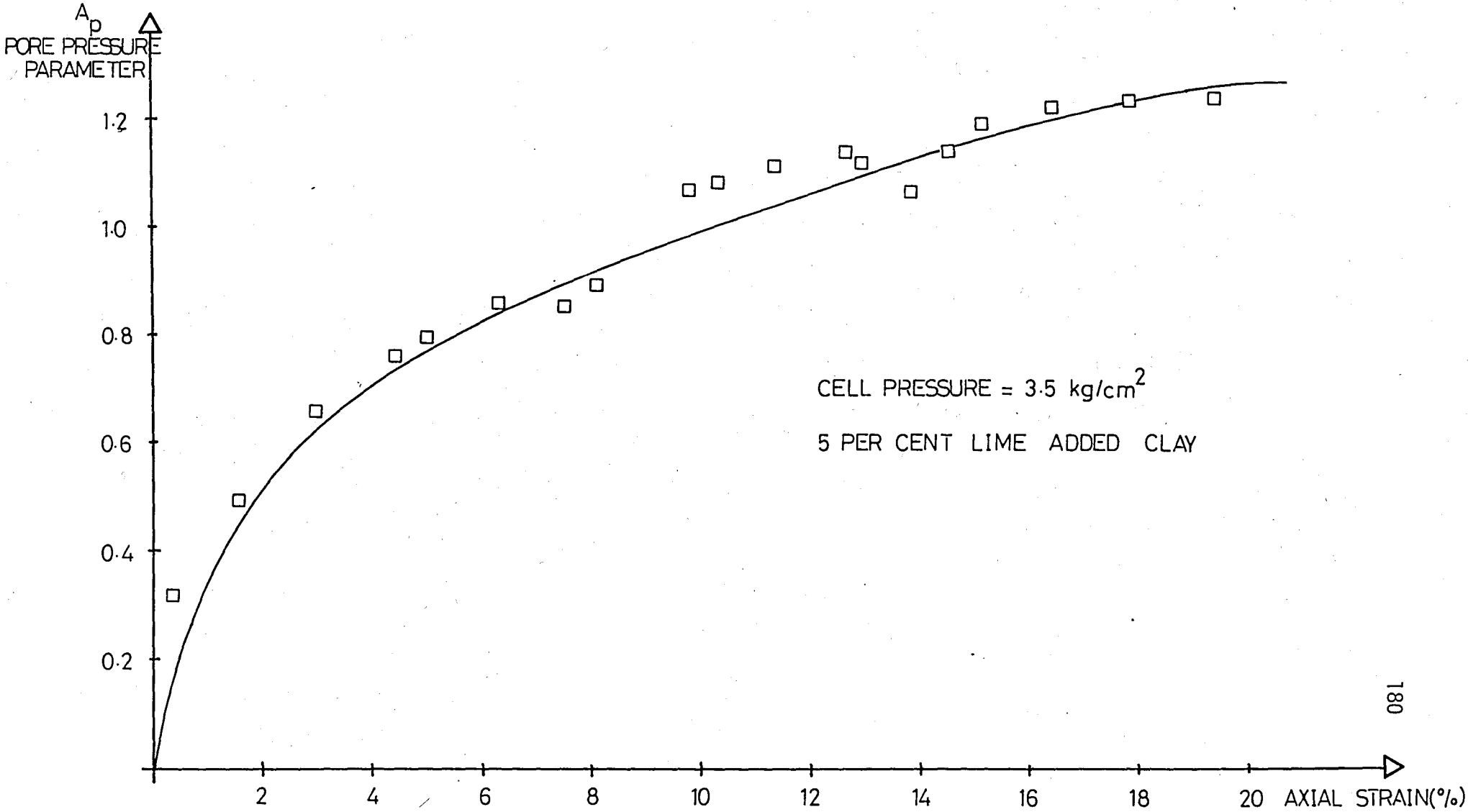

Fig. D.2.2. Relationship Between Pore-pressure Parameter A_p and Axial Strain ε_a

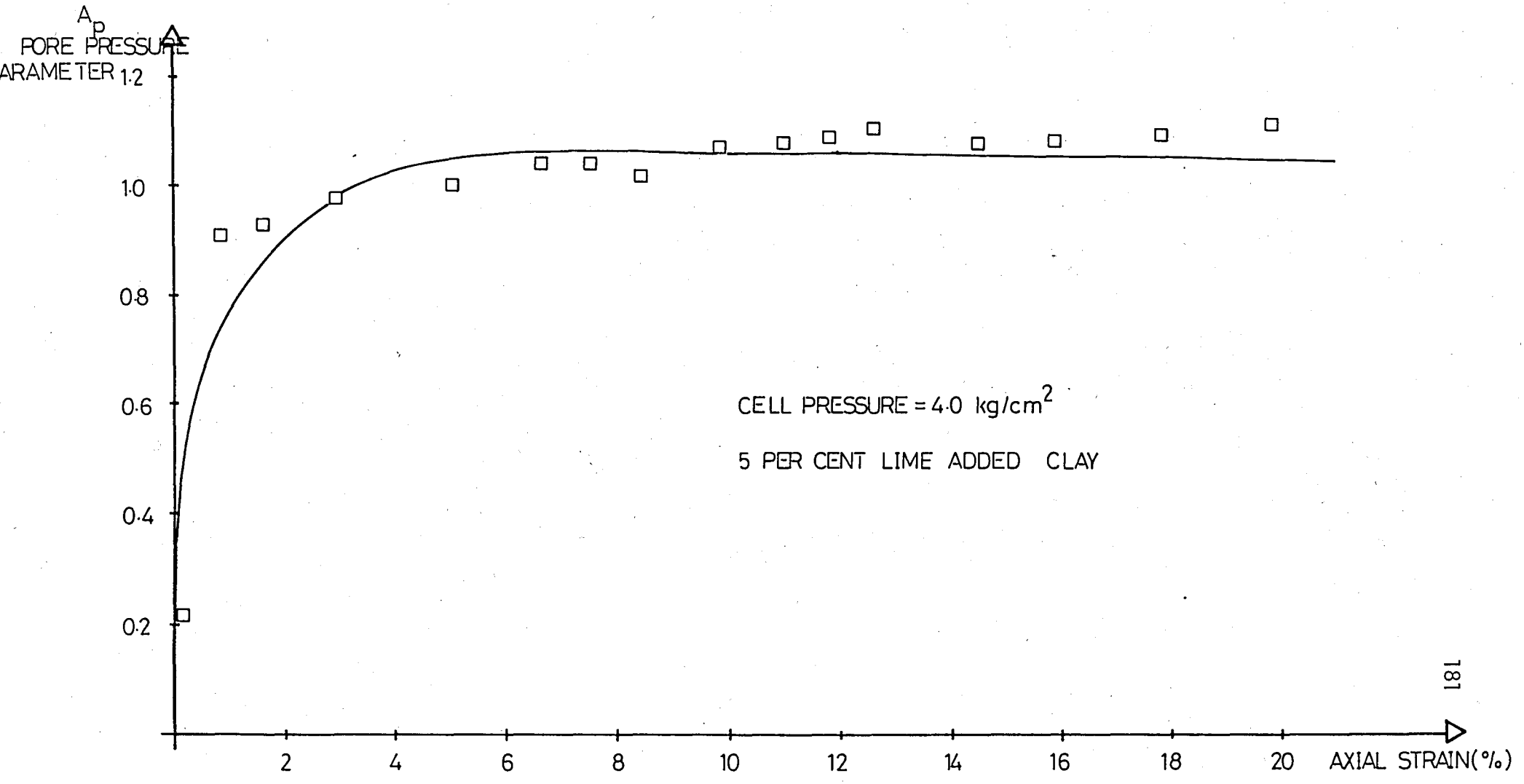

Fig. D 2.3. Relationship Between Pore-pressure Parameter A_p and Axial Strain ε_a

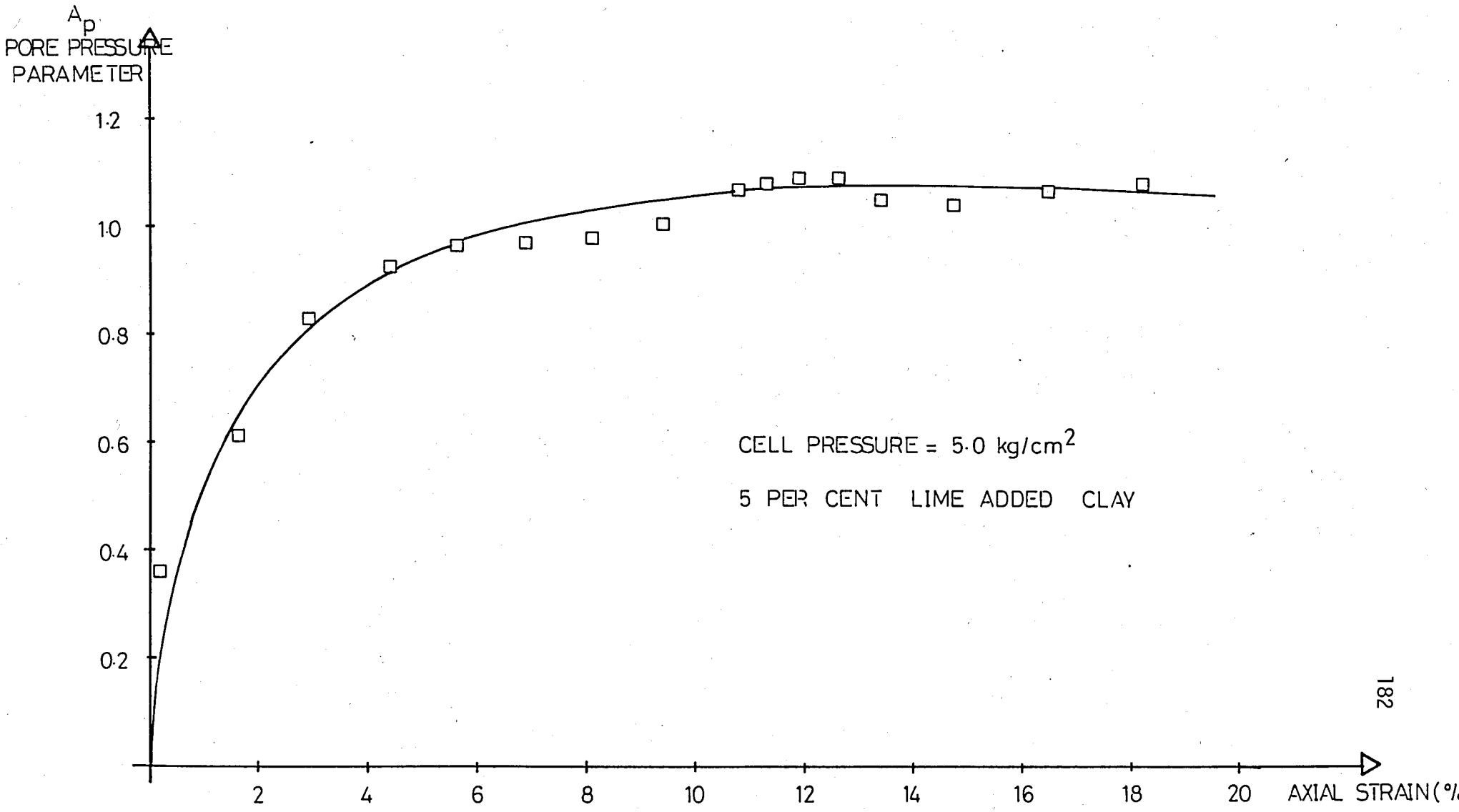

Fig. D 2.4. Relationship Between Pore-pressure Parameter A_p and Axial Strain ϵ_1

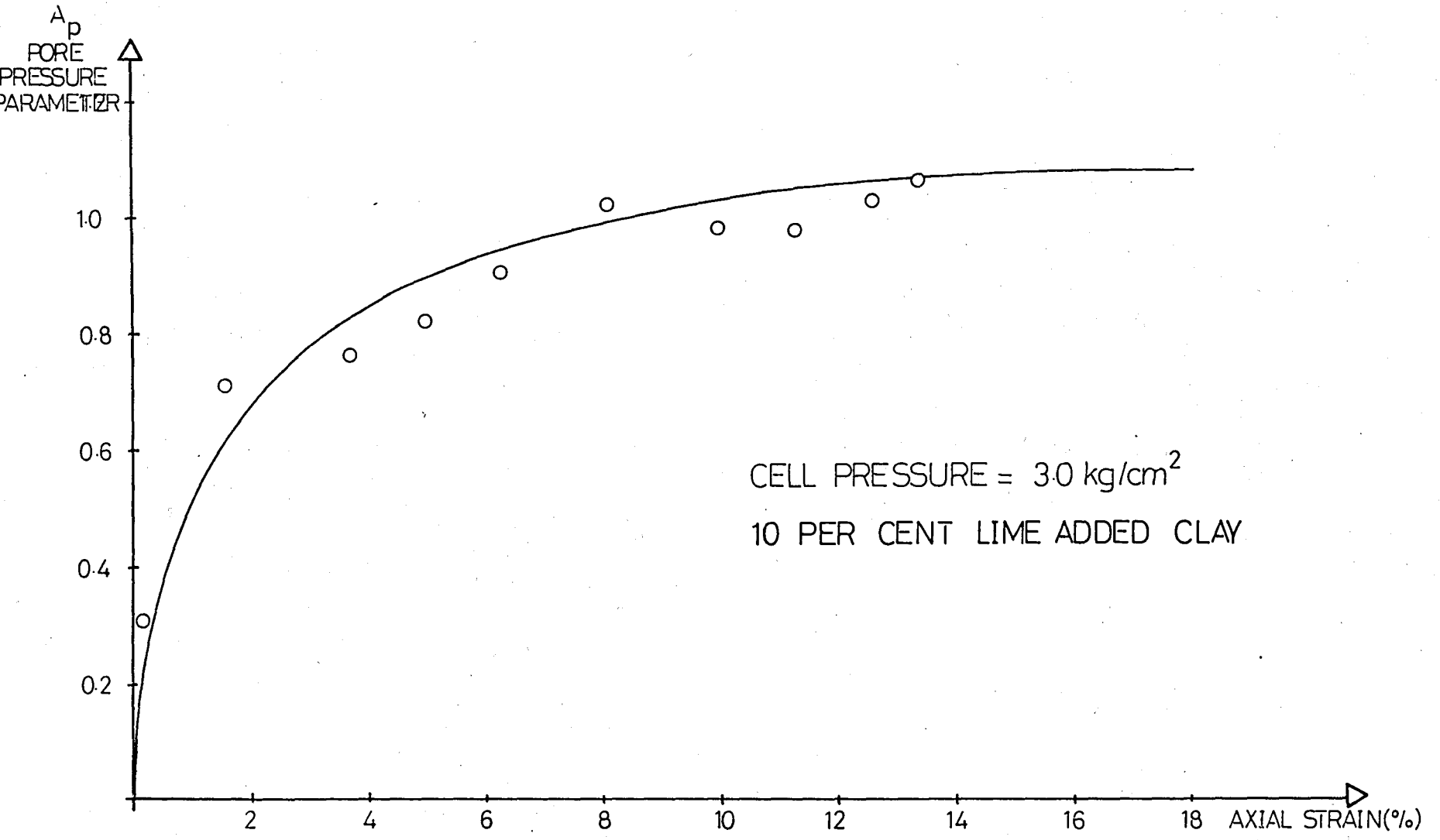

Fig. D.3.1. Relationship Between Pore-pressure Parameter A_p and Axial Strain ε_a

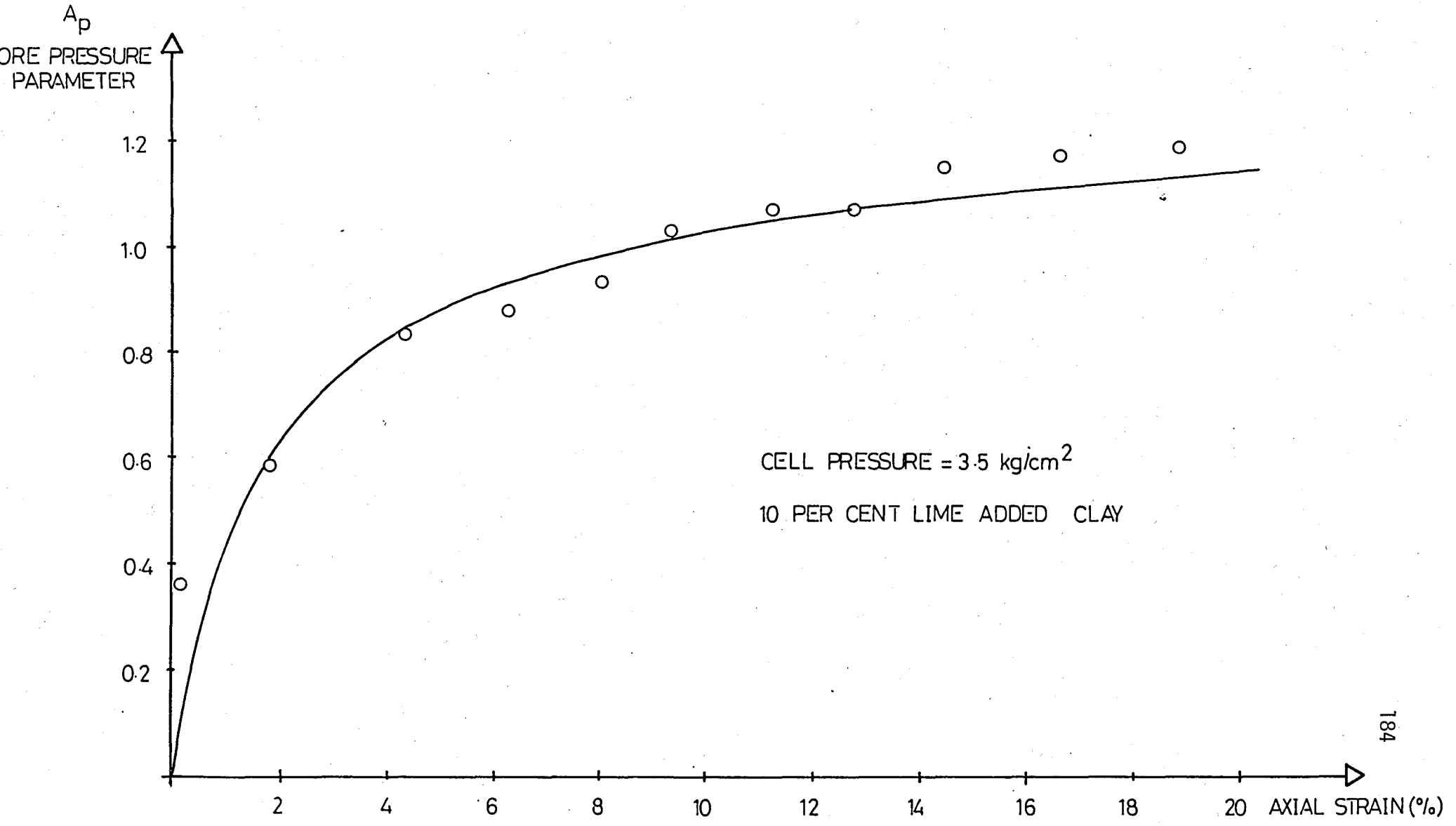

Fig.D.3.2. Relationship Between Pore-pressure Parameter A_p and Axial Strain ε_α

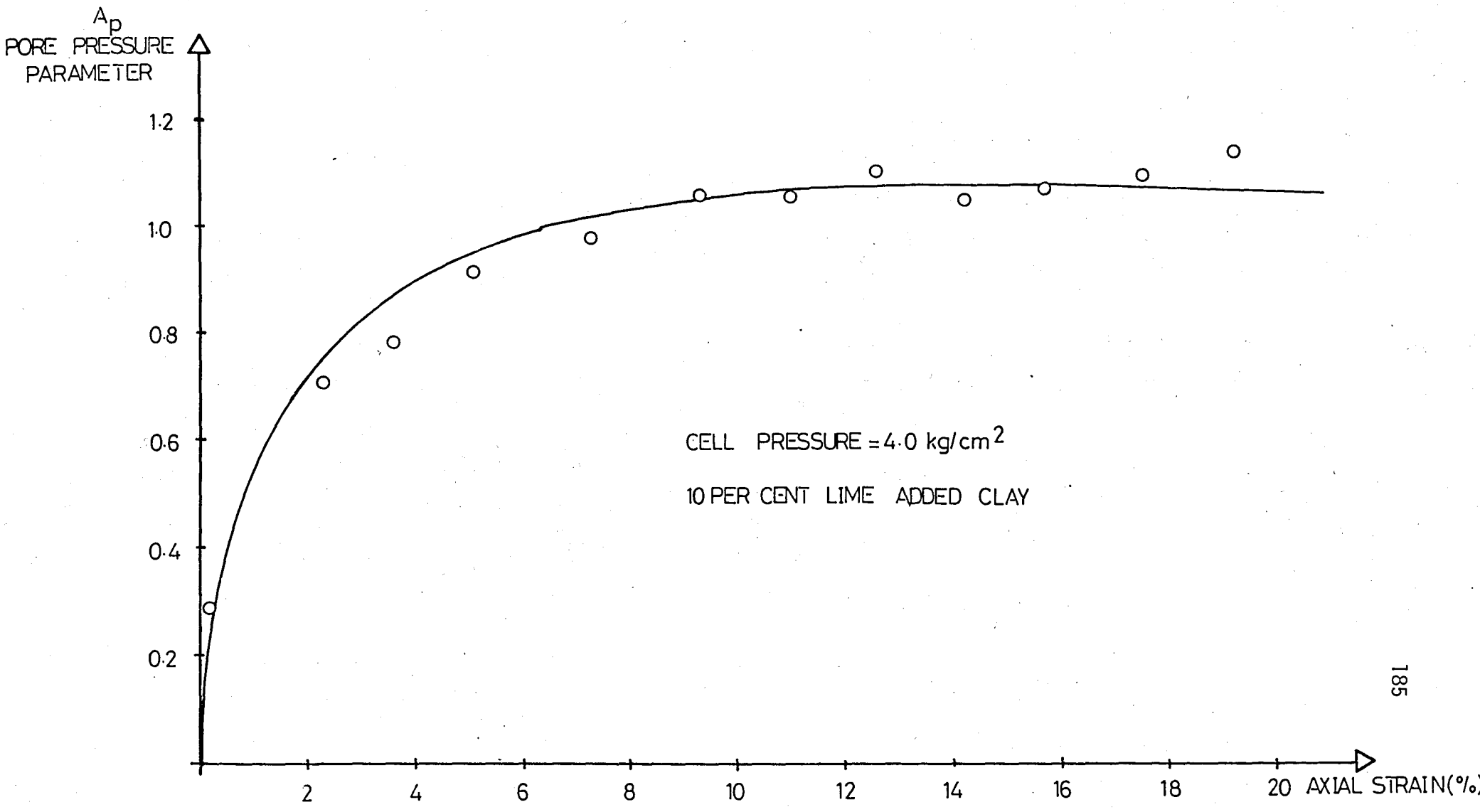

Fig.D.3.3. Relationship Between Pore-pressure Parameter A_p and Axial Strain ε_α

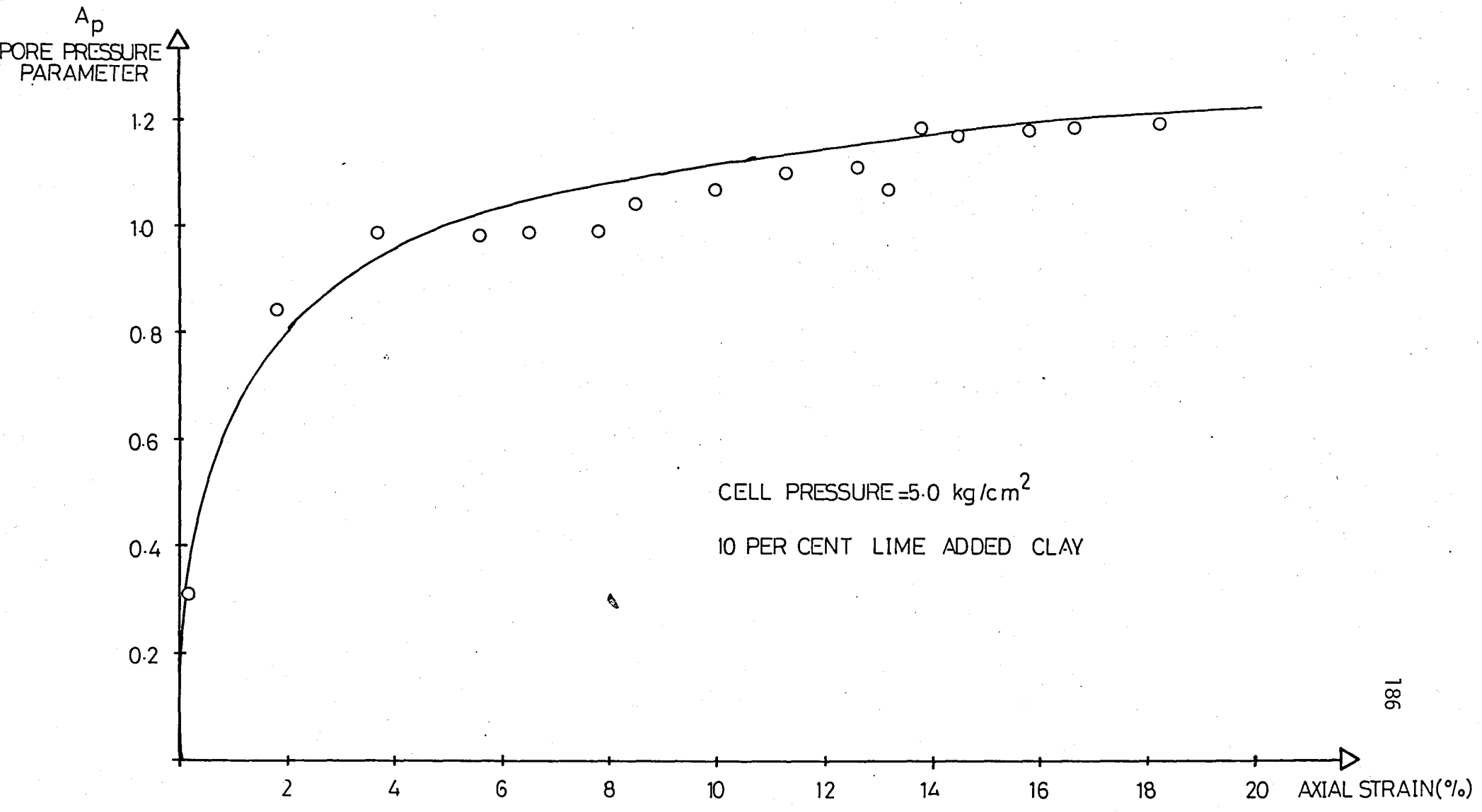

Fig.D.3.4. Relationship Between Pore-pressure Parameter A_p and Axial Strain ε_α

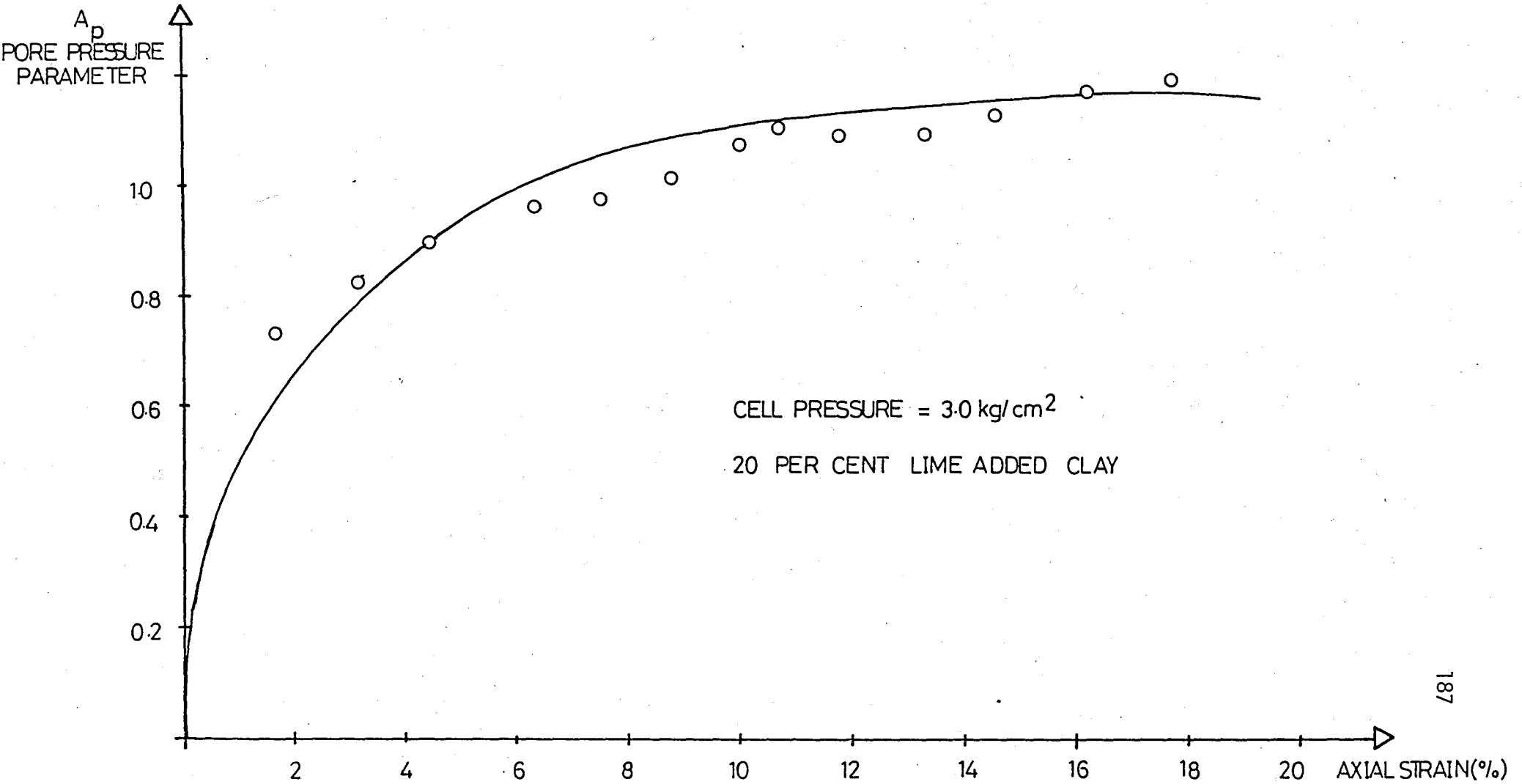

Fig. D.4.1. Relationship Between Pore-pressure Parameter A_p and Axial Strain ε_α

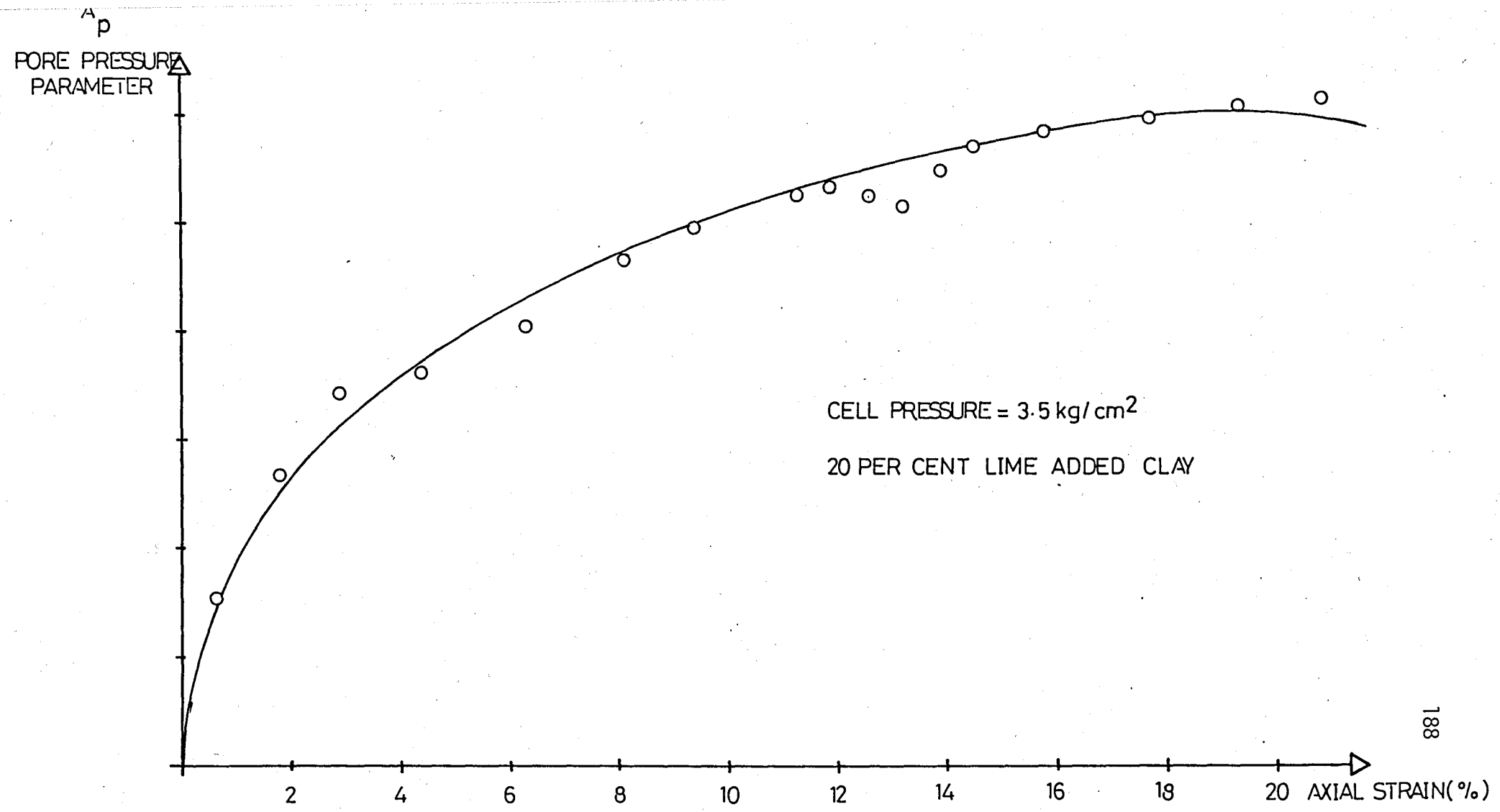

Fig.D.4.2. Relationship Between Pore-pressure Parameter A_p and Axial Strain ε_α

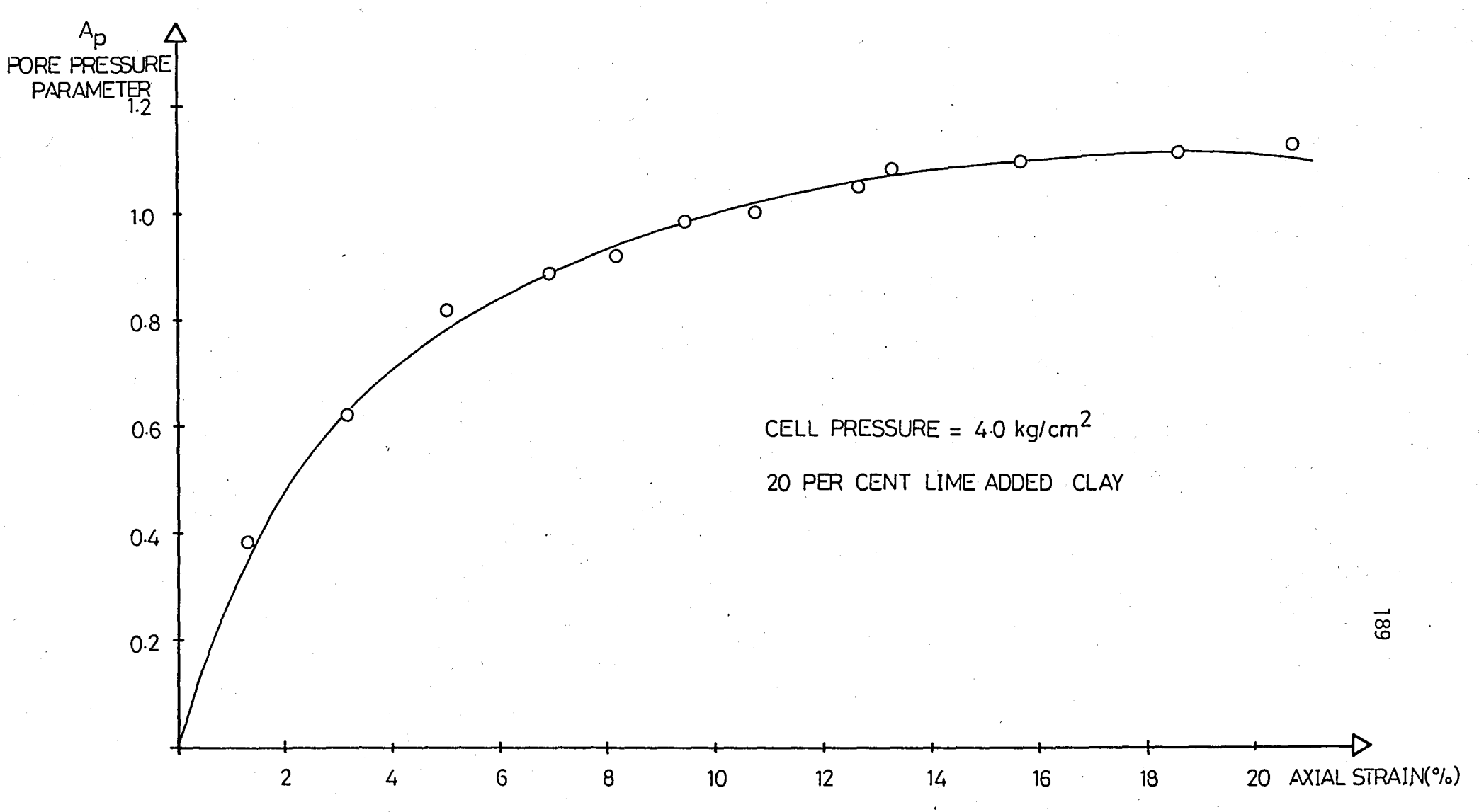

Fig D.4.3. Relationship Between Pore.pressure Parameter A_p and Axial Strain ε_α

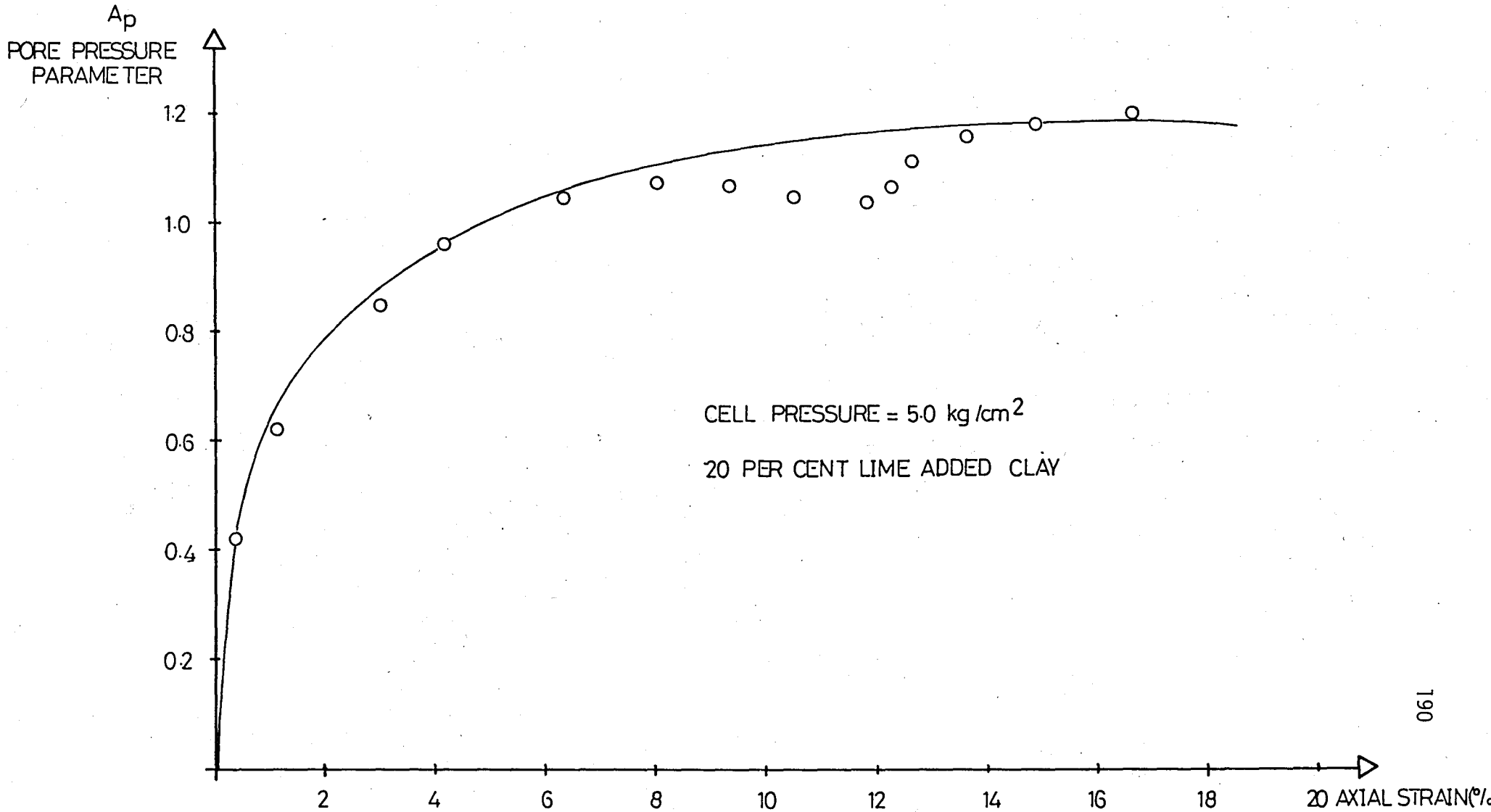

Fig. D.4.4. Relationship Between Pore-pressure Parameter A_p and Axial Strain ε_α

APPENDIX E

A_p : p' CURVES

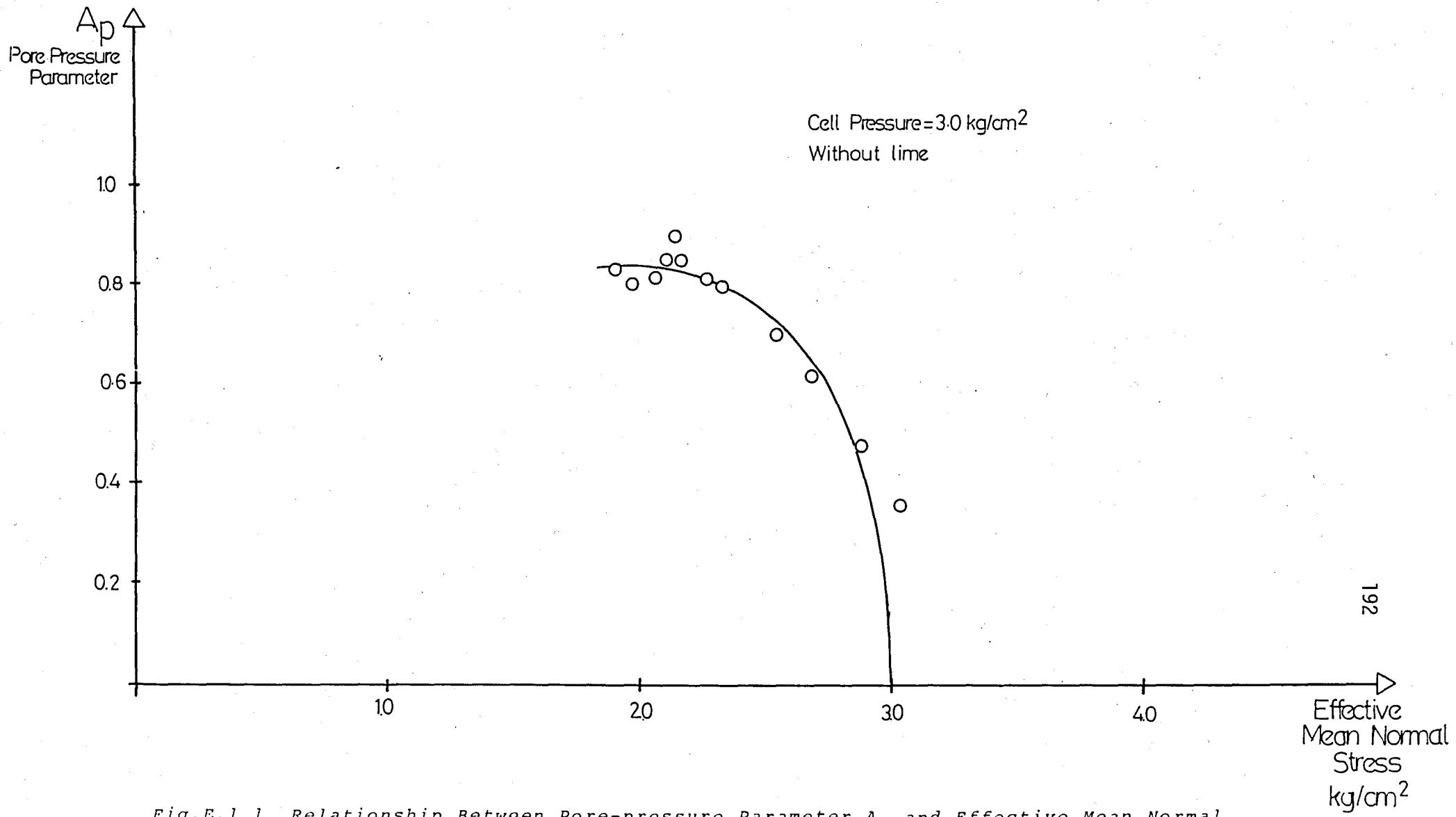

Fig.E.1.1. Relationship Between Pore-pressure Parameter A_p and Effective Mean Normal Stress p'

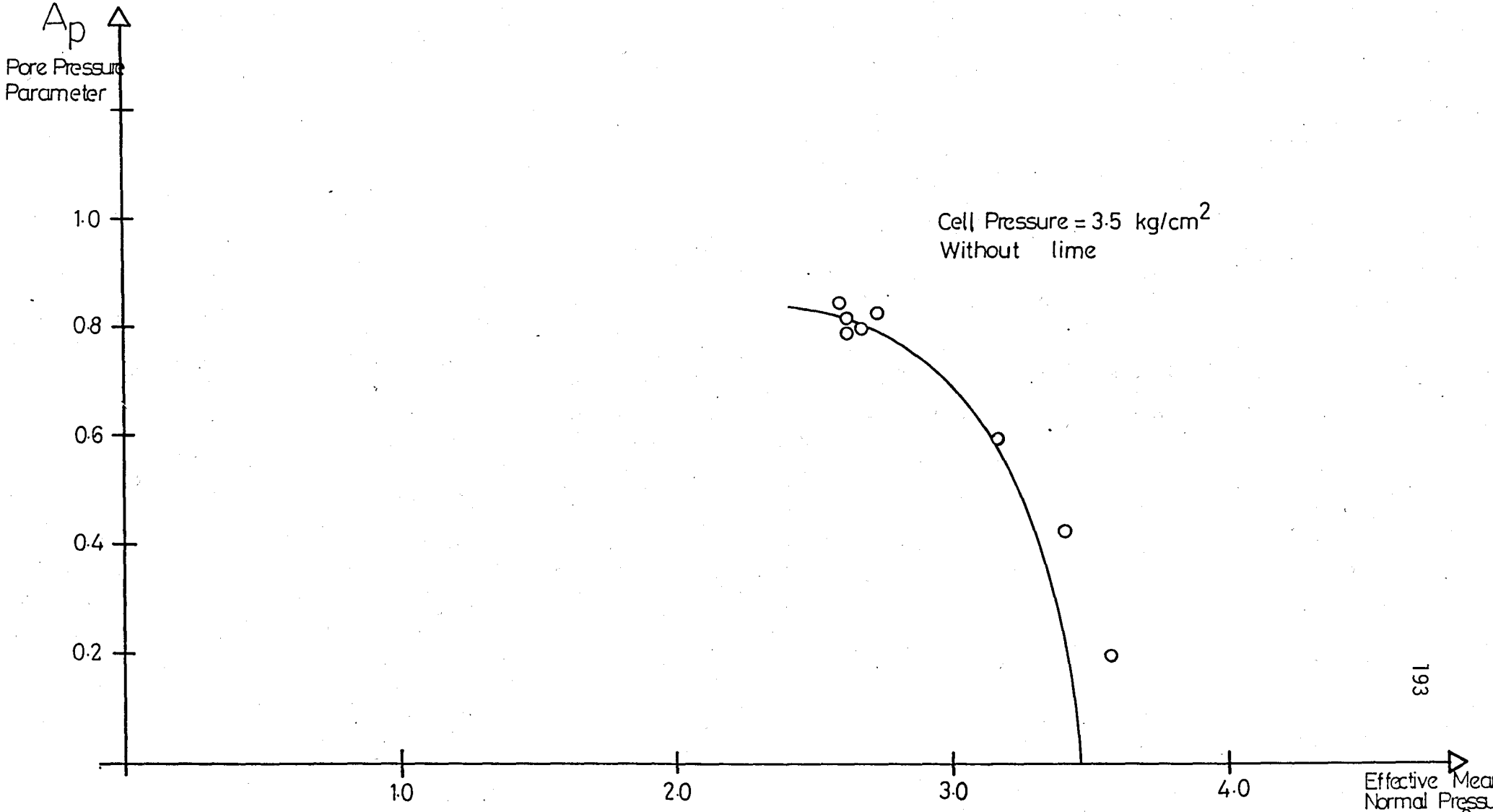

Fig.E.1.2. Relationship Between Pore-pressure Parameter A_p and Effective Mean Normal Stress p'

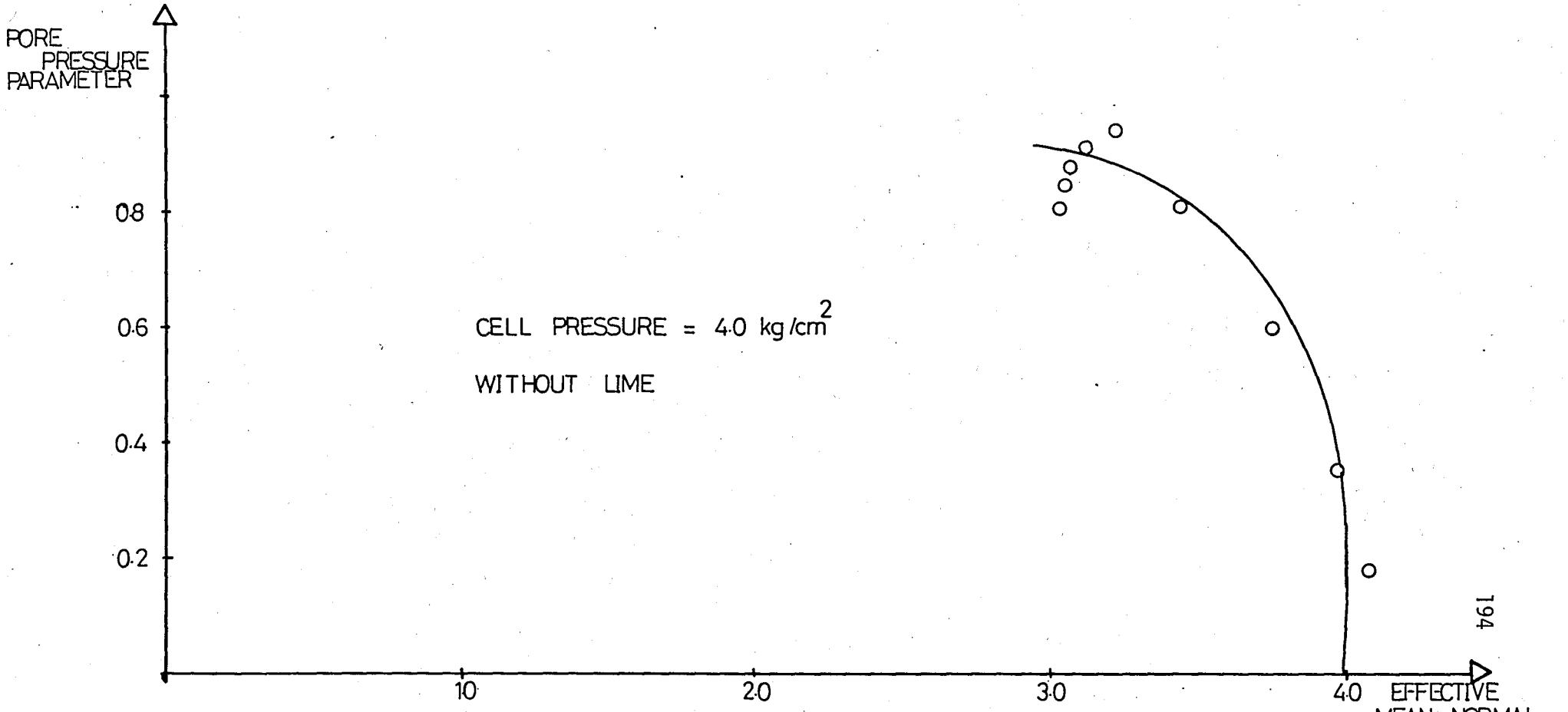

Fig.E.1.3. Relationship Between Pore-pressure Parameter A_p and Effective Mean Normal Stress p'

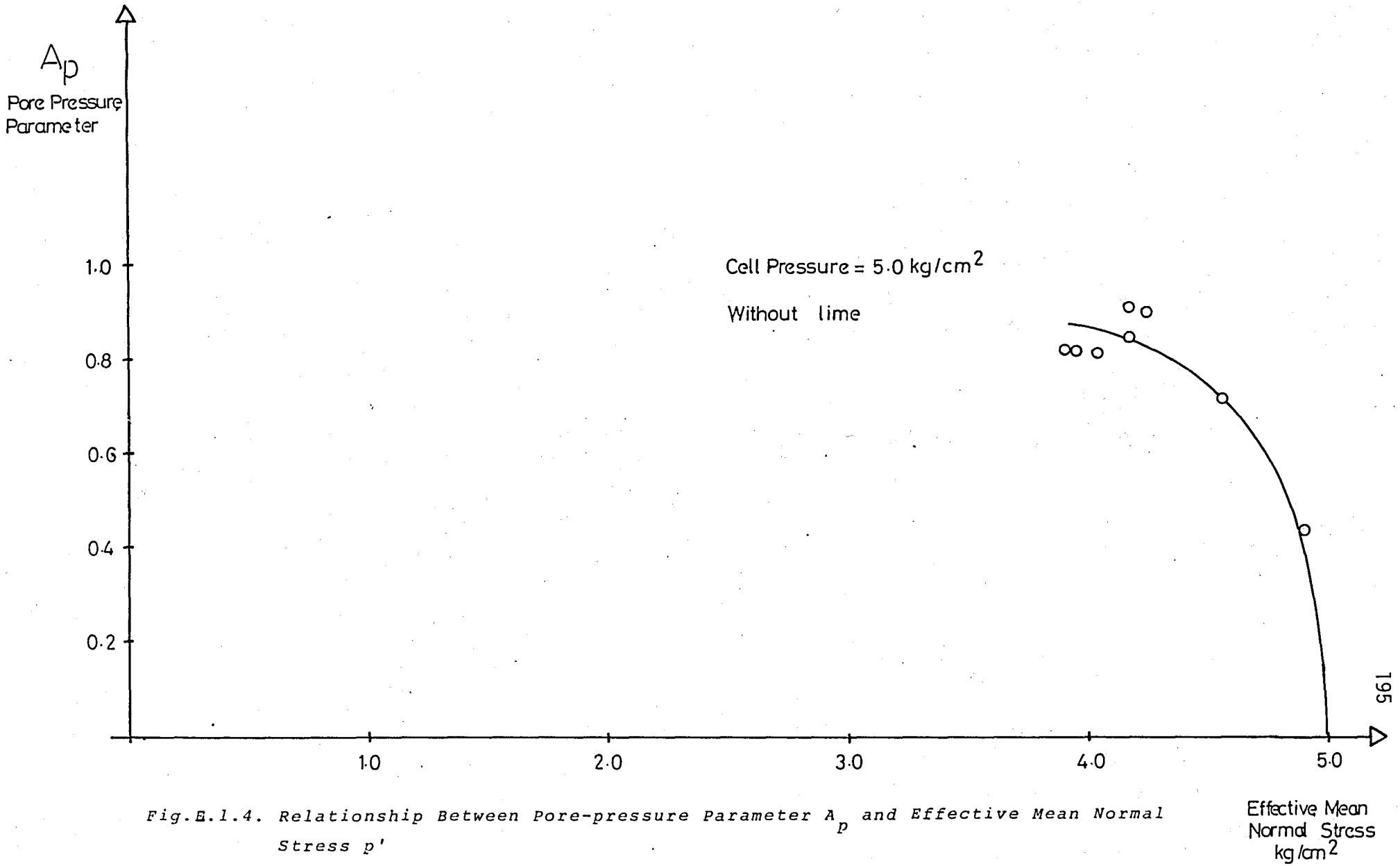

Fig.E.1.4. Relationship Between Pore-pressure Parameter A_p and Effective Mean Normal Stress p'

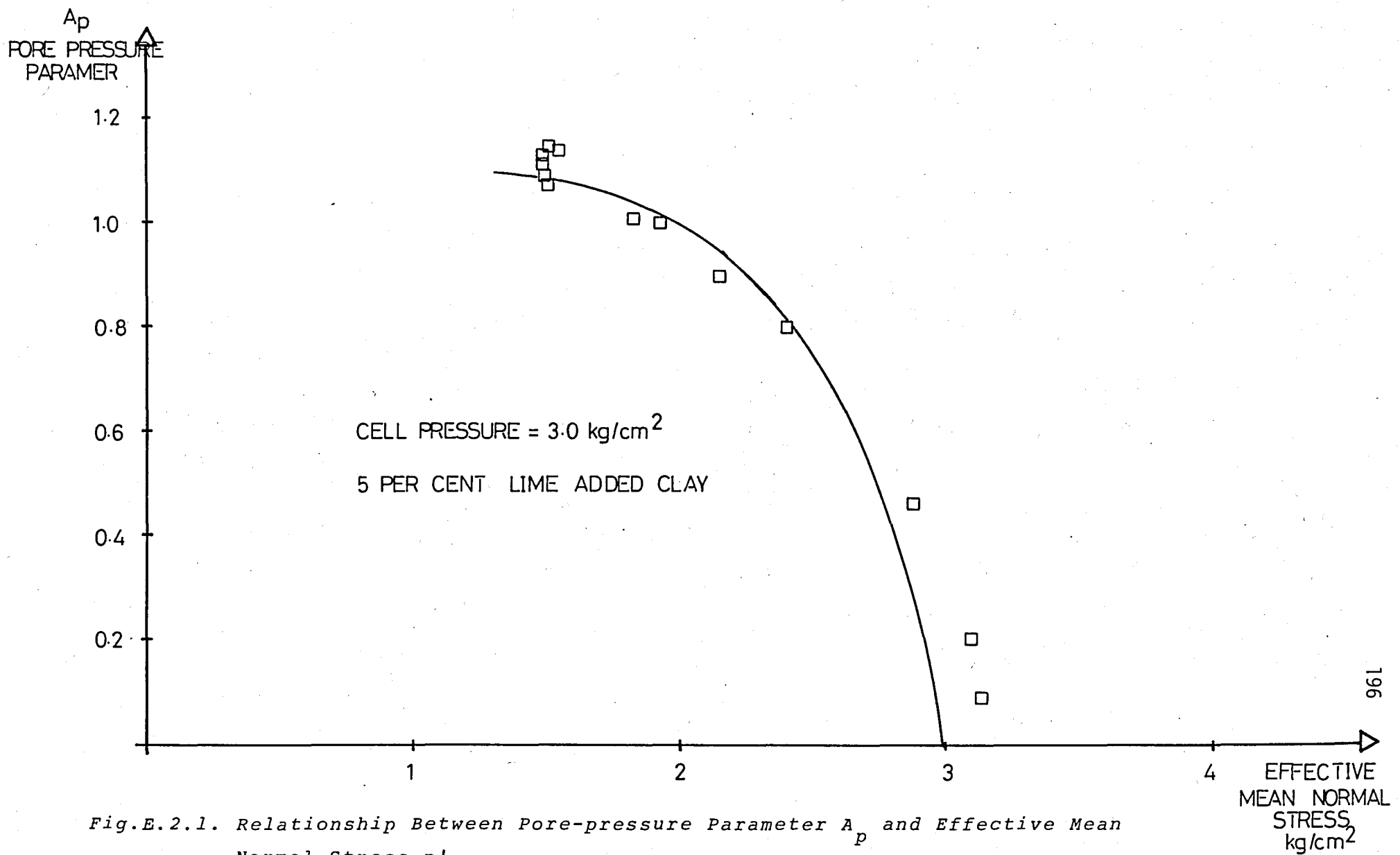

Fig.E.2.1. Relationship Between Pore-pressure Parameter A_p and Effective Mean Normal Stress p'

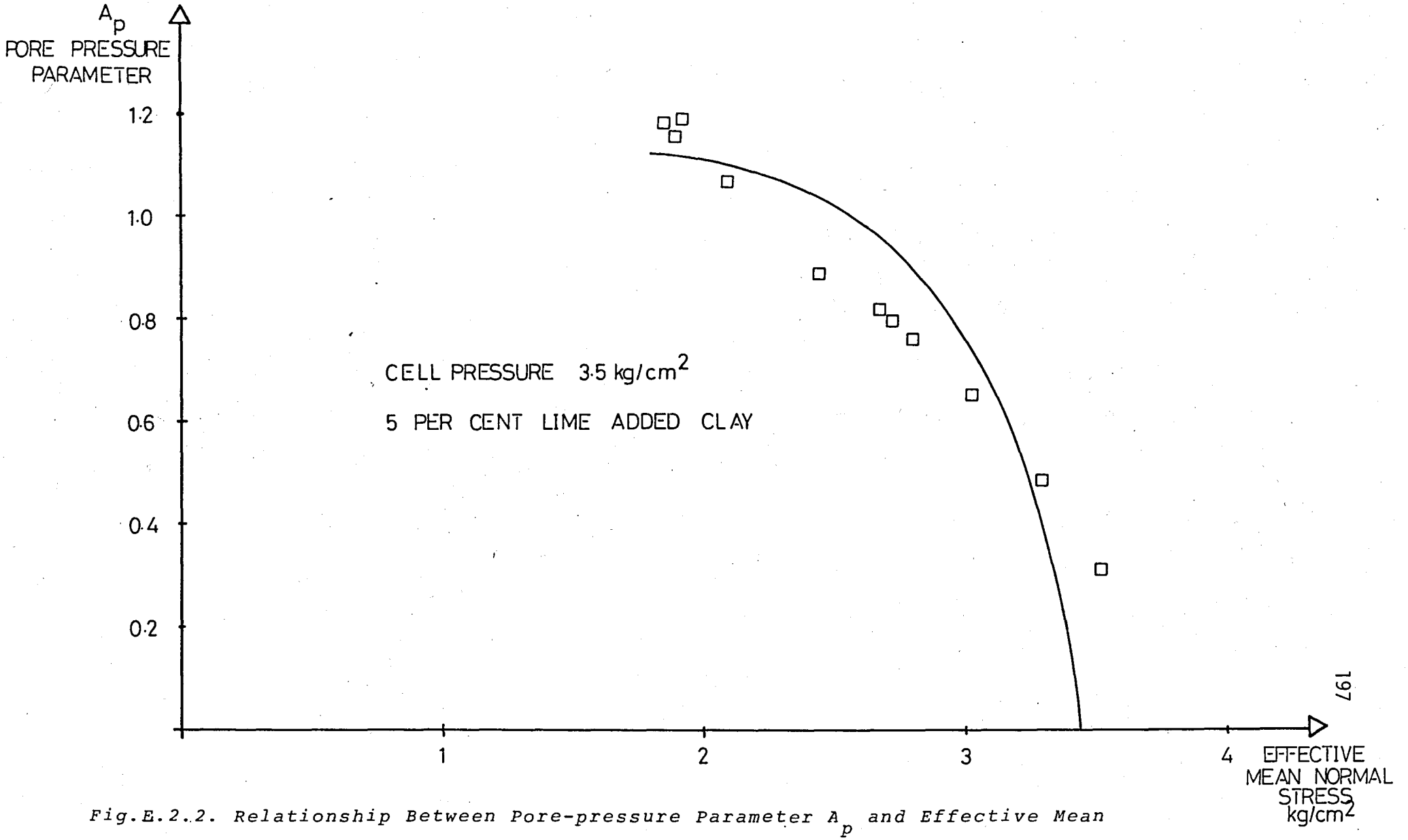

Fig.E.2.2. Relationship Between Pore-pressure Parameter A_p and Effective Mean Normal Stress p'

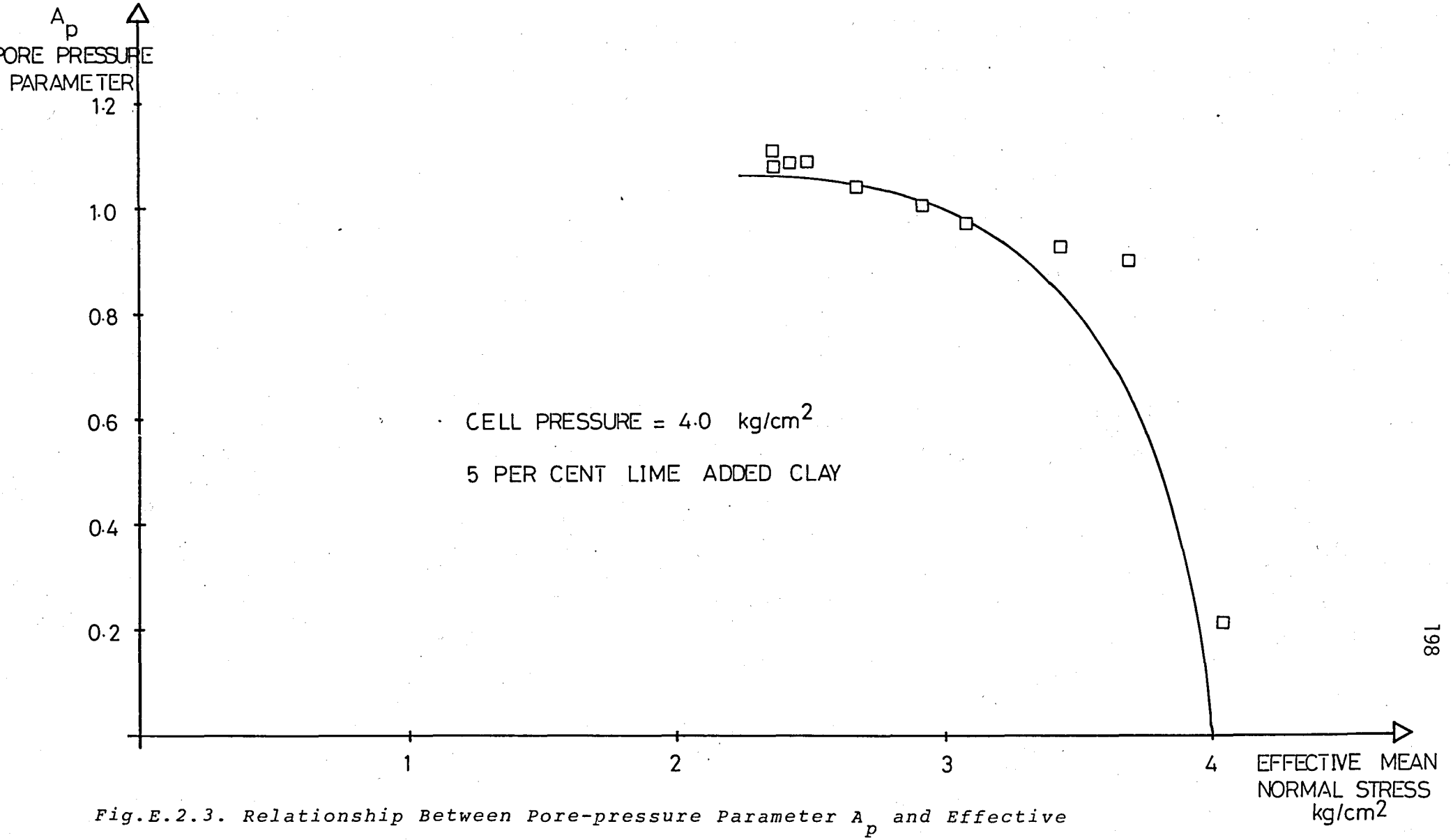

Fig.E.2.3. Relationship Between Pore-pressure Parameter A_p and Effective Mean Normal Stress p'

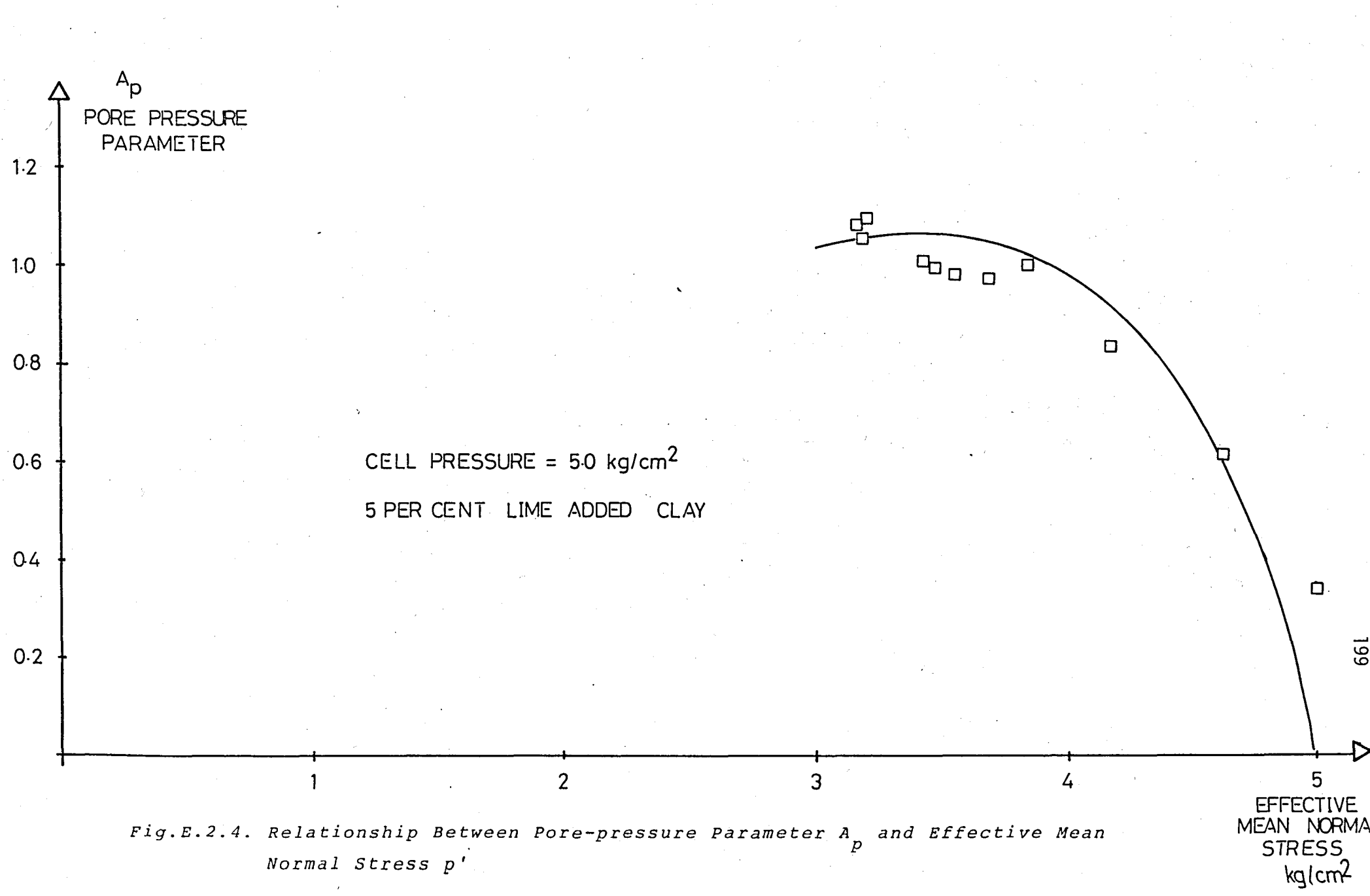

Fig.E.2.4. Relationship Between Pore-pressure Parameter A_p and Effective Mean Normal Stress p'

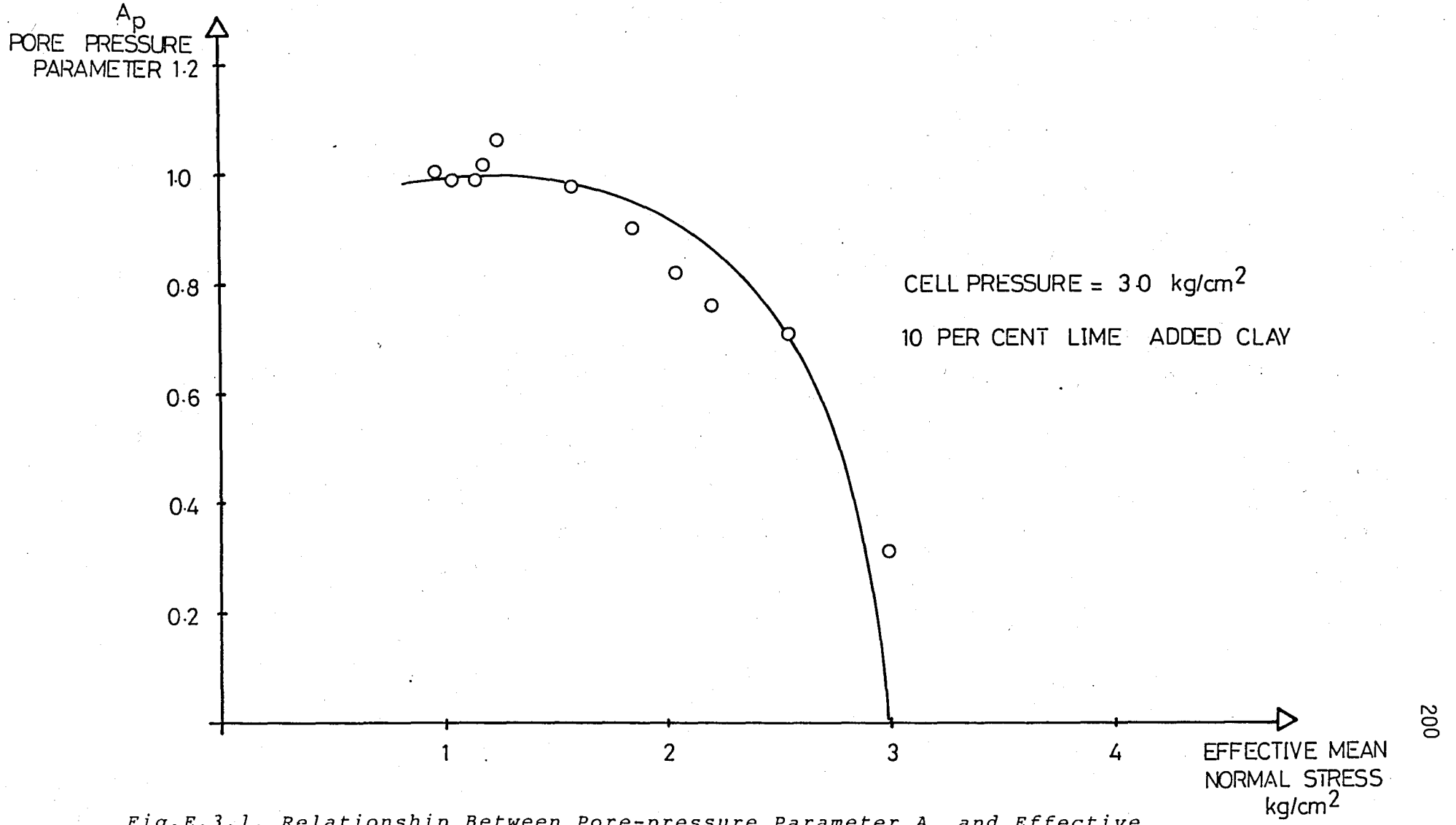

Fig.E.3.1. Relationship Between Pore-pressure Parameter A_p and Effective Mean Normal Stress p'

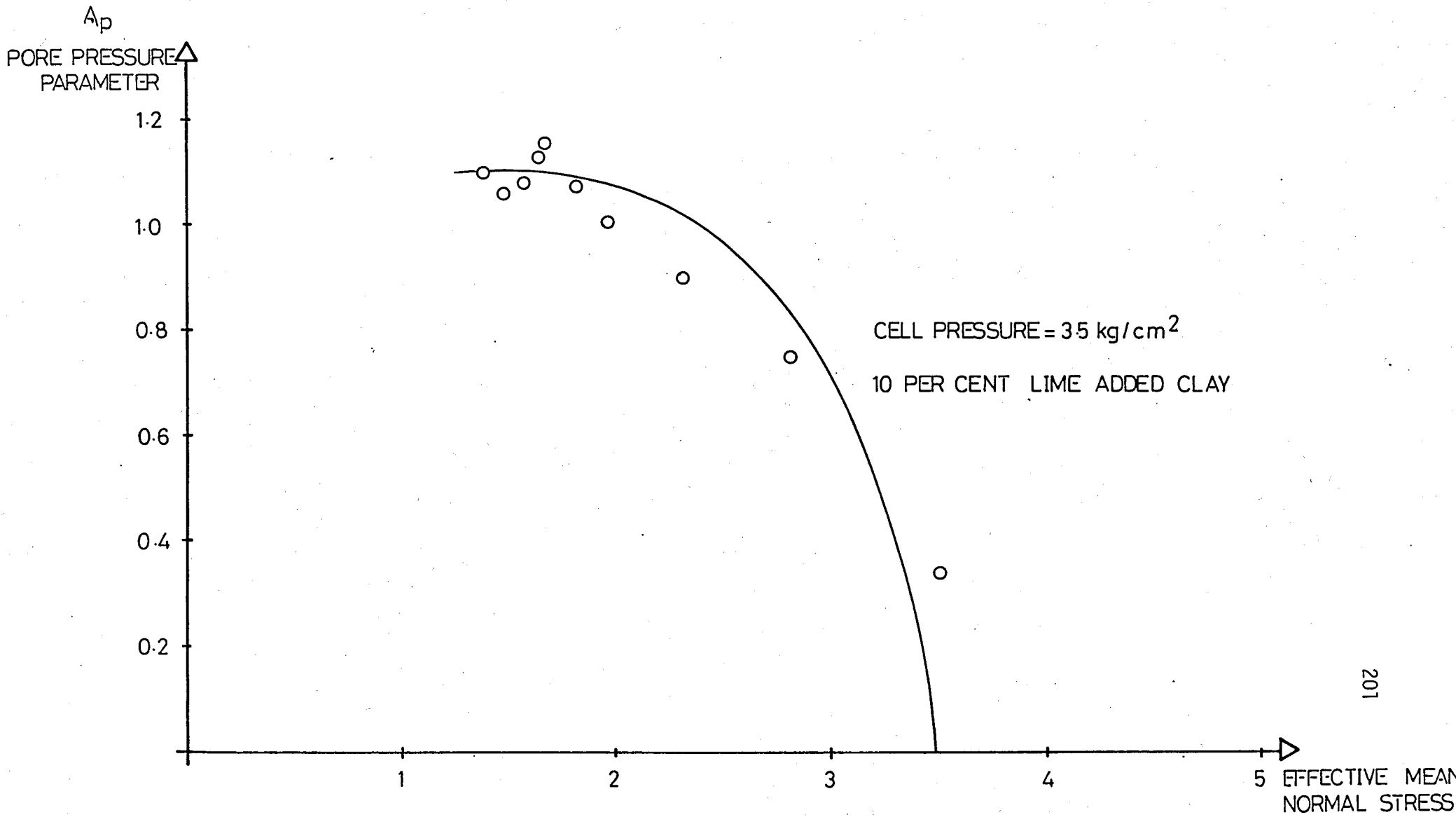

Fig.E.3.2. Relationship Between Pore-pressure Parameter A_p and Effective Mean Normal Stress p'

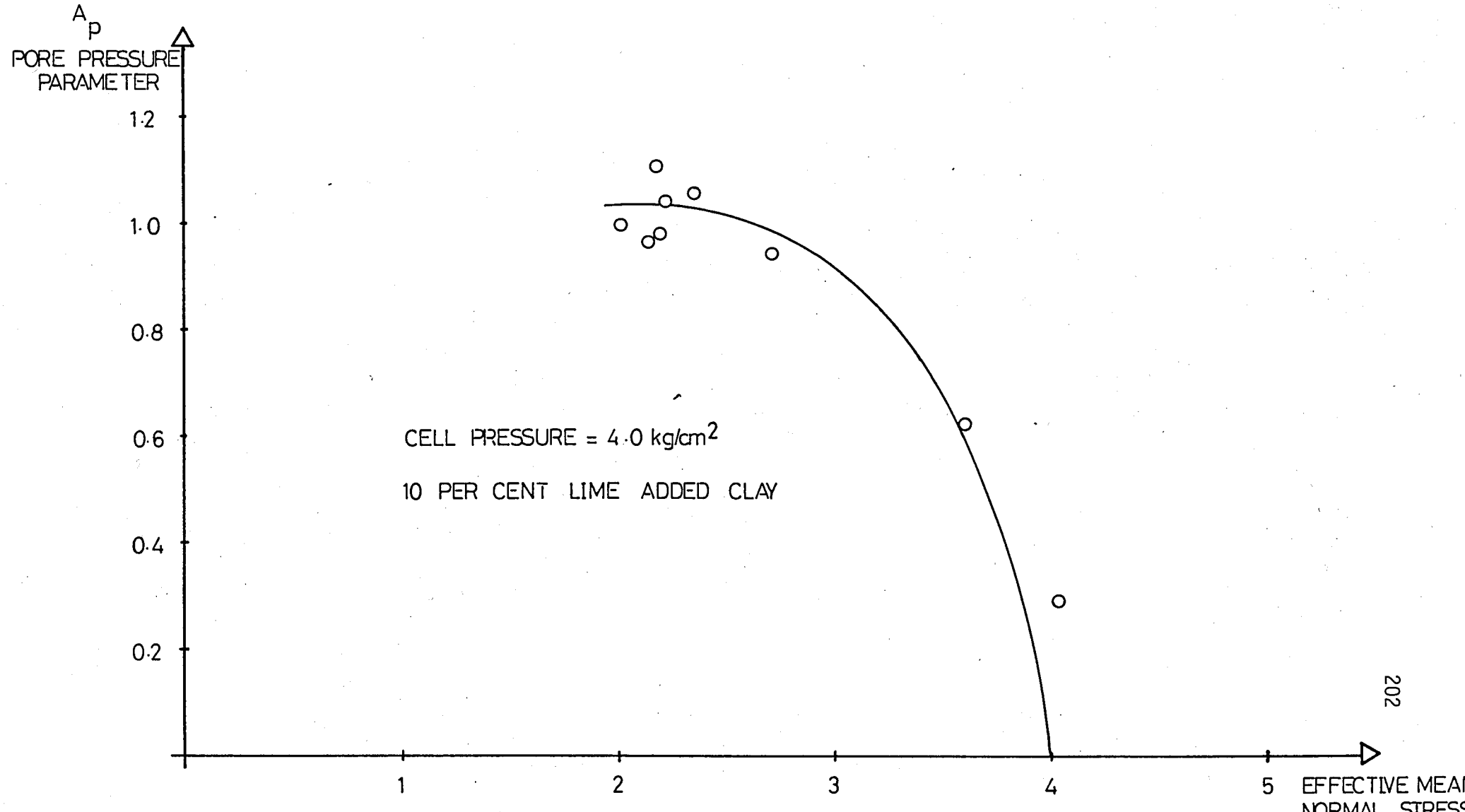

Fig.E.3.3. Relationship Between Pore-pressure Parameter A_p and Effective Mean Normal Stress p'

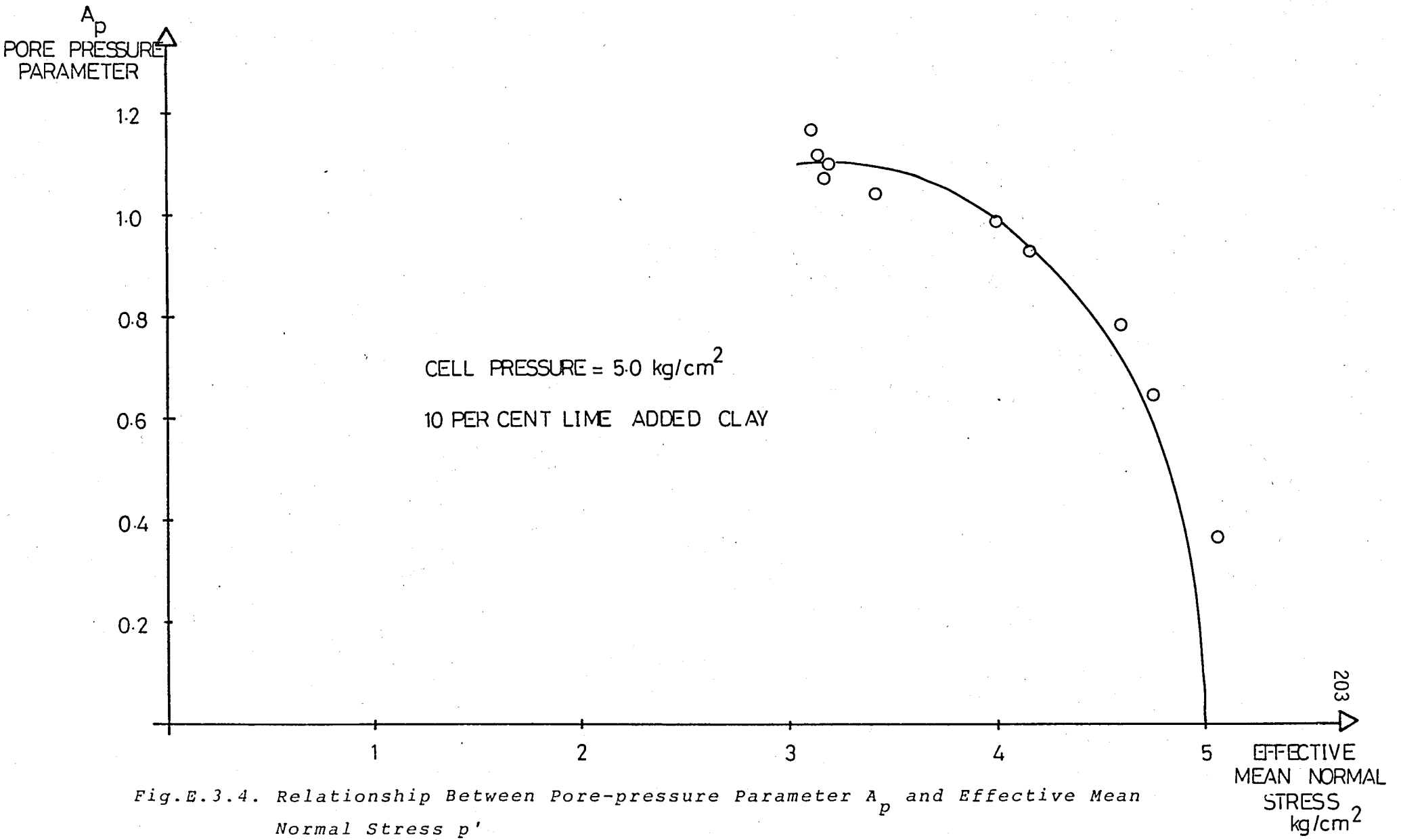

Fig.E.3.4. Relationship Between Pore-pressure Parameter A_p and Effective Mean Normal Stress p'

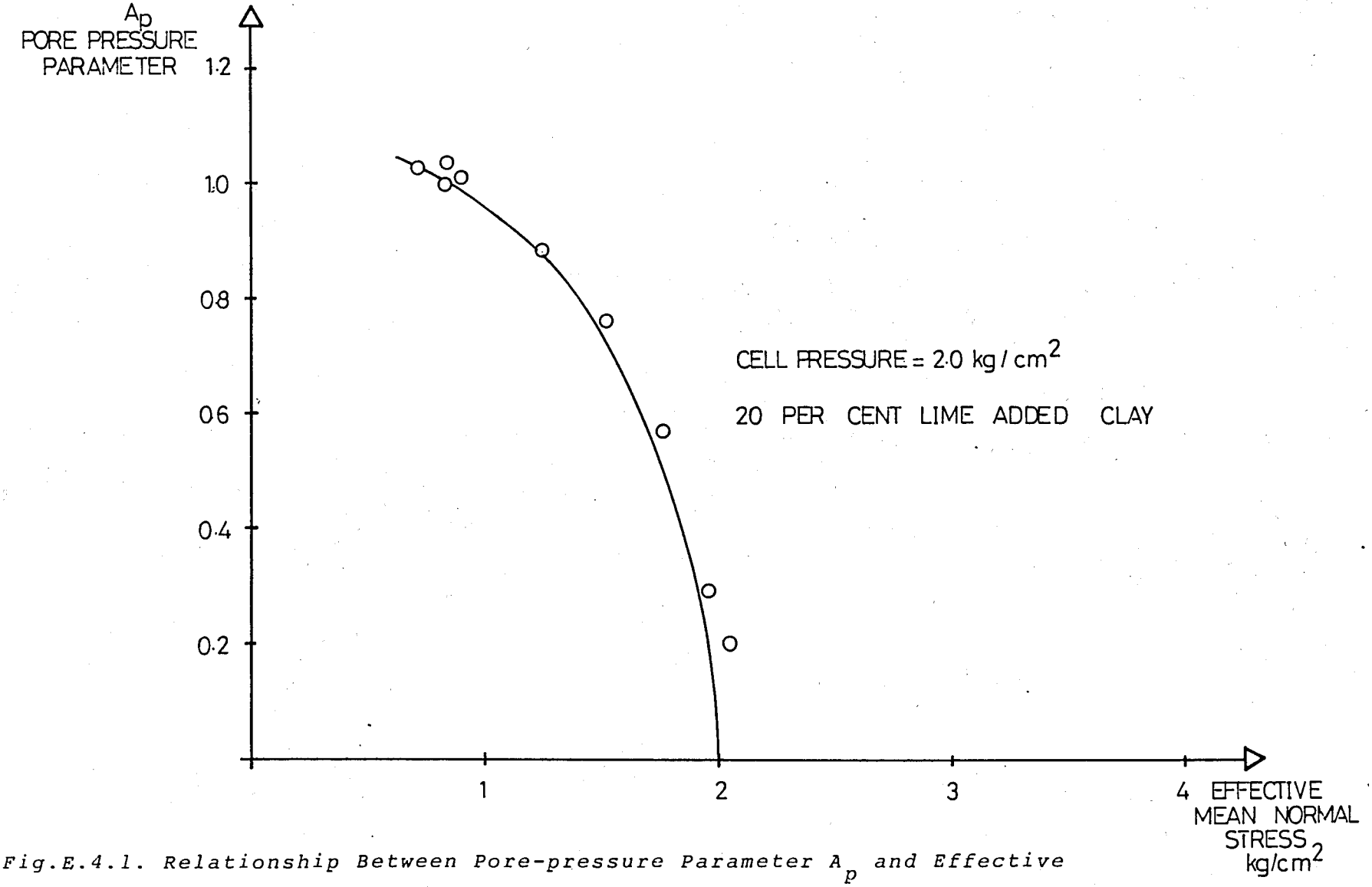

Fig.E.4.1. Relationship Between Pore-pressure Parameter A_p and Effective Mean Normal Stress p'

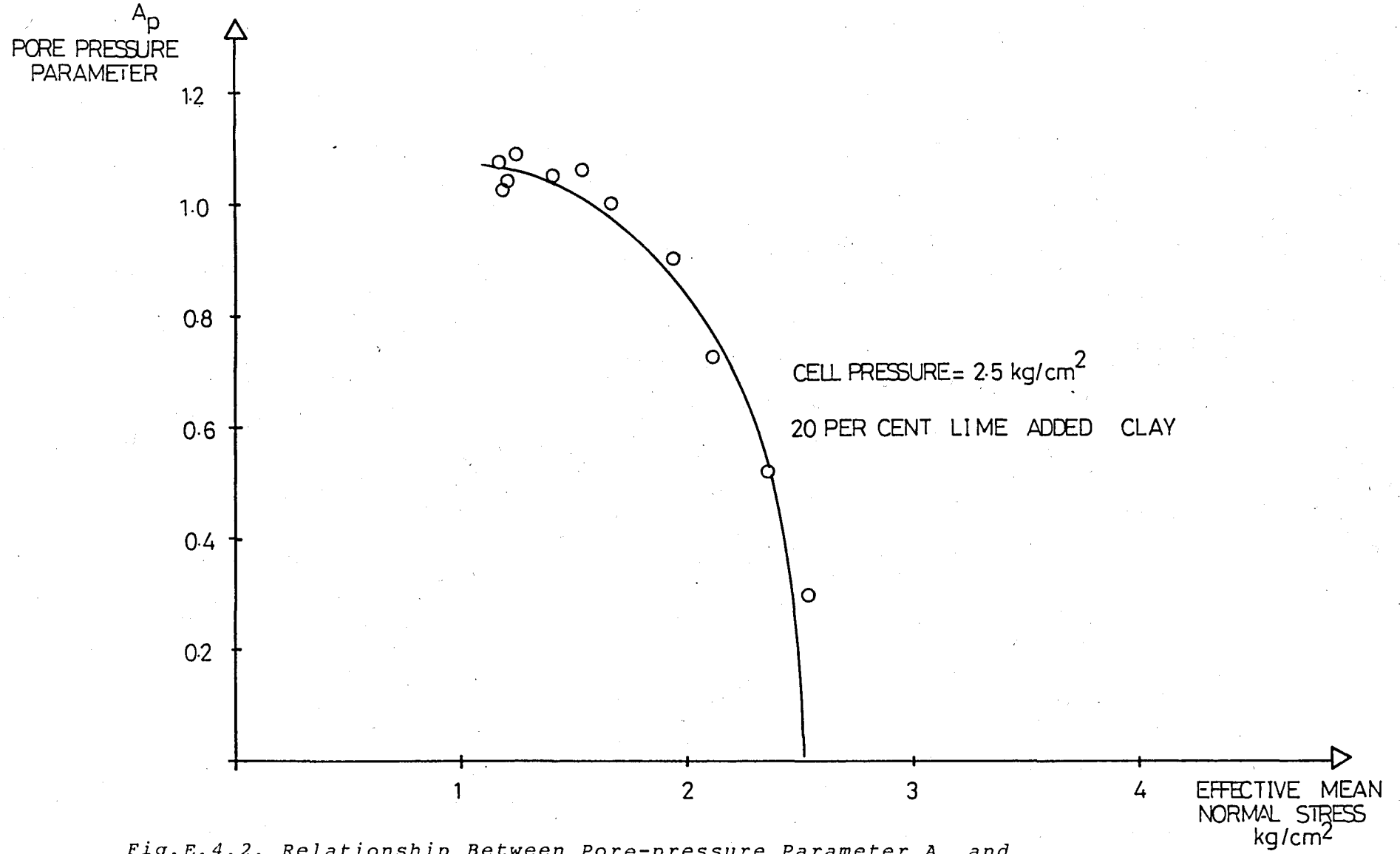

Fig.E.4.2. Relationship Between Pore-pressure Parameter A_p and Effective Mean Normal Stress p'

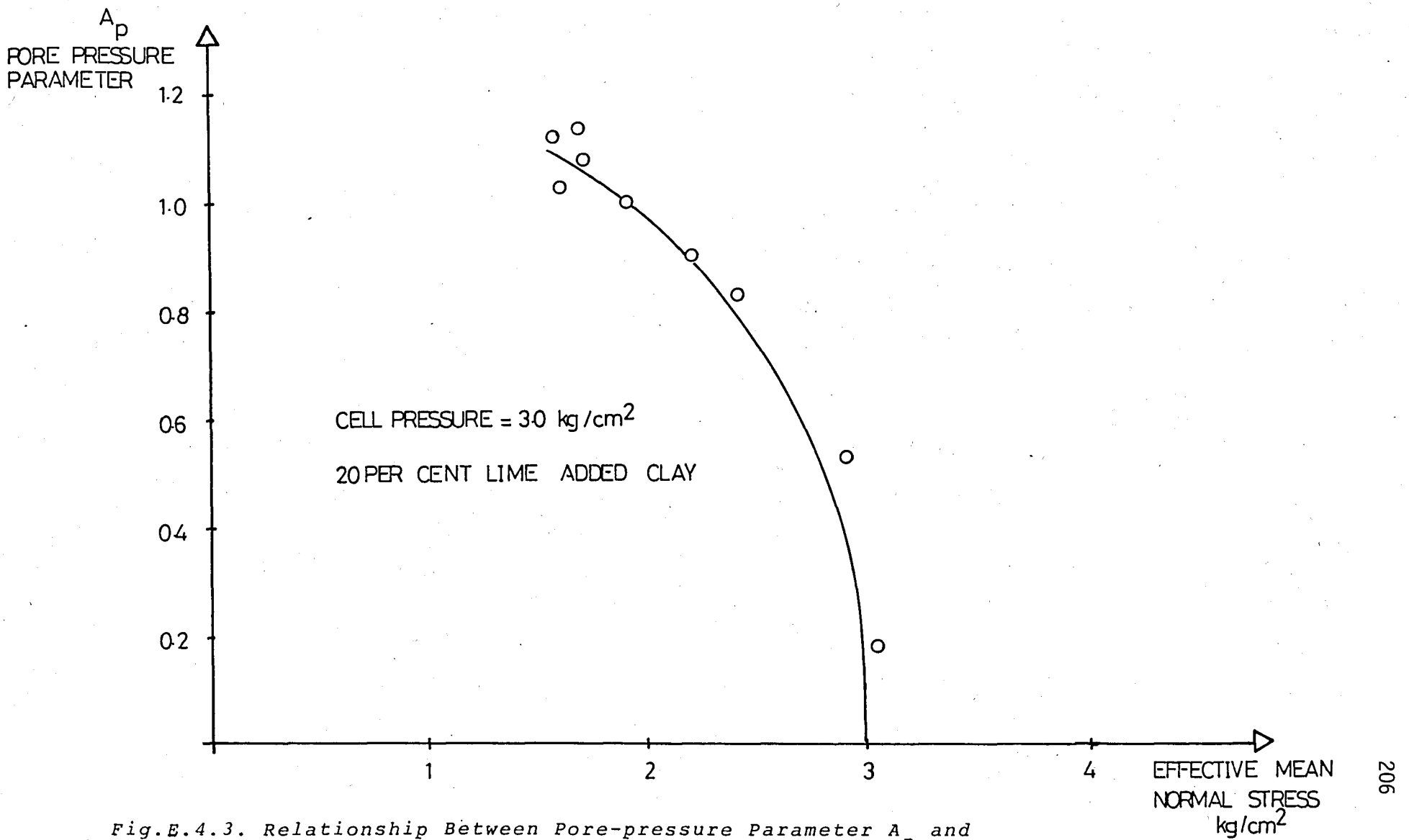

Fig.E.4.3. Relationship Between Pore-pressure Parameter A_p and Effective Mean Normal Stress p'

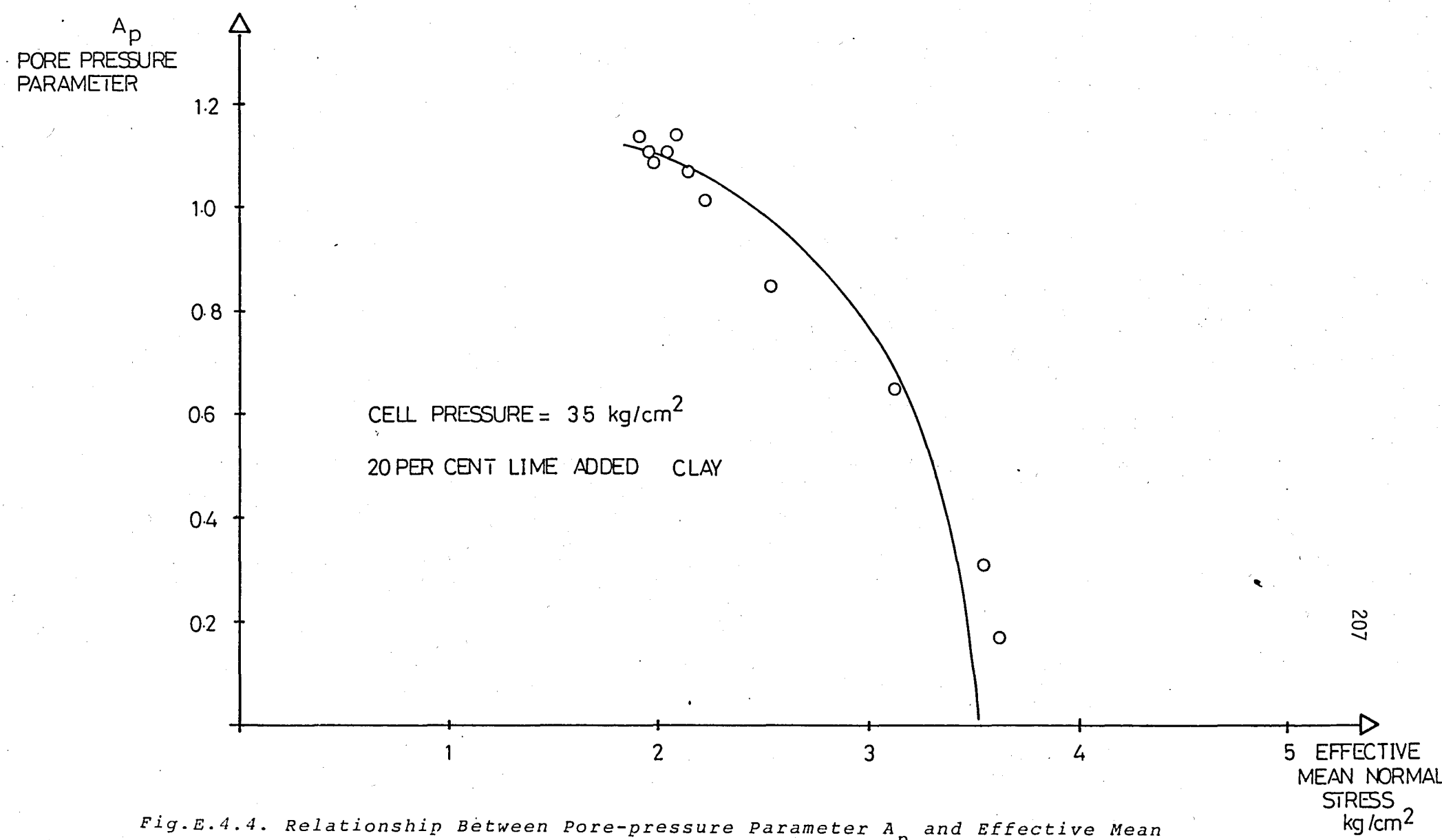

Fig.E.4.4. Relationship Between Pore-pressure Parameter A_p and Effective Mean Normal Stress p'

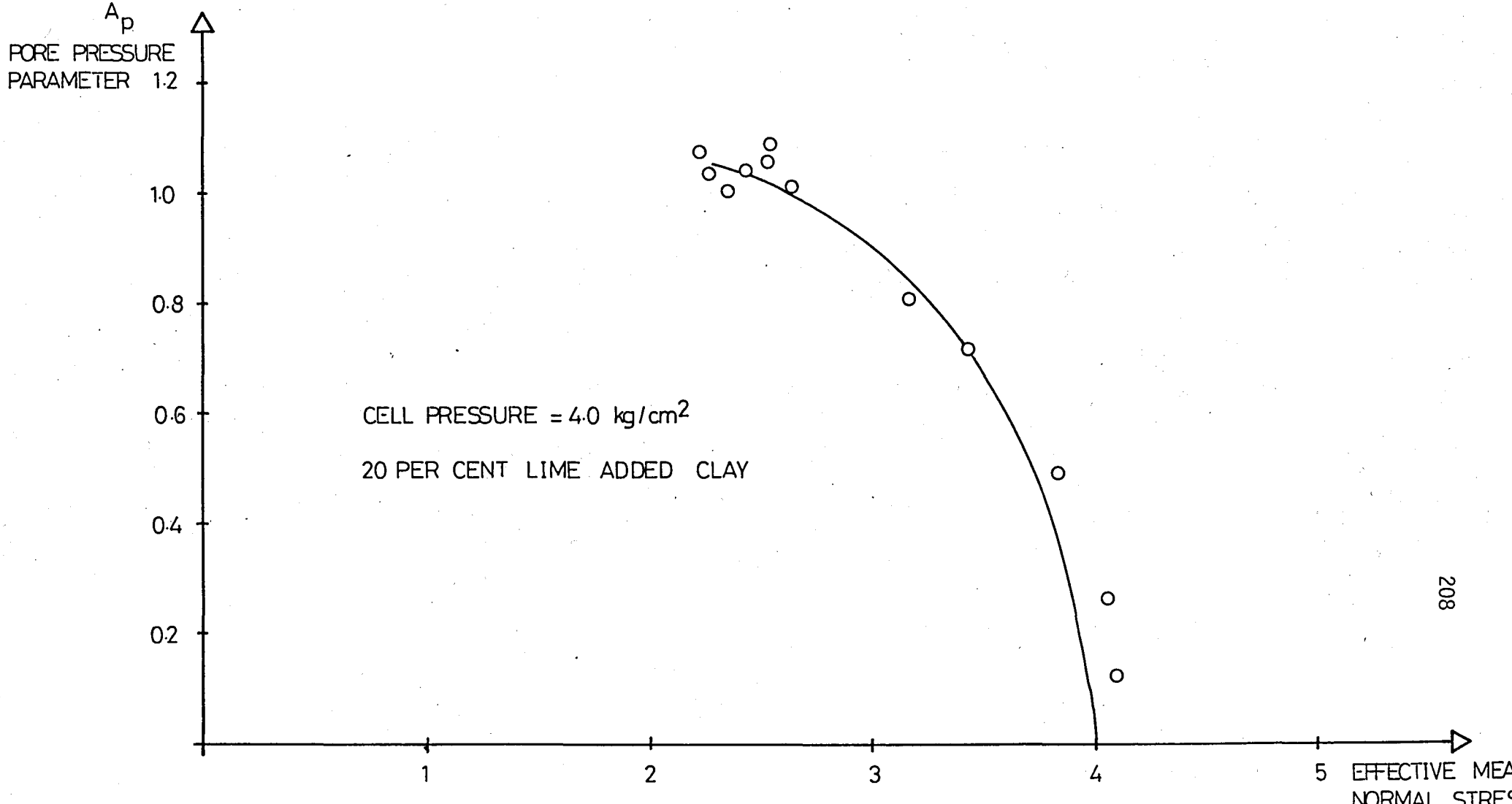

Fig.E.4.5. Relationship Between Pore-pressure Parameter A_p and Effective Mean Normal Stress p'

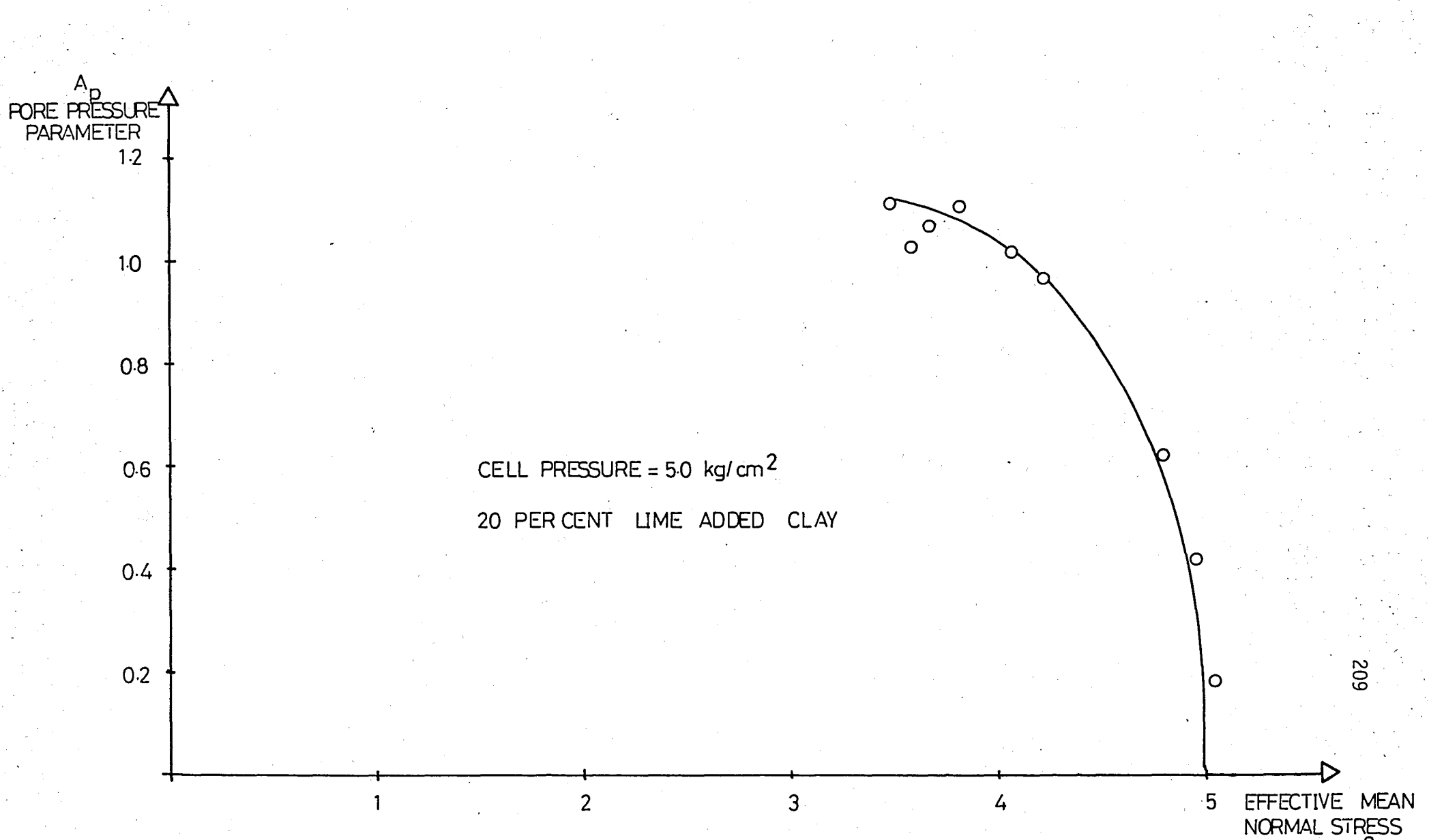

Fig.E.4.6. Relationship Between Pore-pressure Parameter A_p and Effective Mean Normal Stress p'